

FORMATION CONTROL AND FAULT  
ACCOMMODATION FOR A TEAM OF AUTONOMOUS  
UNDERWATER VEHICLES

SAHAR SEDAGHATI

A THESIS  
IN  
THE DEPARTMENT  
OF  
ELECTRICAL ENGINEERING

PRESENTED IN PARTIAL FULFILLMENT OF THE REQUIREMENTS  
FOR THE DEGREE OF MASTER OF APPLIED SCIENCE (ELECTRICAL AND  
COMPUTER ENGINEERING)  
CONCORDIA UNIVERSITY  
MONTRÉAL, QUÉBEC, CANADA

AUGUST 2015

© SAHAR SEDAGHATI, 2015

CONCORDIA UNIVERSITY  
School of Graduate Studies

This is to certify that the thesis prepared

By: **Sahar Sedaghati**

Entitled: **Formation Control and Fault Accommodation for a Team  
of Autonomous Underwater Vehicles**

and submitted in partial fulfillment of the requirements for the degree of

**Master of Applied Science (Electrical and Computer Engineering)**

complies with the regulations of this University and meets the accepted standards  
with respect to originality and quality.

Signed by the final examining committee:

_____	Chair
Dr. A. G. Aghdam	
_____	Examiner
Dr. A. Dolatabadi	
_____	Examiner
Dr. Y. R. Shayan	
_____	Supervisor
Dr. K. Khorasani	
_____	Co-Supervisor
Dr. F. Abdollahi	

Approved by \_\_\_\_\_  
Department of Electrical and Computer Engineering

\_\_\_\_\_  
Dean  
Faculty of Engineering and Computer Science

# Abstract

## Formation Control and Fault Accommodation for a Team of Autonomous Underwater Vehicles

Sahar Sedaghati

The purpose of this thesis is the development of efficient formation control and fault accommodation algorithms for a team of autonomous underwater vehicles (AUVs). The team of AUVs are capable of performing a wide range of deep water marine applications such as seabed mapping and surveying, oil and gas exploration and extraction, and oil and gas pipeline inspection. However, communication limitations and the presence of undesirable events such as component faults in any of the team members can prevent the whole team to achieve safe, reliable, and efficient performance while executing underwater mission tasks.

In this regard, the semi-decentralized control scheme is developed to achieve trajectory tracking and formation keeping while requiring information exchange only among neighboring agents. To this end, model predictive control (MPC) technique and dynamic game theory are utilized to formulate and solve the formation control problem. Moreover, centralized and decentralized control schemes are developed to assess the performance of the proposed semi-decentralized control scheme in the simulation studies. The simulation results verify that the performance of the proposed semi-decentralized scheme is very close to the centralized scheme with lower control effort cost while it does not impose stringent communication requirements as in the centralized scheme.

Moreover, the semi-decentralized active fault recovery scheme is developed to maintain a graceful degraded performance and to ensure that the team of autonomous

underwater vehicles can satisfy mission objectives when an actuator fault occurs in any of the team members. In this regard, online fault information provided by fault detection and isolation (FDI) modules of each agent and its neighbors are incorporated to redesign the nominal controllers based on the MPC technique and dynamic game theory. Additionally, FDI imperfections such as fault estimation error and time delay are taken into account, and a performance index is derived to show the impact of FDI imperfections on the performance of team members. Moreover, centralized and decentralized active fault recovery schemes are developed to evaluate the performance of the proposed semi-decentralized recovery scheme through comparative simulation studies with various fault scenarios. The comparative simulation studies justify that the proposed semi-decentralized fault recovery scheme meets the design specifications even if the performance of the FDI module is not ideal.

# Acknowledgments

I would like to express my sincere gratitude to my supervisor Professor Khashayar Khorasani. I am thankful to him for giving me the opportunity to join his research group at Concordia University. Completion of my masters would have not been possible without his kind support, motivation, and invaluable guidance. I would also like to acknowledge the advice and guidance of Dr. Farzaneh Abdollahi, who offered useful suggestions. Many thanks for her assistance in the preparation and completion of this study.

I am thankful to all my friends and colleagues in Control and Systems Laboratory of Concordia University who provided me a warm and friendly environment during this period of my life.

Last but not the least, I would like to extend my deepest gratitude to my wonderful family. No word can express how grateful I am for their unconditional love, continuous encouragement, and support throughout my life and especially in this stage of my life. This work is dedicated to them.

# Contents

<b>List of Figures</b>	<b>xi</b>
<b>List of Tables</b>	<b>xvii</b>
<b>1 Introduction</b>	<b>1</b>
1.1 Motivation . . . . .	1
1.2 Literature Review . . . . .	2
1.2.1 Control Structures . . . . .	3
1.2.2 Coordination Methods . . . . .	4
1.2.3 Optimal Control of Autonomous Vehicle Formations . . . . .	6
1.2.4 Game Theoretic Approach to Autonomous Vehicle Formations	9
1.2.5 Fault Tolerant Control Strategies for Formation of Autonomous Vehicles . . . . .	11
1.3 Thesis Objectives and Contributions . . . . .	14
1.4 Organization of The Thesis . . . . .	16
<b>2 Background, Preliminaries and Definitions</b>	<b>17</b>
2.1 Introduction . . . . .	17
2.2 AUV Equations of Motion . . . . .	17
2.2.1 Coordinate Frames . . . . .	18
2.2.2 Attitude Representation by Euler Angles . . . . .	19

2.2.3	AUV Nonlinear Kinematic and Dynamic Equations of Motion	20
2.2.4	AUV Nonlinear Equations of Motion in Horizontal Plane . . .	21
2.2.5	Modeling Environmental Disturbances . . . . .	24
2.2.6	Linearized Equations of Motion . . . . .	26
2.3	Fault Types and Modeling . . . . .	28
2.4	Model Predictive Control Framework . . . . .	30
2.4.1	QP formulation of MPC . . . . .	32
2.4.2	Stability of MPC . . . . .	33
2.5	Dynamic Game Theory . . . . .	35
2.5.1	Cooperative Game . . . . .	36
2.5.2	Non-Cooperative Game . . . . .	38
2.6	Basic Definitions on Multiple AUVs Formation Structure and Modeling	39
2.6.1	Formation Graph Modeling . . . . .	40
2.7	Summary . . . . .	41
<b>3</b>	<b>Centralized, Semi-Decentralized, and Decentralized Control of Au-</b>	
	<b>tonomous Vehicle Formations</b>	<b>42</b>
3.1	Introduction . . . . .	42
3.2	Centralized Control . . . . .	43
3.2.1	Model Predictive Control Approach to Centralized Control . .	45
3.2.2	Non-Cooperative Dynamic Game Approach to Centralized Con-	
	trol . . . . .	47
3.2.3	Cooperative Dynamic Game Approach to Centralized Control	49
3.3	Semi-Decentralized Control . . . . .	52
3.3.1	Model Predictive Control Approach to Semi-Decentralized Con-	
	trol . . . . .	54

3.3.2	Non-Cooperative Dynamic Game Approach to Semi- Decentralized Control . . . . .	56
3.4	Decentralized Control . . . . .	59
3.4.1	Model Predictive Control Approach to Decentralized Control . . . . .	61
3.4.2	Non-Cooperative Dynamic Game Approach to Decentralized Control . . . . .	62
3.5	Simulation Results . . . . .	64
3.5.1	Comparison of Centralized, Semi-Decentralized, and Decentralized MPC-Based Control Schemes . . . . .	67
3.5.2	Comparison of Centralized, Semi-Decentralized, and Decentralized Control Schemes Based on Non-Cooperative Dynamic Game . . . . .	71
3.5.3	Centralized Cooperative Dynamic Game vs. Centralized Non-Cooperative Dynamic Game . . . . .	76
3.6	Summary . . . . .	80
<b>4</b>	<b>Centralized, Semi-Decentralized, and Decentralized Fault Accommodation of Autonomous Vehicle Formations</b>	<b>83</b>
4.1	Introduction . . . . .	83
4.2	Centralized Fault Accommodation . . . . .	84
4.2.1	Model Predictive Control Approach to Centralized Fault Accommodation . . . . .	85
4.2.2	Non-Cooperative Dynamic Game Approach to Centralized Fault Accommodation . . . . .	87
4.2.2.1	Performance Evaluation in the Presence of FDI Imperfections . . . . .	89
4.2.3	Cooperative Dynamic Game Approach to Centralized Fault Accommodation . . . . .	91

4.2.3.1	Performance Evaluation in the Presence of FDI Im-	
	perfections . . . . .	93
4.3	Semi-Decentralized Fault Accommodation . . . . .	95
4.3.1	Model Predictive Control Approach to Semi-Decentralized Fault	
	Accommodations . . . . .	96
4.3.2	Non-Cooperative Dynamic Game Approach to Semi - Decen-	
	tralized Fault Accommodation . . . . .	97
4.3.2.1	Performance Evaluation in the Presence of FDI Im-	
	perfections . . . . .	100
4.4	Decentralized Fault Accommodation . . . . .	102
4.4.1	Model Predictive Control Approach to Decentralized Fault Ac-	
	commodation . . . . .	103
4.4.2	Non-Cooperative Dynamic Game Approach to Decentralized	
	Fault Accommodation . . . . .	104
4.4.2.1	Performance Evaluation in the Presence of FDI Im-	
	perfections . . . . .	106
4.5	Simulation Results . . . . .	108
4.5.1	Simulation Scenarios for MPC-Based Semi-Decentralized Fault	
	Accommodation . . . . .	108
4.5.1.1	Scenario 1: 5% LOE Fault . . . . .	109
4.5.1.2	Scenario 2: 20% LOE Fault . . . . .	112
4.5.1.3	Scenario 3: 40% LOE Fault . . . . .	115
4.5.1.4	Scenario 4: Influence of FDI Time Delay . . . . .	118
4.5.1.5	Scenario 5: Multiple Faulty Agents in the Team . . . . .	120
4.5.2	Simulation Scenarios for Semi-Decentralized Fault Accommo-	
	dation Based on Non-Cooperative Dynamic Game . . . . .	125

4.5.2.1	Scenario 1: 5% LOE Fault . . . . .	125
4.5.2.2	Scenario 2: 20% LOE Fault . . . . .	128
4.5.2.3	Scenario 3: 40% LOE Fault . . . . .	131
4.5.2.4	Scenario 4: Influence of FDI Time Delay . . . . .	134
4.5.2.5	Scenario 5: Multiple Faulty Agents in the Team . . .	137
4.5.3	Simulation Scenario for Centralized Cooperative vs. Central- ized Non-Cooperative Dynamic Game . . . . .	142
4.6	Summary . . . . .	145
<b>5</b>	<b>Conclusions and Future Work</b>	<b>151</b>

# List of Figures

1.1	Formation of AUVs working underwater [1] . . . . .	2
1.2	Classification of Games . . . . .	10
2.1	Coordinate frames and AUV motion variables [2] . . . . .	19
3.1	Centralized Control System . . . . .	43
3.2	Information Exchange Structure of Semi-Decentralized Control System	53
3.3	Decentralized Control System . . . . .	59
3.4	Error Signals Along $X$ -axis for Cenetralized, Semi-Decentralized, and Decentralized MPC-Based Control Schemes . . . . .	69
3.5	Error Signals Along $Y$ -axis for Cenetralized, Semi-Decentralized, and Decentralized MPC-Based Control Schemes . . . . .	69
3.6	Error Signals about $Z$ -axis for Cenetralized, Semi-Decentralized, and Decentralized MPC-Based Control Schemes . . . . .	70
3.7	Surge Velocity Error Signals for Cenetralized, Semi-Decentralized, and Decentralized MPC-Based Control Schemes . . . . .	70
3.8	Thruster Forces along $X$ -axis for Cenetralized, Semi-Decentralized, and Decentralized MPC-Based Control Schemes . . . . .	71
3.9	Error Signals Along $X$ -axis for Centralized, Semi-Decentralized, and Decentralized Control Schemes Based on Non-Cooperative Dynamic Game . . . . .	73

3.10	Error Signals Along $Y$ -axis for Centralized, Semi-Decentralized, and Decentralized Control Schemes Based on Non-Cooperative Dynamic Game . . . . .	74
3.11	$Yaw$ Angle Error Signals about $Z$ -axis for Centralized, Semi-Decentralized, and Decentralized Control Schemes Based on Non-Cooperative Dynamic Game . . . . .	74
3.12	Surge Velocity Error Signals for Centralized, Semi-Decentralized, and Decentralized Control Schemes Based on Non-Cooperative Dynamic Game . . . . .	75
3.13	Thruster Forces along $X$ -axis for Centralized, Semi-Decentralized, and Decentralized Control Schemes Based on Non-Cooperative Dynamic Game . . . . .	75
3.14	Error Signals Along $X$ -axis for Centralized Control Scheme Based on Cooperative and Non-Cooperative Dynamic Game . . . . .	77
3.15	Error Signals Along $Y$ -axis for Centralized Control Scheme Based on Cooperative and Non-Cooperative Dynamic Game . . . . .	78
3.16	Error Signals about $Z$ -axis for Centralized Control Scheme Based on Cooperative and Non-Cooperative Dynamic Game . . . . .	78
3.17	Surge Velocity Error Signals for Centralized Control Scheme Based on Cooperative and Non-Cooperative Dynamic Game . . . . .	79
3.18	Thruster Forces along $X$ -axis for Centralized Control Scheme Based on Cooperative and Non-Cooperative Dynamic Game . . . . .	79
4.1	Error Signals Along $X$ -axis for Cenetralized, Semi-Decentralized, and Decentralized MPC-Based Control Schemes, Fault Scenario 1 . . . . .	110
4.2	Surge Velocity Error Signals for Cenetralized, Semi-Decentralized, and Decentralized MPC-Based Control Schemes, Fault Scenario 1 . . . . .	111

4.3	Thruster Forces along $X$ -axis for Cenetralized, Semi-Decentralized, and Decentralized MPC-Based Control Schemes, Fault Scenario 1 . . .	111
4.4	Error Signals Along $X$ -axis for Cenetralized, Semi-Decentralized, and Decentralized MPC-Based Accommodation Schemes, Fault Scenario 2	113
4.5	Surge Velocity Error Signals for Cenetralized, Semi-Decentralized, and Decentralized MPC-Based Accommodation Schemes, Fault Scenario 2	114
4.6	Thruster Forces along $X$ -axis for Cenetralized, Semi-Decentralized, and Decentralized MPC-Based Accommodation Schemes, Fault Scenario 2 . . . . .	114
4.7	Error Signals Along $X$ -axis for Cenetralized, Semi-Decentralized, and Decentralized MPC-Based Accommodation Schemes, Fault Scenario 3	116
4.8	Surge Velocity Error Signals for Cenetralized, Semi-Decentralized, and Decentralized MPC-Based Accommodation Schemes, Fault Scenario 3	117
4.9	Thruster Forces along $X$ -axis for Cenetralized, Semi-Decentralized, and Decentralized MPC-Based Accommodation Schemes, Fault Scenario 3 . . . . .	117
4.10	Error Signals Along $X$ -axis for Semi-Decentralized MPC-Based Accommodation Scheme, Fault Scenario 4 . . . . .	119
4.11	Surge Velocity Error Signals for Semi-Decentralized MPC-Based Accommodation Scheme, Fault Scenario 4 . . . . .	119
4.12	Thruster Forces along $X$ -axis for Semi-Decentralized MPC-Based Accommodation Scheme, Fault Scenario 4 . . . . .	120
4.13	Error Signals Along $X$ -axis for Centralized and Semi-Decentralized MPC-Based Accommodation Schemes, First Case in Fault Scenario 5 . . . . .	122

4.14	Surge Velocity Error Signals for Centralized and Semi-Decentralized MPC-Based Accommodation Schemes, First Case in Fault Scenario 5	123
4.15	Thruster Forces along $X$ -axis for Centralized and Semi-Decentralized MPC-Based Accommodation Schemes, First Case in Fault Scenario 5	123
4.16	Error Signals Along $X$ -axis for Centralized and Semi-Decentralized MPC-Based Accommodation Schemes, Second Case in Fault Scenario 5	124
4.17	Surge Velocity Error Signals for Centralized and Semi-Decentralized MPC-Based Accommodation Schemes, Second Case in Fault Scenario 5	124
4.18	Thruster Forces along $X$ -axis for Centralized and Semi-Decentralized MPC-Based Accommodation Schemes, Second Case in Fault Scenario 5	125
4.19	Error Signals Along $X$ -axis for Centralized, Semi-Decentralized, and Decentralized Accommodation Schemes Based on Non-Cooperative Game, Fault Scenario 1 . . . . .	127
4.20	Surge Velocity Error Signals for Centralized, Semi-Decentralized, and Decentralized Accommodation Schemes Based on Non-Cooperative Game, Fault Scenario 1 . . . . .	127
4.21	Thruster Forces along $X$ -axis for Centralized, Semi-Decentralized, and Decentralized Accommodation Schemes Based on Non-Cooperative Game, Fault Scenario 1 . . . . .	128
4.22	Error Signals Along $X$ -axis for Centralized, Semi-Decentralized, and Decentralized Accommodation Schemes Based on Non-Cooperative Game, Fault Scenario 2 . . . . .	130
4.23	Surge Velocity Error Signals for Centralized, Semi-Decentralized, and Decentralized Accommodation Schemes Based on Non-Cooperative Game, Fault Scenario 2 . . . . .	130

4.24 Thruster Forces along $X$ -axis for Centralized, Semi-Decentralized, and Decentralized Accommodation Schemes Based on Non-Cooperative Game, Fault Scenario 2 . . . . .	131
4.25 Error Signals Along $X$ -axis for Centralized, Semi-Decentralized, and Decentralized Accommodation Schemes Based on Non-Cooperative Game, Fault Scenario 3 . . . . .	133
4.26 Surge Velocity Error Signals for for Centralized, Semi-Decentralized, and Decentralized Accommodation Schemes Based on Non-Cooperative Game, Fault Scenario 3 . . . . .	133
4.27 Thruster Forces along $X$ -axis for for Centralized, Semi-Decentralized, and Decentralized Accommodation Schemes Based on Non-Cooperative Game, Fault Scenario 3 . . . . .	134
4.28 Error Signals Along $X$ -axis for Semi-Decentralized Accommodation Scheme Based on Non-Cooperative Game, Fault Scenario 4 . . . . .	135
4.29 Surge Velocity Error Signals for Semi-Decentralized Accommodation Scheme Based on Non-Cooperative Game, Fault Scenario 4 . . . . .	136
4.30 Thruster Forces along $X$ -axis for Semi-Decentralized Accommodation Scheme Based on Non-Cooperative Game, Fault Scenario 4 . . . . .	136
4.31 Error Signals Along $X$ -axis for Centralized, Semi-Decentralized, and Decentralized Accommodation Schemes Based on Non-Cooperative Game, Fault Scenario 5.1 . . . . .	139
4.32 Surge Velocity Error Signals for Centralized, Semi-Decentralized, and Decentralized Accommodation Schemes Based on Non-Cooperative Game, Fault Scenario 5.1 . . . . .	140

4.33 Thruster Forces along $X$ -axis for Centralized, Semi-Decentralized, and Decentralized Accommodation Schemes Based on Non-Cooperative Game, Fault Scenario 5.1 . . . . .	140
4.34 Error Signals Along $X$ -axis for Centralized, Semi-Decentralized, and Decentralized Accommodation Schemes Based on Non-Cooperative Game, Fault Scenario 5.2 . . . . .	141
4.35 Surge Velocity Error Signals for Centralized, Semi-Decentralized, and Decentralized Accommodation Schemes Based on Non-Cooperative Game, Fault Scenario 5.2 . . . . .	141
4.36 Thruster Forces along $X$ -axis for Centralized, Semi-Decentralized, and Decentralized Accommodation Schemes Based on Non-Cooperative Game, Fault Scenario 5.2 . . . . .	142
4.37 Error Signals Along $X$ -axis for Centralized Accommodation Scheme Based on Cooperative and Non-Cooperative Game . . . . .	144
4.38 Surge Velocity Error Signals for Centralized Accommodation Scheme Based on Cooperative and Non-Cooperative Game . . . . .	144
4.39 Thruster Forces along $X$ -axis for Centralized Accommodation Scheme Based on Cooperative and Non-Cooperative Game . . . . .	145

# List of Tables

2.1	Nomenclature for AUV Parameters . . . . .	24
3.1	AUV Parameters [3] . . . . .	65
3.2	Initial Conditions . . . . .	66
3.3	Desired Formation Configuration . . . . .	66
3.4	Controller Parameters . . . . .	66
3.5	Performance Measures . . . . .	67
3.6	Performance and Time Response Evaluation of Centralized, Semi-Decentralized, and Decentralized MPC-Based Control Schemes . . . . .	68
3.7	Performance and Time Response Evaluation of Centralized, Semi-Decentralized, and Decentralized Control Schemes based on Non-Cooperative Dynamic Game . . . . .	73
3.8	Performance and Time Response Evaluation Between Cooperative and Non-Cooperative Dynamic Game Approaches to Centralized Control . . . . .	77
3.9	Summary of Performance and Time Response Characteristics of Centralized, Semi-Decentralized, and Decentralized Control Schemes . . . . .	82
4.1	Performance and Time Response Evaluation of Centralized, Semi-Decentralized, and Decentralized MPC-Based Controllers, 5% LOE Fault with No FDI and Recovery . . . . .	110

4.2	Performance and Time Response Evaluation of Centralized, Semi-Decentralized, and decentralized MPC-Based Fault Accommodation mechanisms, 20% LOE Fault with 20% FDI Inaccuracy . . . . .	113
4.3	Performance and Time Response Evaluation of Centralized, Semi-Decentralized, and Decentralized MPC-Based Fault Accommodation mechanisms, 40% LOE Fault with 7% FDI Inaccuracy . . . . .	116
4.4	Performance and Time Response Evaluation of MPC-Based Semi-Decentralized Fault Accommodation under Various FDI Time Delays, 40% LOE Fault with 7% FDI Inaccuracy . . . . .	118
4.5	Performance and Time Response Evaluation of Centralized and Semi-Decentralized MPC-Based Fault Accommodation Mechanisms, 40% LOE Fault with 7% FDI Inaccuracy in AUVs #2 and #4 . . . . .	121
4.6	Performance and Time Response Evaluation of Centralized and Semi-Decentralized MPC-Based Fault Accommodation Mechanisms, Different LOE Faults in AUVs #2, #4, and #5 . . . . .	122
4.7	Performance and Time Response Evaluation of Centralized, Semi-Decentralized, and Decentralized Controllers Based on Non-Cooperative Dynamic Game, 5% LOE Fault with No FDI and Recovery . . . . .	126
4.8	Performance and Time Response Evaluation of Centralized, Semi-Decentralized, and Decentralized Fault Accommodation Based on Non-Cooperative Dynamic Game, 20% LOE Fault with 20% FDI Inaccuracy . . . . .	129
4.9	Performance and Time Response Evaluation of Centralized, Semi-Decentralized, and Decentralized Fault Accommodation Based on Non-Cooperative Dynamic Game, 40% LOE Fault with 7% FDI Inaccuracy . . . . .	132

4.10	Performance and Time Response Evaluation of Semi-Decentralized Fault Accommodation Based on Non-Cooperative Dynamic Game under Various FDI Time Delays, 40% LOE Fault with 7% FDI Inaccuracy . . .	135
4.11	Performance and Time Response Evaluation of Centralized, Semi-Decentralized, and Decentralized Fault Accommodation Based on Non-Cooperative Dynamic Game, 40% LOE Fault with 7% FDI Inaccuracy in AUVs #2 and #4 . . . . .	138
4.12	Performance and Time Response Evaluation of Centralized, Semi-Decentralized, and Decentralized Fault Accommodation Based on Non-Cooperative Dynamic Game, Different LOE Faults in AUVs #2, #4, and #5 . .	139
4.13	Performance and Time Response Evaluation of Centralized Fault Accommodation Based on Non-Cooperative and Cooperative Dynamic Game, Different LOE Faults in AUVs #2, #4, and #5 . . . . .	143
4.14	Summary of Performance and Time Response Characteristics of Centralized, Semi-Decentralized, and Decentralized fault Accommodation Schemes, Fault Scenarios 1, 2, 3 . . . . .	148
4.15	Summary of Performance and Time Response Characteristics of MPC-Based and Non-Cooperative Dynamic Game-Based Semi-Decentralized fault Accommodation Schemes, Fault Scenario 4 . . . . .	149
4.16	Summary of Performance and Time Response Characteristics of Centralized and Semi-Decentralized fault Accommodation Schemes, Fault Scenario 5, Multiple Faulty Agents . . . . .	150

# Chapter 1

## Introduction

### 1.1 Motivation

The use of multiple cooperative autonomous underwater vehicles has the potential to perform difficult and complex underwater applications, namely seabed mapping, ocean sampling, oil and gas exploration and extraction, and monitoring oil and gas pipelines [4]. Multiple AUVs can outperform a single AUV by providing significant benefits such as precision, efficiency, reliability, and robustness in case of single point of failure.

The cooperation and coordination of vehicles require inter-vehicle information exchange. In underwater applications, information exchange among AUVs is typically achieved using acoustic modems which are known to be unreliable due to their limited bandwidth [5, 6]. Hence, the aforementioned issue highlights the requirement of coordinated control strategies that can achieve the desired performance while keeping the information exchange restricted to a minimum .

In addition, multiple AUVs are generally involved in high-precision and costly missions that call for reliability considerations. Physical restrictions and anomalies in

each individual member such as actuator saturation and faults are considered as reliability issues that can cause severe performance deterioration and system instability, resulting in the loss of one or more vehicles and mission failure. Therefore, effective control algorithms and accommodation strategies that consider physical restrictions and actuator faults play a crucial role in accomplishing strict high-precision missions.

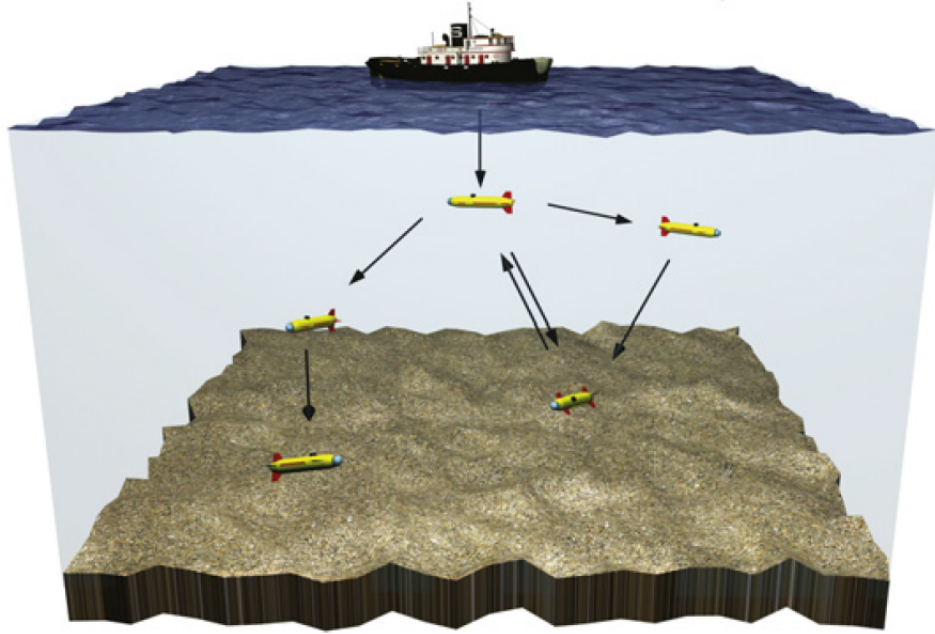


**Figure 1.1:** Formation of AUVs working underwater [1]

Tackling the above-mentioned issues and limitations in motion coordination and formation of multiple AUVs provide motivation for this thesis to address and develop suitable control and accommodation strategies to achieve cooperative objectives while maintaining acceptable level of formation performance and precision.

## 1.2 Literature Review

Formation control has been one of the most important research topics that covers a wide variety of applications in cooperative control of multi-agent systems with the hope of achieving better performance over the control of a single agent. The formation

control is referred to as the ability of agents to coordinately form and maintain the position and orientation relative to each other or relative to a reference according to a desired geometrical configuration [7, 8].

The following subsections will review specifications for formation control of multi-agent systems, namely, control structures, coordination methods, and the control design methodologies.

### 1.2.1 Control Structures

Formation control challenges mainly arise in the development of control schemes where agents need to coordinately achieve their objectives considering their limited sensing, physical, and computational capabilities. According to the admissible level of information exchange, the control structures for formation and coordination of multi-agent systems can be categorized into

- **Centralized** : In the centralized control design scheme, control actions are determined based on the information of all agents and the entire team objectives. From the implementation perspective, the central unit receives the information of all agents, processes this information, and then sends back the corresponding control actions to be implemented by the individual agents. Although this strategy can achieve a globally optimal solution, it has the problem of computational complexity, stringent communication requirements, and reliability issues in the case of failure in the central unit [9, 10, 11, 12, 13].
- **Decentralized** : In the decentralized control design scheme, depends on the degree of decentralization, local control input of each agent is designed and implemented independently. In this control design scheme, the state information of each agent and its neighbors are incorporated. This scheme is less affected by communication and computation limitations and has the benefit of scalability

and robustness to the loss of individual agents. The difficulty with decentralized scheme is that local controller design requires more challenges in order to achieve cooperative behavior [14, 15, 16, 17, 18, 19, 20]. Moreover, the reduced amount of available information to each agent, as well as neglecting the coupling effects due to neighboring agents control inputs, may result in a degraded or even poor achievable performance.

- **Semi-Decentralized** : In the semi-decentralized scheme proposed in [21], local optimization problem constrained by each individual local dynamics is considered to derive control inputs of individual agents. This scheme surpasses its decentralized counterpart by introducing the notion of interaction terms in each individual control law. Therefore, the local controllers are not fully decentralized in the conventional sense due to considering the coupling effects among neighboring agents.
- **Distributed** : The distributed control scheme is viewed as a middle ground between centralized and decentralized control structures. In this control structure, cooperative control laws are designed based on common objectives among neighboring agents. Therefore, state information, as well as control actions of neighboring agents, are involved in the process of distributed control design of each individual [22, 23, 24].

### 1.2.2 Coordination Methods

Existing coordination methods mainly fall into three categories, namely, leader-follower, virtual structure, and behavior-based [25].

- **Leader-Follower** : In this structure, one or more agents are considered as leaders to pursue a global objective while others act as followers to track transformed coordinates of the leaders with some predefined offsets. The positive point of this structure is that the formation problem can be easily considered as regulation and tracking problem. However, this structure depends heavily on the leader. Moreover, the lack of explicit feedback from the followers to the leader leads to poor disturbance rejection and fault tolerance properties. This structure is mainly formulated and solved as two feedback controller schemes, namely, separation-bearing and separation-separation [26]. Classical control approaches can be suitably employed to achieve formation objectives in leader-follower architecture [27, 3, 28, 29].
- **Virtual Structure** : In this structure, the entire formation is treated as a single entity that tracks the desired trajectories specified by translation of the desired trajectory of a virtual center. The main advantage of this structure is that the rigid geometrical shape of the formation can be maintained very well during the maneuvers; however, it shows limitations while formation shape needs to be reconfigured [30, 31, 32, 33].
- **Behavior-Based** : In this structure, control strategies are derived based on a set of desired behaviors for each member of the team such as trajectory tracking, formation keeping, and collision avoidance [34]. Generally, the desired behaviors are interpreted via potential functions [35]. The positive feature of this structure is that the feedback controller explicitly depends on the distances among neighboring agents; however due to the difficulty in the mathematical analysis of this structure the convergence of the formation to a desired configuration cannot be guaranteed explicitly [36, 37].

### 1.2.3 Optimal Control of Autonomous Vehicle Formations

Optimal control design strategies have been widely used for cooperative control of multi-agent systems and more specifically formation control of autonomous vehicles, in which the aim is to derive stabilizing control laws for each agent such that a given performance index is minimized.

Due to the limitation imposed by information exchange topology, considering a centralized optimal control problem where agents know the state of all the other agents is not applicable. In addition, solving a centralized optimal control problem is not computationally tractable. Therefore, it is essential to design locally optimal controllers where each agent minimizes its own cost. Toward this goal, different optimal control design methodologies have been proposed to attain a performance comparable to globally optimal solution of centralized controller design [38, 39, 40, 41, 42, 24].

Authors in reference [38], set up the linear quadratic regulator (LQR) problem for the control of a network of autonomous agents with a given information flow topology. Since deriving optimal controllers with a prescribed structure is a difficult task, a sub-optimal LQR controller is proposed which is computationally more tractable. Moreover, it is shown that the sub-optimal controller with centralized architecture will result in the lowest cost value whereas the decentralized architecture will increase the resulting cost value. In reference [39], a distributed LQR design for identical dynamically coupled systems is presented. In this work, special properties of the local LQR problem is derived, which enable the construction of stabilizing distributed controllers independently of the choice of local weighting matrices. Authors in [41], design a consensus protocol for a network of multi-agent system based on the linear matrix inequality (LMI) formulation of optimal control problem with a global cost. Moreover, through the proposed formulation of the consensus problem, the partial

information availability is taken into account as an additional LMI constraint. In [42], authors provide a sufficient condition on the graph topology to guarantee the existence of distributed control laws which solve a global optimal LQR control problem.

The above-mentioned references mainly aim to derive optimal structured control laws based on the structure of information exchange topology in an offline manner. Therefore, any controller redesign demands for availability of centralized information to all agents.

In addition to aforementioned approaches, another optimal control technique that has been widely used in the cooperative control of multi-agent systems is model predictive control. In this strategy, the finite time optimal control problem is formulated as quadratic programming (QP) optimization problem with the sequence of future control inputs as its optimization variable. Then, the optimal control input is computed and applied in real-time at each sampling interval [43, 44]. The key advantage of MPC over other control strategies is its ability to explicitly handle system constraints whilst optimizing a performance criterion. Moreover, real-time implementation of MPC can reflect changes in the system model and environment.

Previous work on MPC based formation control are reported in [45, 46, 47, 48, 49, 50, 51].

In [52, 53], first centralized MPC algorithm is developed to solve formation control problem in which the objective of individual agents are added together to form a common formation objective. In order to solve the optimization problem, it is assumed that the initial condition and perfect knowledge of dynamics of all agents are available to each agent. To avoid high computation and communication requirements, distributed implementation of MPC is then proposed in which each agent is designated to solve its own optimal control problem. The cooperation of neighboring

agents is incorporated as coupling terms in the individual cost function. The distinctive point in this work is that agents do not view one another as bounded contracting disturbances. To ensure the stability, the notion of compatibility constraints is introduced to guarantee that actual and planned state trajectories of each agent are not too far from one another.

In [47], authors propose a decentralized receding horizon control (RHC) algorithm for dynamically decoupled agents with common local objectives and constraints. In this scheme, agents locally solve optimization-based control problem for both their own control input and the control inputs of neighboring agents based on local state information. They also formulate local stability tests and show that increasing information update rate is needed as each agent converges to its equilibrium. Therefore, such algorithm leads to increase in computation time and decrease in the level of decentralization. It is worth noting that authors apply their algorithm to formation flight with some practical modifications [54, 55]. In their work, emergency controllers based on invariant sets and protection zones are designed to guarantee collision avoidance when the feasibility of the optimization problem is lost.

In [48], the cooperative control problem of a team of autonomous vehicles is developed based on a completely decentralized receding horizon control algorithm. Each agent evolves in discrete-time by means of a locally computed control laws. The stabilizing control laws depend on the local state variables (feedback action) and on delayed information gathered from neighboring agents (feed-forward action) which is treated as being fixed.

In [56, 49], decentralized and distributed robust model predictive controllers are proposed for the team of unmanned aerial vehicles (UAVs). The problem is to generate a local plan over a short horizon while guaranteeing the robust constraint satisfaction. In this work, all UAVs have to reach their goals in minimum time while maintaining

minimum distances from neighbors. It is shown that the implementation of proposed architecture results in significant computational improvement as compared to its centralized counterpart.

In the context of autonomous underwater vehicles, the MPC technique is applied to achieve collision free triangular formations in [57, 50, 51]. The decentralized model predictive controller is developed based on the geometry of leader-follower formation in which the tracking error prediction model is developed for each follower based on the relative distance to its corresponding leader.

#### **1.2.4 Game Theoretic Approach to Autonomous Vehicle Formations**

Game theory is a mathematical framework that has its origin in economics by the pioneering works presented in [58] and [59], which then has been widely applied to other areas of applications. Game theory is basically utilized to characterize the resulting behavior of multiple decision makers whose outcomes are functions of not only their own actions but also depends on the actions of others.

Multi-agent systems can be formulated as the dynamic game problem. In brief, dynamic game is called cooperative if agents jointly collaborate to improve their cost functions. Hence, a single cost function which is the weighted sum of all individual costs should be minimized. The solution to this type of game is called Pareto optimal solution. On the contrary, the non-cooperative game framework outlines a type of game where each agent minimizes its own cost independently while considering the actions of others. The resulting solution is called Nash equilibrium. This solution implies that unilateral deviation of each agent from its action will lead to worse value of its cost function [60]. In figure 1.2, the classification of dynamic game theory is given.

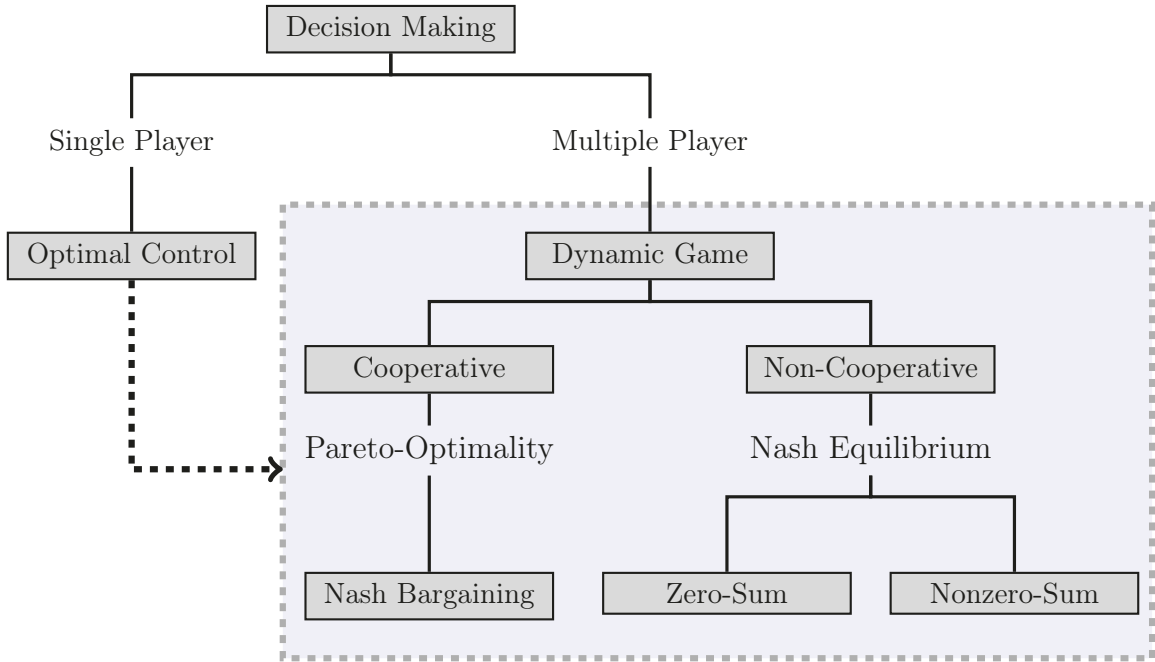


**Figure 1.2:** Classification of Games

In the literature, dynamic game theory is considered in [61, 62, 63, 64, 65, 66, 67] for formation control and consensus seeking.

In [61], cooperative game theory is utilized for consensus seeking problem to ensure a lower individual as well as team cost value. In this work, minimization of a unique team cost is formulated as an LMI problem in order to add constraints due to the consensus condition and the information structure. The solution to this minimization problem is a set of Pareto optimal solutions. In order to choose the best solution, Nash bargaining strategy is employed to maximize the difference between the cost obtained through cooperative approach and semi-decentralized optimal control approach.

In [62], authors formulate formation control problem as a finite horizon open-loop Nash differential game. The corresponding Nash equilibrium is derived as the solution to a set of coupled Riccati differential equations. The resulting control law can be implemented in a distributed fashion through the selection of weighting matrices

which only relate each agent to its neighbors. This work is then extended to time-varying formations in [64].

In [63], formation control problem for a team of UAVs is considered where each agent has its own performance index in terms of terminal formation errors and control efforts. The problem is formulated as a differential game problem. As the control structure of each agent should conform to information graph, a distributed state estimation algorithm is combined with the classical open-loop Nash differential game to construct distributed controllers.

Reference [65], integrates cooperative control, reinforcement learning, and dynamic game theory to find online solution of team games while considering information graph topology. The notion of interactive Nash equilibrium along with cooperative policy iteration algorithm is proposed. It is shown that the algorithm converges to the best response when the neighbors of each agent do not update their policies, and to the cooperative Nash equilibrium when all agents update their policies simultaneously.

### **1.2.5 Fault Tolerant Control Strategies for Formation of Autonomous Vehicles**

Developing fault tolerant multi-agent systems is crucial for the sake of safety and reliability considerations since malfunctioning of any agent may cause reduction in efficiency and even overall mission failure. Therefore, individual controllers need to be equipped with a proper fault tolerant mechanism to maintain acceptable performance in terms of achieving mission objectives, reduce cost, and ensure stability of the whole team.

In general, fault tolerant control (FTC) design approaches can be categorized as passive method and active method [68, 69]. In passive FTC systems, a robust fixed

structure controller is designed which is able to deal with anticipated faults. This approach is attractive from computational point of view. However, decreased nominal performance at the expense of robustness to restricted class of faults is the downside of this method [70, 71]. On the other hand, active FTC systems utilize on-line information from FDI module to compensate for the effect of faults. This can be done either by selection of predefined controllers or by controller redesign [72, 73, 74, 75, 76]. The performance of active methods are superior to passive methods. However, integration of fault detection and isolation (FDI) module and FTC mechanism can arise challenging issues due to probable imperfections in fault estimates. Therefore, FTC mechanism should be able to guarantee acceptable post-fault system performance while considering uncertainties and time delays in FDI information [77].

Based on classical FTC design approaches, previous work on fault tolerant multi-agent systems are reported in [78, 79, 80, 81, 82, 83, 84, 85, 86, 87, 88].

In [79], two adaptive fault tolerant control laws, namely sliding mode controller and non-singular terminal sliding mode controller are developed for satellite formation flying to achieve high precision formation in the presence of actuator and sensor faults. Then, the control methodology is improved in [89] by introducing fast terminal sliding mode as an FTC strategy for distributed cooperative attitude synchronization. A fuzzy logic system is utilized as an uncertainty estimator to update controller parameters in case of actuator faults. In [86], distributed controller for multi-robot systems is derived based on dynamic surface control technique to handle LOE faults. In addition, adaptive mechanism is applied to estimate effectiveness factor and uncertainty bounds. It is worth noting that aforementioned methods, suffer from chattering phenomenon due to the adoption of sign function.

Authors in [78], investigate the effect of various actuator fault types on the performance of modified leader-follower architecture. It is shown that stability and consensus achievement are maintained under faulty situation. However, the transient behavior of the team is deteriorated.

In reference [87], distributed reconfigurable controller is designed on-line to guarantee consensus achievement with minimum cost in the presence of actuator faults and FDI uncertainty. The reconfiguration scheme is formulated such that only the faulty agent needs to reconfigure its control law. In this regard, sufficient conditions are derived as a set of linear matrix inequalities for existence of a reconfigurable controller. Moreover, a metric is defined to have a measure of FDI information accuracy.

In [81], a fault tolerant linear cooperative protocol is developed for target aggregation problem. The fault tolerant algorithm is proposed to adjust the weights associated with shortest path from active agents who have access to target point and faulty individuals. The proposed algorithm ensures that sufficient conditions are satisfied and the target point still can be reached.

In [82], a two-level fault recovery scheme is suggested for satellites formation flying. In the low level recovery mechanism, asymptomatic closed loop stability is ensured. However, in case that fault estimates are biased, faulty satellites are partially recovered, and therefore formation tracking errors are deteriorated. As a remedy, formation level mechanism is formulated as an optimization problem to reduce tracking error bound. Therefore, other satellites compensate for the effect of partially recovered agent by allocating more control efforts.

In [83], virtual actuator technique is suggested to compensate the effect of actuator faults in individual agents for consensus tracking control problem. Moreover, sliding mode observer is designed for estimating the faults. The effect of estimation error is studied, and sufficient condition for bounded tracking error of all followers in terms of

the estimation error is derived. It is worth noting that the tracking errors of healthy individuals converge to zero, and tracking errors of faulty agents remain bounded only once accurate fault estimates are available.

In [84], decentralized fault tolerant formation controller is developed for UAVs in leader-follower structure in which the FTC mechanism is only needed for faulty agent rather than the entire team. As actuator faults occur, a compensation term is added to nominal controller to remove the effect of such permanent faults. Moreover, The effect of intermittent faults is discussed using switch system approach. It is shown that system stability can be maintained under certain condition without the requirement of any FTC mechanism. It should be noted that this scheme requires highly efficient FDI mechanism to rapidly detect intermittent faults.

### 1.3 Thesis Objectives and Contributions

In this thesis, formation control and fault accommodation of a team of autonomous underwater vehicles are addressed based on the MPC technique and dynamic game theory. Our first goal is to consider the problem of limited information availability in underwater applications. In the first part, a semi-decentralized control scheme is developed to solve the tracking and formation keeping control problems with minimum communication requirement. Moreover, centralized and decentralized control schemes are developed to have a comparative evaluation for the performance of our proposed semi-decentralized control scheme. Since underwater vehicle actuators are very prone to malfunctioning, our second goal is to ensure mission objectives in the presence of such anomalies. In the second part, a semi-decentralized active fault recovery scheme is developed to maintain acceptable tracking and formation keeping performance of the entire team in the presence of actuator fault. Moreover, centralized and decentralized active fault recovery schemes are developed to have a comparative evaluation

for the performance of our proposed semi-decentralized fault recovery scheme.

In the following the main contributions of this thesis are summarized:

1. A semi-decentralized MPC-based control scheme is developed to solve the tracking and formation keeping control problems of a team of autonomous underwater vehicles with reduced amount of computational complexity and communication requirements.
2. A semi-decentralized dynamic game-based control scheme is proposed to solve the tracking and formation keeping control problems of a team of autonomous underwater vehicles with reduced amount of communication requirement.
3. A semi-decentralized MPC-based active fault accommodation scheme is developed to maintain a graceful degraded performance of a team of autonomous underwater vehicles in the presence of LOE actuator faults and actuator saturation constraints.
4. A semi-decentralized dynamic-game based active fault accommodation scheme is developed to maintain a graceful degraded performance of a team of autonomous underwater vehicles in the presence of LOE actuator faults.
5. The performance and effectiveness of semi-decentralized active fault accommodation schemes based on the MPC technique and dynamic game theory are validated through various fault scenarios such as the presence of FDI imperfections and multiple faulty agents.
6. The centralized and decentralized active fault accommodation schemes based on the MPC technique and dynamic game theory are developed and compared with the corresponding proposed semi-decentralized active fault accommodation

schemes through quantitative simulation studies, and the improvements and limitations are illustrated.

## 1.4 Organization of The Thesis

The organization of this thesis is explained briefly as follows.

In Chapter 2, preliminaries and background information are provided. First, a brief description on nonlinear dynamical model of the AUV using Euler angles along with the environmental disturbances which affect the AUV dynamics are presented. Then, linear model of an AUV is derived. In the next section, a general description on model predictive control framework and dynamic game theory is stated. Finally, some concepts and ingredients of formation graph modeling are explained.

In Chapter 3, MPC technique and dynamic game theory are utilized to solve the problem of tracking and formation keeping of a team of autonomous agents under three schemes, namely centralized, semi-decentralized, and decentralized control schemes. At the end of the chapter, a set of comparative simulation studies are conducted on a team of AUVs, and then the performance of proposed control strategies are interpreted and discussed quantitatively.

In Chapter 4, active fault recovery strategies based on the MPC technique and dynamic game theory are developed for all aforementioned control schemes introduced in Chapter 3. At the end of the chapter, comparative simulations of various faulty scenarios are performed on a team of AUVs to investigate the performance and effectiveness of proposed active fault recovery strategies in the presence of LOE actuator faults.

In Chapter 5, concluding remarks and recommendations for future work are provided.

# Chapter 2

## Background, Preliminaries and Definitions

### 2.1 Introduction

In this chapter, background information required for the derivation of the nonlinear and linearized model of autonomous underwater vehicles is provided. Moreover, dominant source of environmental disturbances is explained and modeled. Afterward, basic concepts of faults and the model of the faulty system with loss of effectiveness (LOE) actuator faults are provided. In the next sections, model predictive control and dynamic game theory are briefly explained. Finally, some basic definitions and concepts in graph theory which are used for formation modeling are given.

### 2.2 AUV Equations of Motion

The representation of translational and rotational motion of the AUV in six degrees of freedom (DOF) depends on the choice of coordinate frames. In the following sections, the coordinate frames and attitude representation technique which are commonly used

in underwater applications are presented.

### 2.2.1 Coordinate Frames

There are two coordinate frames that are commonly used to precisely describe the equations of motion of an underwater vehicle in six degrees of freedom. These two coordinate systems are specified as

- Earth-fixed coordinate frame,  $\{E\} := (O_E, X_E, Y_E, Z_E)$
- Body-fixed coordinate frame,  $\{B\} := (O_B, X_B, Y_B, Z_B)$

The earth-fixed frame  $\{E\}$  is composed of the orthonormal axes  $\{X_E, Y_E, Z_E\}$ , where the  $X$ -axis points to the north, the  $Y$ -axis to the east and the  $Z$ -axis to the center of the earth. The body-fixed frame with orthonormal axes  $\{X_B, Y_B, Z_B\}$  is coupled to the vehicle, where the  $X$ -axis points to the forward direction, the  $Y$ -axis to the right of the vehicle and the  $Z$ -axis vertically down. The origin  $O_B$  of the body-fixed frame is chosen to coincide with the center of gravity of the vehicle. The directions of coordinate frames are indicated in Figure 2.1 where the degrees of freedom of the  $\{B\}$  are named surge, sway, heave, roll, pitch and yaw.

The common notation used for marine vehicles according to the SNAME notation [90] is used to demonstrate the 6 DOF motion of vehicle in vector form by the following

- $\eta = [\eta_1^T, \eta_2^T]^T$  where  $\eta_1 = [p_x, p_y, p_z]^T$ , and  $\eta_2 = [p_\varphi, p_\theta, p_\psi]^T$  denote the position and orientation of  $\{B\}$  expressed in  $\{E\}$ , respectively.
- $\nu = [\nu_1^T, \nu_2^T]^T$  where  $\nu_1 = [v_u, v_v, v_w]^T$ , and  $\nu_2 = [v_p, v_q, v_r]^T$  denote the linear velocities and angular velocities of the vehicle expressed in  $\{B\}$ , respectively.
- $\tau = [\tau_1^T, \tau_2^T]^T$  where  $\tau_1 = [X, Y, Z]^T$ , and  $\tau_2 = [K, M, N]^T$  denote the total forces and moments acting on the vehicle expressed in  $\{B\}$ , respectively.

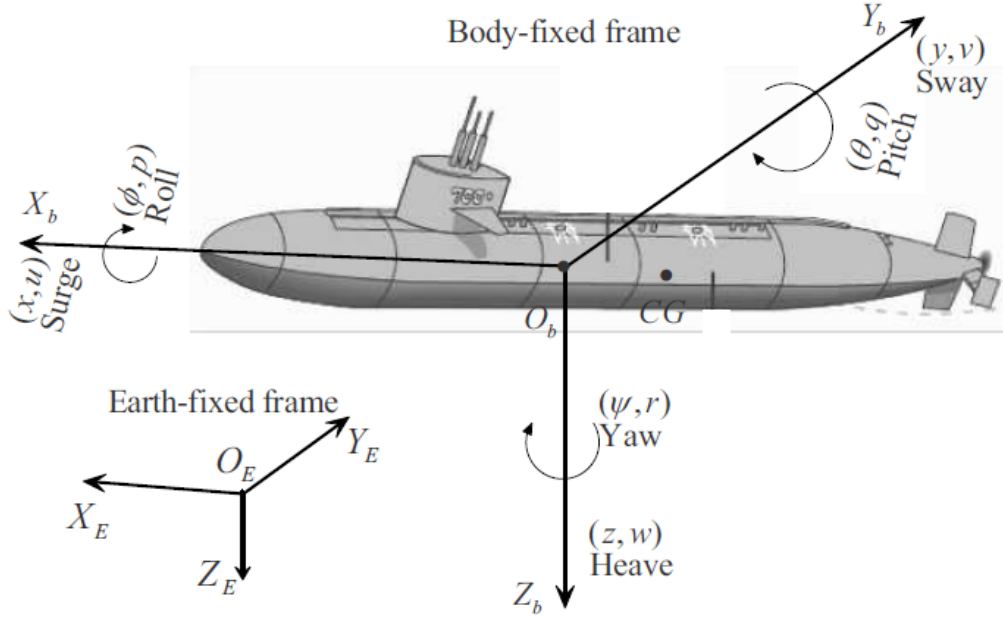


**Figure 2.1:** Coordinate frames and AUV motion variables [2]

### 2.2.2 Attitude Representation by Euler Angles

The orientation of a rigid body in three dimensional space can be represented either by using Euler angles or quaternions (Euler Parameters). In this thesis, as it is common in the marine terminology, we use Euler angles for AUV attitude representation. However, there exist several control strategies that use the quaternion in order to avoid the representation singularities that might arise by the use of Euler angles. In Euler angles representation, a set of sequential coordinate transformations is performed to relate the body-fixed frame to the earth-fixed frame in terms of orientation. The Euler convention used to describe the orientation from body to world is the  $Z$ - $Y$ - $X$  convention that corresponds to the rotation angles of yaw ( $p_\psi$ ), pitch ( $p_\theta$ ), and roll ( $p_\phi$ ), respectively. The rotation matrix used to describe the orientation of the body-fixed frame with respect to the earth-fixed frame is given by

$$R_B^E(\eta_2) = R_z(p_\psi)R_y(p_\theta)R_x(p_\phi) \quad (2.1a)$$

$$R_B^E(\eta_2)^{-1} = R_E^B(\eta_2) \quad (2.1b)$$

where

$$R_x(p_\varphi) = \begin{bmatrix} 1 & 0 & 0 \\ 0 & \cos(p_\varphi) & -\sin(p_\varphi) \\ 0 & \sin(p_\varphi) & \cos(p_\varphi) \end{bmatrix} \quad (2.2a)$$

$$R_y(p_\theta) = \begin{bmatrix} \cos(p_\theta) & 0 & \sin(p_\theta) \\ 0 & 1 & 0 \\ -\sin(p_\theta) & 0 & \cos(p_\theta) \end{bmatrix} \quad (2.2b)$$

$$R_z(p_\psi) = \begin{bmatrix} \cos(p_\psi) & -\sin(p_\psi) & 0 \\ \sin(p_\psi) & \cos(p_\psi) & 0 \\ 0 & 0 & 1 \end{bmatrix} \quad (2.2c)$$

The coordinate transformation matrix that relates body-fixed angular velocity with roll, pitch, and yaw rates can be written as

$$T_B^E(\eta_2) = \begin{bmatrix} 1 & \sin(p_\varphi)\tan(p_\theta) & \cos(p_\varphi)\tan(p_\theta) \\ 0 & \cos(p_\varphi) & -\sin(p_\varphi) \\ 0 & \sin(p_\varphi)/\cos(p_\theta) & \cos(p_\varphi)/\cos(p_\theta) \end{bmatrix} \quad (2.3a)$$

$$T_B^E(\eta_2)^{-1} = T_E^B(\eta_2) \quad (2.3b)$$

The consequence of using Euler angles to describe the vehicle's motion is that  $T_B^E(\eta_2)$  can not be defined for a pitch angle  $p_\theta = \pm\pi/2$ . However, due to physical restrictions, the AUV will always operate far from the singular point.

### 2.2.3 AUV Nonlinear Kinematic and Dynamic Equations of Motion

Based on the notations and coordinate transformation introduced in previous sections, we are ready to introduce equations of motion of a single AUV. It is convenient to collect the kinematic equations of AUV relative to the earth-fixed frame into the

following compact 6-dimensional matrix form

$$\dot{\eta} = J(\eta)\nu \iff \begin{bmatrix} \dot{\eta}_1 \\ \dot{\eta}_2 \end{bmatrix} = \begin{bmatrix} R_B^E(\eta_2) & 0 \\ 0 & T_B^E(\eta_2) \end{bmatrix} \begin{bmatrix} \nu_1 \\ \nu_2 \end{bmatrix} \quad (2.4)$$

The overall 6 DOF nonlinear dynamics of an AUV in body-fixed frame can be derived based on Newton-Euler equation of a rigid body in fluid according to the following compact form

$$M\dot{\nu} + C(\nu)\nu + D(\nu)\nu + g(\eta) = \tau \quad (2.5)$$

where

$$M = M_{RB} + M_A \quad (2.6a)$$

$$C(\nu) = C_{RB}(\nu) + C_A(\nu) \quad (2.6b)$$

$$D(\nu) = D(\nu)_l + D(\nu)_q \quad (2.6c)$$

In equation (2.5),  $M$  denotes the total mass and inertia matrix consists of rigid body mass  $M_{RB}$  and added mass  $M_A$  terms;  $C(\nu)$  is the total Coriolis and centripetal matrix consists of a rigid body mass  $C_{RB}(\nu)$  and added mass  $C_A(\nu)$  terms;  $D(\nu)$  is the quadratic and linear drag matrix;  $g(\eta)$  is the gravitational and buoyancy matrix; and  $\tau$  is the vector of thruster forces and torques.

## 2.2.4 AUV Nonlinear Equations of Motion in Horizontal Plane

In this thesis, the motion of AUV in the horizontal plane is considered which covers wide range of underwater missions, namely, seabed surveying, mapping, and reconnaissance. It is worth mentioning that the AUV is symmetric in all planes and the

origin of the body-fixed frame  $O_B$ , the center of gravity  $C_G$ , and the center of buoyancy  $C_B$  of the AUV coincide with each other, i.e.  $O_B = C_G = C_B = [0 \ 0 \ 0]$ , then the kinematics and dynamics equations of motion in the surge, sway, and yaw degrees of freedom can be defined as

$$\dot{p}_x = v_u \cos(p_\psi) - v_v \sin(p_\psi) \quad (2.7a)$$

$$\dot{p}_y = v_u \sin(p_\psi) + v_v \cos(p_\psi) \quad (2.7b)$$

$$\dot{p}_\psi = v_r \quad (2.7c)$$

$$m_u \dot{v}_u - m_v v_v v_r + d_u v_u = \tau_u \quad (2.7d)$$

$$m_v \dot{v}_v + m_u v_u v_r + d_v v_v = \tau_v \quad (2.7e)$$

$$m_r \dot{v}_r + (m_v - m_u) v_u v_v + d_r v_r = \tau_r \quad (2.7f)$$

which can be rewritten into the following compact matrix form

$$M\dot{\nu} + C(\nu)\nu + D\nu = \tau \quad (2.8a)$$

$$\dot{\eta} = J(p_\psi)\nu \quad (2.8b)$$

where  $\nu = [v_u \ v_v \ v_r]^T$  and  $\eta = [p_x \ p_y \ p_\psi]^T$  are the vectors of linear and angular velocities, and absolute positions and orientation in the earth-fixed frame.

The transformation matrix  $J(p_\psi)$  from  $\{B\}$  to  $\{E\}$  for the reduced order 3 DOF model in equation (2.8b) can be written as

$$J(p_\psi) = \begin{bmatrix} \cos(p_\psi) & -\sin(p_\psi) & 0 \\ \sin(p_\psi) & \cos(p_\psi) & 0 \\ 0 & 0 & 1 \end{bmatrix} \quad (2.9)$$

The diagonal matrix

$$M = \begin{bmatrix} m_u & 0 & 0 \\ 0 & m_v & 0 \\ 0 & 0 & m_r \end{bmatrix} \quad (2.10)$$

is the total inertia matrix due to rigid body mass and added mass with  $m_u$ ,  $m_v$ ,  $m_r$  as the total mass and inertia constant parameters along  $X$ ,  $Y$ , and about  $Z$  axes, respectively.

The diagonal matrix

$$D = \begin{bmatrix} d_u & 0 & 0 \\ 0 & d_v & 0 \\ 0 & 0 & d_r \end{bmatrix} \quad (2.11)$$

denotes the total linear and quadratic drag with  $d_u$ ,  $d_v$ ,  $d_r$  as its constant parameters along  $X$ ,  $Y$ , and about  $Z$  axes, respectively.

The skew-symmetric matrix  $C(\nu)$  is the coriolis and centripetal matrix that can be shown as

$$C(\nu) = \begin{bmatrix} 0 & 0 & -m_v v_v \\ 0 & 0 & m_u v_u \\ m_v v_v & -m_u v_u & 0 \end{bmatrix} \quad (2.12)$$

The vector

$$\tau = \begin{bmatrix} \tau_u \\ \tau_v \\ \tau_r \end{bmatrix} \quad (2.13)$$

is the control input with  $\tau_u$ ,  $\tau_v$ , and  $\tau_r$  as the total forces and torques produced by the actuators in surge, sway, and yaw directions, respectively.

The parameters of a simplified AUV model are defined as  $m_u = m - X_{\dot{u}}$ ,  $m_v =$

$$m - Y_{\dot{v}}, m_r = I_z - N_{\dot{r}}, d_u = -X_u - X_{u|u}|v_u|, d_v = -Y_v - Y_{v|v}|v_v|, d_r = -N_r - N_{r|r}|v_r|.$$

The detailed description on model parameters is illustrated as in table 2.1.

**Table 2.1:** Nomenclature for AUV Parameters

Name	Description	Unit
$m$	Weight of the AUV	$kg$
$I_z$	Moment of inertia in yaw	$kg\ m^2$
$X_{\dot{u}}$	Added mass in surge	$kg$
$X_u$	Linear damping coefficient in surge	$kg/s$
$X_{u u }$	Quadratic damping coefficient in surge	$kg/m$
$Y_{\dot{v}}$	Added mass in sway	$kg$
$Y_v$	Linear damping coefficient in sway	$kg/s$
$Y_{v v }$	Quadratic damping coefficient in sway	$kg/m$
$N_{\dot{r}}$	Added mass in yaw	$kg\ m^2$
$N_r$	Linear damping coefficient in yaw	$kg\ m/s$
$N_{r r }$	Quadratic damping coefficient in yaw	$kg\ m$

### 2.2.5 Modeling Environmental Disturbances

Different types of environmental disturbances can be considered to act on an AUV including wind, waves, and currents. In the case of fully submerged AUV, the main environmental disturbance is due to ocean currents. Ocean currents are horizontal and vertical circulating systems of ocean water, produced by gravity, wind friction and water density variation in different parts of the ocean [91], [92].

In the literature, there are generally two ways to consider the effect of ocean current in the dynamical model of AUV. Readers are referred to [93] for more information on the existing methods and their applications.

• **Method 1**

In this method, the nonlinear dynamical model of AUV introduced in equation (2.8a) is rewritten in terms of relative velocity. In this regard, the earth-fixed current velocity is modeled as a Gauss-Markov process with a limiter as follows

$$\dot{V}_c(t) + \mu_c V_c(t) = \omega_c \quad (2.14a)$$

$$V_{c_{min}} \leq V_c(t) \leq V_{c_{max}}$$

where  $\omega_c(t)$  is a zero mean Gaussian white noise and  $\mu_c > 0$  is a constant that is mostly considered to be zero. Assuming that the fluid is irrotational, the projected current velocity vector in the earth-fixed reference frame is given by

$$\nu_c^E = [V_{cx} \ V_{cy} \ 0]^T \quad (2.15)$$

where  $V_c = \sqrt{V_{cx}^2 + V_{cy}^2}$ ,  $V_{cx} = V_c \cos(\alpha)$ , and  $V_{cy} = V_c \sin(\alpha)$ , and the angle  $\alpha$  describes the orientation of the  $V_c$  about the  $Z$ -axis. Then, the body-fixed current velocity can be computed by the transposed Euler angle rotation matrix given in equation (2.9):

$$\nu_c^B = J(p_\psi)^{-1} \nu_c^E \quad (2.16)$$

$$\nu_c^B = [v_{uc}^B \ v_{vc}^B \ 0]^T \quad (2.17)$$

where  $v_{uc}^B$  and  $v_{vc}^B$  denote the current velocity in surge and sway, respectively. This results in the body-fixed frame relative velocity  $\nu_r = [v_u - v_{uc}^B \ v_v - v_{vc}^B \ v_r]^T$ . Then, the dynamical model of AUV with relative velocity  $\nu_r$  must be modified to

$$M\dot{\nu}_r + C(\nu_r)\nu_r + D\nu_r = \tau \quad (2.18a)$$

$$\dot{\eta} = J(p_\psi)\nu = J(p_\psi)\nu_r + \nu_c^E \quad (2.18b)$$

This model is introduced in [90] and is further used in references [94] and [95].

- **Method 2**

In this method, the effect of ocean currents are all considered as drift forces acting at the force level on the AUV as follows

$$M\dot{\nu} + C(\nu)\nu + D\nu = \tau + J(p_\psi)^{-1} d_c \quad (2.19a)$$

$$\dot{\eta} = J(p_\psi)\nu \quad (2.19b)$$

where the current loads  $d_c = [d_{cx} \ d_{cy} \ 0]^T$  are usually defined in the earth-fixed frame and are modeled as a constant or slowly varying bias as

$$\dot{d}_c = w_d \quad (2.20)$$

where  $w_d$  is a vector of zero mean Gaussian white noise processes.

This model is usually utilized as a basis for derivation of model-based controllers for path following and tracking of AUVs [92, 96, 97]. In this thesis, we resort to this method and consider the effect of ocean currents through the input channels of AUVs in the simulation studies.

## 2.2.6 Linearized Equations of Motion

The nonlinear reduced order equations of motion introduced in Subsection 2.2.4 without considering the effect of disturbance and noise can be described by the following

continuous-time nonlinear state space model

$$\dot{\bar{x}}(t) = f(\bar{x}(t), \bar{u}(t)) \quad (2.21a)$$

$$\bar{z}(t) = g(\bar{x}(t)) \quad (2.21b)$$

where  $\bar{x} = [p_x \ p_y \ p_\psi \ v_u \ v_v \ v_r]^T \in \mathbb{R}^6$  is the state vector,  $\bar{u} = [\tau_u \ \tau_v \ \tau_r]^T \in \mathbb{R}^3$  is the vector of control inputs generated by actuators along surge, sway, and yaw axes, respectively, and  $\bar{z} = [p_x \ p_y \ p_\psi]^T \in \mathbb{R}^3$  is the vector of position measurements.

The corresponding linear model that defines the dynamic behavior of the system can be derived based on the Taylor series expansion about any valid operating point  $(x_o, u_o)$ . The resultant linear continuous-time state space model will take the following form

$$\dot{x}(t) = A_c x(t) + B_c u(t) \quad (2.22a)$$

$$z(t) = C x(t) \quad (2.22b)$$

where  $x = \bar{x} - x_o$  and  $u = \bar{u} - u_o$  are respectively state and input error vectors around specific operating point. Moreover, the matrices  $A_c$ ,  $B_c$ , and  $C$  can be defined as follows

$$A_c = \left. \frac{\partial f}{\partial x} \right|_{(x_o, u_o)} = \begin{bmatrix} 0 & 0 & -v_{v_o} \cos(p_{\psi_o}) - v_{u_o} \sin(p_{\psi_o}) & \cos(p_{\psi_o}) & -\sin(p_{\psi_o}) & 0 \\ 0 & 0 & v_{u_o} \cos(p_{\psi_o}) - v_{v_o} \sin(p_{\psi_o}) & \sin(p_{\psi_o}) & \cos(p_{\psi_o}) & 0 \\ 0 & 0 & 0 & 0 & 0 & 1 \\ 0 & 0 & 0 & \frac{-d_u}{m_u} & \frac{m_v}{m_u} v_{r_o} & \frac{m_v}{m_u} v_{v_o} \\ 0 & 0 & 0 & \frac{-m_u}{m_v} v_{r_o} & \frac{-d_v}{m_v} & \frac{-m_u}{m_v} v_{u_o} \\ 0 & 0 & 0 & \frac{(m_u - m_v)}{m_r} v_{v_o} & \frac{(m_u - m_v)}{m_r} v_{u_o} & \frac{-d_r}{m_r} \end{bmatrix} \quad (2.23a)$$

$$B_c = \frac{\partial f}{\partial u}|_{(x_o, u_o)} = \begin{bmatrix} 0 & 0 & 0 \\ 0 & 0 & 0 \\ 0 & 0 & 0 \\ \frac{1}{m_u} & 0 & 0 \\ 0 & \frac{1}{m_v} & 0 \\ 0 & 0 & \frac{1}{m_r} \end{bmatrix} \quad (2.23b)$$

$$C = \begin{bmatrix} 1 & 0 & 0 & 0 & 0 & 0 \\ 0 & 1 & 0 & 0 & 0 & 0 \\ 0 & 0 & 1 & 0 & 0 & 0 \end{bmatrix} \quad (2.23c)$$

By discretizing linear continuous-time state space model (2.22), using zero-order-hold method, the discrete-time linear state space model over the sampling period  $T_s$  can be obtained as

$$x(k+1) = Ax(k) + Bu(k) \quad (2.24a)$$

$$z(k) = Cx(k) \quad (2.24b)$$

where  $A = e^{A_c T_s}$  and  $B = \int_0^{T_s} e^{A_c t} B_c dt$ .

## 2.3 Fault Types and Modeling

A fault is defined as an unpermitted deviation of at least one characteristic property or variable of the system from the accepted standard condition that may lead to malfunction or failure in the system [98]. Faults can be classified based on several criteria, such as the time characteristics of faults, physical locations in the system and the effect of faults on the system performance. The time dependency of faults can be distinguished as abrupt fault (stepwise), incipient fault (drift-like) or intermittent

fault. When faults are classified according to their physical locations, three main faults can be defined, namely, actuator faults, sensor faults, and plant component faults. If faults are to be classified according to their induced effects on the system performance, they can be classified into additive and multiplicative faults [99].

Since an actuator is often considered as the entrance to the system, actuator faults have serious consequences on the system performance. To incorporate the effect of actuator faults in the nominal system, multiplicative modeling is commonly used. An abrupt change of the nominal control action from  $u$  to  $u^f$  based on the severity of actuator faults ranging from loss of partial control effectiveness (stuck at a fixed value) to a complete loss of control authority can be classified as

$$u^f = \begin{cases} \Gamma u & \Gamma = 1, \forall t \geq 0 & \text{No Failure} \\ \Gamma u & 0 < \epsilon < \Gamma < 1, \forall t \geq t_f & \text{Loss of Effectiveness (LOE)} \\ \Gamma u & \Gamma = 0, \forall t \geq t_f & \text{Float} \\ \Gamma u + u^{Lock} & \Gamma = 0, \forall t \geq t_f & \text{Lock-In-Place (LIP)} \\ \Gamma u + u^{min} \text{ or } u^{max} & \Gamma = 0, \forall t \geq t_f & \text{Hard Over Failure (HOF)} \end{cases} \quad (2.25)$$

where  $u^f$  corresponds to the actual input that is produced by the faulty actuator,  $u$  is the input commanded by the controller,  $t_f$  denotes the time when a fault is injected, and  $\Gamma$  represents the effectiveness coefficient of the actuator.  $u^{min}$  and  $u^{max}$  are the minimum and maximum possible actuation, and  $u^{Lock}$  ( $u^{min} < u^{Lock} < u^{max}$ ) is a constant level of actuation.

Substituting the nominal control action  $u(k)$  in equation (2.24) with the faulty

control action  $u^f(k)$  results in the following state-space model

$$x(k+1) = Ax(k) + B\Gamma u(k) \quad (2.26a)$$

$$z(k) = Cx(k) \quad (2.26b)$$

In this thesis, we are interested in the most common actuator fault named as Loss of Effectiveness fault where the actual control input becomes a lower percent of the desired control input. The Loss of Effectiveness actuator fault can be represented by the multiplicative matrix  $\Gamma$  as

$$\Gamma = \begin{bmatrix} \gamma^1 & 0 & 0 \\ 0 & \gamma^2 & 0 \\ 0 & 0 & \gamma^3 \end{bmatrix} \quad (2.27)$$

where  $0 < \gamma^k < 1$ ,  $k = 1, \dots, 3$  indicates the effectiveness factor of the corresponding actuator forces and torque in three directions, namely, surge, sway, and yaw.

## 2.4 Model Predictive Control Framework

In general, the idea behind the predictive control strategy includes (I) A model of the plant which is used to predict the future response of the system at future time instants, (II) the calculation of a sequence of control action minimizing an optimal control problem using system's current states as the initial condition, and (III) the receding strategy which involves the application of the first control action at each step, so that the horizon moves towards the future at each instant. Practically, this combination of feed-forward and feedback makes MPC to outperform passive feedback control. Briefly, the benefits of MPC are referred to as its ability to include generic models and constraints in the optimal control problem and its reconfigurability to redefine cost functions and constraints as needed to reflect changes in the system and

environment [100, 101].

Assume that the discrete-time linear dynamical model of the system is given by

$$x(k+1) = Ax(k) + Bu(k) \quad (2.28a)$$

$$z(k) = Cx(k) \quad (2.28b)$$

where  $x(k) \in \mathbb{R}^n$ ,  $u(k) \in \mathbb{R}^m$ , and  $z(k) \in \mathbb{R}^p$  are the state, control input, and output vectors respectively. The MPC implementation can be formulated by introducing the following open-loop optimization problem at every time interval  $k$ :

$$\min_{u(\cdot)} J(u(\cdot), x(k)) \quad (2.29a)$$

subject to:

$$x(k+h+1 | k) = Ax(k+h | k) + Bu(k+h | k) \quad (2.29b)$$

$$z(k+h | k) = Cx(k+h | k) \quad (2.29c)$$

$$z_{min} < z(k+h | k) < z_{max}, \quad h = 1, \dots, N_p - 1 \quad (2.29d)$$

$$u_{min} < u(k+h | k) < u_{max}, \quad h = 1, \dots, N_m - 1 \quad (2.29e)$$

The performance index is defined as

$$\begin{aligned} J(u(\cdot), x(k)) = & \sum_{h=0}^{N_p-1} \left\{ z^T(k+h | k) Q z(k+h | k) + u^T(k+h | k) R u(k+h | k) \right\} \\ & + x^T(k+N_p | k) Q_N x(k+N_p | k) \end{aligned} \quad (2.30)$$

where  $Q \in \mathbb{R}^{p \times p}$ , and  $Q_N \in \mathbb{R}^{n \times n}$  are positive semi-definite, and  $R \in \mathbb{R}^{m \times m}$  is positive definite penalty matrices.  $N_p$  and  $N_m$  denote the length of the prediction horizon and the length of the control horizon, respectively. Usually,  $N_p \geq N_m$ . The

first term of performance index is called state penalty , the second term is called control penalty and the third term is called terminal penalty.

### 2.4.1 QP formulation of MPC

All predicted variables can be formulated in terms of current state variable information  $x(k)$  and the future control movement  $u(k+h|k)$ ,  $h = 1, \dots, N_m$  as follows

$$\mathcal{Z} = \mathcal{S}^z x(k) + \mathcal{S}^u U \quad (2.31)$$

where the predicted variables are

$$\mathcal{Z} = [z^T(k|k) \ z^T(k+1|k) \ z^T(k+2|k) \ \cdots \ z^T(k+N_p|k)]^T \quad (2.32a)$$

$$U = [u^T(k|k) \ u^T(k+1|k) \ u^T(k+2|k) \ \cdots \ u^T(k+N_c-1|k)]^T \quad (2.32b)$$

and the batched matrices  $\mathcal{S}^z$  and  $\mathcal{S}^u$  are

$$\mathcal{S}^z = \begin{bmatrix} C \\ CA \\ CA^2 \\ \vdots \\ CA^{N_p} \end{bmatrix}; \quad \mathcal{S}^u = \begin{bmatrix} 0 & 0 & 0 & \cdots & 0 \\ CB & 0 & 0 & \cdots & 0 \\ CAB & CB & 0 & \cdots & 0 \\ \vdots & \vdots & \vdots & \ddots & \vdots \\ CA^{N_p-1}B & CA^{N_p-2}B & CA^{N_p-3}B & \cdots & CA^{N_p-N_c}B \end{bmatrix} \quad (2.33)$$

Using the compact equation (2.31), the finite horizon cost function (2.30) can be written as

$$\begin{aligned} J(U, x(k)) &= \mathcal{Z}^T \bar{Q} \mathcal{Z} + U^T \bar{R} U \\ &= U^T H U + 2x(k)^T F U + x(k)^T G x(k) \end{aligned} \quad (2.34)$$

where  $\bar{Q} \triangleq \text{blkdiag}\{Q, Q, \dots, Q_N\}$ ,  $\bar{R} \triangleq \text{blkdiag}\{R, \dots, R\}$ ,  $H \triangleq \mathcal{S}^{u^T} \bar{Q} \mathcal{S}^u + \bar{R}$ ,  $F = \mathcal{S}^{z^T} \bar{Q} \mathcal{S}^u$ , and  $G = \mathcal{S}^{z^T} \bar{Q} \mathcal{S}^z$ .

Moreover, the inequality constraints of problem (2.29) that indicate the feasibility of the solution sets can be written in the following compact form

$$\begin{bmatrix} 1 \\ -1 \end{bmatrix} U \leq \begin{bmatrix} I_{N_c m \times m} u_{max} \\ -I_{N_c m \times m} u_{min} \end{bmatrix} \quad (2.35a)$$

$$\begin{bmatrix} \mathcal{S}^u \\ -\mathcal{S}^u \end{bmatrix} U \leq \begin{bmatrix} I_{N_p n \times n} x_{max} \\ -I_{N_p n \times n} x_{min} \end{bmatrix} + \begin{bmatrix} -\mathcal{S}^x \\ \mathcal{S}^x \end{bmatrix} x(k) \quad (2.35b)$$

The set of equations (2.34), (2.35a), and (2.35b) define a quadratic programming problem. When the optimal control sequence  $U$  is obtained, only the first control  $u(k | k)$  is applied to the system. The rest of the control sequence is discarded. Then at the next time interval,  $x(k+1)$  is used as the new initial condition of the optimal control problem (2.29) and the algorithm will be repeated.

## 2.4.2 Stability of MPC

In this subsection, a brief review on available methods to guarantee closed loop stability of linear constrained systems using MPC controller is stated. For more reviews on stability analysis of MPC, readers are referred to [43, 44].

The proposed approaches in the literature are mostly relies on Lyapunov methods. These approaches ensure that the MPC cost function is monotonically decreasing, and therefore it can be considered as a Lyapunov function. In this regard, authors in [102], add a zero terminal state equality constraint to the optimization problem. Although this scheme is suitable for a large class of systems, but it has feasibility issue due to adding a strict terminal equality constraint, therefore it is required to consider a relatively long horizon to ensure feasibility of the optimization problem.

For stable linear systems, reference [103] removes the need for terminal equality constraint by adding the terminal quadratic state cost. In this scheme, no control action is considered after the end of prediction horizon, therefore the terminal penalty matrix can be found as the solution to the Lyapunov matrix equation associated with open loop system. This work is then extended in [104] for unstable linear systems in which the unstable modes are derived to origin at the end of optimization problem and the terminal state penalty is applied to stable modes. A rather more general approach is introduced in [105] to ensure decreasing property of the MPC cost function by introducing the terminal cost associated with the sub-optimal feedback control law derived from the infinite horizon unconstrained LQR method. Moreover, the feasibility of the sub-optimal feedback control law is translated into the convex quadratic constraint on the terminal state.

In this thesis, we are dealing with unstable linear systems in which the triple  $(A, B, C)$  is controllable and observable, therefore we will use the approach proposed in [104] to ensure the stability of the closed loop system. This scheme is formally stated in the following theorem.

**Theorem 2.1.** Consider the optimization problem (2.29) where the pair  $(A, B)$  of the prediction model is stabilizable with  $r < N_p$  unstable modes, then  $x(k) = 0$  is an asymptotically stable solution of closed loop MPC with objective function (2.30) where  $Q \geq 0$ ,  $Q_N \geq 0$ , and  $R > 0$ , and with feasible initial state  $x(0)$  satisfying the constraint equations (2.29d), (2.29e), and an extra terminal equality constraint on unstable modes, namely

$$\tilde{V}_u x(k + N_p) = 0 \tag{2.36}$$

where  $\tilde{V}_u$  is determined from Jordan form of matrix  $A$  partitioned into stable and

unstable parts in which the unstable eigenvalues are contained in  $J_u$

$$A = \begin{bmatrix} V_u & V_s \end{bmatrix} \begin{bmatrix} J_u & 0 \\ 0 & J_s \end{bmatrix} \begin{bmatrix} \tilde{V}_u \\ \tilde{V}_s \end{bmatrix} \quad (2.37)$$

Moreover, the terminal penalty matrix  $Q_N$  for stable modes is determined by

$$Q_N = \tilde{V}_s^T \Pi \tilde{V}_s \quad (2.38)$$

where  $\Pi$  is the solution of matrix Lyapunov equation

$$\Pi = V_s^T C^T Q C V_s + J_s^T \Pi J_s \quad (2.39)$$

**Proof:** The proof of Theorem 2.1 can be found in [104]. ■

## 2.5 Dynamic Game Theory

In the dynamic game of  $N_v$  players, a dynamic equation governs the entire game which is influenced by all players as

$$x(k+1) = A x(k) + \sum_{i=1}^{N_v} B_i u_i(k) \quad (2.40)$$

where  $x$  is the team state vector,  $u_i$  is the control variable of  $i$ th player,  $A$ , and  $B_i$  are constant matrices. In this game, each player wants to minimize its own quadratic cost as follows

$$J_i = \sum_{k=0}^{\infty} x^T(k) Q_i x(k) + u_i^T(k) R_i u_i(k) \quad (2.41)$$

where  $Q_i$  and  $R_i$  are positive semi-definite and positive definite matrices, respectively. The objective functions can be conflicting meaning that the optimal solution associated with player  $i$  may interfere with the state evolution from another player point of view. In this regard, based on how players collaborate to achieve their goals, there are cooperative and non-cooperative games.

### 2.5.1 Cooperative Game

In cooperative games, control actions of players are jointly determined such that total cost of the team is minimized. Therefore, if players choose any other control strategy, then at least one of the players has higher cost value. This solution set is known as Pareto optimal solution of the game. In the following, the definition of Pareto optimal solution is explicitly stated.

**Definition 2.1.** [60] For  $N_v$  player game defined by dynamic equation in (2.40) and objective functions in (2.41), the set of control strategies  $u^* = [u_1^*, \dots, u_{N_v}^*]$  constitute Pareto optimal solution if the set of inequalities

$$J_i(u) \leq J_i(u^*), \quad i = 1, \dots, N_v \quad (2.42)$$

do not hold with at least one strict inequality. The corresponding point  $J^* = (J_1^*, \dots, J_{N_v}^*)$  is called a Pareto solution. The set of all Pareto solutions is called the Pareto frontier.

The Pareto optimal control strategies can be derived by minimizing the convex combination of all players objective functions, namely

$$u^*(\alpha) = \underset{u}{\operatorname{argmin}} \sum_{i=1}^{N_v} \alpha_i J_i \quad \text{subject to (2.40)} \quad (2.43)$$

where  $\alpha \in \mathcal{A} = \{[\alpha_1, \dots, \alpha_{N_v}] \mid \alpha \geq 0 ; \sum_{i=1}^{N_v} \alpha_i = 1\}$ . The set of control strategies  $u^*(\alpha)$  and the corresponding Pareto optimal solution set  $J^*(u^*(\alpha))$  obtained from above optimization problem are functions of parameter  $\alpha$ , and therefore are not generally unique. In order to cooperatively choose the best solution among a set of Pareto optimal solutions, it is required to exploit from bargaining theory.

In bargaining theory, players cooperatively select a unique Pareto optimal solution among Pareto frontier, since they understand that better outcome will be achieved compared to the non-cooperative outcome. The non-cooperative outcome of the game is known as threat point and here is denoted by  $d$ .

In axiomatic bargaining theory, a number of solutions have been proposed. In [106], a survey is given on this theory. In this thesis, the Nash bargaining solution is adopted, as it provides a reasonable cooperative solution due to satisfaction of Pareto-optimality and symmetry.

The Nash bargaining solution  $N(S, d)$ , select for a given set  $(J_1, \dots, J_{N_v}) \in S$  a point at which the product of utility gains, i.e. the difference between the solution and the threat point of players, is maximized, namely

$$N(S, d) = \operatorname{argmax}_{J \in S} \prod_{i=1}^{N_v} (d_i - J_i), \quad J \leq d \quad (2.44)$$

As previously stated, Nash bargaining solution has Pareto-optimality property, meaning that  $N(S, d)$  lies on the Pareto frontier, and therefore is dependent on weighting parameter  $\alpha$ . Hence, N-solution can also be obtained by

$$\alpha^N = \operatorname{argmax}_{\alpha \in \mathcal{A}} \prod_{i=1}^{N_v} (d_i - J_i(u^*(\alpha))) \quad (2.45)$$

In Nash bargaining problem, players agree that the more utility gain a player

receives from cooperation the less weight it will get in the minimization problem. In another words, the following relationship holds between the value of the cost functions at  $N$ -solution  $J^N = (J_1^N, \dots, J_{N_v}^N)$ , the threat point  $d$ , and the weighting parameter  $\alpha^N = (\alpha_1^N, \dots, \alpha_{N_v}^N)$ , namely

$$\alpha_1^N (J_1^d - J_1^N) = \alpha_2^N (J_2^d - J_2^N) = \dots = \alpha_{N_v}^N (J_{N_v}^d - J_{N_v}^N) \quad (2.46)$$

## 2.5.2 Non-Cooperative Game

In non-cooperative game framework, each player focuses only on minimizing its own cost function under the possible influence of other players control actions. The non-cooperative aspect indicates that the players are assumed not to collaborate in trying to attain their objectives. A typical solution to the non-cooperative game is the well-known Nash equilibrium introduced in [59]. In the following, the definition of Nash equilibrium is formally stated.

**Definition 2.2.** [107] An admissible set of actions  $u = [u_1^*, \dots, u_{N_v}^*]^T$  is a Nash equilibrium for  $N_v$  player game defined by dynamic equation (2.40) and a set of cost functions in (2.41), if for all admissible  $u = [u_1, \dots, u_{N_v}]^T$  the following inequalities hold:

$$J_i(u_1^*, \dots, u_i^*, \dots, u_{N_v}^*) \leq J_i(u_1^*, \dots, u_i, \dots, u_{N_v}^*), \quad i = 1, \dots, N_v \quad (2.47)$$

The above-mentioned definition implies that none of the players have incentive to change their control actions unilaterally, since any deviation from Nash equilibrium point will lead to the worst cost value.

The Nash equilibrium solution associated with non-cooperative dynamic game

of linear quadratic type which is characterized by (2.40) and (2.41) can be found explicitly according to the following theorem.

**Theorem 2.2.** Let  $K_i$ ,  $i \in \{1, \dots, N_v\}$ , be defined by the following linear matrix equation

$$(B_i^T P_i B_i + R_i) K_i + B_i^T P_i \sum_{j \neq i} B_j K_j = B_i^T P_i A, \quad i \in \{1, \dots, N_v\} \quad (2.48)$$

where  $P_i$ , is the solution to the set of coupled algebraic Riccati equations (AREs), namely

$$P_i = (A - \sum_{j \in N_v} B_j K_j)^T P_i (A - \sum_{j \in N_v} B_j K_j) + Q_i + K_i^T R_i K_i, \quad i \in \{1, \dots, N_v\} \quad (2.49)$$

Then,  $N_v$  player linear quadratic dynamic game defined by (2.40) and (2.41) with  $Q_i \geq 0$  and  $R_i > 0$  admits a unique Nash equilibrium solution if, and only if, (2.48) admits a unique solution set  $\{K_i^*; i \in \{1, \dots, N_v\}\}$  in which Nash equilibrium control strategies are given by

$$u_i^*(k) = -K_i^* x(k), \quad i \in \{1, \dots, N_v\} \quad (2.50)$$

**Proof:** The proof of theorem 2.2 can be found in [107]. ■

## 2.6 Basic Definitions on Multiple AUVs Formation Structure and Modeling

In this thesis, a virtual vehicle formation coordination method is considered to achieve individual and cooperative objectives depending on their significance to individuals,

namely (I) reference tracking, and (II) formation keeping, i.e. maintaining the position of team members relative to each other. These team objectives can be interpreted into suitable cost function in model predictive control framework.

The aforementioned control objectives are in conformity with the wide range of underwater mission tasks including seabed surveying and mapping, oil and gas exploration and extraction, monitoring oil and gas pipelines, and reconnaissance just to name a few.

At each sampling intervals, the evaluated control inputs of individuals according to the MPC technique and minimization of cost function which is established based on agents cumulative formation keeping and reference tracking errors are the implicit feedback control law of local and neighbors information as in equation (2.51). It is worth mentioning that the tracking error vector will only appear in the cost function of the leader that has access to the global reference.

$$u_i = k_i^{mpc}(z_i, \{z_j\}_{j \in N_i}) \quad (2.51)$$

### 2.6.1 Formation Graph Modeling

In this section, basic concepts in graph theory are provided to model information flow structure and interactions among agents in the formation control of multiple AUVs.

In a graph-based formation network [108, 109], each agent can be identified as the vertex of the time-invariant, and connected formation graph  $\mathcal{G} \triangleq (\mathcal{V}, \mathcal{E})$ , where

- $\mathcal{V} \triangleq \{1, 2, \dots, N\}$  is the set of vertices that labels each agent in the team of  $N$  vehicles.
- $\mathcal{E} \subseteq \{(i, j) \in \mathcal{V} \times \mathcal{V} \mid i \neq j\}$  is the set of edges describing the interconnection topology of the systems.

- $N_i \triangleq \{j \mid (j, i) \in \mathcal{E}\}$  is the open set of  $i$ th agent neighbors with  $|N_i|$  as its cardinality which is also called the degree of vertex  $i$ . Then, the closed set of  $i$ th agent neighbors, denoted by  $\bar{N}_i$ , is  $N_i \cup \{i\}$  with the cardinality  $|\bar{N}_i|$ .
- The graph  $\mathcal{G}$  is assumed to be undirected meaning that every edge is bidirectional, i.e.  $(i, j) \in \mathcal{E}$ , indicates  $(j, i) \in \mathcal{E}$ .
- The adjacency matrix of an undirected graph  $\mathcal{G}$  with  $N \times N$  vertices is denoted by symmetric matrix  $\mathcal{A} = [a_{ij}]_{N \times N}$  in which  $a_{ij} = 1$  if and only if  $(i \sim j) \in \mathcal{E}$  and  $a_{ij} = 0$  otherwise. The corresponding degree matrix is denoted by  $\mathcal{D} = \text{diag}\{d_{ii}\}$  and is defined to be the diagonal matrix with  $d_{ii} = \sum_{j \in \mathcal{V}} a_{ij}$ , i.e. the number of edges leaving from vertex  $i$ .
- The Laplacian matrix associated with graph  $\mathcal{G}$  can be defined as

$$\mathcal{L} = \mathcal{D} - \mathcal{A} \tag{2.52}$$

where for an undirected and connected graph, the Laplacian matrix is symmetric positive semi-definite and has a simple zero eigenvalue.

## 2.7 Summary

In this chapter, AUV nonlinear and linearized equations of motion in horizontal plane are derived. To this end, fundamental concepts on coordinate systems and attitude representation by Euler angles are introduced. Furthermore, the definition, general classification, and multiplicative model of actuator faults are explained. Then, a brief description on model predictive control technique, cooperative game framework, and non-cooperative game framework are given. Finally, the graph based formation model representation used in this thesis is illustrated.

# Chapter 3

## Centralized, Semi-Decentralized, and Decentralized Control of Autonomous Vehicle Formations

### 3.1 Introduction

In this chapter, formation control algorithms are developed to achieve desired team objectives using the MPC technique and dynamic game theory. Toward this end, various controller design structures including centralized, semi-decentralized, and decentralized are introduced.

In the centralized control, a central unit with a global control algorithm computes the control commands to each agent based on the collected information from the whole team members. Although this structure provides good performance in achieving formation objectives, it has several issues such as the requirement of high computational capacity, large amount of information exchange, and the possibility of

single point of failure. On the contrary, in the decentralized control, individual control commands are independently designed considering the state information of each agent and its neighbors. This scheme lifts the requirement of high level of information exchange while considerably decrease formation performance due to neglecting couplings among team members. The semi-decentralized control provides a trade-off between aforementioned control design structures where control inputs of agents are designed by incorporating neighboring agents state information while additionally taking into account the coupling effect due to neighboring agents control inputs.

The above-mentioned control design structures will be more elaborated throughout this chapter. Moreover, simulations are performed for a team of AUVs to evaluate and analyze the effectiveness of the proposed control algorithms.

## 3.2 Centralized Control

In the centralized formation control, as shown in Figure 3.1, the state information and control objectives of the entire team are incorporated in the control design of each agent.

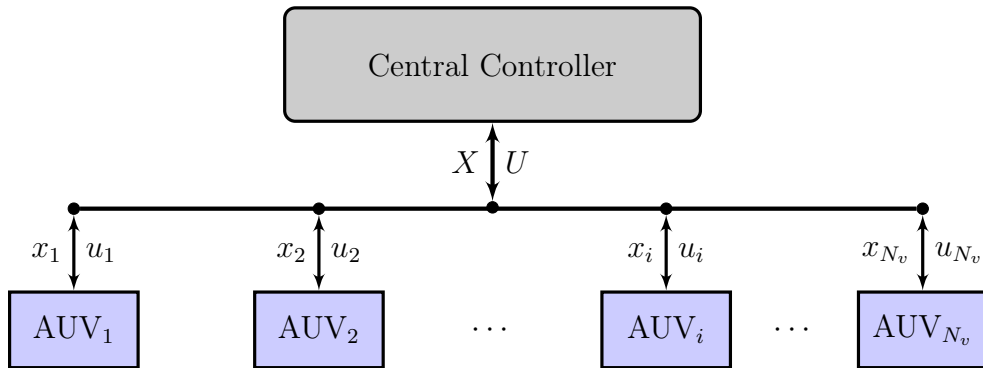


**Figure 3.1:** Centralized Control System

To this end, it is required to derive the overall centralized formation error model.

First, consider the dynamics of each agent  $i = \{1, \dots, N_v\}$  represented by

$$x_i(k+1) = A x_i(k) + B u_i(k) \quad (3.1a)$$

$$z_i(k) = C e_i(k) \quad (3.1b)$$

where  $x_i \in \mathbb{R}^6$ ,  $u_i \in \mathbb{R}^3$ ,  $e_i \in \mathbb{R}^3$ , and  $z_i \in \mathbb{R}^3$  are the state, control input, centralized formation error, and output vectors of  $i$ th agent, respectively.

The centralized information exchange topology among  $N_v$  agents is described by a fully connected graph with  $W = \mathcal{L} + G \in \mathbb{R}^{N_v \times N_v}$  where  $G = \text{diag}\{g_i\}$  is used to denote the connection of agents to global trajectories. The global trajectories can be generated by the following dynamic equation, namely

$$x_i^*(k+1) = A x_i^*(k) + B u^* \quad (3.2)$$

where the desired constant control command  $u^*$  is assumed to be available to each agent. The desired formation configuration between each pair of agents can be represented by a constant vector  $x_{ij}^* = x_i^* - x_j^*$ . Then, the centralized formation error vector  $e_i \in \mathbb{R}^3$  associated with each agent can be defined by

$$e_i(k) = \sum_{j \in \mathcal{V} - \{i\}} a_{ij} (x_i(k) - x_j(k) - x_{ij}^*) + g_i (x_i(k) - x_i^*(k)) \quad (3.3)$$

and its corresponding dynamics is given by

$$e_i(k+1) = A e_i(k) + \sum_{j \in \mathcal{V}} w_{ij} B \delta u_j(k) \quad (3.4a)$$

$$z_i(k) = C e_i(k) \quad (3.4b)$$

where  $a_{ij}$  is the  $ij$ th element of the adjacency matrix  $\mathcal{A}$ ,  $g_i > 0$  is the  $i$ th element of

diagonal matrix  $G$ , and  $w_{ij}$  is the  $ij$ th element of matrix  $W$ . Moreover,  $\delta u_j = u_j - u^*$  is the control input error variable.

Finally, the augmented formation errors of  $N_v$  agents can be represented in a compact form as follows

$$E = (W \otimes I_6) \delta X \quad (3.5)$$

and its dynamics can be given by

$$E(k+1) = \bar{A} E(k) + \bar{B} \delta U(k) \quad (3.6a)$$

$$Z(k) = \bar{C} E(k) \quad (3.6b)$$

where  $\delta X = [(x_1 - x_1^*)^T \dots (x_{N_v} - x_{N_v}^*)^T]^T$ ,  $E = [e_1^T \dots e_{N_v}^T]^T$ ,  $\delta U = [\delta u_1^T \dots \delta u_{N_v}^T]^T$ , and  $Z = [z_1^T \dots z_{N_v}^T]^T$  are the augmented state error, formation error, control input, and output vectors, respectively. Furthermore,  $\bar{A} = I_{N_v} \otimes A$ ,  $\bar{B} = W \otimes B$ , and  $\bar{C} = I_{N_v} \otimes C$ .

In the following subsection, the centralized control design problem using MPC control technique will be demonstrated based on aforementioned definitions.

### 3.2.1 Model Predictive Control Approach to Centralized Control

To derive centralized MPC-based controllers, let us consider the following finite horizon cost for each agent  $i \in \mathcal{V}$  which penalizes each individual centralized formation error and control input as follows

$$J_i(z_i(k), u_i(\cdot)) = \sum_{h=0}^{N_p-1} \{ \|z_i(h|k)\|_{Q_i}^2 + \|u_i(h|k) - u^*\|_{R_i}^2 \} + \|x_i(N_p|k)\|_{Q_{iN}}^2 \quad (3.7)$$

where  $Q_i \in \mathbb{R}^{3 \times 3}$ ,  $Q_{iN} \in \mathbb{R}^{6 \times 6}$  are positive semi-definite, and  $R_i \in \mathbb{R}^{3 \times 3}$  is positive definite penalty matrices. Then, the centralized formation cost is the sum of all individual costs as follows

$$J_c(Z(k), U(\cdot)) = \sum_{h=0}^{N_p-1} \left\{ \sum_{i \in \mathcal{V}} \|z_i(h|k)\|_{Q_i}^2 + \|\delta u_i(h|k)\|_{R_i}^2 \right\} + \sum_{i \in \mathcal{V}} \|x_i(N_p|k)\|_{Q_{iN}}^2 \quad (3.8)$$

In the following, the centralized MPC-based control problem is formally stated.

**Problem 3.1.** At each time step  $k$ , given the current augmented formation error vector  $E(k)$ , find the entire formation control input sequence  $\delta \tilde{U}(k) = [\delta U(k)^T, \delta U(k+1)^T, \dots, \delta U(k+N_c-1)^T]^T$  as the solution to the following constrained finite time optimal control problem

$$\min_{\delta \tilde{U}} J_c(Z(k), \delta \tilde{U}(k)) =: \quad (3.9a)$$

$$\min_{\delta \tilde{U}} \sum_{h=0}^{N_p-1} \left\{ \|Z(h|k)\|_Q^2 + \|\delta U(h|k)\|_R^2 \right\} + \|E(N_p|k)\|_{Q_N}^2$$

s.t.

$$E(h+1|k) = \bar{A} E(h|k) + \bar{B} \delta U(h|k) \quad (3.9b)$$

$$Z(h|k) = \bar{C} E(h|k) \quad h = 0, 1, \dots, N_p - 1 \quad (3.9c)$$

$$\delta U_{min} \leq \delta U(h|k) \leq \delta U_{max} \quad h = 0, 1, \dots, N_c - 1 \quad (3.9d)$$

$$\delta U(h|k) = \delta U(N_c - 1|k) \quad N_c \leq h \leq N_p - 1 \quad (3.9e)$$

$$\tilde{V}_u E(k + N_p) = 0 \quad (3.9f)$$

where  $N_c$ ,  $N_p$  are the control horizon and the prediction horizon, respectively. In order to decrease the computational complexity, the control horizon is selected to be less than the prediction horizon. The output penalty matrix  $Q = blkdiag\{Q_{i \in \mathcal{V}}\} \in$

$\mathbb{R}^{3N_v \times 3N_v}$  and terminal state penalty matrix  $Q_N \in \mathbb{R}^{6N_v \times 6N_v}$  are positive semi-definite, and the input penalty matrix  $R = \text{blkdiag}\{R_{i \in \mathcal{V}}\} \in \mathbb{R}^{3N_v \times 3N_v}$  is positive definite. The triple  $(\bar{A}, \bar{B}, \bar{C})$  considered in the prediction model is controllable and observable with  $3N_v$  unstable modes on the unit circle. In order to ensure stability of closed loop system, the terminal equality constraint (3.9f) associated with unstable modes and the terminal penalty matrix  $Q_N$  are computed as explained in Theorem 2.1.

**Remark 3.1.** The above constrained optimization problem can be solved at each time step using QP algorithms such as interior point, active set and trust-region reflective.

### 3.2.2 Non-Cooperative Dynamic Game Approach to Centralized Control

In this subsection, we will use non-cooperative nonzero-sum dynamic game to formulate and solve centralized formation control problem. It is worth noting that, the objective for each player is the minimization of his own cost function constrained by the underlying centralized formation error dynamics as introduced in (3.6). Therefore, for a formation consists of  $N_v$  agents, control actions of all agents are determined simultaneously to reach irrevocable set of control actions which is known as Nash equilibrium. In this regard, let us consider the following infinite horizon cost associated with each agent

$$J_i(Z(k), \delta u_i(k)) = \sum_{k=0}^{\infty} \|Z(k)\|_{\bar{Q}_i}^2 + \|\delta u_i(k)\|_{R_i}^2, \quad i \in \mathcal{V} \quad (3.10)$$

where  $\bar{Q}_i = \text{blkdiag}\{0_{3 \times 3} \dots Q_i \dots 0_{3 \times 3}\} \in \mathbb{R}^{3N_v \times 3N_v}$  and  $Q_i \in \mathbb{R}^{3 \times 3}$  are positive semi-definite, and  $R_i \in \mathbb{R}^{3 \times 3}$  is positive definite penalty matrices. In the following

problem, this scheme is formally stated.

**Problem 3.2.** For non-cooperative nonzero-sum dynamic game of  $N_v$  agents with fully connected information exchange topology, find the set of control strategies  $\delta U^*(k) = [\delta u_1^*(k), \dots, \delta u_{N_v}^*(k)]^T$  as the solution to the set of  $N_v$  simultaneous global minimization problems, namely

$$\delta u_i^*(k) = \underset{\delta u_i}{\operatorname{argmin}} J_i(Z(k), \delta u_i(k)) , \quad i \in \mathcal{V} \quad (3.11a)$$

subject to

$$E(k+1) = \bar{A} E(k) + \sum_{i \in \mathcal{V}} \bar{B}_i \delta u_i(k) \quad (3.11b)$$

$$Z(k) = \bar{C} E(k) \quad (3.11c)$$

where each individual cost  $J_i$  is defined in (3.10). Moreover, the error dynamics considered in the minimization problem is the rearranged form of centralized formation error dynamics defined in (3.6) in which  $\bar{B}_i = w_i^T \otimes B$  and  $w_i$  is the  $i$ th row of matrix  $W$  that characterizes the underlying information graph.

**Solution:**

The non-cooperative dynamic game outlined in Problem 3.2 is in the standard form due to the full information availability and centralized nature of the problem. Hence, the local control strategies that constitute global Nash equilibrium  $\delta U^*(k) = [\delta u_1^{*T}(k), \dots, \delta u_{N_v}^{*T}(k)]^T$  as stated in Theorem 2.2 can be given by

$$\delta u_i^*(k) = -\bar{K}_i E(k) \quad \forall i \in \mathcal{V} \quad (3.12)$$

where the control gain matrices  $\bar{K}_{i \in \mathcal{V}} \in \mathbb{R}^{3 \times 6N_v}$  are defined by

$$\bar{K}_i = (R_i + \bar{B}_i^T \bar{P}_i \bar{B}_i)^{-1} \bar{B}_i^T \bar{P}_i (\bar{A} - \sum_{j \in \mathcal{V} - \{i\}} \bar{B}_j \bar{K}_j) \quad \forall i \in \mathcal{V} \quad (3.13)$$

where  $\bar{P}_{i \in \mathcal{V}} \in \mathbb{R}^{6N_v \times 6N_v}$  are the solutions to coupled AREs as follows

$$\bar{P}_i = \bar{C}^T \bar{Q}_i \bar{C} + \bar{K}_i^T R_i \bar{K}_i + (\bar{A} - \sum_{j \in \mathcal{V}} \bar{B}_j \bar{K}_j)^T \bar{P}_i (\bar{A} - \sum_{j \in \mathcal{V}} \bar{B}_j \bar{K}_j) \quad \forall i \in \mathcal{V} \quad (3.14)$$

It should be noted that  $\bar{P}_i$  is the unique positive semi-definite solutions to the  $i$ th coupled ARE given in (3.14) if and only if the pair  $(\bar{A} - \sum_{j \in \mathcal{V} - \{i\}} \bar{B}_j \bar{K}_j, \bar{B}_i)$  is stabilizable and the pair  $(\bar{A} - \sum_{j \in \mathcal{V} - \{i\}} \bar{B}_j \bar{K}_j, \bar{Q}_i^{1/2} \bar{C})$  is detectable.

**Remark 3.2.** The solution to above-mentioned coupled AREs is determined numerically using iterative algorithms in [110, 111].

### 3.2.3 Cooperative Dynamic Game Approach to Centralized Control

In this subsection, we exploit from cooperative dynamic game theory and Nash bargaining solution as an agreement strategy to solve the centralized control design problem. We expect to achieve a cooperative behavior in terms of individual cost values as compared to the cost values that are obtained by the optimal control without any agreement strategy. Hence, each agent benefits from cooperation in a fair way while promising simultaneous minimization of individual costs.

In this regard, let us consider the infinite horizon cost associated with each agent as defined in (3.10). Then, the centralized formation cost is defined by the convex

combination of all individual costs, as follows

$$J_c(Z(k), \delta U(k), \alpha) = \sum_{i \in \mathcal{V}} \alpha_i J_i(Z(k), \delta u_i(k)) \quad (3.15)$$

where  $\alpha \in \Lambda = \{[\alpha_1, \dots, \alpha_{N_v}] \mid \alpha \geq 0, \sum_{i \in \mathcal{V}} \alpha_i = 1\}$ .

We are now ready to formally state centralized control problem using cooperative dynamic game.

**Problem 3.3.** For a cooperative dynamic game of  $N_v$  agents, find a set of Pareto-efficient control strategies denoted by  $\delta U^*(\alpha, k)$  for  $\forall \alpha \in \Lambda$  which provides the solutions to the following global minimization problem, namely

$$\delta U^*(\alpha, k) = \underset{\delta U}{\operatorname{argmin}} J_c(Z(k), \delta U(k), \alpha) \quad (3.16a)$$

subject to

$$E(k+1) = \bar{A} E(k) + \sum_{i \in \mathcal{V}} \bar{B}_i \delta u_i(k) \quad (3.16b)$$

$$Z(k) = \bar{C} E(k) \quad (3.16c)$$

where the dynamic equation considered in the minimization problem is the rearranged form of centralized formation error dynamics defined in (3.6) in which  $\bar{B}_i = w_i^T \otimes B$  and  $w_i$  is the  $i$ th row of matrix  $W$  which characterizes the underlying information graph.

**Solution:**

The local control strategies that constitute Pareto-efficient solution  $\delta U(\alpha^*) = [\delta u_1^T(\alpha^*), \dots, \delta u_{N_v}^T(\alpha^*)]^T$  can be given by

$$\delta u_i^*(\alpha, k) = -\bar{K}_i(\alpha) E(k) \quad \forall i \in \mathcal{V} \quad (3.17)$$

where the control gain matrices  $\bar{K}_{i \in \mathcal{V}}(\alpha) \in \mathbb{R}^{3 \times 6N_v}$  are defined by

$$\bar{K}_i(\alpha) = (\alpha_i R_i + \bar{B}_i^T \bar{P}(\alpha) \bar{B}_i)^{-1} \bar{B}_i^T \bar{P}(\alpha) (\bar{A} - \sum_{j \in \mathcal{V} - \{i\}} \bar{B}_j \bar{K}_j(\alpha)) \quad \forall i \in \mathcal{V} \quad (3.18)$$

where  $\bar{P}(\alpha) \in \mathbb{R}^{6N_v \times 6N_v}$  is the solution to the following ARE, namely

$$\bar{P}(\alpha) = \sum_{i \in \mathcal{V}} \{ \alpha_i \bar{C}^T \bar{Q}_i \bar{C} + \bar{K}_i^T(\alpha) \alpha_i R_i \bar{K}_i(\alpha) \} + (\bar{A} - \sum_{j \in \mathcal{V}} \bar{B}_j \bar{K}_j(\alpha))^T \bar{P}(\alpha) (\bar{A} - \sum_{j \in \mathcal{V}} \bar{B}_j \bar{K}_j(\alpha)) \quad (3.19)$$

It should be noted that  $\bar{P}(\alpha)$  is the positive semi-definite solution to ARE (3.19) which is not unique in general.

**Remark 3.3.** The cooperative linear quadratic dynamic game is a regular linear quadratic optimal control problem which depends on parameter  $\alpha$ . Therefore, the existence of a solution to Problem 3.3 depends on the existence of solution to ARE given in (3.19).

As can be observed from above discussion, the local Pareto-efficient control strategies are functions of  $\alpha \in \Lambda$ . Hence, we need to find the best possible solution that all agents can agree on. In this regard, we resort to Nash bargaining theory to obtain a reasonable cooperative solution to Problem 3.3. The Algorithm 3.1 given in [60] will be used in conjunction to equations (3.19) and (3.18) to find a unique  $\alpha^*$ , Pareto optimal solution  $[J_1(\alpha^*), \dots, J_{N_v}(\alpha^*)]$ , and the corresponding Pareto-efficient control strategy  $\delta U(\alpha^*) = [\delta u_1^T(\alpha^*), \dots, \delta u_{N_v}^T(\alpha^*)]^T$ .

**Remark 3.4.** It is worth noting that the cost values of each agent derived in Subsection 3.2.2 are considered as non-cooperative cost values  $J_{i \in \mathcal{V}}^d$  used in Algorithm 3.1.

```

1 Start with an initial  $\alpha_0 = [\frac{1}{N_v}, \dots, \frac{1}{N_v}] \in \Lambda$ ;
2 Compute  $\delta U^*(\alpha^0, k) = \underset{\delta U}{\operatorname{argmin}} J_c(Z(k), \delta U(k), \alpha^0)$ ;
3 if  $J_i(\delta u^*) > J_i^d$  for  $i \in \mathcal{V}$  then
4   update  $\alpha_i^0 = \alpha_i^0 + 0.01$ , and  $\alpha_j^0 = \alpha_j^0 - \frac{0.01}{N_v - 1}$  for  $j \neq i$  and return to Step 2
5 else
6   Calculate  $\hat{\alpha}_i^N = \frac{\prod_{j \in \mathcal{V} - \{i\}} (J_j^d - J_j(\delta u_j^*(\alpha_j^0)))}{\sum_{j \in \mathcal{V}} \prod_{l \in \mathcal{V} - \{j\}} (J_l^d - J_l(\delta u_l^*(\alpha_l^0)))}$ ;
7   if  $|\hat{\alpha}_i^N - \alpha_i^0| < 0.01$  for  $i \in \mathcal{V}$  then
8     Terminate the algorithm and set  $\alpha^N = \hat{\alpha}^N$ 
9   else
10     $\alpha_i^0 = 0.8\alpha_i^0 + 0.2\hat{\alpha}_i^N$  and return to Step 2
11  end
12 end

```

**Algorithm 3.1:** Algorithm to Calculate N-Solution of Centralized Cooperative Dynamic Game Problem 3.3

### 3.3 Semi-Decentralized Control

This section concerns with developing semi-decentralized controller in which information exchange is allowed only among neighboring agents. This information includes states and control actions of neighboring agents as depicted in Figure 3.2. In this regard, non-cooperative nonzero-sum dynamic game theory and model predictive control strategy are utilized to formulate and solve semi-decentralized formation control problem.

The semi-decentralized information exchange topology among  $N_v$  agents is described by a connected graph with  $W = \mathcal{L} + G \in \mathbb{R}^{N_v \times N_v}$  where  $G = \operatorname{diag}\{g_i\}$  is used

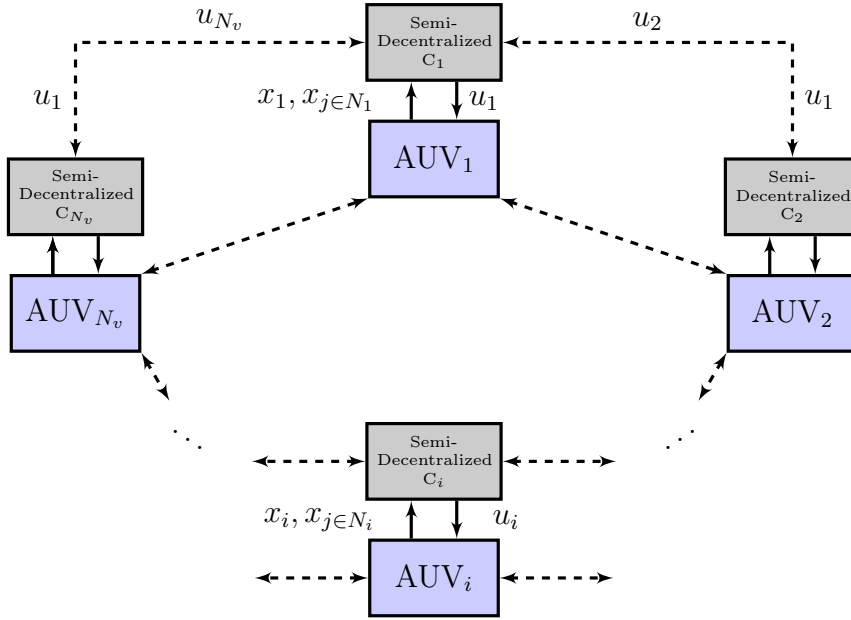


**Figure 3.2:** Information Exchange Structure of Semi-Decentralized Control System

to denote the connection of agents to global trajectory. We have  $g_i > 0$  if agent  $i$  is connected to the virtual leader and  $g_i = 0$  otherwise.

**Remark 3.5.** The second smallest eigenvalue of the Laplacian matrix  $\lambda_2(\mathcal{L})$  associated with the undirected and connected graph considered in semi-decentralized controller design depends on the number of communication links among agents. By increasing the number of connections among agents, the value of  $\lambda_2(\mathcal{L})$  increases, and therefore better stability margin of closed-loop system and formation performance will be achieved.

For each agent  $i \in \mathcal{V}$  with the state space dynamic equation given in (3.1), and the desired global trajectory and formation configuration as defined in (3.2), the formation error vector associated with  $i$ th agent while considering the information exchange topology can be represented as follows

$$e_i(k) = \sum_{j \in N_i} a_{ij} (x_i(k) - x_j(k) - x_{ij}^*) + g_i (x_i(k) - x^*(k)) \quad (3.20)$$

or equivalently, we can rewrite equation (3.20) in the following compact form using augmented state error vector, namely

$$e_i(k) = (w_i \otimes I_6) \delta X(k) \quad (3.21)$$

Then, the formation error dynamics can be written as

$$e_i(k+1) = A e_i(k) + \sum_{j \in \bar{N}_i} w_{ij} B \delta u_j(k) \quad (3.22a)$$

$$z_i(k) = C e_i(k) \quad (3.22b)$$

where  $\delta X = [(x_1 - x_1^*)^T \dots (x_{N_v} - x_{N_v}^*)^T]^T$  is the augmented state error vector and  $\delta u_i = u_i - u^*$  is the control input error vector of  $i$ th agent. Moreover,  $a_{ij}$  is the  $ij$ th element of the adjacency matrix  $\mathcal{A}$ ,  $g_i$  is the  $i$ th element of diagonal matrix  $G$ . The row vector  $w_i$  and  $w_{ij}$  are the  $i$ th row and  $ij$ th element of matrix  $W$  which characterizes the underlying information graph, respectively.

### 3.3.1 Model Predictive Control Approach to Semi-Decentralized Control

To derive semi-decentralized MPC-based controller, let us consider the following finite horizon cost for each agent  $i \in \mathcal{V}$  which penalizes each individual formation error defined in (3.20) and its control input as follows

$$J_i(z_i(k), u_i(\cdot)) = \sum_{h=0}^{N_p-1} \{ \|z_i(h|k)\|_{Q_i}^2 + \|u_i(h|k) - u^*\|_{R_i}^2 \} + \|x_i(N_p|k)\|_{Q_{iN}}^2 \quad (3.23)$$

where  $Q_i \in \mathbb{R}^{3 \times 3}$ ,  $Q_{iN} \in \mathbb{R}^{6 \times 6}$  are positive semi-definite, and  $R_i \in \mathbb{R}^{3 \times 3}$  is positive definite penalty matrices. In the following problem, the semi-decentralized control

design using MPC control technique is illustrated.

**Problem 3.4.** At each time step  $k$ , given the current formation error vector of  $i$ th agent  $e_i(k)$ , and neighboring agents previous optimal control inputs  $\delta\tilde{u}(k-1)_{j \in N_i}$ , find  $i$ th agent control input sequence  $\delta\tilde{u}_i(k) = [\delta u_i(k)^T, \delta u_i(k+1)^T, \dots, \delta u_i(k+N_c-1)^T]^T$  as the solution to the following constrained finite time optimal control problem

$$\min_{\delta\tilde{u}_i} J_i(z_i(k), \delta\tilde{u}_i(k)) =: \quad (3.24a)$$

$$\min_{\delta\tilde{u}_i} \sum_{h=0}^{N_p-1} \{ \|z_i(h|k)\|_{Q_i}^2 + \|\delta u_i(h|k)\|_{R_i}^2 \} + \|e_i(N_p|k)\|_{Q_i^{N_p}}^2$$

s.t.

$$e_i(h+1|k) = A e_i(h|k) + w_{ii} B \delta u_i(h|k) + \sum_{j \in N_i} w_{ij} B \delta u_j(h|k-1) \quad (3.24b)$$

$$z_i(h|k) = C e_i(h|k) \quad h = 0, 1, \dots, N_p - 1 \quad (3.24c)$$

$$\delta u_{min} \leq \delta u_i(h|k) \leq \delta u_{max} \quad h = 0, 1, \dots, N_c - 1 \quad (3.24d)$$

$$\delta u_i(h|k) = \delta u_i(N_c - 1|k) \quad N_c \leq h \leq N_p - 1 \quad (3.24e)$$

$$\tilde{V}_i e_i(k + N_p) = 0 \quad (3.24f)$$

where  $N_c$  and  $N_p$  are the control horizon and the prediction horizon, respectively. In order to decrease the computational complexity, the control horizon is selected to be less than the prediction horizon. The triple  $(A, w_{ii} B, C)$  considered in the prediction model of  $i$ th agent is controllable and observable with 3 unstable modes on the unit circle. In order to ensure stability of closed loop system, the terminal equality constraint (3.24f) associated with unstable modes and the terminal penalty matrix  $Q_{iN}$  are computed as explained in Theorem 2.1.

**Remark 3.6.** The above constrained optimization problem can be solved at each

time step using iterative quadratic programming algorithms such as interior point, active set and trust-region reflective.

### 3.3.2 Non-Cooperative Dynamic Game Approach to Semi- Decentralized Control

In this subsection, the semi-decentralized formation control is formulated as a non-cooperative nonzero-sum dynamic game in which each agent tries to minimize its objective function, while its error dynamics is coupled to the neighboring agents. Therefore, the value of each individual cost function is implicitly affected by the control actions pursued by its neighbors.

To develop semi-decentralized control algorithm based on non-cooperative dynamic game, let us consider the infinite horizon cost function associated with each agent as follows

$$J_i(z_i(k), u_i(k)) = \sum_0^{\infty} \|z_i(k)\|_{Q_i}^2 + \|\delta u_i(k)\|_{R_i}^2, \quad \forall i \in \mathcal{V} \quad (3.25)$$

where  $Q_i \in \mathbb{R}^{3 \times 3}$ , and  $R_i \in \mathbb{R}^{3 \times 3}$  are positive semi-definite, and positive definite penalty matrices, respectively. The following problem, formally states the semi-decentralized control using non-cooperative dynamic game while the information exchange topology is not fully connected.

**Problem 3.5.** For non-cooperative nonzero-sum dynamic game of  $N_v$  agents with connected information exchange topology, find the set of local control strategies  $\delta U^*(k) = [\delta u_1^{*T}(k) \dots \delta u_{N_v}^{*T}(k)]^T$  as the solution to the set of  $N_v$  simultaneous local minimization problems, namely

$$\delta u_i^*(k) = \underset{\delta u_i}{\operatorname{argmin}} J_i(z_i(k), \delta u_i(k)), \quad \forall i \in \mathcal{V} \quad (3.26a)$$

subject to

$$e_i(k+1) = A e_i(k) + \sum_{j \in \bar{N}_i} w_{ij} B \delta u_j(k) \quad (3.26b)$$

$$z_i(k) = C e_i(k) \quad (3.26c)$$

**Solution:**

In the semi-decentralized control, the information exchange topology is not fully connected, and the information available to each agent is restricted to its neighboring set. If we stack all error dynamics defined in (3.22) and using the standard coupled AREs given in Theorem 2.2, as what we did in Subsection 3.2.2, the solution will be a full matrix. In this way, the centralized information must be available to all agents to implement the resulting set of control strategies which constitute global Nash equilibrium.

To overcome aforementioned issue, we will solve a set of  $N_v$  local minimization problems simultaneously as defined in Problem 3.5 to find irrevocable set of control strategies  $\delta U^*(k) = [\delta u_1^{*T}(k), \dots, \delta u_{N_v}^{*T}(k)]^T$  such that each agent and its neighbors constitute local Nash equilibrium  $[\delta u_i^{*T}(k), \{\delta u_j^{*T}(k)\}_{j \in N_i}]^T$  for  $\forall i \in \mathcal{V}$ .

Since the local error dynamics associated with each agent is affected by its own control input as well as control inputs of its neighbors, we need to construct augmented error dynamics for each agent  $i \in \mathcal{V}$  to solve the corresponding local minimization problem as follows

$$\begin{bmatrix} e_i(k+1) \\ \vdots \\ e_j(k+1) \\ \vdots \end{bmatrix} = \underbrace{\begin{bmatrix} A & & & \\ & \ddots & & \\ & & A & \\ & & & \ddots \end{bmatrix}}_{A_i} \underbrace{\begin{bmatrix} e_i(k) \\ \vdots \\ e_j(k) \\ \vdots \end{bmatrix}}_{\bar{e}_i} + \sum_{n \in \bar{N}_i} \underbrace{\begin{bmatrix} w_{in} B \\ \vdots \\ w_{jn} B \\ \vdots \end{bmatrix}}_{B_{in}} \delta u_n(k) \quad (3.27a)$$

$$z_i = \underbrace{\begin{bmatrix} C & 0_{3 \times 6N_i} \end{bmatrix}}_{C_{ii}} \begin{bmatrix} e_i(k) \\ \vdots \\ e_j(k) \\ \vdots \end{bmatrix} \quad (3.27b)$$

In this model, it is assumed that non-neighboring agents are at steady state, therefore the effect of their control actions are ignored.

The set of local control strategies that provides Nash equilibrium solution to the set of  $N_v$  local minimization problems defined in (3.26) and subject to the new dynamics given in (3.27) can be given by

$$\delta u_i^*(k) = K_i \bar{e}_i(k) \quad \forall i \in \mathcal{V} \quad (3.28)$$

where the control gain matrices  $K_i \in \mathbb{R}^{3 \times 6\bar{N}_i}$  are defined by

$$K_i = (R_i + B_{ii}^T P_i B_{ii})^{-1} B_{ii}^T P_i (A_i - \sum_{j \in N_i} B_{ij} \hat{K}_j) \quad \forall i \in \mathcal{V} \quad (3.29)$$

where  $P_i \in \mathbb{R}^{6\bar{N}_i \times 6\bar{N}_i}$  are the solutions to the coupled AREs as follows

$$P_i = Q_{ii} + K_i^T R_i K_i + (A_i - B_{ii} K_i - \sum_{j \in N_i} B_{ij} \hat{K}_j)^T P_i (A_i - B_{ii} K_i - \sum_{j \in N_i} B_{ij} \hat{K}_j) \quad \forall i \in \mathcal{V} \quad (3.30)$$

where  $Q_{ii} = C_{ii}^T Q_i C_{ii} \in \mathbb{R}^{6\bar{N}_i \times 6\bar{N}_i}$  is positive semi-definite, and  $R_i \in \mathbb{R}^{3 \times 3}$  is positive definite. The control gain matrices  $\hat{K}_{j \in N_i}$  are the rearrange form of communicated control gain matrices of neighboring agents, i.e.  $K_{j \in N_i}$ , in order to be suitably incorporated in the coupled ARE of  $i$ th agent. Moreover,  $P_i$  is the unique positive semi-definite solution of  $i$ th algebraic Riccati equation given in (3.30) if and only if the pair  $(A_i - \sum_{j \in N_i} B_{ij} \hat{K}_j, B_{ii})$  is stabilizable, and the pair  $(A_i - \sum_{j \in N_i} B_{ij} \hat{K}_j, Q_{ii}^{1/2})$  is

detectable.

Since the formation graph is connected, ultimately the information from each agent propagates to all others. Therefore, if each agent and its neighbors reach irrevocable set of local control inputs  $[\delta u_i^{*T}(k), \{\delta u_j^{*T}(k)\}_{j \in N_i}]^T$  for  $i \in \mathcal{V}$ , this will imply that the whole set of local control inputs, i.e.  $[\delta u_1^*(k), \dots, \delta u_i^*(k), \dots, \delta u_{N_v}^*(k)]$  constitute Nash equilibrium.

**Remark 3.7.** The solution to above-mentioned coupled algebraic Riccati equations are determined numerically using algorithms proposed in [110, 111].

### 3.4 Decentralized Control

In this section, decentralized formation control algorithms are developed in which the information exchange is restricted to the neighboring set of each agent. The exchanged information among neighboring agents only includes their state information as depicted in Figure 3.3.

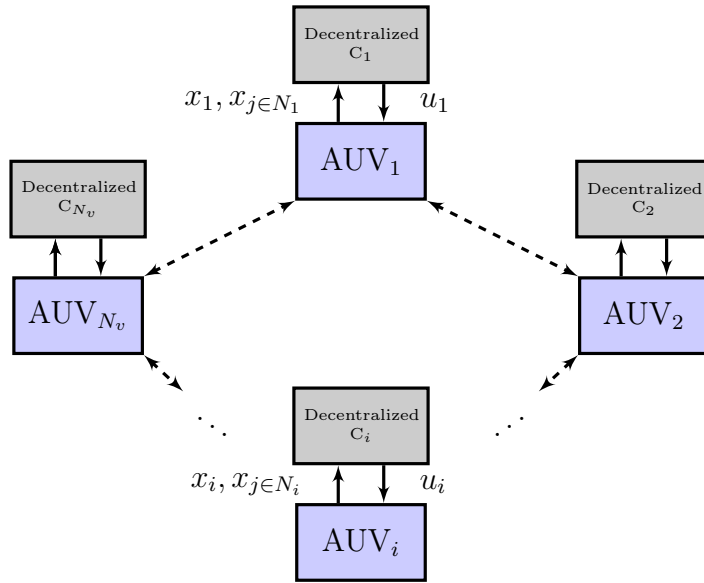


**Figure 3.3:** Decentralized Control System

The decentralized information exchange topology is described by the same graph defined for semi-decentralized control. Hence, we can similarly express the formation error dynamics associated with  $i$ th agent as given in (3.22). Since control inputs are not exchanged, each agent needs to compute its control action as well as the control actions of its neighbors, i.e.  $\{\delta u_j\}_{j \in \bar{N}_i}$  locally. In this regard, it is required to construct augmented error dynamics to design decentralized controller for each agent  $i \in \mathcal{V}$ . The augmented error dynamics of each agent can be formed by stacking its own error dynamics and the error dynamics of its neighbors as

$$\begin{bmatrix} e_i(k+1) \\ \vdots \\ e_j(k+1) \\ \vdots \end{bmatrix} = \underbrace{\begin{bmatrix} A & & \\ & \ddots & \\ & & A \end{bmatrix}}_{A_i} \underbrace{\begin{bmatrix} e_i(k) \\ \vdots \\ e_j(k) \\ \vdots \end{bmatrix}}_{\bar{e}_i} + \sum_{n \in \bar{N}_i} \underbrace{\begin{bmatrix} w_{in} B \\ \vdots \\ w_{jn} B \\ \vdots \end{bmatrix}}_{B_{in}} \delta u_n(k) \quad (3.31a)$$

$$\underbrace{\begin{bmatrix} z_i(k) \\ \vdots \\ z_j(k) \\ \vdots \end{bmatrix}}_{\bar{z}_i} = \underbrace{\begin{bmatrix} C & & \\ & \ddots & \\ & & C \end{bmatrix}}_{C_i} \begin{bmatrix} e_i(k) \\ \vdots \\ e_j(k) \\ \vdots \end{bmatrix} \quad (3.31b)$$

In model (3.31), it is assumed that non-neighboring agents are at steady state, therefore the effect of their control actions are ignored. At the implementation level,  $\delta u_i$  will be applied and the rest of neighboring agents control actions computed locally via  $i$ th agent will be only used to control augmented error dynamics in open loop. Hence, the decentralized control has the problem of dynamical model error due to not exchanging the control actions among neighboring agents.

### 3.4.1 Model Predictive Control Approach to Decentralized Control

To derive decentralized MPC-based controller, let us consider the following finite horizon cost for each agent  $i \in \mathcal{V}$  which penalizes each individual formation error defined in (3.20) and its own control input as well as control inputs of neighboring agents, as follows

$$J_i(\bar{z}_i(k), \{u_j(\cdot)\}_{j \in \bar{N}_i}) = \sum_{h=0}^{N_p-1} \{ \|\bar{z}_i(h|k)\|_{\bar{Q}_i}^2 + \sum_{j \in \bar{N}_i} \|u_j(h|k) - u^*\|_{R_j}^2 \} + \|\bar{e}_i(N_p|k)\|_{\bar{Q}_{iN}}^2 \quad (3.32)$$

where  $\bar{Q}_i = \text{blkdiag}\{Q_{j \in \bar{N}_i}\} \in \mathbb{R}^{3\bar{N}_i \times 3\bar{N}_i}$  and  $\bar{Q}_{iN} \in \mathbb{R}^{6\bar{N}_i \times 6\bar{N}_i}$  are respectively positive semi-definite output and terminal state penalty matrices, and  $\{R_j\}_{j \in \bar{N}_i} \in \mathbb{R}^{3 \times 3}$  are positive definite input penalty matrices.

In the following problem, the decentralized control design using MPC control technique is illustrated.

**Problem 3.6.** At each time step  $k$ , given the current augmented state error vector of  $i$ th agent  $\bar{e}_i(k)$ , find  $i$ th agent decentralized control input sequence  $\delta\tilde{u}_i(k) = [\delta u_i(k)^T, \delta u_i(k+1)^T, \dots, \delta u_i(k+N_c-1)^T]^T$  as the solution to the following constrained finite time optimal control problem

$$\begin{aligned} & \min_{\{\delta\tilde{u}_j\}_{j \in \bar{N}_i}} J_i(\bar{e}_i(k), \{\delta\tilde{u}_j(k)\}_{j \in \bar{N}_i}) =: \\ & \min_{\{\delta\tilde{u}_j\}_{j \in \bar{N}_i}} \sum_{h=0}^{N_p-1} \{ \|\bar{z}_i(h|k)\|_{\bar{Q}_i}^2 + \sum_{j \in \bar{N}_i} \|\delta u_j(h|k)\|_{R_j}^2 \} + \|\bar{e}_i(N_p|k)\|_{\bar{Q}_{iN}}^2 \end{aligned} \quad (3.33a)$$

s.t.

$$\bar{e}_i(h+1|k) = A_i \bar{e}_i(h|k) + \sum_{j \in \bar{N}_i} B_{ij} \delta u_j(h|k) \quad (3.33b)$$

$$\bar{z}_i(h|k) = C_i \bar{e}_i(h|k) \quad h = 0, 1, \dots, N_p - 1 \quad (3.33c)$$

$$\delta u_{min} \leq \delta u_j(h|k) \leq \delta u_{max}, \quad j \in \bar{N}_i \quad h = 0, 1, \dots, N_c - 1 \quad (3.33d)$$

$$\delta u_j(h|k) = \delta u_j(N_c - 1|k), \quad j \in \bar{N}_i \quad N_c \leq h \leq N_p - 1 \quad (3.33e)$$

$$\tilde{V}_i \bar{e}_i(k + N_p) = 0 \quad (3.33f)$$

where  $N_c$  and  $N_p$  are the control horizon and the prediction horizon, respectively. In order to decrease the computational complexity, the control horizon is selected to be less than the prediction horizon. The triple  $(A_i, [B_{ii}, B_{ij \in \bar{N}_i}], C_i)$  considered in the prediction model of  $i$ th agent is controllable and observable with  $3\bar{N}_i$  unstable modes on the unit circle. In order to ensure stability of closed loop system, the terminal equality constraint (3.33f) associated with unstable modes and the terminal penalty matrix  $\bar{Q}_{iN}$  are computed as explained in Theorem 2.1.

**Remark 3.8.** The above constrained optimization problem can be solved at each time step using iterative quadratic programming algorithms such as interior point, active set and trust-region reflective.

### 3.4.2 Non-Cooperative Dynamic Game Approach to Decentralized Control

In this subsection, the decentralized formation control is formulated as non-cooperative nonzero-sum dynamic game. Since in this scheme, control actions are not exchanged, each agent has to perform a set of  $|\bar{N}_i|$  minimization problems constrained by the augmented error dynamics given in (3.31). In this regard, let us consider the infinite horizon cost function associated with each agent in the closed neighboring set of  $i$ th

agent as follows

$$J_j(\bar{z}_i, \delta u_j(k)) = \sum_0^{\infty} \|\bar{z}_i(k)\|_{Q_{ij}}^2 + \|\delta u_j(k)\|_{R_j}^2, \quad j \in \bar{N}_i \quad (3.34)$$

where  $Q_{ij} = \text{blkdiag}\{0_{3 \times 3} \dots Q_j \dots 0_{3 \times 3}\} \in \mathbb{R}^{3\bar{N}_i \times 3\bar{N}_i}$  is positive semi-definite and  $R_j \in \mathbb{R}^{3 \times 3}$  is positive definite penalty matrices. The non-cooperative dynamic game formulation of decentralized control is formally stated in the following problem.

**Problem 3.7.** For non-cooperative nonzero-sum dynamic game of  $|\bar{N}_i|$  agents associated with  $i$ th agent, find the set of control strategies  $\{\delta u_j^*\}_{j \in \bar{N}_i}$ , as the solution to the set of  $|\bar{N}_i|$  local minimization problems, namely

$$\delta u_j^*(k) = \text{argmin} J_j(\bar{z}_i(k), \delta u_j(k)) \quad j \in \bar{N}_i \quad (3.35a)$$

subject to

$$\bar{e}_i(k+1) = A_i \bar{e}_i(k) + \sum_{j \in \bar{N}_i} B_{ij} \delta u_j(k) \quad (3.35b)$$

$$\bar{z}_i(k) = C_i \bar{e}_i(k) \quad (3.35c)$$

**Solution:**

The set of  $|\bar{N}_i|$  control strategies that are computed locally by  $i$ th agent and provides Nash equilibrium solution to Problem 3.7 can be given by

$$\delta u_j^*(k) = -K_{ij} \bar{e}_i(k), \quad \forall j \in \bar{N}_i \quad (3.36)$$

where the control gain matrices  $K_{ij \in \bar{N}_i} \in \mathbb{R}^{3 \times 6\bar{N}_i}$  are defined by

$$K_{ij} = (R_j + B_{ij}^T P_{ij} B_{ij})^{-1} B_{ij}^T P_{ij} (A_i - \sum_{j \in \bar{N}_i - \{j\}} B_{ij} K_{ij}), \quad \forall j \in \bar{N}_i \quad (3.37)$$

where  $P_{ij \in \bar{N}_i} \in \mathbb{R}^{6\bar{N}_i \times 6\bar{N}_i}$  are the solutions to coupled AREs solved by  $i$ th agent, namely

$$P_{ij} = C_i^T Q_{ij} C_i + K_{ij} R_j K_{ij} + (A_i - \sum_{j \in \bar{N}_i} B_{ij} K_{ij})^T P_{ij} (A_i - \sum_{j \in \bar{N}_i} B_{ij} K_{ij}), \quad \forall j \in \bar{N}_i \quad (3.38)$$

It should be noted that  $P_{ij}$  is the unique positive semi-definite solutions to  $j$ th coupled ARE given in (3.38) if and only if the pair  $(A_i - \sum_{j \in \bar{N}_i - \{j\}} B_{ij} K_{ij}, B_{ij})$  is stabilizable, and the pair  $(A_i - \sum_{j \in \bar{N}_i - \{j\}} B_{ij} K_{ij}, Q_{ij}^{1/2} C_i)$  is detectable.

As mentioned before, the control action which is implemented by  $i$ th agent is  $\delta u_i^*(k) = K_{ii} \bar{e}_i(k)$  and the rest of locally computed control actions are only used to control  $i$ th agent augmented error dynamics in open loop.

**Remark 3.9.** The solution to above-mentioned coupled algebraic Riccati equations are determined numerically using algorithms proposed in [110, 111].

## 3.5 Simulation Results

In this section, simulation results are presented to compare performance of the proposed control structures. The simulations are conducted for a team of five AUVs. The details on dynamical model parameters of each AUV are given in Table 3.1. Without loss of generality, the topology of semi-decentralized and decentralized structures is assumed to be a ring topology. Table 3.2 summarizes the initial state values for each agent. The desired formation configuration is presented in Table 3.3 that characterizes the straight line formation on the horizontal plane in which AUVs sweep along  $X$ -axis with desired surge velocity equal to  $1 \text{ m/s}$ . The effects of environmental disturbances due to irrotational ocean currents are all considered as

slowly varying drift forces acting on the input channels of each AUV along  $X$  and  $Y$  axes. The ocean current drift forces are produced according to the equation given in (2.20). In this model, the mean values of drift forces are initially assumed to be  $[4 \ 4 \ 0]^T N$ . Moreover,  $\omega_d$  is assumed to be zero-mean Gaussian white noise with standard deviation of  $\sigma_\omega = [5 \times 10^{-3} \ 5 \times 10^{-3} \ 0]^T N$ . The measurement noise is also modeled as zero-mean Gaussian white noise with standard deviation of  $\sigma_v = [5 \times 10^{-3} m \ 5 \times 10^{-3} m \ 5 \times 10^{-3} rad]^T$ .

The upper bound of the steady state tracking error is assumed to be  $J_x^s \approx 0.1$  to meet the precision requirements of potential underwater missions such as seabed mapping and pipeline inspection. The control parameters provided in Table 3.4 are chosen such that the effect of environmental disturbances are attenuated and the steady state design specification are satisfied. Moreover, the performance of all control schemes are evaluated according to the performance measures provided in Table 3.5.

It is worth noting that simulations are conducted in MATLAB on a computer equipped with 4-cored processor operating at 1.6 GHz, and is managed by 64-bit operating system.

**Table 3.1:** AUV Parameters [3]

Total mass and inertia matrix	M=diag [200 250 80] <i>kg</i>
Linear drag matrix	D=diag [170 100 50] <i>N.s/m</i>
X-axes and Y-axes maximum thruster force	400 <i>N</i>
Yaw-axes maximum thruster torque	100 <i>N.m</i>
Sampling time	0.2 <i>sec</i>

**Table 3.2:** Initial Conditions

	$[p_x(0) \ p_y(0) \ p_\psi(0) \ v_u(0) \ v_v(0) \ v_r(0)]^T$
AUV <sub>1</sub>	$[0.2 \ 0.3 \ \frac{\pi}{15} \ 0 \ 0 \ 0]^T$
AUV <sub>2</sub>	$[0.3 \ 0.3 \ \frac{\pi}{20} \ 0 \ 0 \ 0]^T$
AUV <sub>3</sub>	$[0.25 \ 0.3 \ \frac{\pi}{15} \ 0 \ 0 \ 0]^T$
AUV <sub>4</sub>	$[0.25 \ 0.25 \ \frac{\pi}{20} \ 0 \ 0 \ 0]^T$
AUV <sub>5</sub>	$[0.25 \ 0.3 \ \frac{\pi}{20} \ 0 \ 0 \ 0]^T$

**Table 3.3:** Desired Formation Configuration

$(p_{x_{12}}^*, p_{y_{12}}^*, p_{\psi_{12}}^*)$	$(p_{x_{23}}^*, p_{y_{23}}^*, p_{\psi_{23}}^*)$	$(p_{x_{34}}^*, p_{y_{34}}^*, p_{\psi_{34}}^*)$	$(p_{x_{45}}^*, p_{y_{45}}^*, p_{\psi_{45}}^*)$	$(p_{x_{51}}^*, p_{y_{51}}^*, p_{\psi_{51}}^*)$
(0, 2, 0)	(0, 2, 0)	(0, -6, 0)	(0, -2, 0)	(0, 4, 0)

**Table 3.4:** Controller Parameters

	MPC-based	Game-based
Output penalty matrix $Q_{i \in \mathcal{V}}$	$10^5 \times I_{3 \times 3}$	$10^5 \times I_{3 \times 3}$
Control penalty matrix $R_{i \in \mathcal{V}}$	$I_{3 \times 3}$	$10 \times I_{3 \times 3}$
Prediction Horizon $N_p$	9	
Control horizon $N_c$	1	

**Table 3.5:** Performance Measures

Tracking error cost	$J_x = \sum_{i \in \mathcal{V}} \frac{1}{40} \int_0^{40} \ x_i(t) - x_i^*(t)\ ^2 dt$
Formation error cost	$J_{\tilde{x}} = \sum_{i \in \mathcal{V}} \sum_{j \in \mathcal{V} - \{i\}} \frac{1}{40} \int_0^{40} \ x_{ij}(t) - x_{ij}^*\ ^2 dt$
Steady state tracking error	$J_x^s = \sum_{i \in \mathcal{V}} \ x_i(40) - x_i^*(40)\ $
Steady state formation error	$J_{\tilde{x}}^s = \sum_{i \in \mathcal{V}} \sum_{j \in \mathcal{V} - \{i\}} \ x_{ij}(40) - x_{ij}^*\ $
Control Cost	$J_u = \sum_{i \in \mathcal{V}} \frac{1}{40} \int_0^{40} \ \delta u_i(t)\ ^2 dt$
Total Cost	$J_{total} = \sum_{i \in \mathcal{V}} \int_0^{40} \ (x_i(t) - x_i^*(t))\ ^2 + \left\  \sum_{j \in \mathcal{V} - \{i\}} (x_{ij}(t) - x_{ij}^*) \right\ ^2 dt$

### 3.5.1 Comparison of Centralized, Semi-Decentralized, and Decentralized MPC-Based Control Schemes

In this subsection, the performance of centralized, semi-decentralized, and decentralized MPC-based controllers are investigated. The position errors along  $X$ -axis and  $Y$ -axis, orientation errors along  $Z$ -axis, surge velocity errors, and thruster forces along  $X$ -axis are depicted in Figures 3.4, 3.5, 3.6, 3.7, and 3.8, respectively. Moreover, performance measures and time response characteristics are quantitatively reported in Table 3.6.

Based on the values of tracking and formation keeping costs given in Table 3.6, the centralized scheme has the lowest  $J_x$  and  $J_{\tilde{x}}$  values, and the corresponding cost values obtained by semi-decentralized scheme are less than the decentralized scheme. Based on the obtained results for steady-state cost values, it can be observed that the semi-decentralized scheme has the lowest steady state error among all schemes, and the steady state error of centralized scheme is less than the decentralized scheme. Moreover, the settling time characteristics of centralized and decentralized schemes

are relatively close to each other, and the settling time characteristics of decentralized scheme are noticeably worst than all other schemes. In the centralized control scheme, lower total cost value is obtained which is due to solving global optimization problem for the entire team, and after that the semi-decentralized scheme has lower total cost value than the decentralized scheme.

To summarize above-mentioned observations, we can conclude that the transient performance of centralized scheme is superior to the semi-decentralized and the decentralized schemes, but at the cost of higher control effort. However, the steady-state characteristics obtained by semi-decentralized scheme is better than two other schemes. Another positive aspect of semi-decentralized scheme is that it can achieve acceptable performance close to centralized scheme while requiring lower control effort cost, and computation and communication loads.

**Table 3.6:** Performance and Time Response Evaluation of Centralized, Semi-Decentralized, and Decentralized MPC-Based Control Schemes

	Centralized MPC	Semi-Decentralized MPC	Decentralized MPC
$J_x$	2.52	2.58	3.82
$J_{\tilde{x}}$	56.8	58.5	61
$J_x^s$	0.13	0.10	1.38
$J_{\tilde{x}}^s$	$3.0e - 05$	$8.6e - 09$	$2.5e - 05$
$J_u$	$2.9e + 04$	$2.5e + 04$	$2.6e + 04$
$J_{total}$	$1.18e + 04$	$1.22e + 04$	$1.29e + 04$
$t_s$	15.4	15.8	22
$\tilde{t}_s$	9.7	7	12
$t_{solve}$	0.53	0.06	0.25

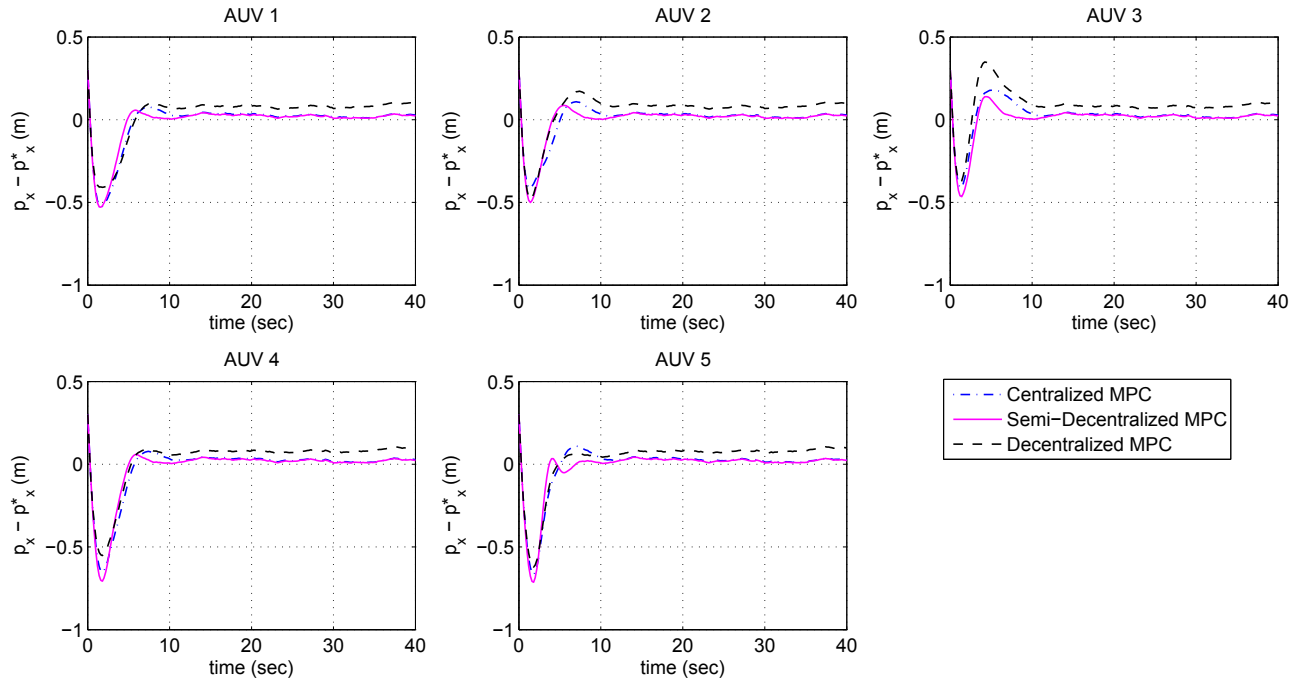


**Figure 3.4:** Error Signals Along  $X$ -axis for Cenetralized, Semi-Decentralized, and Decen-  
tralized MPC-Based Control Schemes

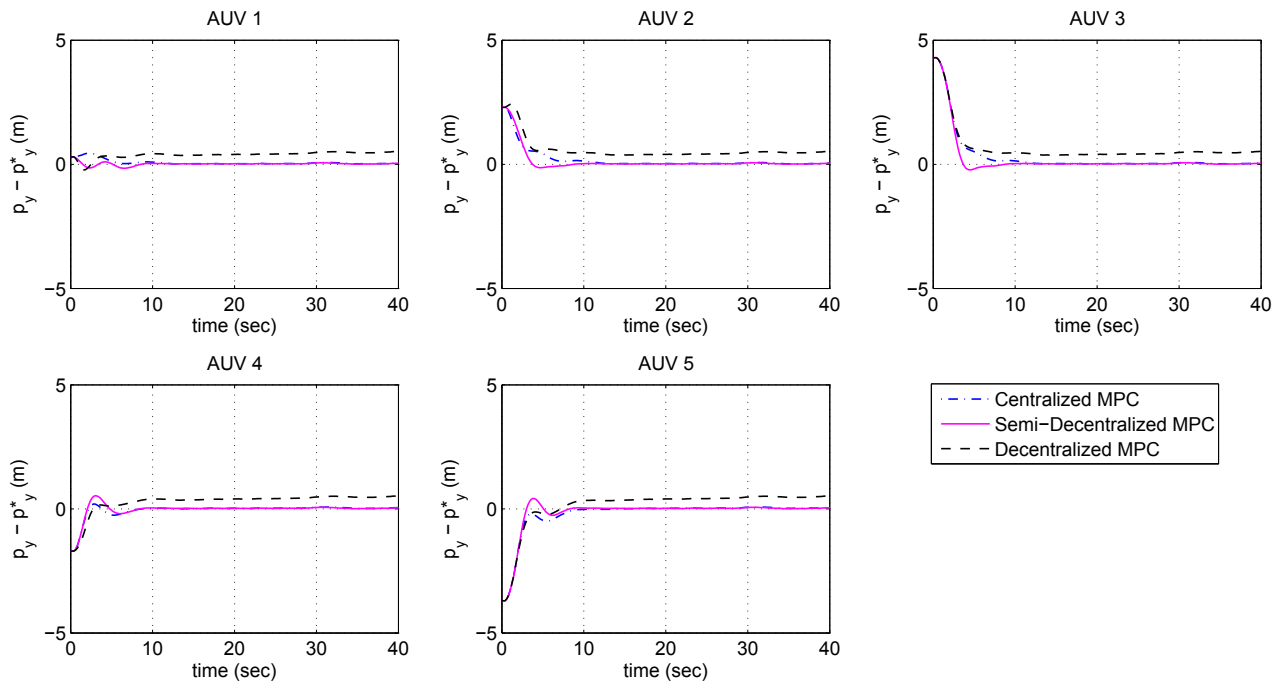


**Figure 3.5:** Error Signals Along  $Y$ -axis for Cenetralized, Semi-Decentralized, and Decen-  
tralized MPC-Based Control Schemes

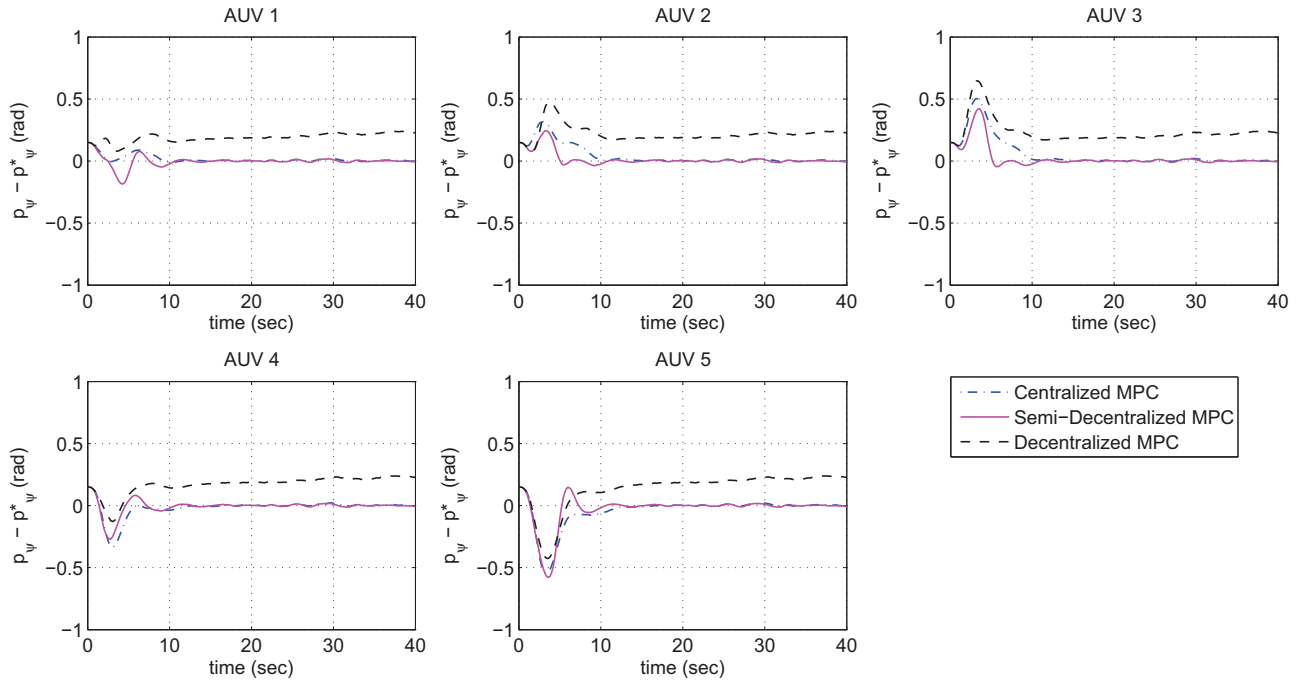


**Figure 3.6:** Error Signals about Z-axis for Cenetralized, Semi-Decentralized, and Decen-tralized MPC-Based Control Schemes

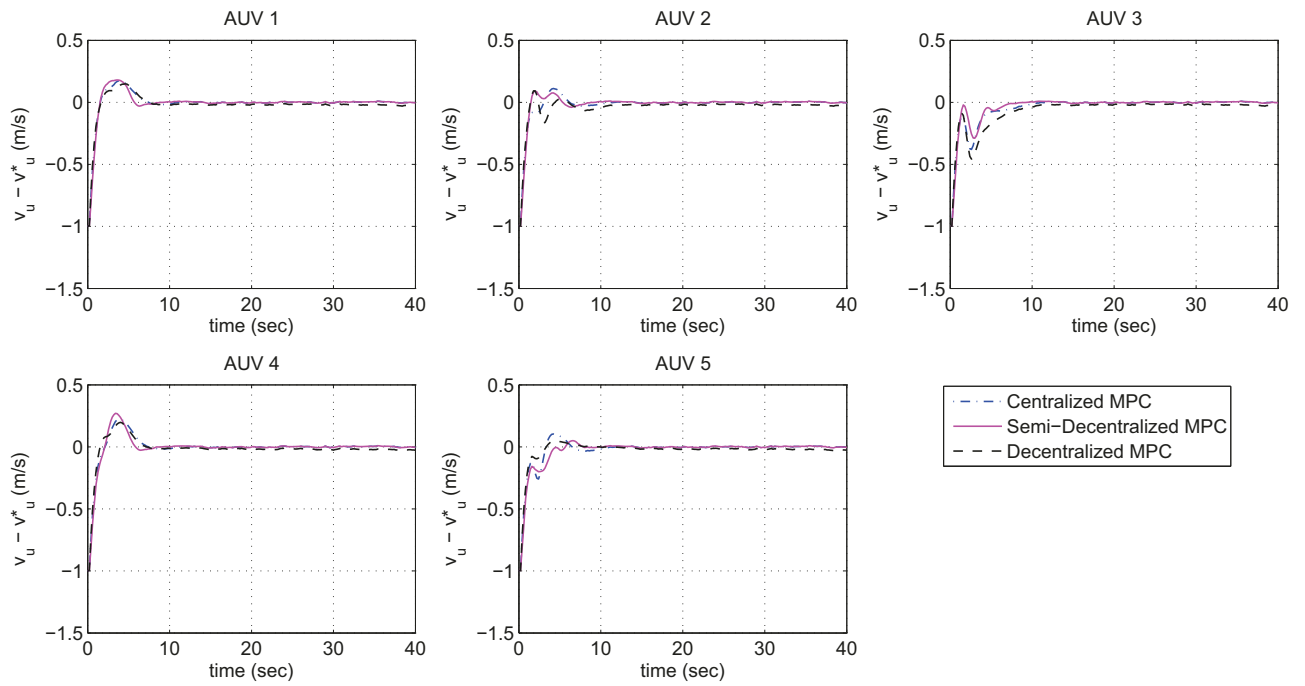


**Figure 3.7:** Surge Velocity Error Signals for Cenetralized, Semi-Decentralized, and Decen-tralized MPC-Based Control Schemes

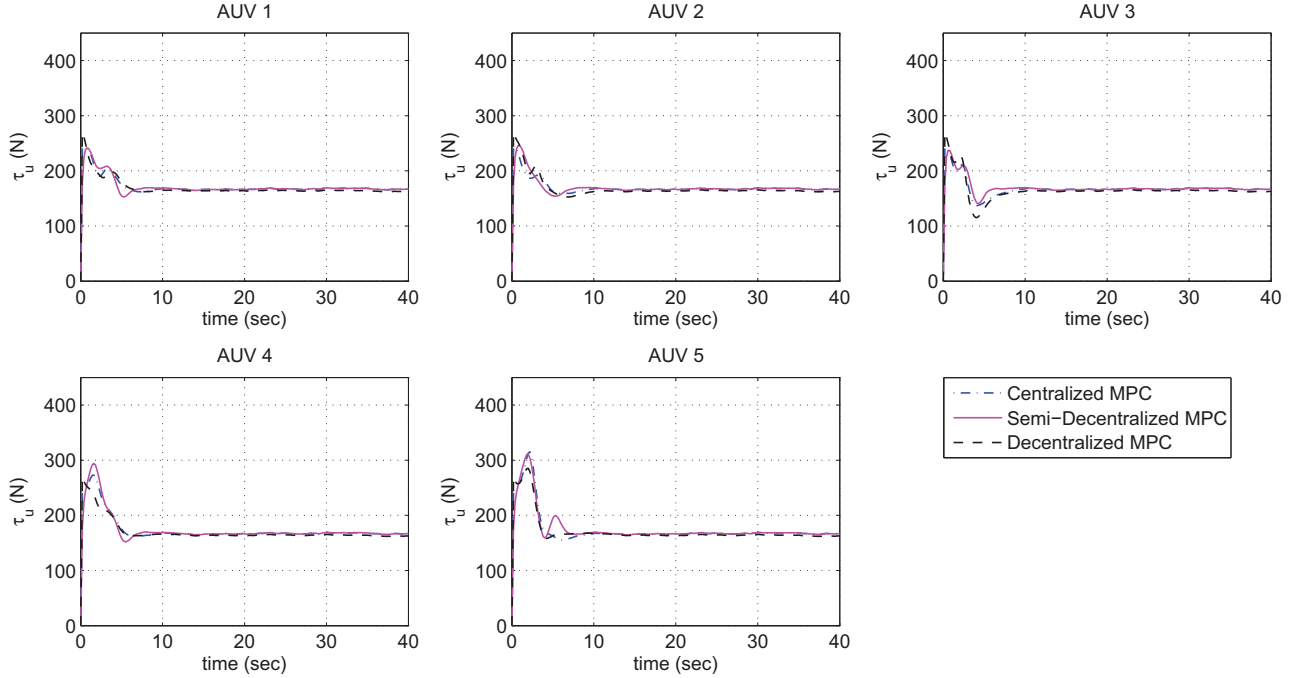


**Figure 3.8:** Thruster Forces along  $X$ -axis for Cenetralized, Semi-Decentralized, and Decentralized MPC-Based Control Schemes

### 3.5.2 Comparison of Centralized, Semi-Decentralized, and Decentralized Control Schemes Based on Non-Cooperative Dynamic Game

In this subsection, the performance of centralized, semi-decentralized, and decentralized schemes based on non-cooperative dynamic game approach are demonstrated. The position errors along  $X$ -axis and  $Y$ -axis, orientation errors along  $Z$ -axis, surge velocity errors, and thruster forces along  $X$ -axis are depicted in Figures 3.9, 3.10, 3.11, 3.12, and 3.13, respectively. Moreover, the performance measures and time response characteristics are evaluated and summarized in Table 3.7.

By comparing the evaluated tracking and formation keeping cost values, it can be observed that lower  $J_x$  and  $J_{\hat{x}}$  are obtained in the centralized scheme, and after that the semi-decentralized scheme has lower tracking and formation keeping cost

values than the decentralized scheme. Moreover, the steady-state tracking error cost  $J_x^s$  obtained by semi-decentralized controller is less than two other schemes, and its steady-state formation keeping error  $J_x^s$  is very close to centralized scheme and extremely lower than the decentralized scheme. It can be also seen that the settling time of formation keeping error in the centralized scheme is lower than two other schemes. However, the semi-decentralized scheme has the lowest tracking error settling time. The lowest total cost value is obtained in the centralized scheme which is due to considering the global team dynamics in the minimization problem of each agent, and it is lower in the semi-decentralized scheme in comparison to decentralized scheme.

Finally, we can conclude from above-mentioned observations that the overall performance of centralized scheme is better than the two other schemes, but at the cost of higher control effort. The superiority of centralized scheme is especially more visible in its formation keeping behavior. However, the tracking performance and the corresponding time response characteristics of semi-decentralized scheme are very close to centralized scheme while requiring lower control effort and communication load. Moreover, the increase in total cost value of semi-decentralized scheme as a result of reduction in communication load is quite negligible as compared to centralized scheme.

**Table 3.7:** Performance and Time Response Evaluation of Centralized, Semi-Decentralized, and Decentralized Control Schemes based on Non-Cooperative Dynamic Game

	Centralized Non-Cooperative	Semi-Decentralized Non-Cooperative	Decentralized Non-Cooperative
$J_x$	1.89	1.92	2.04
$J_{\tilde{x}}$	43.7	44.8	46.1
$J_x^s$	0.07	0.06	0.10
$J_{\tilde{x}}^s$	$1.8e - 13$	$7.7e - 12$	0.01
$J_u$	$8.2e + 04$	$5.2e + 04$	$4.1e + 04$
$J_{total}$	$9.1e + 03$	$9.3e + 03$	$9.6e + 03$
$t_s$	15	14.5	17.8
$\tilde{t}_s$	4.4	5.1	6.8
$t_{Iter}$	43	34	37

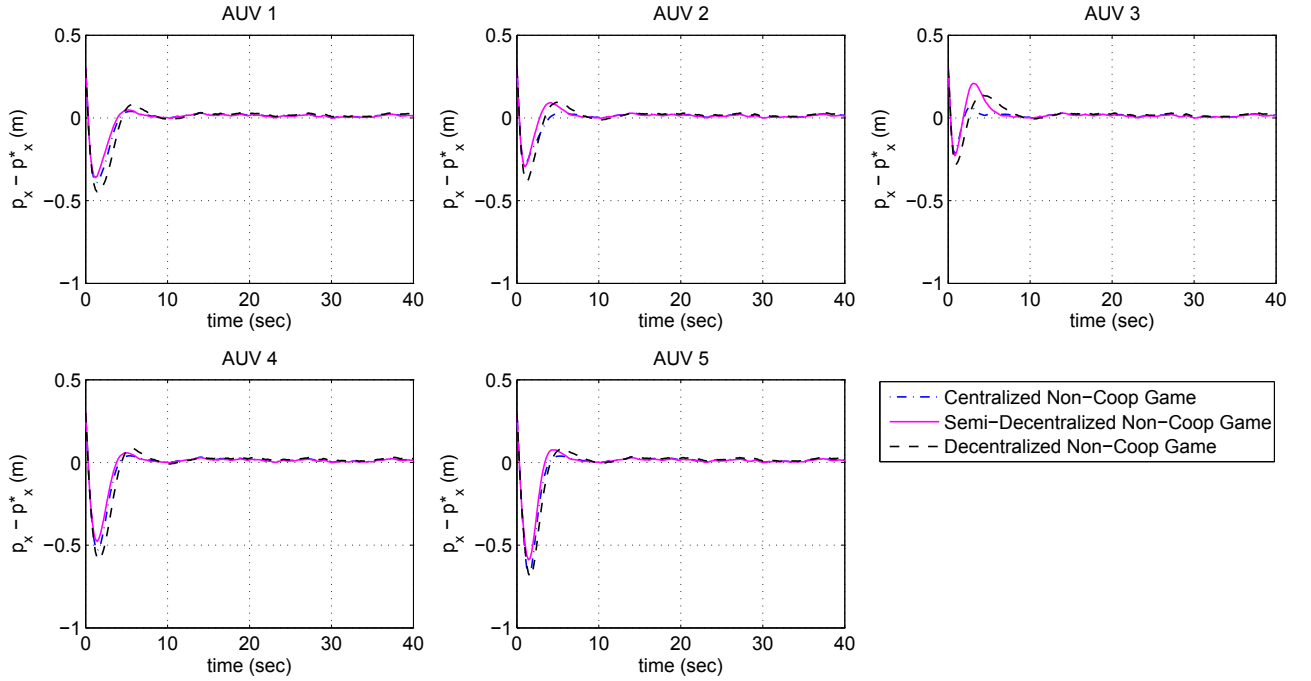


**Figure 3.9:** Error Signals Along  $X$ -axis for Centralized, Semi-Decentralized, and Decentralized Control Schemes Based on Non-Cooperative Dynamic Game

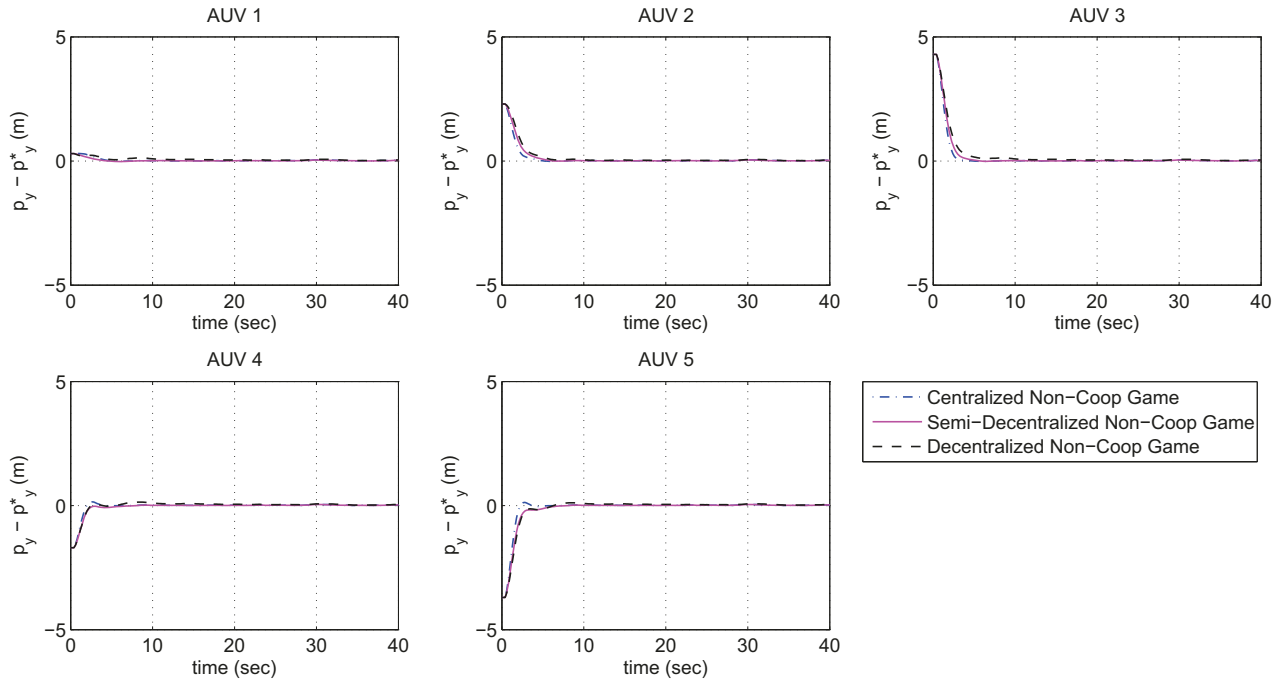


**Figure 3.10:** Error Signals Along Y-axis for Centralized, Semi-Decentralized, and Decentralized Control Schemes Based on Non-Cooperative Dynamic Game

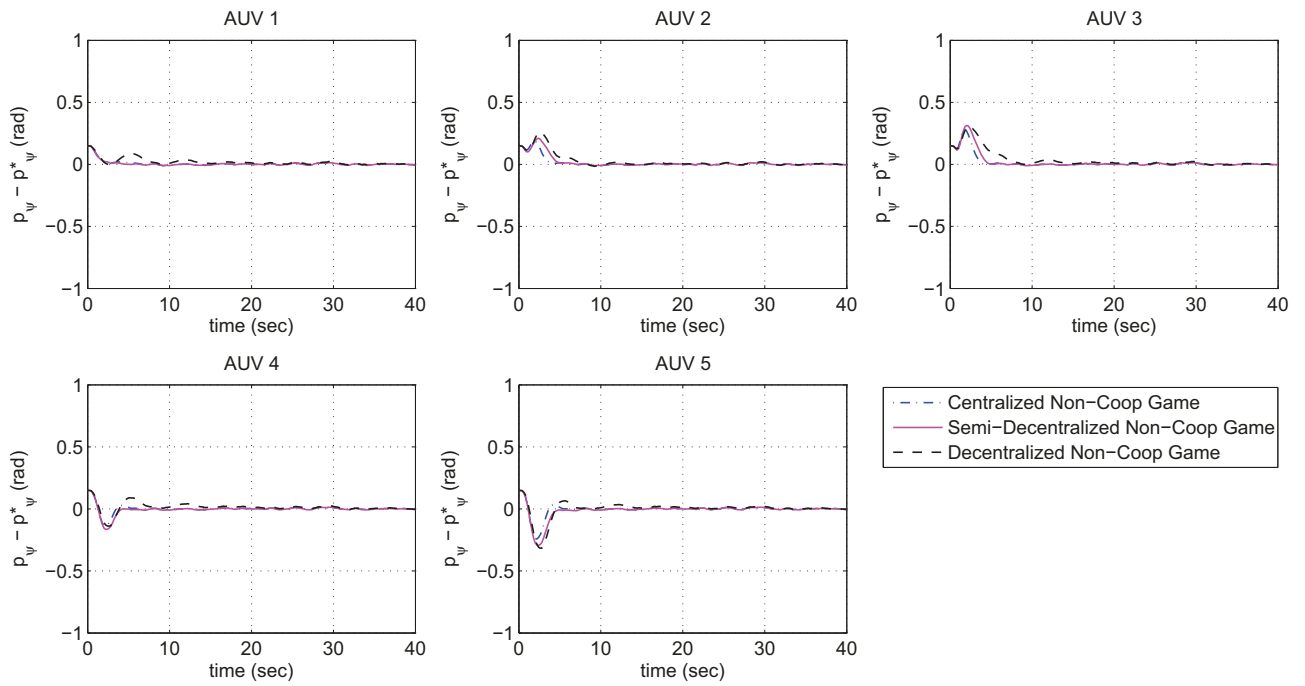


**Figure 3.11:** Yaw Angle Error Signals about Z-axis for Centralized, Semi-Decentralized, and Decentralized Control Schemes Based on Non-Cooperative Dynamic Game

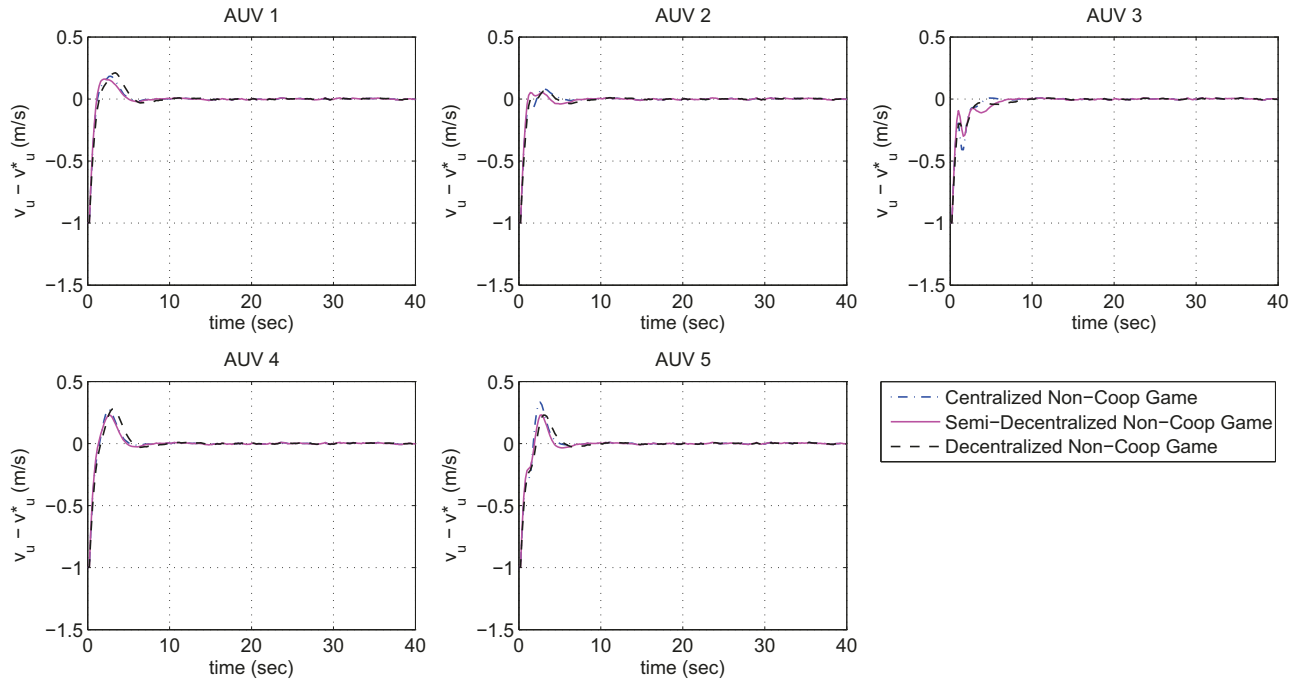


**Figure 3.12:** Surge Velocity Error Signals for Centralized, Semi-Decentralized, and Decentralized Control Schemes Based on Non-Cooperative Dynamic Game

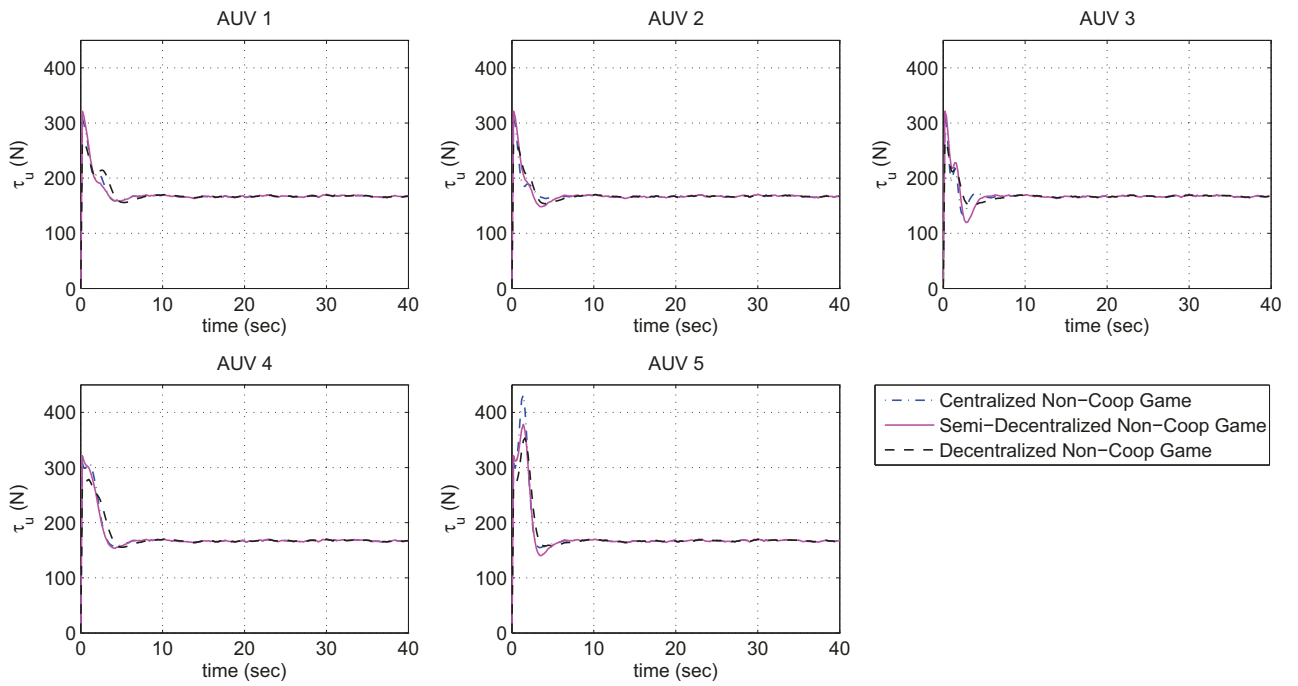


**Figure 3.13:** Thruster Forces along  $X$ -axis for Centralized, Semi-Decentralized, and Decentralized Control Schemes Based on Non-Cooperative Dynamic Game

### 3.5.3 Centralized Cooperative Dynamic Game vs. Centralized Non-Cooperative Dynamic Game

In this subsection, the effectiveness of both cooperative and non-cooperative dynamic game approaches to centralized control is investigated. The position errors along  $X$ -axis and  $Y$ -axis, orientation error along  $Z$ -axis, surge velocity error, and thruster force along  $X$ -axis are depicted in Figures 3.14, 3.15, 3.16, 3.17, and 3.18, respectively. Moreover, the cost performance and time response characteristics are reported in Table 3.8.

Based on the quantitative results provided in Table 3.8, it can be observed that the formation keeping cost  $J_x$  of centralized cooperative scheme is lower than the non-cooperative scheme, while its tracking cost  $J_x$  is higher than that of non-cooperative scheme. The same behavior can be seen in the obtained results associated with steady-state tracking and formation keeping errors of both schemes. Moreover, the cooperative scheme has lower formation keeping settling time, while it has higher tracking settling time than the non-cooperative scheme which indicates that agents in the non-cooperative centralized scheme achieve tracking behavior prior to formation keeping, but the resulting behavior in cooperative scheme is reversed. The featuring point of cooperative scheme is that it has lower total cost value than its non-cooperative counterpart which is due to solving global minimization problem with one global team cost.

To summarize the aforementioned observations, we can conclude that the cooperative centralized scheme can achieve higher accuracy in term of formation keeping and cooperative performance, whereas the non-cooperative centralized scheme can obtain higher accuracy in terms of tracking performance.

**Table 3.8:** Performance and Time Response Evaluation Between Cooperative and Non-Cooperative Dynamic Game Approaches to Centralized Control

	Centralized Non-Cooperative	Centralized Cooperative
$J_x$	1.8	1.9
$J_{\dot{x}}$	43.7	43.3
$J_x^s$	0.07	0.14
$J_{\dot{x}}^s$	$1.8e - 13$	$3.8e - 15$
$J_u$	$8.2e + 04$	$9.4e + 04$
$J_{total}$	$9.11e + 03$	$9.05e + 03$
$t_s$	15	18
$\tilde{t}_s$	4.4	4.2
$t_{Iter}$	43	50

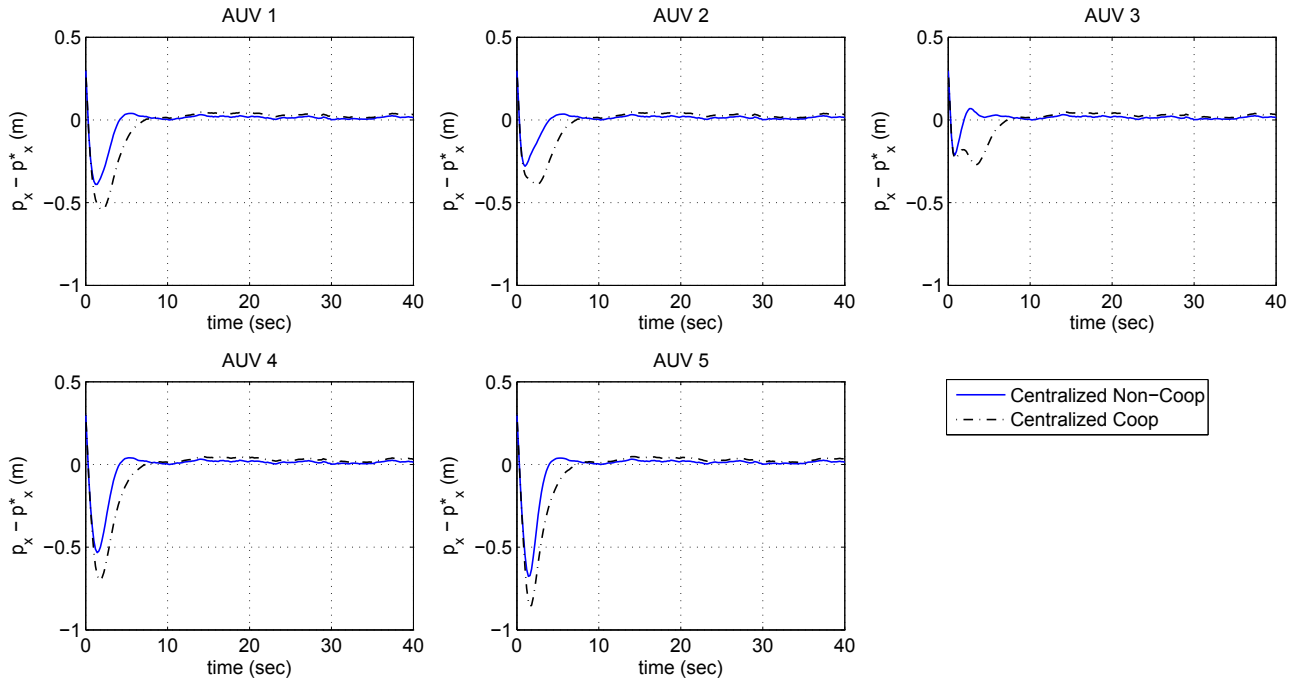


**Figure 3.14:** Error Signals Along X-axis for Centralized Control Scheme Based on Cooperative and Non-Cooperative Dynamic Game

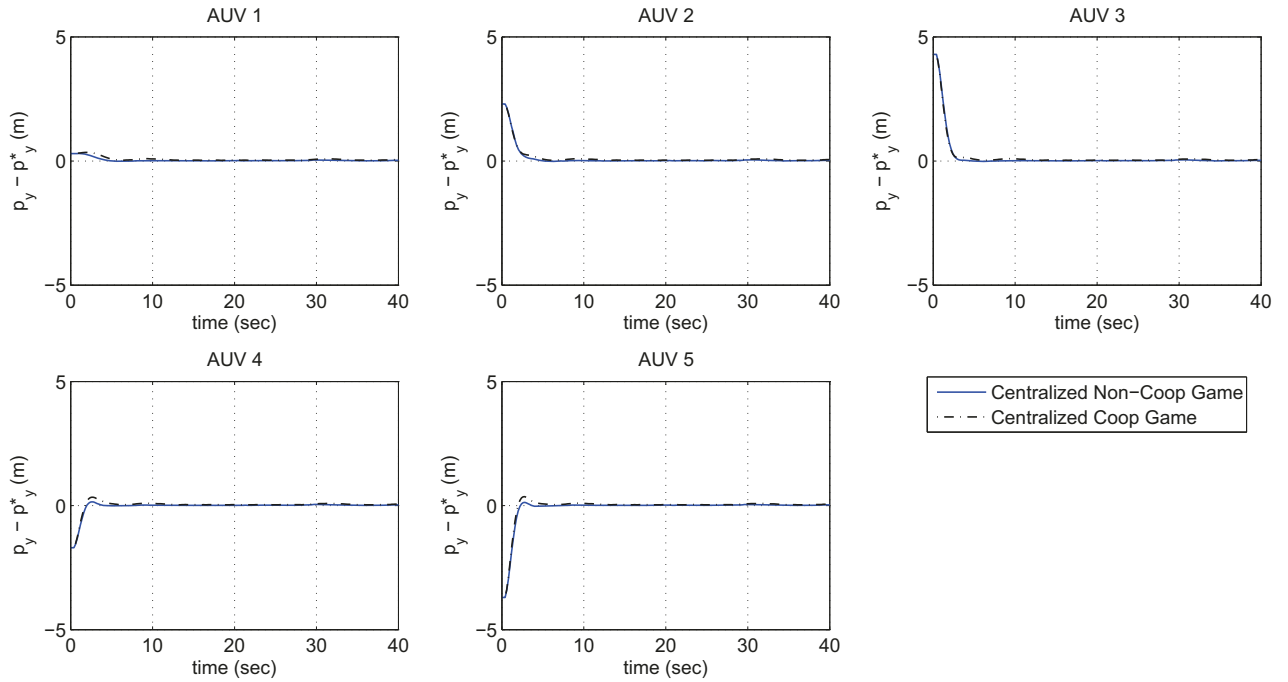


**Figure 3.15:** Error Signals Along Y-axis for Centralized Control Scheme Based on Cooperative and Non-Cooperative Dynamic Game

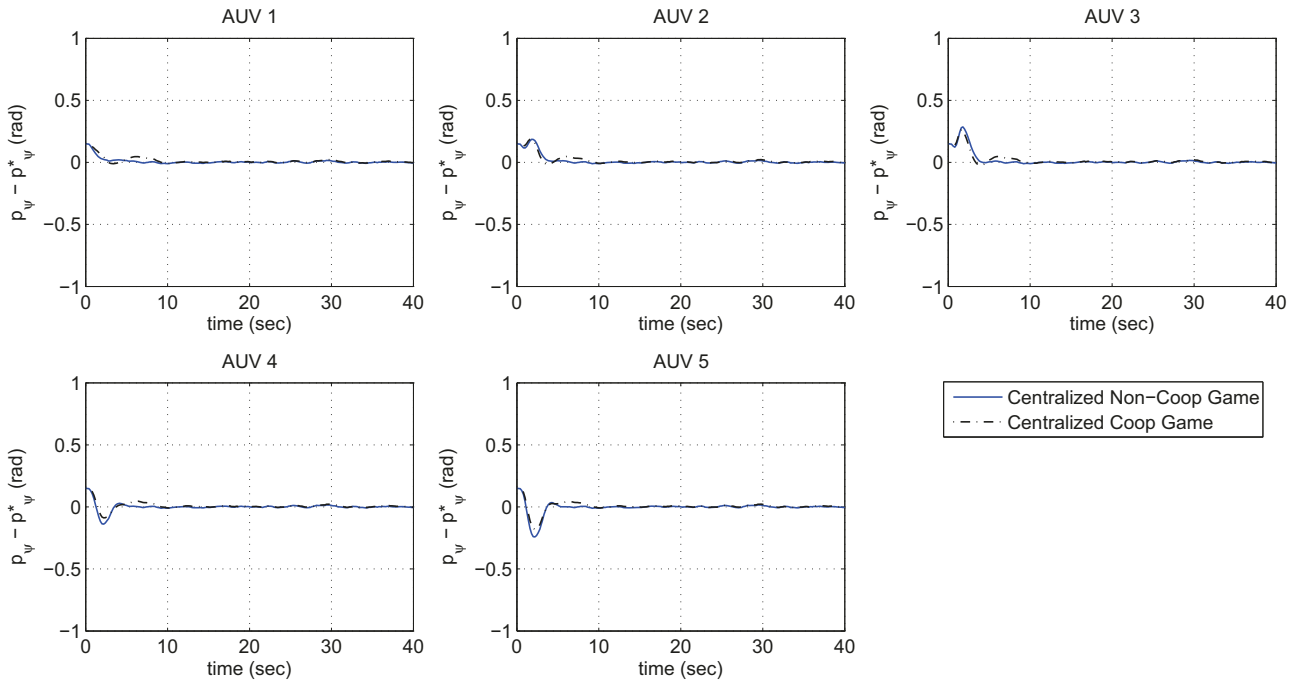


**Figure 3.16:** Error Signals about Z-axis for Centralized Control Scheme Based on Cooperative and Non-Cooperative Dynamic Game

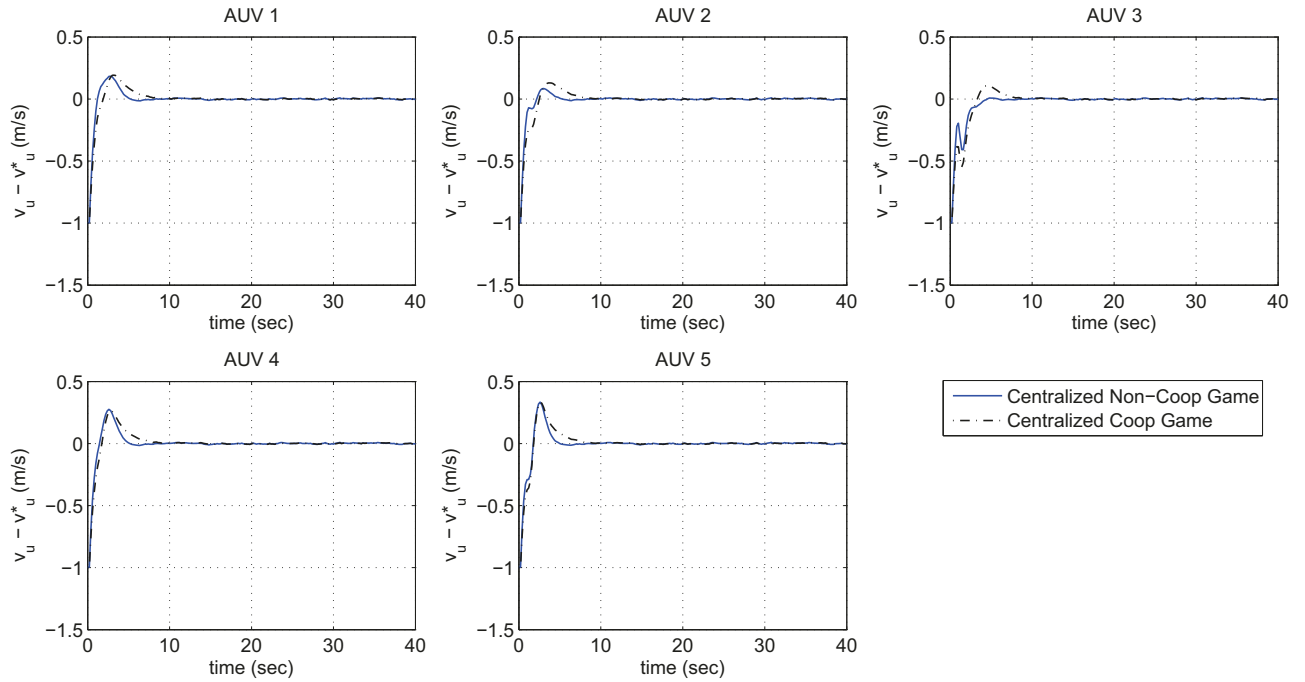


**Figure 3.17:** Surge Velocity Error Signals for Centralized Control Scheme Based on Cooperative and Non-Cooperative Dynamic Game

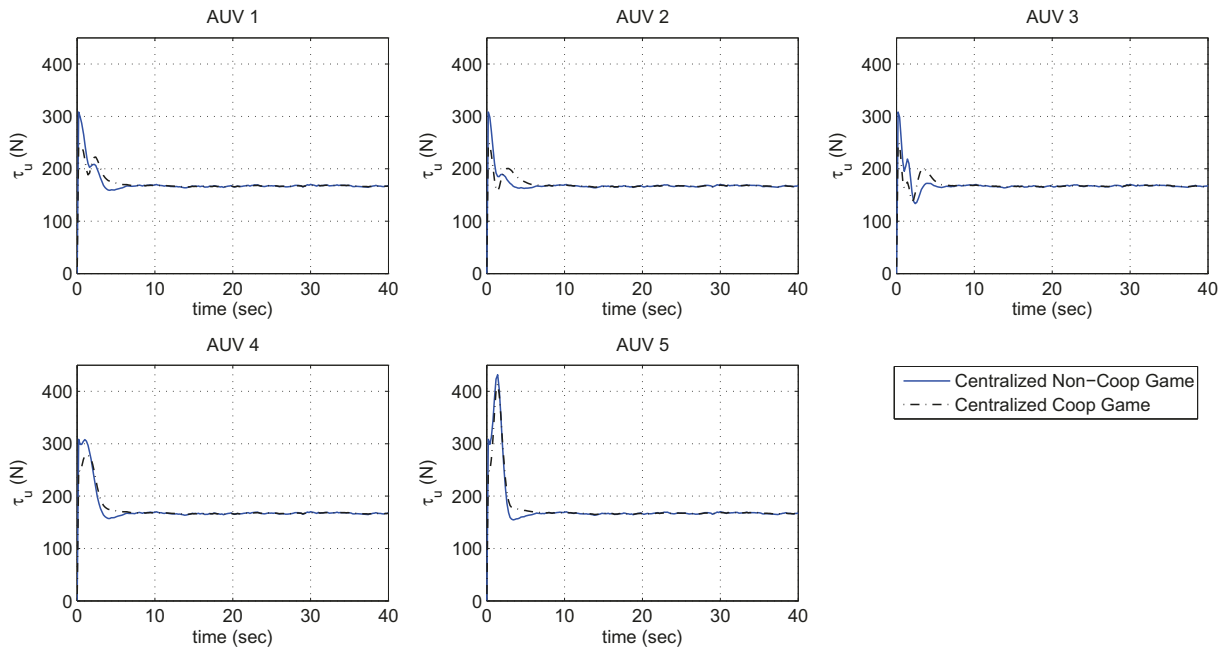


**Figure 3.18:** Thruster Forces along X-axis for Centralized Control Scheme Based on Cooperative and Non-Cooperative Dynamic Game

## 3.6 Summary

In this chapter, three cooperative control schemes, namely centralized, semi-decentralized, and decentralized control schemes are developed. In each one of control schemes, we first adopt an optimal control approach, namely the MPC technique to solve the tracking and formation keeping control problems for a team of autonomous agents. Next, we exploit from dynamic game theory to design controller that can fulfill aforementioned objectives for a team of autonomous agents. At the end of the chapter, a set of comparative simulation studies are conducted on a team of autonomous underwater vehicles to demonstrate the effectiveness and to highlight pros and cons of the proposed control schemes. Table 3.9 summarizes all the quantitative results we have obtained in this chapter. Furthermore, the following conclusions briefly state our obtained results.

The transient behavior of MPC-based centralized scheme according to the tracking and formation keeping costs, i.e.  $J_x$  and  $J_{\bar{x}}$  is shown to be the best in comparison to two other MPC-based schemes. Similarly, the dynamic game-based centralized scheme has also the best tracking and formation keeping performance as compared to other dynamic game-based schemes. More precisely, the centralized non-cooperative scheme has the best tracking performance, and the centralized cooperative scheme has the best formation keeping performance. It should be noted that better transient performance obtained by centralized scheme is at the cost of higher control effort; however, both MPC-based and dynamic game-based semi-decentralized schemes can achieve the transient performance very close to centralized scheme with lower control effort cost.

The steady-state behavior of MPC-based semi-decentralized scheme according to steady-state tracking and formation keeping costs, i.e.  $J_x$  and  $J_{\bar{x}}$  is shown to be the

best as compared to other MPC-based schemes. Moreover, in dynamic game framework, the steady-state tracking error of semi-decentralized scheme is also better than other dynamic game-based schemes. However, the centralized cooperative scheme leads to the lowest steady-state formation keeping error as compared to all other schemes.

The tracking error settling time characteristics of both centralized and semi-decentralized MPC-based schemes are very close to each other, and also much lower than the decentralized scheme. However, the semi-decentralized scheme has the lowest formation keeping settling time among all other schemes. In the dynamic game framework, the centralized and semi-decentralized game-based schemes have also lower values for settling time of tracking error. However, the centralized cooperative framework obtained lower settling time associated with formation keeping error.

In both MPC and dynamic game frameworks, lowest total cost values are obtained by centralized schemes. This feature is due to solving global minimization problem for the entire team.

The final conclusion that can be derived from these results is that the proposed semi-decentralized controller provides a satisfactory performance as compared to the centralized controller while imposing less amount of communication and computation loads on the team members. Furthermore, the semi-decentralized controller is more reliable as compared to its decentralized counterpart.

**Table 3.9:** Summary of Performance and Time Response Characteristics of Centralized, Semi-Decentralized, and Decentralized Control Schemes

	MPC			Dynamic Game			
	Centralized	Semi-Decentralized	Decentralized	Non-Cooperative			
				Cooperative	Centralized	Semi-Decentralized	Decentralized
$J_x$	2.52	2.58	3.82	1.97	1.89	1.92	2.04
$J_{\tilde{x}}$	56.8	58.5	61	43.3	43.7	44.8	46.1
$J_x^s$	0.13	0.10	1.38	0.14	0.07	0.06	0.10
$J_{\tilde{x}}^s$	$3.0e - 05$	$8.6e - 09$	$2.5e - 05$	$3.8e - 15$	$1.8e - 13$	$7.7e - 12$	0.01
$J_u$	$2.9e + 04$	$2.5e + 04$	$2.6e + 04$	$9.4e + 04$	$8.2e + 04$	$5.2e + 04$	$4.1e + 04$
$J_{total}$	$1.18e + 04$	$1.22e + 04$	$1.29e + 04$	$9.05e + 03$	$9.11e + 03$	$9.34e + 03$	$9.63e + 03$
$t_s$	15.4	15.8	22	18.4	15	14.5	17.8
$\tilde{t}_s$	9	7	12	4.2	4.4	5.1	6.8
$t_{solve}, t_{Iter}$	0.53	0.06	0.25	50	43	34	37

## Chapter 4

# Centralized, Semi-Decentralized, and Decentralized Fault Accommodation of Autonomous Vehicle Formations

### 4.1 Introduction

In this chapter, active fault accommodation mechanisms are developed in accordance with each one of control design structures introduced in previous chapter, namely centralized, semi-decentralized, and decentralized control structures.

If any agent in the team becomes faulty, not only the tracking performance of faulty agent will be deteriorated but also it can cause tracking and formation keeping performance deterioration of healthy agents and the entire team. The impact of faulty agent on the performance of the entire team depends on the level of couplings considered to derive control strategy for each individual. Therefore, it is crucial to develop proper fault recovery mechanism based on the allowable amount of information transmitted among agents such that the team objectives can be still achieved with

acceptable performance. In this regard, we intend to incorporate on-line fault information provided by FDI module to design active fault accommodation mechanisms. In the centralized accommodation mechanism, the fault information of all agents are involved in the recovery process. In the semi-decentralized accommodation mechanism, fault information is exchanged among neighboring agents. Therefore, faulty individual and its neighbors are involved in fault accommodation process. On the contrary, in the decentralized accommodation mechanism, no fault information is exchanged, and faulty agent is recovered independently.

The focus of this chapter is on loss of effectiveness actuator fault. We also consider imperfections in the FDI module, namely FDI fault estimation error and FDI time delay while developing active fault accommodation mechanisms. At the end of the chapter, simulations are conducted on a team of AUVs to show the effectiveness of proposed fault accommodation mechanisms.

## 4.2 Centralized Fault Accommodation

In this section, centralized active fault accommodation mechanism is developed in which a central unit is connected to all agents and receives fault information from their FDI modules to derive the accommodated controllers for each agent. In the forthcoming subsections, the MPC technique and dynamic game theory are utilized to recover the team from LOE actuator fault.

To this end, redesigning the controller must be performed based on faulty system dynamics. Let us consider the state equation associated with  $i$ th agent with LOE actuator fault as

$$x_i(k+1) = Ax_i(k) + B\Gamma_i u_i(k) \quad (4.1a)$$

$$z_i(k) = Ce_i(k) \quad (4.1b)$$

where  $\Gamma_i \in R^{3 \times 3}$  is the control effectiveness matrix of  $i$ th agent. Then, in the same way as in previous chapter, the centralized error dynamics of  $i$ th agent under faulty condition becomes

$$e_i(k+1) = A e_i(k) + \sum_{j \in \mathcal{V}} w_{ij} B \Gamma_j \delta u_j(k) \quad (4.2a)$$

$$z_i(k) = C e_i(k) \quad (4.2b)$$

where the control input error variable of  $i$ th agent is  $\delta u_i = u_i - \frac{u^*}{\Gamma_i}$ . Finally, the augmented centralized formation error dynamics which is developed in (3.6) can be rewritten as

$$E(k+1) = \bar{A} E(k) + \bar{B} \Gamma \delta U \quad (4.3a)$$

$$Z(k) = \bar{C} E(k) \quad (4.3b)$$

where  $\Gamma = \text{blkdiag}\{\dots \Gamma_i \dots\} \in R^{3N_v \times 3N_v}$ .

### 4.2.1 Model Predictive Control Approach to Centralized Fault Accommodation

In this subsection, the previously introduced MPC-based centralized controller is accommodated based on the centralized faulty error dynamics introduced in (4.3) and the centralized finite horizon team cost given in (3.8). The following problem formally states this scenario.

**Problem 4.1.** At each sampling time  $t_k \in [t_f + t_d, \infty)$ , given the current augmented formation error vector  $E(k)$  as well as the fault information estimates provided by FDI module of all agents, namely  $\hat{\Gamma}$ , find the entire formation accommodated control input sequence  $\delta \tilde{U}(k) = [\delta U(k)^T, \delta U(k+1)^T, \dots, \delta U(k+N_c-1)^T]^T$  as the solution

to the following constrained finite time optimal control problem

$$\min_{\delta\tilde{U}} J_c(Z(k), \delta\tilde{U}(k)) =: \quad (4.4a)$$

$$\min_{\delta\tilde{U}} \sum_{h=0}^{N_p-1} \left\{ \|Z(h|k)\|_Q^2 + \|\delta U(h|k)\|_R^2 \right\} + \|E(N_p|k)\|_{Q_N}^2$$

s.t.

$$E(h+1|k) = \bar{A}E(h|k) + \bar{B}\hat{\Gamma}\delta U(h|k) \quad (4.4b)$$

$$Z(h|k) = \bar{C}E(h|k) \quad h = 0, 1, \dots, N_p - 1 \quad (4.4c)$$

$$\delta U_{min}^f \leq \delta U(h|k) \leq \delta U_{max}^f \quad h = 0, 1, \dots, N_c - 1 \quad (4.4d)$$

$$\delta U(h|k) = \delta U(N_c - 1|k) \quad N_c \leq h \leq N_p - 1 \quad (4.4e)$$

$$\tilde{V}_u E(k + N_p) = 0 \quad (4.4f)$$

where  $t_f$  is the time instant in which the fault has occurred, and  $t_d$  is the time takes for FDI module to detect and identify the fault, and then activates control accommodation mechanism. The matrix  $\hat{\Gamma} \in \mathbb{R}^{3N_v \times 3N_v}$  is the estimate of control effectiveness matrix  $\Gamma$  provided by FDI module of all agents. Moreover,  $N_c$  and  $N_p$  are the control horizon and the prediction horizon, respectively. In order to decrease the computational complexity, the control horizon is selected to be less than the prediction horizon. The output penalty matrix  $Q = blkdiag\{Q_{i \in \mathcal{V}}\} \in \mathbb{R}^{3N_v \times 3N_v}$  and terminal state penalty matrix  $Q_N \in \mathbb{R}^{6N_v \times 6N_v}$  are positive semi-definite, and the input penalty matrix  $R = blkdiag\{R_{i \in \mathcal{V}}\} \in \mathbb{R}^{3N_v \times 3N_v}$  is positive definite. The triple  $(\bar{A}, \bar{B}\hat{\Gamma}, \bar{C})$  considered in the faulty prediction model is both controllable and observable with  $3N_v$  unstable modes on the unit circle. In order to ensure stability of closed loop system, the terminal equality constraint (4.4f) associated with unstable modes and the terminal penalty matrix  $Q_N$  are computed as explained in Theorem 2.1.

## 4.2.2 Non-Cooperative Dynamic Game Approach to Centralized Fault Accommodation

In this subsection, the previously introduced centralized controller based on non-cooperative dynamic game is accommodated and redesigned using the fault estimates provided by FDI module of all agents. In this case, infinite horizon cost of all agents as given in (3.10) are simultaneously minimized considering the centralized faulty error dynamics presented in (4.3). Finally, the accommodated control actions of all agents will constitute an irrevocable set known as Nash equilibrium. As a result, each agent can obtain minimum cost value while considering the effects of accommodated control actions pursued by all other agents. The following problem formally states this scenario.

**Problem 4.2.** For non-cooperative nonzero-sum dynamic game of  $N_v$  agents with fully connected information exchange topology, given the FDI fault estimate  $\hat{\Gamma}$  of the entire team at sampling time  $t_k = t_f + t_d$ , find the set of accommodated control strategies  $\delta U^*(k) = [\delta u_1^{*T}(k), \dots, \delta u_{N_v}^{*T}(k)]^T$  as the solution to the set of  $N_v$  simultaneous global minimization problems, namely

$$\delta u_i^*(k) = \underset{\delta u_i}{\operatorname{argmin}} J_i(Z(k), \delta u_i(k)) , \quad i \in \mathcal{V} \quad (4.5a)$$

subject to

$$E(k+1) = \bar{A} E(k) + \sum_{j \in \mathcal{V}} \bar{B}_j \Gamma_j \delta u_j(k) \quad (4.5b)$$

$$Z(k) = \bar{C} E(k) \quad (4.5c)$$

where  $t_f$  is the time instant in which the fault has occurred, and  $t_d$  is the time takes for FDI module to detect and identify the fault, and then activates control accommodation mechanism. Each individual cost  $J_i$  is defined in (3.10). Moreover,

the faulty error dynamics considered in the optimization problem is the rearranged form of centralized faulty error dynamics defined in (4.3) in which  $\bar{B}_i = w_i^T \otimes B$  and  $w_i$  is the  $i$ th row of matrix  $W$  that characterizes the underlying information graph.

**Solution:**

The accommodated local control strategies which constitute global Nash equilibrium  $\delta U^*(k) = [\delta u_1^{*T}(k), \dots, \delta u_{N_v}^{*T}(k)]^T$  can be given by

$$\delta u_i^*(k) = -\bar{K}_i^a E(k) \quad \forall i \in \mathcal{V} \quad (4.6)$$

where the accommodated control gain matrices  $\bar{K}_{i \in \mathcal{V}}^a \in \mathbb{R}^{3 \times 6N_v}$  are defined by

$$\bar{K}_i^a = (R_i + \hat{\Gamma}_i^T \bar{B}_i^T \bar{P}_i^a \bar{B}_i \hat{\Gamma}_i)^{-1} \hat{\Gamma}_i^T \bar{B}_i^T \bar{P}_i^a (\bar{A} - \sum_{j \in \mathcal{V} - \{i\}} \bar{B}_j \hat{\Gamma}_j \bar{K}_j^a) \quad \forall i \in \mathcal{V} \quad (4.7)$$

where  $\bar{P}_{i \in \mathcal{V}}^a \in \mathbb{R}^{6N_v \times 6N_v}$  are the solutions to coupled AREs while incorporating the estimates of control effectiveness matrices  $\hat{\Gamma}_{i \in \mathcal{V}}$  provided by FDI module of all agents, namely

$$\bar{P}_i^a = \bar{C}^T \bar{Q}_i \bar{C} + \bar{K}_i^{aT} R_i \bar{K}_i^a + (\bar{A} - \sum_{j \in \mathcal{V}} \bar{B}_j \hat{\Gamma}_j \bar{K}_j^a)^T \bar{P}_i^a (\bar{A} - \sum_{j \in \mathcal{V}} \bar{B}_j \hat{\Gamma}_j \bar{K}_j^a) \quad \forall i \in \mathcal{V} \quad (4.8)$$

It should be noted that  $\bar{P}_i^a$  is the unique positive semi-definite solutions to  $i$ th coupled ARE given in (4.8) if and only if the pair  $(\bar{A} - \sum_{j \in \mathcal{V} - \{i\}} \bar{B}_j \hat{\Gamma}_j \bar{K}_j^a, \bar{B}_i \hat{\Gamma}_i)$  is stabilizable and the pair  $(\bar{A} - \sum_{j \in \mathcal{V} - \{i\}} \bar{B}_j \hat{\Gamma}_j \bar{K}_j^a, \bar{Q}_i^{1/2} \bar{C})$  is detectable.

#### 4.2.2.1 Performance Evaluation in the Presence of FDI Imperfections

In this part, the minimum cost value obtained by each agent after the occurrence of LOE fault is evaluated. Moreover, the effects of FDI imperfections such as time delay and fault estimation error on the value of the cost are investigated. To this end, we split the minimum cost value obtained by  $i$ th agent in to two terms as

$$J_i^*(Z(k), \delta u_i^*(k), [t_f, \infty)) = J_i^*(Z(k), \delta u_i^*(k), [t_f, t_f + t_d)) + J_i^*(Z(k), \delta u_i^*(k), [t_f + t_d, \infty)) \quad (4.9)$$

The first term in (4.9) is the minimum cost value when the multi-agent system is faulty, but the FDI fault estimates are not available, and the nominal controllers are still applied. Therefore, its value can be calculated as follows

$$J_i^*(Z(k), \delta u_i^*(k), [t_f, t_f + t_d)) = E(f)^T \bar{P}_i E(f) - E(f + d)^T \bar{P}_i E(f + d) \quad (4.10)$$

that can be rewritten as

$$J_i^*(Z(k), \delta u_i^*(k), [t_f, t_f + t_d)) = E(f)^T \left[ \bar{P}_i - (\bar{A} - \sum_{j \in \mathcal{V}} \bar{B}_j \Gamma_j \bar{K}_j)^{d^T} \bar{P}_i (\bar{A} - \sum_{j \in \mathcal{V}} \bar{B}_j \Gamma_j \bar{K}_j)^d \right] E(f) \quad (4.11)$$

The second term in (4.9) is the minimum cost value when the multi-agent system is faulty, and the accommodated controllers are applied. Therefore, its value can be calculated as

$$\begin{aligned} J_i^*(Z(k), \delta u_i^*(k), [t_f + t_d, \infty)) &= E(f + d)^T (\bar{C} \bar{Q}_i \bar{C} + \bar{K}_i^{a^T} R_i \bar{K}_i^a) E(f + d) \\ &+ E(f + d + 1)^T \bar{P}_i^a E(f + d + 1) \end{aligned} \quad (4.12)$$

that can be rewritten as

$$\begin{aligned}
J_i^*(Z(k), \delta u_i^*(k), [t_f + t_d, \infty)) &= E(f + d)^T \bar{P}_i^a E(f + d) \\
&+ E(f + d)^T \left[ (-2 \sum_{j \in \mathcal{V}} \bar{B}_j \varepsilon_j \bar{K}_j^a)^T \bar{P}_i^a (\bar{A} - \sum_{j \in \mathcal{V}} \bar{B}_j \hat{\Gamma}_j \bar{K}_j^a) \right] E(f + d) \\
&+ E(f + d)^T \left[ (2 \sum_{j \in \mathcal{V}} \bar{B}_j \varepsilon_j \bar{K}_j^a)^T \bar{P}_i^a (2 \sum_{j \in \mathcal{V}} \bar{B}_j \varepsilon_j \bar{K}_j^a) \right] E(f + d) \quad (4.13)
\end{aligned}$$

where the last two terms in equation (4.13) are the costs incurred due to the FDI estimation error, i.e.  $\varepsilon_i = \Gamma_i - \hat{\Gamma}_i$ . It should be noted that the value of the last term is negligible. Finally, the evaluated minimum cost obtained by  $i$ th agent after the occurrence of LOE fault can be defined as

$$\begin{aligned}
J_i^*(Z(k), \delta u_i^*(k), [t_f, \infty)) &= E(f)^T \left[ \bar{P}_i + (\bar{A} - \sum_{j \in \mathcal{V}} \bar{B}_j \Gamma_j \bar{K}_j)^{dT} [-\bar{P}_i + \bar{P}_i^a \right. \\
&+ \left. (-2 \sum_{j \in \mathcal{V}} \bar{B}_j \varepsilon_j \bar{K}_j^a)^T \bar{P}_i^a (\bar{A} - \sum_{j \in \mathcal{V}} \bar{B}_j \hat{\Gamma}_j \bar{K}_j^a)] (\bar{A} - \sum_{j \in \mathcal{V}} \bar{B}_j \Gamma_j \bar{K}_j)^d \right] E(f) \quad (4.14)
\end{aligned}$$

**Remark 4.1.** The existence of the solution to Problem 4.2 does not necessarily mean that it is satisfactory. The minimum cost value of each agent  $J_i^*(Z(k), \delta u_i^*(k), [t_f, \infty))$  is said to be admissible if it is lower than some predefined upper bound for the minimum cost value  $\bar{J}_i^*$ , i.e.  $J_i^*(Z(k), \delta u_i^*(k), [t_f, \infty)) \leq \bar{J}_i^*$ . However, it is worth noting that, under bounded FDI time delay and estimation error, it is possible to derive the guaranteed cost accommodated controller based on a cost function with modified weighting matrices.

### 4.2.3 Cooperative Dynamic Game Approach to Centralized Fault Accommodation

In this subsection, the centralized controller based on cooperative dynamic game approach is accommodated and redesigned using the fault estimates provided by FDI module of all agents. In this case, the weighted sum of all individual objective functions as given in (3.15) is minimized considering the centralized faulty error dynamics presented in (4.3). Along with the main global minimization problem, the bargaining protocol is utilized to allocate appropriate weights to each agent when LOE fault occurs. The following problem formally states this scenario.

**Problem 4.3.** For cooperative dynamic game of  $N_v$  agents, given the FDI fault estimates of the entire team  $\hat{\Gamma}$  at sampling time  $t_k = t_f + t_d$ , find the set of Pareto efficient control strategies denoted by  $\delta U^*(\alpha, k) = [\delta u_1^{*T}(\alpha, k), \dots, \delta u_{N_v}^{*T}(\alpha, k)]^T$  for  $\forall \alpha \in \Lambda$  which provides the solution to the following global minimization problem, namely

$$\delta U^*(\alpha, k) = \underset{\delta U}{\operatorname{argmin}} J_c(Z(k), \delta U(k), \alpha) \quad (4.15a)$$

subject to

$$E(k+1) = \bar{A} E(k) + \sum_{j \in \mathcal{V}} \bar{B}_j \Gamma_j \delta u_j(k) \quad (4.15b)$$

$$Z(k) = \bar{C} E(k) \quad (4.15c)$$

where  $t_f$  is the time instant in which the fault has occurred, and  $t_d$  is the time takes for FDI module to detect and identify the fault, and then activates control accommodation mechanism. The dynamic equation considered in the minimization problem is the rearranged form of centralized formation error dynamics defined in (4.3) in which  $\bar{B}_i = w_i^T \otimes B$  and  $w_i$  is the  $i$ th row of matrix  $W$  which characterizes

the underlying information graph.

**Solution:**

The accommodated Pareto-efficient local control strategies can be given by

$$\delta u_i^*(\alpha, k) = -\bar{K}_i^a(\alpha) E(k) \quad \forall i \in \mathcal{V} \quad (4.16)$$

where the accommodated control gain matrices  $\bar{K}_i^a(\alpha) \in \mathbb{R}^{3 \times 6N_v}$  are defined by

$$\bar{K}_i^a(\alpha) = (\alpha_i R_i + \hat{\Gamma}_i^T \bar{B}_i^T \bar{P}^a(\alpha) \bar{B}_i \hat{\Gamma}_i)^{-1} \hat{\Gamma}_i^T \bar{B}_i^T \bar{P}^a(\alpha) (\bar{A} - \sum_{j \in \mathcal{V} - \{i\}} \bar{B}_j \hat{\Gamma}_j \bar{K}_j^a(\alpha)) \quad \forall i \in \mathcal{V} \quad (4.17)$$

where  $\bar{P}^a(\alpha) \in \mathbb{R}^{6N_v \times 6N_v}$  is the solution to the following ARE while incorporating the estimates of control effectiveness matrices  $\hat{\Gamma}_{i \in \mathcal{V}}$  provided by FDI module of all agents, namely

$$\begin{aligned} \bar{P}^a(\alpha) = & \sum_{i \in \mathcal{V}} \{ \alpha_i \bar{C}^T \bar{Q}_i \bar{C} + \bar{K}_i^{aT}(\alpha) \alpha_i R_i \bar{K}_i^a(\alpha) \} \\ & + (\bar{A} - \sum_{j \in \mathcal{V}} \bar{B}_j \hat{\Gamma}_j \bar{K}_j^a(\alpha))^T \bar{P}^a(\alpha) (\bar{A} - \sum_{j \in \mathcal{V}} \bar{B}_j \hat{\Gamma}_j \bar{K}_j^a(\alpha)) \end{aligned} \quad (4.18)$$

where  $\bar{P}^a(\alpha)$  is the positive semi-definite solution to ARE (4.18) which is not unique in general.

As already explained, the accommodated local Pareto-efficient control strategies are functions of  $\alpha \in \Lambda$ . In this regard, Algorithm 3.1 introduced in previous chapter is used in conjunction with equations (4.18) and (4.17) to recalculate a unique  $\alpha^*$ , Pareto optimal solution  $[J_1(\alpha^*), \dots, J_{N_v}(\alpha^*)]$ , and the corresponding accommodated Pareto-efficient control strategy  $\delta U(\alpha^*) = [\delta u_1^T(\alpha^*), \dots, \delta u_{N_v}^T(\alpha^*)]^T$ . As a result of employing bargaining protocol, lower weight will be allocated to the objective function of faulty

agent in the global optimization problem, and hence the cost of cooperation will be decreased during the fault recovery process.

**Remark 4.2.** It worth noting that the cost values of each agent derived in Subsection 4.2.2 are considered as non-cooperative cost values  $J_{i \in \mathcal{V}}^d$  used in Algorithm 3.1.

#### 4.2.3.1 Performance Evaluation in the Presence of FDI Imperfections

In this part, the minimum cost value obtained by the entire team after the occurrence of LOE fault is evaluated. Moreover, the effects of FDI imperfections such as time delay and fault estimation error on the value of the cost are investigated. To this end, we split the minimum cost value of the team in to two terms as

$$\begin{aligned} J_c^*(Z(k), \delta U^*(\alpha^*, k), [t_f, \infty)) &= J_c^*(Z(k), \delta U^*(\alpha^*, k), [t_f, t_f + t_d)) \\ &\quad + J_c^*(Z(k), \delta U^*(\alpha^*, k), [t_f + t_d, \infty)) \end{aligned} \quad (4.19)$$

The first term in (4.19) is the minimum cost value when the multi-agent system is faulty, but the FDI fault estimates are not available, and the nominal controllers are still applied. Therefore, its value can be calculated as follows

$$J_c^*(Z(k), \delta U^*(\alpha^*, k), [t_f, t_f + t_d)) = E(f)^T \bar{P}(\alpha^*) E(f) - E(f + d)^T \bar{P}(\alpha^*) E(f + d) \quad (4.20)$$

that can be rewritten as

$$\begin{aligned} J_c^*(Z(k), \delta U^*(\alpha^*, k), [t_f, t_f + t_d)) &= E(f)^T \left[ \bar{P}(\alpha^*) - (\bar{A} - \sum_{j \in \mathcal{V}} \bar{B}_j \Gamma_j \bar{K}_j(\alpha^*))^{dT} \bar{P}(\alpha^*) \right. \\ &\quad \left. (\bar{A} - \sum_{j \in \mathcal{V}} \bar{B}_j \Gamma_j \bar{K}_j(\alpha^*))^d \right] E(f) \end{aligned} \quad (4.21)$$

The second term in (4.19) is the minimum cost value when the multi-agent system is faulty, and the accommodated controllers are applied. Therefore, its value can be calculated as

$$\begin{aligned} J_c^*(Z(k), \delta U^*(\alpha^*, k), [t_f + t_d, \infty)) &= E(f + d + 1)^T \bar{P}^a(\alpha^*) E(f + d + 1) \\ &+ E(f + d)^T \left[ \sum_{i \in \mathcal{V}} \{ \alpha_i^* \bar{C}^T \bar{Q}_i \bar{C} + \bar{K}_i^{aT}(\alpha^*) \alpha_i^* R_i \bar{K}_i^a(\alpha^*) \} \right] E(f + d) \end{aligned} \quad (4.22)$$

that can be rewritten as

$$\begin{aligned} J_c^*(Z(k), \delta U^*(\alpha^*, k), [t_f + t_d, \infty)) &= E(f + d)^T \bar{P}^a(\alpha^*) E(f + d) \\ &+ E(f + d)^T \left[ (-2 \sum_{j \in \mathcal{V}} \bar{B}_j \varepsilon_j \bar{K}_j^a(\alpha^*))^T \bar{P}^a(\alpha^*) (\bar{A} - \sum_{j \in \mathcal{V}} \bar{B}_j \hat{\Gamma}_j \bar{K}_j^a(\alpha^*)) \right] E(f + d) \\ &+ E(f + d)^T \left[ (2 \sum_{j \in \mathcal{V}} \bar{B}_j \varepsilon_j \bar{K}_j^a(\alpha^*))^T \bar{P}^a(\alpha^*) (2 \sum_{j \in \mathcal{V}} \bar{B}_j \varepsilon_j \bar{K}_j^a(\alpha^*)) \right] E(f + d) \end{aligned} \quad (4.23)$$

where the last two terms in equation (4.23) are the costs incurred due to the FDI estimation error, i.e.  $\varepsilon_i = \Gamma_i - \hat{\Gamma}_i$ . It should be noted that the value of the last term is negligible. Finally, the evaluated minimum cost obtained by the entire team after the occurrence of LOE fault can be defined as

$$\begin{aligned} J_c^*(Z(k), \delta U^*(\alpha^*, k), [t_f, \infty)) &= E(f)^T \left[ \bar{P}(\alpha^*) + (\bar{A} - \sum_{j \in \mathcal{V}} \bar{B}_j \Gamma_j \bar{K}_j(\alpha^*))^{dT} [-\bar{P}(\alpha^*) + \bar{P}^a(\alpha^*) \right. \\ &\left. + (-2 \sum_{j \in \mathcal{V}} \bar{B}_j \varepsilon_j \bar{K}_j^a(\alpha^*))^T \bar{P}^a(\alpha^*) (\bar{A} - \sum_{j \in \mathcal{V}} \bar{B}_j \hat{\Gamma}_j \bar{K}_j^a(\alpha^*)) \right] (\bar{A} - \sum_{j \in \mathcal{V}} \bar{B}_j \Gamma_j \bar{K}_j(\alpha^*))^d \right] E(f) \end{aligned} \quad (4.24)$$

**Remark 4.3.** The existence of the solution to Problem 4.3 does not necessarily mean that it is satisfactory. The minimum cost value of the team  $J_c^*(Z(k), \delta U^*(\alpha^*, k), [t_f, \infty))$  is said to be admissible if it is lower than some predefined upper bound for the minimum cost value  $\bar{J}_c^*$ , i.e.  $J_c^*(Z(k), \delta U^*(\alpha^*, k), [t_f, \infty)) \leq \bar{J}_c^*$ . However, it is worth

noting that, under bounded FDI time delay and estimation error, it is possible to derive the guaranteed cost accommodated controller based on a cost function with modified weighting matrices.

### 4.3 Semi-Decentralized Fault Accommodation

In this section, semi-decentralized active fault accommodation mechanism is developed while incorporating on-line information provided by FDI module of neighboring agents. In the forthcoming subsections, the MPC technique and dynamic game theory are utilized to recover the team from LOE actuator fault.

To this end, redesigning the controller must be performed based on faulty system dynamics. Let us consider the faulty state equation associated with  $i$ th agent with LOE actuator fault as defined in (4.1), then formation error dynamics of  $i$ th agent under faulty condition while considering information exchange topology can be written as

$$e_i(k+1) = A e_i(k) + \sum_{j \in \bar{N}_i} w_{ij} B \Gamma_j \delta u_j(k) \quad (4.25a)$$

$$z_i(k) = C e_i(k) \quad (4.25b)$$

where  $\Gamma_i \in \mathbb{R}^{3 \times 3}$  is the control effectiveness matrix of  $i$ th agent, and  $\delta u_i = u_i - \frac{u^*}{\Gamma_i}$  is the control input error variable of  $i$ th agent.

### 4.3.1 Model Predictive Control Approach to Semi-Decentralized Fault Accommodations

In this subsection, the previously introduced MPC-based semi-decentralized controller is accommodated considering the finite horizon cost given in (3.23) and the semi-decentralized faulty error dynamics presented in equation (4.25). The following problem formally states this scenario.

**Problem 4.4.** At each sampling time  $t_k \in [t_f + t_d, \infty)$ , given the current formation error vector of  $i$ th agent  $e_i(k)$ , and neighboring agents previous optimal control inputs  $\delta \tilde{u}(k-1)_{j \in N_i}$ , as well as the fault information estimates of  $i$ th agent and its neighbors, i.e.  $\hat{\Gamma}_{j \in \bar{N}_i}$ , find  $i$ th agent accommodated control input sequence  $\delta \tilde{u}_i(k) = [\delta u_i(k)^T, \delta u_i(k+1)^T, \dots, \delta u_i(k+N_c-1)^T]^T$  as the solution to the following constrained finite time optimal control problem

$$\min_{\delta \tilde{u}_i} J_i(z_i(k), \delta \tilde{u}_i(k)) =: \quad (4.26a)$$

$$\min_{\delta \tilde{u}_i} \sum_{h=0}^{N_p-1} \{ \|z_i(h|k)\|_{Q_i}^2 + \|\delta u_i(h|k)\|_{R_i}^2 \} + \|e_i(N_p|k)\|_{Q_i}^2$$

s.t.

$$e_i(h+1|k) = A e_i(h|k) + w_{ii} B \hat{\Gamma}_i \delta u_i(h|k) + \sum_{j \in N_i} w_{ij} B \hat{\Gamma}_j \delta u_j(h|k-1) \quad (4.26b)$$

$$z_i(h|k) = C e_i(h|k) \quad h = 0, 1, \dots, N_p - 1 \quad (4.26c)$$

$$\delta u_{min}^f \leq \delta u_i(h|k) \leq \delta u_{max}^f \quad h = 0, 1, \dots, N_c - 1 \quad (4.26d)$$

$$\delta u_i(h|k) = \delta u_i(N_c - 1|k) \quad N_c \leq h \leq N_p - 1 \quad (4.26e)$$

$$\tilde{V}_i e_i(k + N_p) = 0 \quad (4.26f)$$

where  $t_f$  is the time that fault has occurred, and  $t_d$  is the time takes for FDI module to detect and identify the fault and then activates the control accommodation mechanism. The matrices  $\hat{\Gamma}_{i \in \bar{N}_i} \in \mathbb{R}^{3 \times 3}$  are the estimates of control effectiveness matrices  $\Gamma_{i \in \bar{N}_i}$  provided by FDI module of  $i$ th agent and its neighbors. Moreover,  $N_c$  and  $N_p$  are the control horizon and the prediction horizon, respectively. In order to decrease the computational complexity, the control horizon is selected to be less than the prediction horizon. The triple  $(A, w_{ii} B \hat{\Gamma}_i, C)$  considered in the prediction model of  $i$ th agent is controllable and observable with 3 unstable modes on the unit circle. In order to ensure stability of closed loop system, the terminal equality constraint (4.26f) associated with unstable modes and the terminal penalty matrix  $Q_{iN}$  are computed as explained in Theorem 2.1.

### 4.3.2 Non-Cooperative Dynamic Game Approach to Semi - Decentralized Fault Accommodation

In this subsection, the previously introduced semi-decentralized controller based on non-cooperative dynamic game is accommodated and redesigned using the fault estimates provided by FDI module of each agent and its neighbors. In this case, infinite horizon cost of all agents as given in (3.25) are simultaneously minimized considering their faulty formation error dynamics presented in (4.25). Therefore, each agent can obtain minimum cost value under the effects of accommodated control actions pursued by its neighbors. The following problem formally states this scenario.

**Problem 4.5.** For non-cooperative dynamic game of  $N_v$  agents with connected information exchange topology, given the fault estimates by FDI module of each agent and its neighbors  $\hat{\Gamma}_{j \in \bar{N}_i}$  at sampling time  $t_k = t_f + t_d$ , find the set of accommodated control strategies  $\delta U^*(k) = [\delta u_1^{*T}(k), \dots, \delta u_{N_v}^{*T}(k)]^T$  as the solution to the set of  $N_v$

simultaneous local minimization problems, namely

$$\delta u_i^*(k) = \underset{\delta u_i}{\operatorname{argmin}} J_i(z_i(k), \delta u_i(k)) , \quad \forall i \in \mathcal{V} \quad (4.27a)$$

subject to

$$e_i(k+1) = A e_i(k) + \sum_{j \in \bar{N}_i} w_{ij} B \Gamma_j \delta u_j(k) \quad (4.27b)$$

$$z_i(k) = C e_i(k) \quad (4.27c)$$

where  $t_f$  is the time instant in which the fault has occurred, and  $t_d$  is the time takes for FDI module to detect and identify the fault, and then activates control accommodation mechanism.

**Solution:**

In order to perform the controller redesign at time  $t_k = t_f + t_d$ , its required to consider the previously introduced augmented error dynamics of each agent  $i \in \mathcal{V}$  given in (3.27) in faulty condition as follows

$$\begin{bmatrix} e_i(k+1) \\ \vdots \\ e_j(k+1) \\ \vdots \end{bmatrix} = \underbrace{\begin{bmatrix} A & & & \\ & \ddots & & \\ & & A & \\ & & & \ddots \end{bmatrix}}_{A_i} \underbrace{\begin{bmatrix} e_i(k) \\ \vdots \\ e_j(k) \\ \vdots \end{bmatrix}}_{\bar{e}_i} + \sum_{n \in \bar{N}_i} \underbrace{\begin{bmatrix} w_{in} B \\ \vdots \\ w_{jn} B \\ \vdots \end{bmatrix}}_{B_{in}} \Gamma_n \delta u_n(k) \quad (4.28a)$$

$$z_i = \underbrace{\begin{bmatrix} C & 0_{3 \times 6N_i} \end{bmatrix}}_{C_{ii}} \begin{bmatrix} e_i(k) \\ \vdots \\ e_j(k) \\ \vdots \end{bmatrix} \quad (4.28b)$$

The set of accommodated local control strategies that provides Nash equilibrium solution to the set of  $N_v$  local minimization problems defined in (4.27) and subject

to the new dynamics given in (4.28) can be given by

$$\delta u_i^*(k) = K_i^a \bar{e}_i(k) \quad \forall i \in \mathcal{V} \quad (4.29)$$

where the accommodated control gain matrices  $K_i^a \in \mathbb{R}^{3 \times 6\bar{N}_i}$  are defined by

$$K_i^a = (R_i + \hat{\Gamma}_i^T B_{ii}^T P_i^a B_{ii} \hat{\Gamma}_i)^{-1} \hat{\Gamma}_i^T B_{ii}^T P_i^a (A_i - \sum_{j \in N_i} B_{ij} \hat{\Gamma}_j \hat{K}_j^a) \quad \forall i \in \mathcal{V} \quad (4.30)$$

where  $P_i^a \in \mathbb{R}^{6\bar{N}_i \times 6\bar{N}_i}$  are the solutions to the coupled AREs while incorporating the estimates of control effectiveness matrices  $\hat{\Gamma}_{i \in \bar{N}_i}$  provided by FDI module of each agent and its neighbors as follows

$$\begin{aligned} P_i^a = & (A_i - B_{ii} \hat{\Gamma}_i K_i^a - \sum_{j \in N_i} B_{ij} \hat{\Gamma}_j \hat{K}_j^a)^T P_i^a (A_i - B_{ii} \hat{\Gamma}_i K_i^a - \sum_{j \in N_i} B_{ij} \hat{\Gamma}_j \hat{K}_j^a) + \\ & + Q_{ii} + K_i^{aT} R_i K_i^a \quad \forall i \in \mathcal{V} \end{aligned} \quad (4.31)$$

where  $Q_{ii} = C_{ii}^T Q_i C_{ii} \in \mathbb{R}^{6\bar{N}_i \times 6\bar{N}_i}$  is positive semi-definite, and  $R_i \in \mathbb{R}^{3 \times 3}$  is positive definite. The accommodated control gain matrices  $\hat{K}_{j \in N_i}^a$  are the rearrange form of communicated control gain matrices of neighboring agents, i.e.  $K_{j \in N_i}^a$ , in order to be suitably incorporated in the coupled ARE of  $i$ th agent. Moreover,  $P_i^a$  is the unique positive semi-definite solution of  $i$ th algebraic Riccati equation given in (4.31) if and only if the pair  $(A_i - \sum_{j \in N_i} B_{ij} \hat{\Gamma}_j \hat{K}_j^a, B_{ii} \hat{\Gamma}_i)$  is stabilizable, and the pair  $(A_i - \sum_{j \in N_i} B_{ij} \hat{\Gamma}_j \hat{K}_j^a, Q_{ii}^{1/2})$  is detectable.

Since the formation graph is connected, ultimately the information from each agent propagates to all others. Therefore, if each agent and its neighbors reach irrevocable set of accommodated local control inputs  $[\delta u_i^{*T}(k), \{\delta u_j^{*T}(k)\}_{j \in N_i}]^T$  for  $i \in \mathcal{V}$ , this will imply that the whole set of accommodated local control inputs, i.e.

$[\delta u_1^*(k), \dots, \delta u_i^*(k), \dots, \delta u_{N_v}^*(k)]$  constitute Nash equilibrium.

#### 4.3.2.1 Performance Evaluation in the Presence of FDI Imperfections

In this part, the minimum cost value obtained by each agent after the occurrence of LOE fault is evaluated. Moreover, the effects of FDI imperfections such as time delay and fault estimation error on the value of the cost are investigated. To this end, we split the minimum cost value obtained by  $i$ th agent in to two terms as

$$J_i^*(\bar{z}_i(k), \delta u_i^*(k), [t_f, \infty)) = J_i^*(\bar{z}_i(k), \delta u_i^*(k), [t_f, t_f + t_d)) + J_i^*(\bar{z}_i(k), \delta u_i^*(k), [t_f + t_d, \infty)) \quad (4.32)$$

The first term in (4.32) is the minimum cost value when the multi-agent system is faulty, but the FDI fault estimates are not available, and the nominal controllers are still applied. Therefore, its value can be calculated as follows

$$J_i^*(\bar{z}_i(k), \delta u_i^*(k), [t_f, t_f + t_d)) = \bar{e}_i(f)^T P_i \bar{e}_i(f) - \bar{e}_i(f + d)^T P_i \bar{e}_i(f + d) \quad (4.33)$$

that can be rewritten as

$$J_i^*(\bar{z}_i(k), \delta u_i^*(k), [t_f, t_f + t_d)) = \bar{e}_i(f)^T \left[ P_i - (A_i - B_{ii} \Gamma_i K_i - \sum_{j \in N_i} B_{ij} \Gamma_j \hat{K}_j)^{d^T} P_i \right. \\ \left. (A_i - B_{ii} \Gamma_i K_i - \sum_{j \in N_i} B_{ij} \Gamma_j \hat{K}_j)^d \right] \bar{e}_i(f) \quad (4.34)$$

The second term in (4.32) is the minimum cost value when the multi-agent system is faulty, and the accommodated controllers are applied. Therefore, its value can be

calculated as

$$\begin{aligned} J_i^*(\bar{z}_i(k), \delta u_i^*(k), [t_f + t_d, \infty)) &= \bar{e}_i(f + d)^T [Q_{ii} + K_i^{aT} R_i K_i^a] \bar{e}_i(f + d) \\ &+ \bar{e}_i(f + d + 1)^T P_i^a \bar{e}_i(f + d + 1) \end{aligned} \quad (4.35)$$

that can be rewritten as

$$\begin{aligned} J_i^*(\bar{z}_i(k), \delta u_i^*(k), [t_f + t_d, \infty)) &= \bar{e}_i(f + d)^T P_i^a \bar{e}_i(f + d) \\ &+ \bar{e}_i(f + d)^T \left[ (-2(B_{ii} \varepsilon_i K_i^a + \sum_{j \in N_i} B_{ij} \varepsilon_j \hat{K}_j^a))^T P_i^a (A_i - B_{ii} \hat{\Gamma}_i K_i^a - \sum_{j \in N_i} B_{ij} \hat{\Gamma}_j \hat{K}_j^a) \right] \bar{e}_i(f + d) \\ &+ \bar{e}_i(f + d)^T \left[ 2(B_{ii} \varepsilon_i K_i^a + \sum_{j \in N_i} B_{ij} \varepsilon_j \hat{K}_j^a) \right]^T P_i^a \left[ 2(B_{ii} \varepsilon_i K_i^a + \sum_{j \in N_i} B_{ij} \varepsilon_j \hat{K}_j^a) \right] \bar{e}_i(f + d) \end{aligned} \quad (4.36)$$

where the last two terms in equation (4.36) are the costs incurred due to the FDI estimation error, i.e.  $\varepsilon_i = \Gamma_i - \hat{\Gamma}_i$ . It should be noted that the value of the last term is negligible. Finally, the evaluated minimum cost obtained by  $i$ th agent after the occurrence of LOE fault can be defined as

$$\begin{aligned} J_i^*(\bar{z}_i(k), \delta u_i^*(k), [t_f, \infty)) &= \bar{e}_i(f)^T \left[ P_i + (A_i - B_{ii} \Gamma_i K_i - \sum_{j \in N_i} B_{ij} \Gamma_j \hat{K}_j)^{dT} [-P_i + P_i^a \right. \\ &+ (-2(B_{ii} \varepsilon_i K_i^a + \sum_{j \in N_i} B_{ij} \varepsilon_j \hat{K}_j^a))^T P_i^a (A_i - B_{ii} \hat{\Gamma}_i K_i^a - \sum_{j \in N_i} B_{ij} \hat{\Gamma}_j \hat{K}_j^a)] \\ &\left. (A_i - B_{ii} \Gamma_i K_i - \sum_{j \in N_i} B_{ij} \Gamma_j \hat{K}_j)^d \right] \bar{e}_i(f) \end{aligned} \quad (4.37)$$

**Remark 4.4.** The existence of the solution to Problem 4.5 does not necessarily mean that it is satisfactory. The minimum cost value of each agent  $J_i^*(\bar{z}_i(k), \delta u_i^*(k), [t_f, \infty))$  is said to be admissible if it is lower than some predefined upper bound for the minimum cost value  $\bar{J}_i^*$ , i.e.  $J_i^*(\bar{z}_i(k), \delta u_i^*(k), [t_f, \infty)) \leq \bar{J}_i^*$ . However, it is worth

noting that, under bounded FDI time delay and estimation error, it is possible to derive the guaranteed cost accommodated controller based on a cost function with modified weighting matrices.

## 4.4 Decentralized Fault Accommodation

In this section, decentralized active fault accommodation mechanism is developed in which each agent is recovered independently using on-line information provided by its own FDI module. In the forthcoming subsections, the MPC technique and dynamic game theory are utilized to recover each agent from LOE actuator fault.

To this end, redesigning the controller must be performed based on faulty system dynamics. Recall from previous chapter that the decentralized error dynamics associated with  $i$ th agent is formed by augmenting each individual error dynamics and the error dynamics of its neighbors as given in (3.31). Then, the corresponding decentralized augmented error dynamics in faulty condition can be rewritten as

$$\begin{bmatrix} e_i(k+1) \\ \vdots \\ e_j(k+1) \\ \vdots \end{bmatrix} = \underbrace{\begin{bmatrix} A & & \\ & \ddots & \\ & & A \end{bmatrix}}_{A_i} \underbrace{\begin{bmatrix} e_i(k) \\ \vdots \\ e_j(k) \\ \vdots \end{bmatrix}}_{\bar{e}_i} + \underbrace{\begin{bmatrix} w_{ii}B \\ \vdots \\ w_{ji}B \\ \vdots \end{bmatrix}}_{B_{ii}} \Gamma_i \delta u_i(k) + \sum_{j \in N_i} \underbrace{\begin{bmatrix} w_{ij}B \\ \vdots \\ w_{jj}B \\ \vdots \end{bmatrix}}_{B_{ij}} \delta u_j(k) \quad (4.38a)$$

$$\underbrace{\begin{bmatrix} z_i(k) \\ \vdots \\ z_j(k) \\ \vdots \end{bmatrix}}_{\bar{z}_i} = \underbrace{\begin{bmatrix} C & & \\ & \ddots & \\ & & C \end{bmatrix}}_{C_i} \begin{bmatrix} e_i(k) \\ \vdots \\ e_j(k) \\ \vdots \end{bmatrix} \quad (4.38b)$$

#### 4.4.1 Model Predictive Control Approach to Decentralized Fault Accommodation

In this subsection, decentralized MPC-based controller introduced in previous chapter is accommodated considering the finite horizon cost given in (3.32) and the decentralized faulty error dynamics defined in (4.38). The following problem formally states this scenario.

**Problem 4.6.** At each sampling time  $t_k = [t_f + t_d, \infty)$ , given the current augmented state error vector of  $i$ th agent  $\bar{e}_i(k)$  as well as the its fault information estimate, namely  $\hat{\Gamma}_i$ , find  $i$ th agent decentralized accommodated control input sequence  $\delta\tilde{u}_i(k) = [\delta u_i(k)^T, \delta u_i(k+1)^T, \dots, \delta u_i(k+N_c-1)^T]^T$  as the solution to the following constrained finite time optimal control problem

$$\begin{aligned} \min_{\{\delta\tilde{u}_j\}_{j \in \bar{N}_i}} J_i(\bar{e}_i(k), \{\delta\tilde{u}_j(k)\}_{j \in \bar{N}_i}) =: \\ \min_{\{\delta\tilde{u}_j\}_{j \in \bar{N}_i}} \sum_{h=0}^{N_p-1} \{ \|\bar{z}_i(h|k)\|_{\bar{Q}_i}^2 + \sum_{j \in \bar{N}_i} \|\delta u_j(h|k)\|_{R_j}^2 \} + \|\bar{e}_i(N_p|k)\|_{\bar{Q}_i}^2 \end{aligned} \quad (4.39a)$$

s.t.

$$\bar{e}_i(h+1|k) = A_i \bar{e}_i(h|k) + B_{ii} \hat{\Gamma}_i \delta u_i(h|k) + \sum_{j \in \bar{N}_i} B_{ij} \delta u_j(h|k) \quad (4.39b)$$

$$\bar{z}_i(h|k) = C_i \bar{e}_i(h|k) \quad h = 0, 1, \dots, N_p - 1 \quad (4.39c)$$

$$\delta u_{min}^f \leq \delta u_j(h|k) \leq \delta u_{max}^f, \quad j \in \bar{N}_i \quad h = 0, 1, \dots, N_c - 1 \quad (4.39d)$$

$$\delta u_j(h|k) = \delta u_j(N_c - 1|k), \quad j \in \bar{N}_i \quad N_c \leq h \leq N_p - 1 \quad (4.39e)$$

$$\tilde{V}_i \bar{e}_i(k + N_p) = 0 \quad (4.39f)$$

where  $t_f$  is the time that fault has occurred, and  $t_d$  is the time takes for FDI module to detect and identify the fault and then activates the control accommodation

mechanism. The matrix  $\hat{\Gamma}_i$  is the estimate of control effectiveness matrix  $\Gamma_i$  provided by FDI modul of  $i$ th agent. Moreover,  $N_c$  and  $N_p$  are the control horizon and the prediction horizon, respectively. In order to decrease the computational complexity, the control horizon is selected to be less than the prediction horizon. The triple  $(A_i, [B_{ii} \hat{\Gamma}_i, B_{ij \in N_i}], C_i)$  considered in the prediction model of  $i$ th agent is controllable and observable with  $3\bar{N}_i$  unstable modes on the unit circle. In order to ensure stability of closed loop system, the terminal equality constraint (4.39f) associated with unstable modes and the terminal penalty matrix  $\bar{Q}_{iN}$  are computed as explained in Theorem 2.1.

#### 4.4.2 Non-Cooperative Dynamic Game Approach to Decentralized Fault Accommodation

In this subsection, the previously introduced decentralized controller based on non-cooperative dynamic game is accommodated and redesigned without exchanging FDI fault estimates among team members. In this case, each agent should locally minimize  $\bar{N}_i$  infinite horizon costs given in (3.34) while considering augmented faulty error dynamics defined in (4.38). The following problem formally states this scenario.

**Problem 4.7.** For non-cooperative nonzero-sum dynamic game of  $|\bar{N}_i|$  agents associated with  $i$ th agent, given its own FDI fault estimate, namely  $\hat{\Gamma}_i$  at sampling time  $t_k = t_f + t_d$ , find the set of accommodated control strategies  $\{\delta u_j^*\}_{j \in \bar{N}_i}$ , as the solution to the set of  $|\bar{N}_i|$  local minimization problems, namely

$$\delta u_j^*(k) = \operatorname{argmin} J_j(\bar{z}_i(k), \delta u_j(k)) \quad j \in \bar{N}_i \quad (4.40a)$$

subject to

$$\bar{e}_i(k+1) = A_i \bar{e}_i(k) + B_{ii} \hat{\Gamma}_i \delta u_i(k) + \sum_{j \in N_i} B_{ij} \delta u_j(k) \quad (4.40b)$$

$$\bar{z}_i(k) = C_i \bar{e}_i(k) \quad (4.40c)$$

**Solution:**

The set of  $|\bar{N}_i|$  accommodated control strategies that are computed locally by  $i$ th agent and provides Nash equilibrium solution to Problem 4.7 can be given by

$$\delta u_j^*(k) = -K_{ij}^a \bar{e}_i(k), \quad \forall j \in \bar{N}_i \quad (4.41)$$

where the control gain matrix of  $i$ th agent, i.e.  $K_{ii}^a \in \mathbb{R}^{3 \times 6\bar{N}_i}$  is defined by

$$K_{ii}^a = (R_i + \hat{\Gamma}_i^T B_{ii}^T P_{ii}^a B_{ii} \hat{\Gamma}_i)^{-1} \hat{\Gamma}_i^T B_{ii}^T P_{ii}^a (A_i - \sum_{j \in N_i} B_{ij} K_{ij}^a), \quad \forall j \in \bar{N}_i \quad (4.42)$$

where  $P_{ii}^a \in \mathbb{R}^{6\bar{N}_i \times 6\bar{N}_i}$  is the solution to the  $i$ th coupled ARE solved by  $i$ th agent, namely

$$\begin{aligned} P_{ii}^a = & (A_i - B_{ii} \hat{\Gamma}_i K_{ii}^a - \sum_{j \in N_i} B_{ij} K_{ij}^a)^T P_{ii}^a (A_i - B_{ii} \hat{\Gamma}_i K_{ii}^a - \sum_{j \in N_i} B_{ij} K_{ij}^a) \\ & + C_i^T Q_{ii} C_i + K_{ii}^a R_j K_{ii}^a, \quad \forall j \in \bar{N}_i \end{aligned} \quad (4.43)$$

It should be noted that  $P_{ii}^a$  is the unique positive semi-definite solution to  $i$ th coupled ARE given in (4.43) if and only if the pair  $(A_i - \sum_{j \in N_i} B_{ij} K_{ij}^a, B_{ii} \hat{\Gamma}_i)$  is stabilizable, and the pair  $(A_i - \sum_{j \in N_i} B_{ij} K_{ij}^a, Q_{ii}^{1/2} C_i)$  is detectable.

As mentioned before, the accommodated control action which is implemented by  $i$ th agent is  $\delta u_i^*(k) = K_{ii}^a \bar{e}_i(k)$  and the rest of locally computed control actions are only used to control  $i$ th agent augmented error dynamics in open loop.

#### 4.4.2.1 Performance Evaluation in the Presence of FDI Imperfections

In this part, the minimum cost value obtained by each agent after the occurrence of LOE fault is evaluated. Moreover, the effects of FDI imperfections such as time delay and fault estimation error on the value of the cost are investigated. To this end, we split the minimum cost value obtained by  $i$ th agent in to two terms as

$$J_i^*(\bar{z}_i(k), \delta u_i^*(k), [t_f, \infty)) = J_i^*(\bar{z}_i(k), \delta u_i^*(k), [t_f, t_f + t_d)) + J_i^*(\bar{z}_i(k), \delta u_i^*(k), [t_f + t_d, \infty)) \quad (4.44)$$

The first term in (4.44) is the minimum cost value when  $i$ th agent is faulty, but its FDI fault estimate is not available, and the nominal controller is still applied. Therefore, its value can be calculated as follows

$$J_i^*(\bar{z}_i(k), \delta u_i^*(k), [t_f, t_f + t_d)) = \bar{e}_i(f)^T P_{ii} \bar{e}_i(f) - \bar{e}_i(f + d)^T P_{ii} \bar{e}_i(f + d) \quad (4.45)$$

that can be rewritten as

$$J_i^*(\bar{z}_i(k), \delta u_i^*(k), [t_f, t_f + t_d)) = \bar{e}_i(f)^T \left[ P_{ii} - (A_i - B_{ii} \Gamma_i K_{ii} - \sum_{j \in N_i} B_{ij} K_{ij})^{d^T} P_{ii} \right. \\ \left. (A_i - B_{ii} \Gamma_i K_{ii} - \sum_{j \in N_i} B_{ij} K_{ij})^d \right] \bar{e}_i(f) \quad (4.46)$$

The second term in (4.44) is the minimum cost value when  $i$ th agent is faulty, and the accommodated controller is applied. Therefore, its value can be calculated as

$$J_i^*(\bar{z}_i(k), \delta u_i^*(k), [t_f + t_d, \infty)) = \bar{e}_i(f + d)^T [C_i^T Q_{ii} C_i + K_{ii}^{a^T} R_i K_{ii}^a] \bar{e}_i(f + d) \\ + \bar{e}_i(f + d + 1)^T P_{ii}^a \bar{e}_i(f + d + 1) \quad (4.47)$$

that can be rewritten as

$$\begin{aligned}
J_i^*(\bar{z}_i(k), \delta u_i^*(k), [t_f + t_d, \infty)) &= \bar{e}_i(f + d)^T P_{ii}^a \bar{e}_i(f + d) \\
&+ \bar{e}_i(f + d)^T \left[ (-2 B_{ii} \varepsilon_i K_{ii}^a)^T P_{ii}^a (A_i - B_{ii} \hat{\Gamma}_i K_{ii}^a - \sum_{j \in N_i} B_{ij} K_{ij}^a) \right] \bar{e}_i(f + d) \\
&+ \bar{e}_i(f + d)^T \left[ (2 B_{ii} \varepsilon_i K_{ii}^a)^T P_{ii}^a (2 B_{ii} \varepsilon_i K_{ii}^a) \right] \bar{e}_i(f + d) \tag{4.48}
\end{aligned}$$

where the last two terms in equation (4.48) are the costs incurred due to the FDI estimation error, i.e.  $\varepsilon_i = \Gamma_i - \hat{\Gamma}_i$ . It should be noted that the value of the last term is negligible. Finally, the evaluated minimum cost obtained by  $i$ th agent after the occurrence of LOE fault can be defined as

$$\begin{aligned}
J_i^*(\bar{z}_i(k), \delta u_i^*(k), [t_f, \infty)) &= \bar{e}_i(f)^T \left[ P_{ii} + (A_i - B_{ii} \Gamma_i K_{ii} - \sum_{j \in N_i} B_{ij} K_{ij})^{dT} [-P_{ii} + P_{ii}^a \right. \\
&+ (-2 B_{ii} \varepsilon_i K_{ii}^a)^T P_{ii}^a (A_i - B_{ii} \hat{\Gamma}_i K_{ii}^a - \sum_{j \in N_i} B_{ij} K_{ij}^a)] \\
&\left. (A_i - B_{ii} \Gamma_i K_{ii} - \sum_{j \in N_i} B_{ij} K_{ij})^d \right] \bar{e}_i(f) \tag{4.49}
\end{aligned}$$

**Remark 4.5.** The existence of the solution to Problem 4.7 does not necessarily mean that it is satisfactory. The minimum cost value of each agent  $J_i^*(\bar{z}_i(k), \delta u_i^*(k), [t_f, \infty))$  is said to be admissible if it is lower than some predefined upper bound for the minimum cost value  $\bar{J}_i^*$ , i.e.  $J_i^*(\bar{z}_i(k), \delta u_i^*(k), [t_f, \infty)) \leq \bar{J}_i^*$ . However, it is worth noting that, under bounded FDI time delay and estimation error, it is possible to derive the guaranteed cost accommodated controller based on a cost function with modified weighting matrices.

## 4.5 Simulation Results

In this section, simulation results are presented to demonstrate the performance of our proposed active fault accommodation mechanisms. The faulty scenarios investigated here are LOE actuator faults with different severities equal to 5%, 20%, and 40%. It is assumed that the LOE fault has occurred in the actuator along X-axis at time  $t_f = 40 \text{ sec}$ . Moreover, the time delay associated with FDI module is assumed to be  $t_d = 4 \text{ sec}$ . The simulations are conducted for a team of five AUVs with the same formation mission specifications outlined in previous chapter. The details on system parameters and disturbance and noise characteristics are similar to previous chapter. Moreover, the selected controller parameters are also similar to the ones given in Table 3.4.

In order to have a quantified analysis of the performance and effectiveness of our proposed active fault accommodation mechanisms, the previously defined performance measures presented in Table 3.5 are considered. Moreover, the upper bound limit for degraded steady state tracking performance is assumed to be  $J_x^s \approx 0.2$ .

### 4.5.1 Simulation Scenarios for MPC-Based Semi-Decentralized Fault Accommodation

In this subsection, the performance of centralized, semi-decentralized, and decentralized MPC-based active fault accommodation mechanisms are compared under various fault scenarios and also different conditions on the availability and accuracy of fault estimates provided by FDI module.

#### 4.5.1.1 Scenario 1: 5% LOE Fault

In this part, simulations are related to a scenario where 5 % LOE fault has occurred in the actuator along X-axis of AUV #2 at time  $t_f = 40 \text{ sec}$ . In Figures 4.1, 4.2, and 4.3, position errors, surge velocity errors, and thruster forces along X-axis for all MPC-based schemes are presented under fault scenario 1. In addition, performance measures and time response characteristics for all MPC-based schemes are quantitatively summarized in Table 4.1.

These figures and also the steady-state performance measures  $J_x^s$  and  $J_x^s$  show that the acceptable tracking and formation keeping specifications in faulty situation are met, and the nominal centralized and semi-decentralized controllers can mitigate the effect of low severity LOE fault without the need for any fault recovery mechanism. However, the steady-state tracking error of nominal decentralized controller violates the acceptable specification. The poor performance of decentralized scheme even for low severity fault is due to the presence of modeling error in open loop augmented error dynamics of each agent in which the effects of any abnormalities such as fault and disturbance are not reflected. The control effort cost and total cost values, i.e.  $J_u$  and  $J_{total}$  after the time that fault occurred in the team are noticeably higher in the decentralized scheme, and the centralized scheme demands for higher control effort than the semi-decentralized scheme because of the fact that in the centralized scheme all agents are affected by faulty agent. Therefore, the MPC-based semi-decentralized scheme is capable of handling low severity actuator faults more efficiently than the centralized scheme.

**Table 4.1:** Performance and Time Response Evaluation of Centralized, Semi-Decentralized, and Decentralized MPC-Based Controllers, 5% LOE Fault with No FDI and Recovery

	Centralized MPC	Semi-Decentralized MPC	Decentralized MPC
$J_x$	0.008	0.005	1.9
$J_{\tilde{x}}$	0.010	0.011	0.013
$J_x^s$	0.12	0.13	1.74
$J_{\tilde{x}}^s$	0.16	0.12	0.13
$J_u$	116	115	$4.4e + 03$
$J_{total}$	14	12	$1.4e + 03$
$t_s$	24	23	67
$\tilde{t}_s$	—	—	—
$t_{solve}$	0.51	0.08	0.26

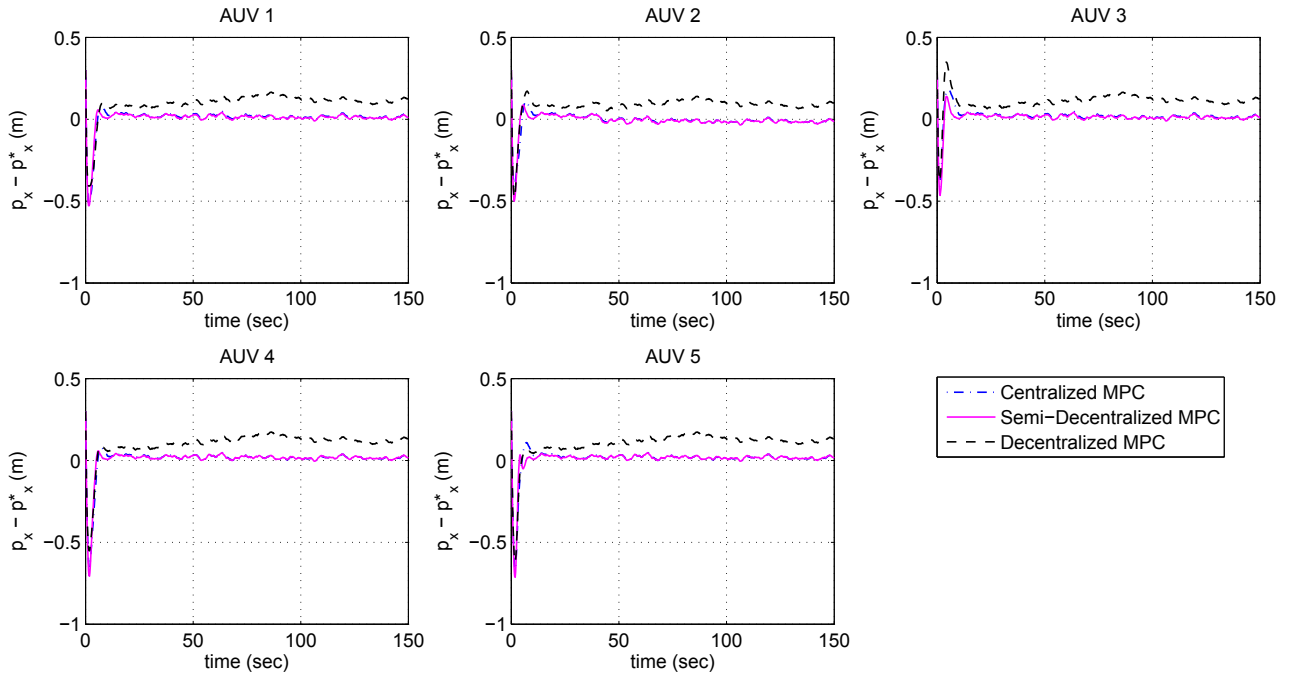


**Figure 4.1:** Error Signals Along X-axis for Cenetralized, Semi-Decentralized, and Decen-  
tralized MPC-Based Control Schemes, Fault Scenario 1

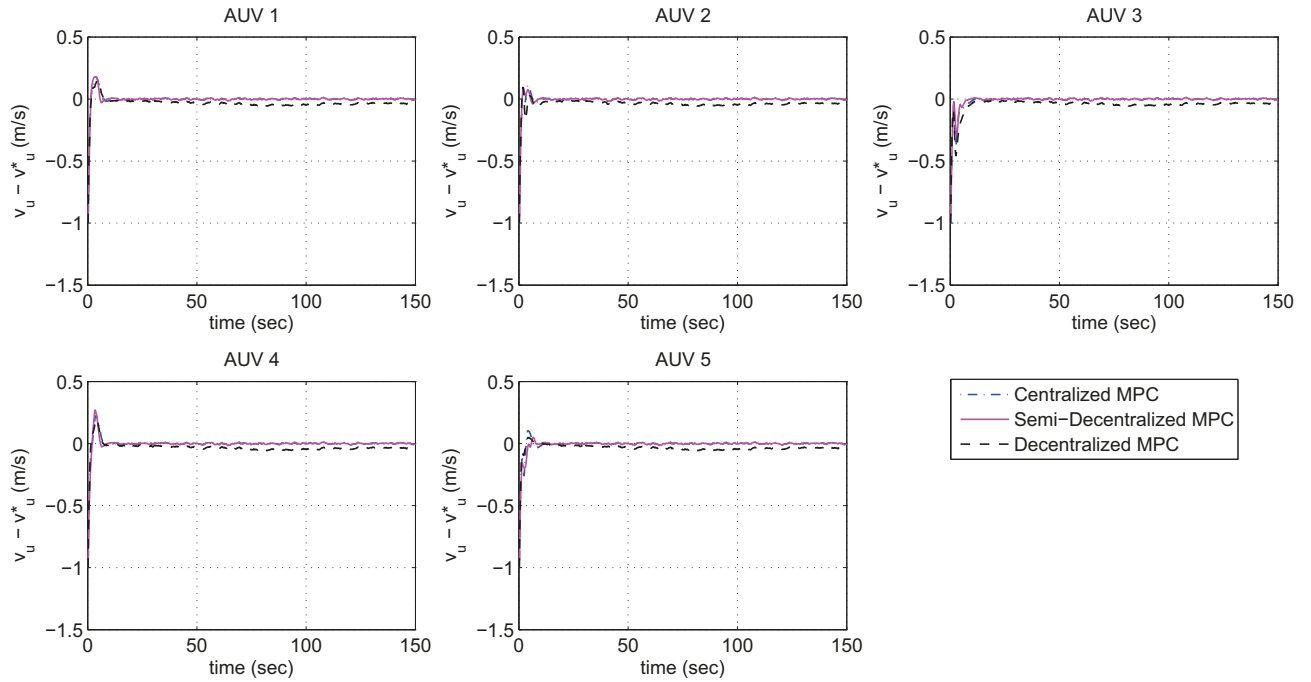


**Figure 4.2:** Surge Velocity Error Signals for Cenetralized, Semi-Decentralized, and Decen-  
 tralized MPC-Based Control Schemes, Fault Scenario 1

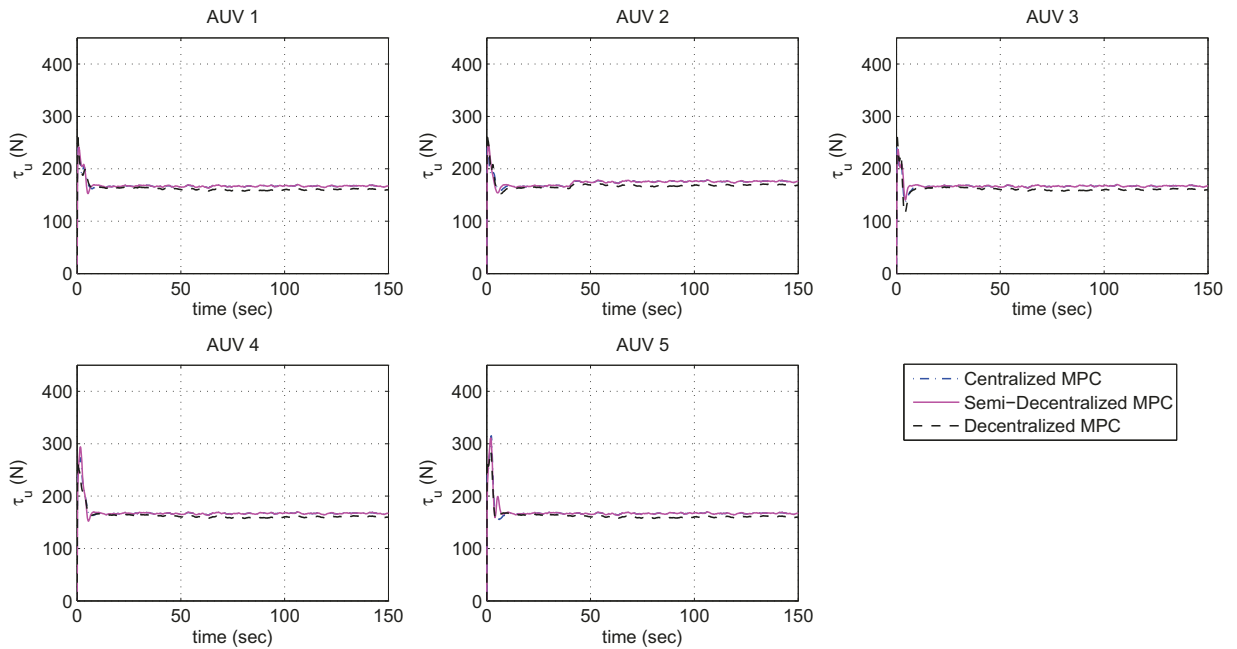


**Figure 4.3:** Thruster Forces along X-axis for Cenetralized, Semi-Decentralized, and De-  
 centralized MPC-Based Control Schemes, Fault Scenario 1

#### 4.5.1.2 Scenario 2: 20% LOE Fault

In this part, simulations are related to a scenario where 20 % LOE fault has occurred in the actuator along X-axis of AUV #2 at time  $t_f = 40 \text{ sec}$ . Moreover, the time delay associated with the FDI module is assumed to be  $t_d = 4 \text{ sec}$ . In Figures 4.4, 4.5, and 4.6, position errors, surge velocity errors, and thruster forces along X-axis for all MPC-based schemes are presented under fault scenario 2. In addition, the performance measures and time response characteristics for all MPC-based schemes are quantitatively summarized in Table 4.2. The maximum allowable FDI inaccuracies of semi-decentralized and centralized schemes in which acceptable degraded steady-state performance can be maintained are evaluated to be 20% and 40%, respectively. In this respect, we compare the performance of decentralized, semi-decentralized, and centralized active fault accommodation mechanisms in the presence of 20% inaccuracy in FDI information.

The obtained results for the steady-state tracking and formation keeping errors verify that MPC-based centralized and semi-decentralized accommodation schemes can maintain acceptable steady-state specifications when a moderate severity LOE fault occurred in the team. However, the steady-state tracking error of decentralized scheme violates the acceptable specification. From Figure 4.4 and also the cost value  $J_x$ , it can be observed that the transient tracking performance of semi-decentralized scheme is less affected in faulty condition. Additionally, the time that takes for centralized and semi-decentralized schemes to mitigate the effect of LOE fault is lower than decentralized scheme. The total cost of accommodation for semi-decentralized scheme has the lowest value, and then the centralized has lower  $J_{total}$  value than the decentralized scheme.

**Table 4.2:** Performance and Time Response Evaluation of Centralized, Semi-Decentralized, and decentralized MPC-Based Fault Accommodation mechanisms, 20% LOE Fault with 20% FDI Inaccuracy

	Centralized MPC	Semi-Decentralized MPC	Decentralized MPC
$J_x$	0.009	0.006	1.95
$J_{\bar{x}}$	0.01	0.02	0.024
$J_x^s$	0.16	0.13	1.74
$J_{\bar{x}}^s$	0.115	0.116	0.13
$J_u$	$1.2e + 03$	$1.2e + 03$	$5.1e + 03$
$J_{total}$	20.4	19.9	$1.4e + 03$
$t_s$	33	23	75
$\tilde{t}_s$	6.2	7.2	7.3
$t_{solve}$	0.51	0.08	0.26

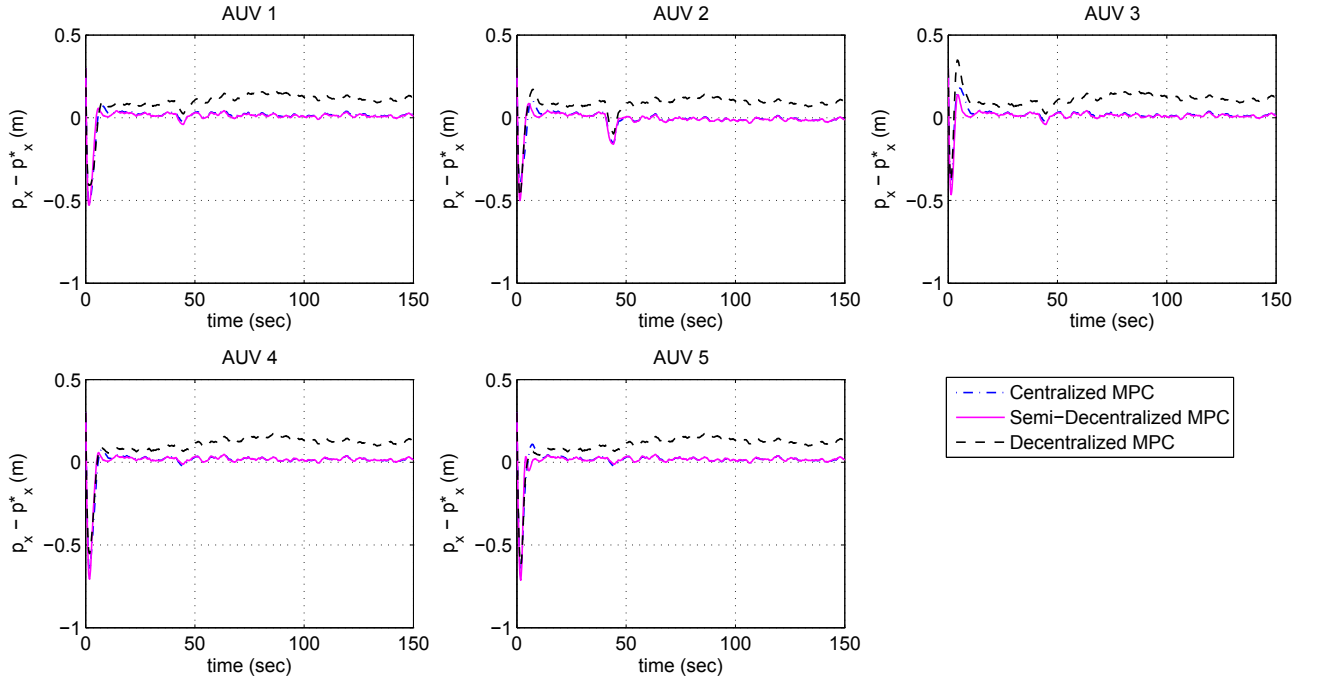


**Figure 4.4:** Error Signals Along X-axis for Cenetralized, Semi-Decentralized, and Decen-  
tralized MPC-Based Accommodation Schemes, Fault Scenario 2

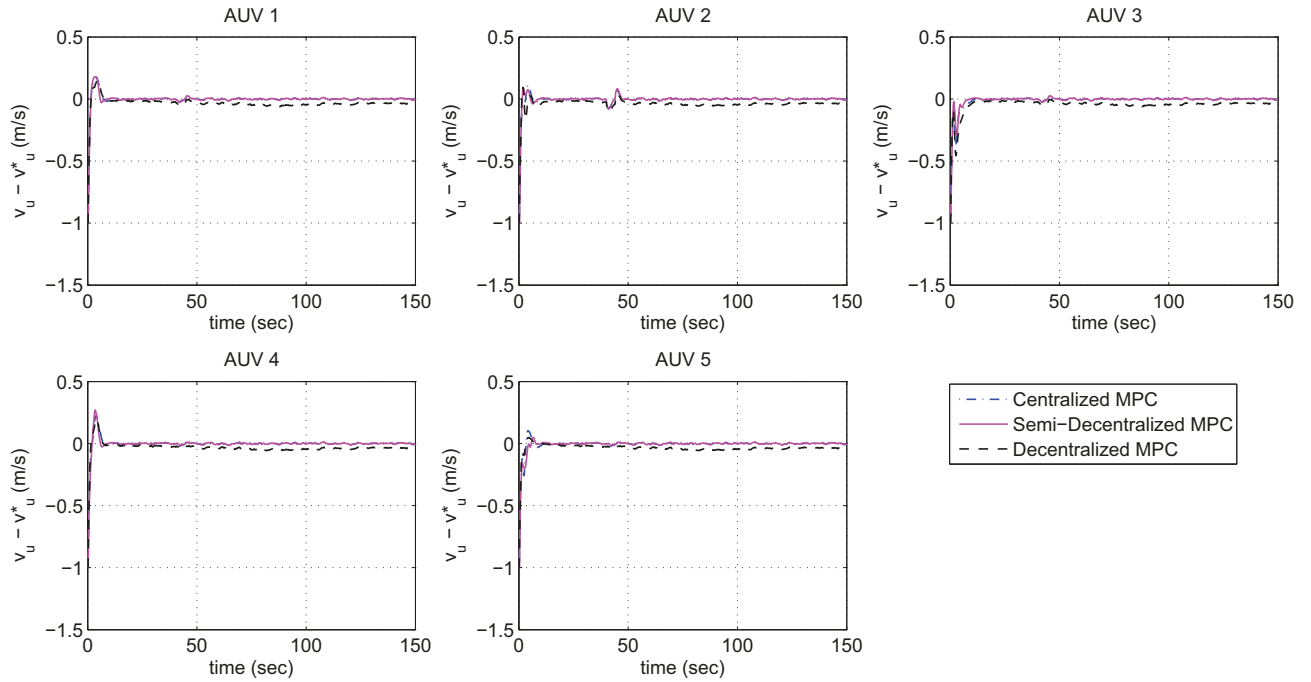


**Figure 4.5:** Surge Velocity Error Signals for Cenetralized, Semi-Decentralized, and Decen-  
 tralized MPC-Based Accommodation Schemes, Fault Scenario 2

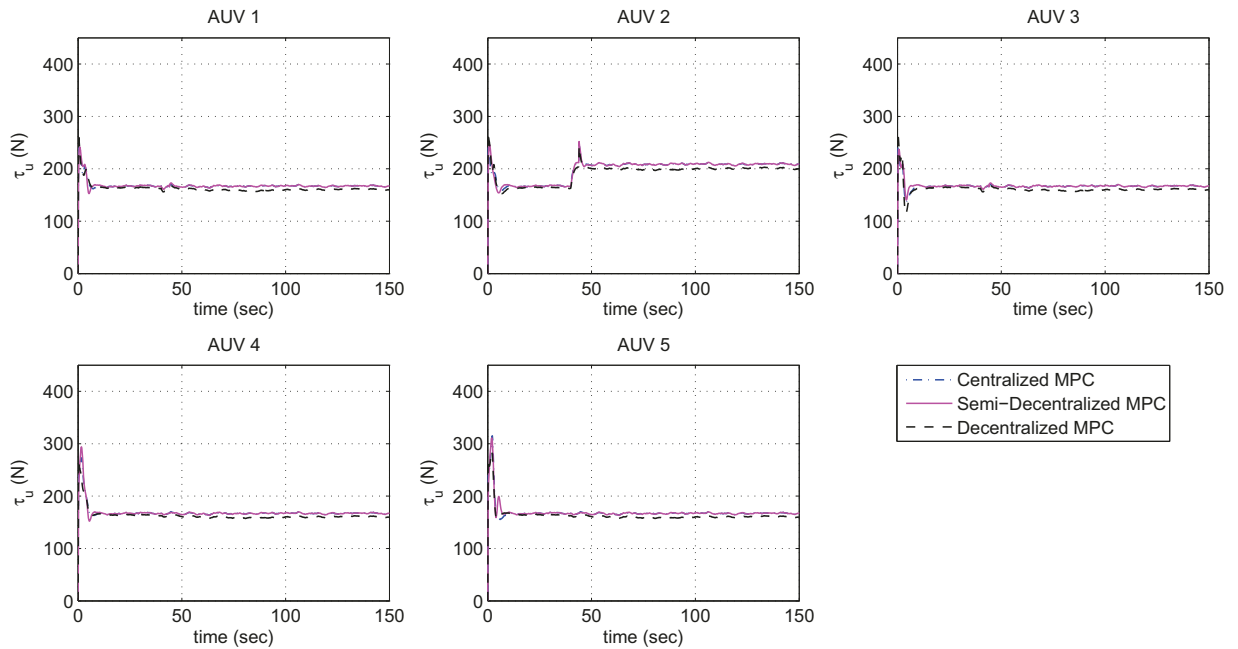


**Figure 4.6:** Thruster Forces along X-axis for Cenetralized, Semi-Decentralized, and De-  
 centralized MPC-Based Accommodation Schemes, Fault Scenario 2

#### 4.5.1.3 Scenario 3: 40% LOE Fault

In this part, simulations are related to 40% LOE fault that is injected to the actuator along  $X$ -axis of AUV #2 at time  $t_f = 40sec$ . Moreover, the time delay associated with FDI module of faulty agent is assumed to be  $t_d = 4 sec$ . In Figures 4.7, 4.8, and 4.9, position errors, surge velocity errors, and thruster forces along  $X$ -axis for all MPC-based schemes are presented under fault scenario 3. In addition, the performance measures and time response characteristics for all MPC-based schemes are quantitatively summarized in Table 4.3. The maximum allowable FDI inaccuracies of semi-decentralized and centralized schemes in which acceptable degraded steady-state performance can be maintained are evaluated to be 7% and 13%, respectively. In this respect, we compare the performance of decentralized, semi-decentralized, and centralized active fault accommodation mechanisms in the presence of 7% inaccuracy in FDI information.

The obtained results for the steady-state tracking and formation keeping errors verify that similar to the moderate severity LOE fault scenario 3, MPC-based centralized and semi-decentralized accommodation schemes can maintain acceptable steady-state specification when a high severity LOE fault occurred in the team. However, the steady-state tracking error of decentralized scheme violates the acceptable specification. From Figure 4.7 and also the cost value  $J_x$ , it can be observed that the transient tracking performance of semi-decentralized scheme is less affected in faulty condition. Additionally, the time that takes for centralized and semi-decentralized schemes to mitigate the effect of LOE fault is lower than decentralized scheme. We can also conclude that the centralized fault accommodation mechanism can mitigate the effect of high severity LOE fault with lower control effort and total costs, and then the semi-decentralized scheme is far more efficient than decentralized scheme.

**Table 4.3:** Performance and Time Response Evaluation of Centralized, Semi-Decentralized, and Decentralized MPC-Based Fault Accommodation mechanisms, 40% LOE Fault with 7% FDI Inaccuracy

	Centralized MPC	Semi-Decentralized MPC	Decentralized MPC
$J_x$	0.013	0.011	1.9
$J_{\bar{x}}$	0.06	0.07	0.08
$J_x^s$	0.16	0.13	1.74
$J_{\bar{x}}^s$	0.095	0.097	0.1
$J_u$	$8.82e + 03$	$8.85e + 03$	$1.15e + 04$
$J_{total}$	56	64	$1.5e + 03$
$t_s$	39	28	87
$\tilde{t}_s$	7	9.1	9.7
$t_{solve}$	0.49	0.07	0.27

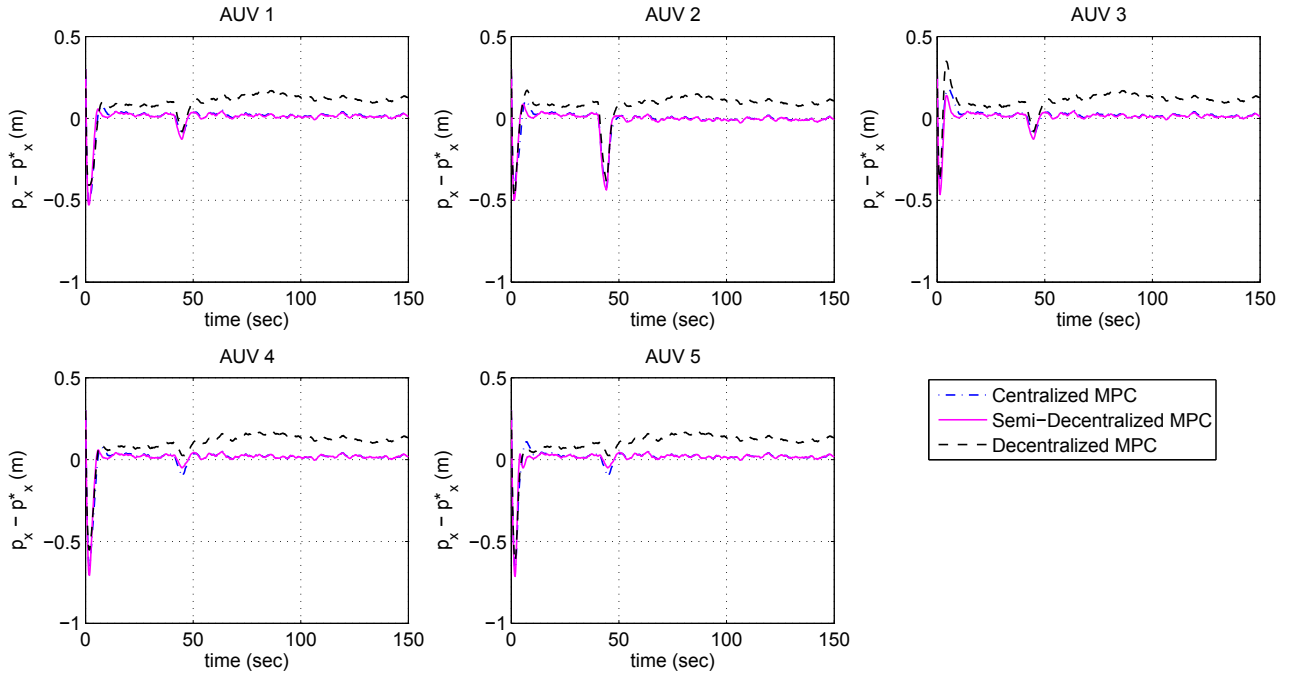


**Figure 4.7:** Error Signals Along X-axis for Cenetralized, Semi-Decentralized, and Decen- tralized MPC-Based Accommodation Schemes, Fault Scenario 3

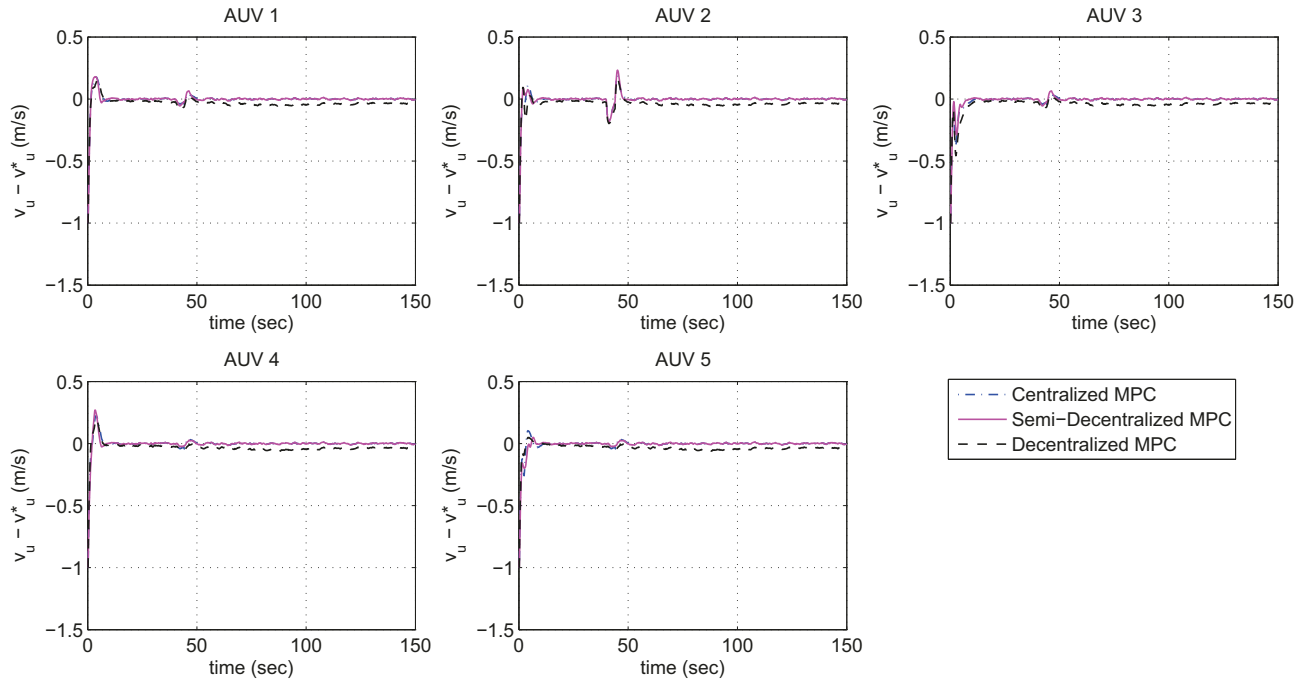


**Figure 4.8:** Surge Velocity Error Signals for Cenetralized, Semi-Decentralized, and Decen-  
 tralized MPC-Based Accommodation Schemes, Fault Scenario 3

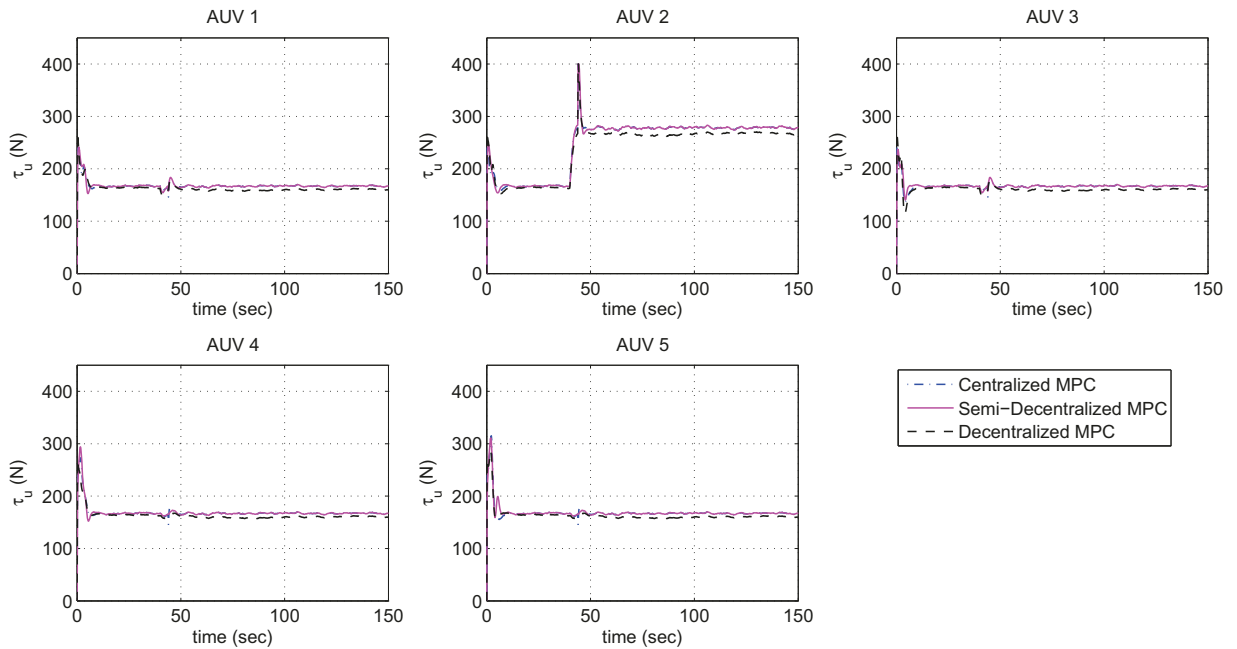


**Figure 4.9:** Thruster Forces along X-axis for Cenetralized, Semi-Decentralized, and De-  
 centralized MPC-Based Accommodation Schemes, Fault Scenario 3

#### 4.5.1.4 Scenario 4: Influence of FDI Time Delay

In this part, the effect of fault detection time delay on the performance of semi-decentralized accommodation mechanism is investigated. In this regard, high severity LOE fault of 40% is injected to the system. Additionally, the maximum allowable FDI estimation error of 7% is considered. In Figures 4.10, 4.11, and 4.12, position errors, surge velocity errors, and thruster forces along  $X$ -axis for MPC-based semi-decentralized scheme are presented under fault scenario 4. In addition, the performance measures and time response characteristics for MPC-based semi-decentralized scheme are quantitatively summarized in Table 4.4. The simulations are conducted under three different FDI time delays, namely  $t_d = 2 \text{ sec}$ ,  $4 \text{ sec}$ , and  $6 \text{ sec}$ . It can be observed that the semi-decentralized accommodation mechanism can recover faulty agent from LOE fault for larger values of FDI time delays, however this will result in poor transient behavior, higher tracking and formation keeping cost values, and also higher accommodation cost.

**Table 4.4:** Performance and Time Response Evaluation of MPC-Based Semi-Decentralized Fault Accommodation under Various FDI Time Delays, 40% LOE Fault with 7% FDI Inaccuracy

	Semi-Decentralized MPC		
	$t_d = 2 \text{ sec}$	$t_d = 4 \text{ sec}$	$t_d = 6 \text{ sec}$
$J_x$	0.007	0.011	0.013
$J_{\tilde{x}}$	0.03	0.07	0.1
$J_x^s$	0.13	0.13	0.13
$J_{\tilde{x}}^s$	0.09	0.09	0.09
$J_u$	$8.83e + 03$	$8.85e + 03$	$8.84e + 03$
$J_{total}$	31	64	90
$t_s$	27	28	29
$\tilde{t}_s$	6	9	11

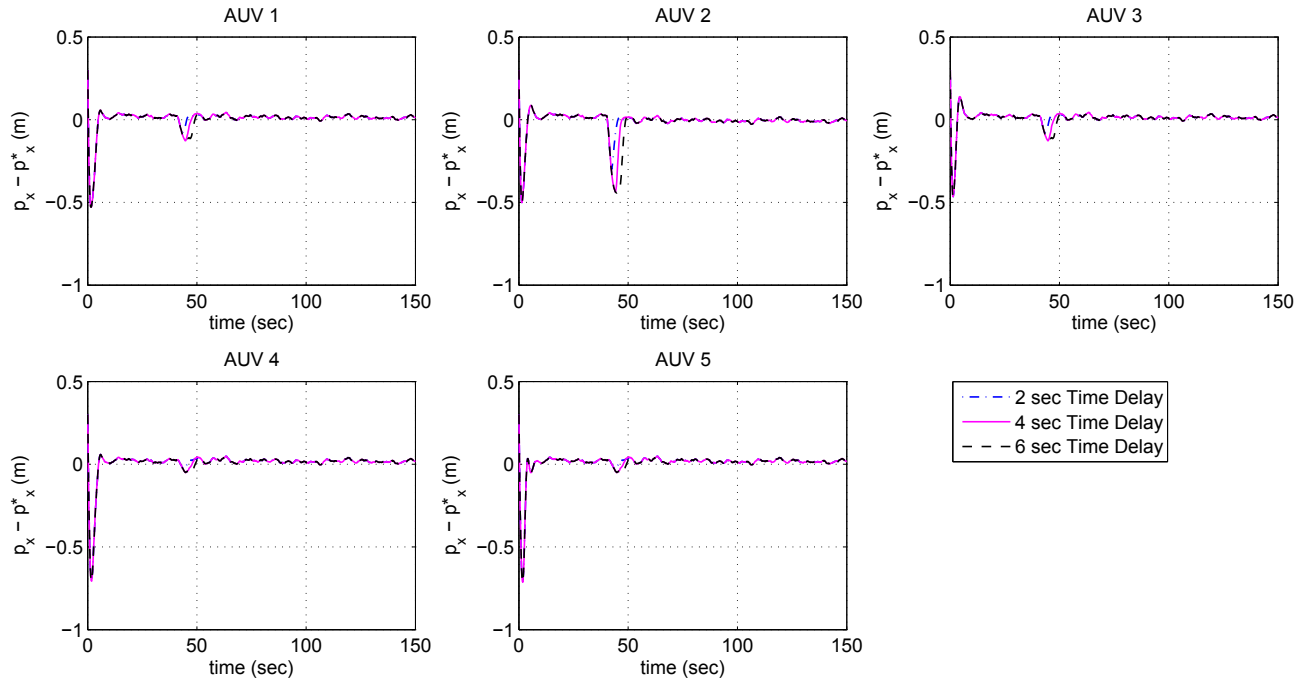


**Figure 4.10:** Error Signals Along  $X$ -axis for Semi-Decentralized MPC-Based Accommodation Scheme, Fault Scenario 4

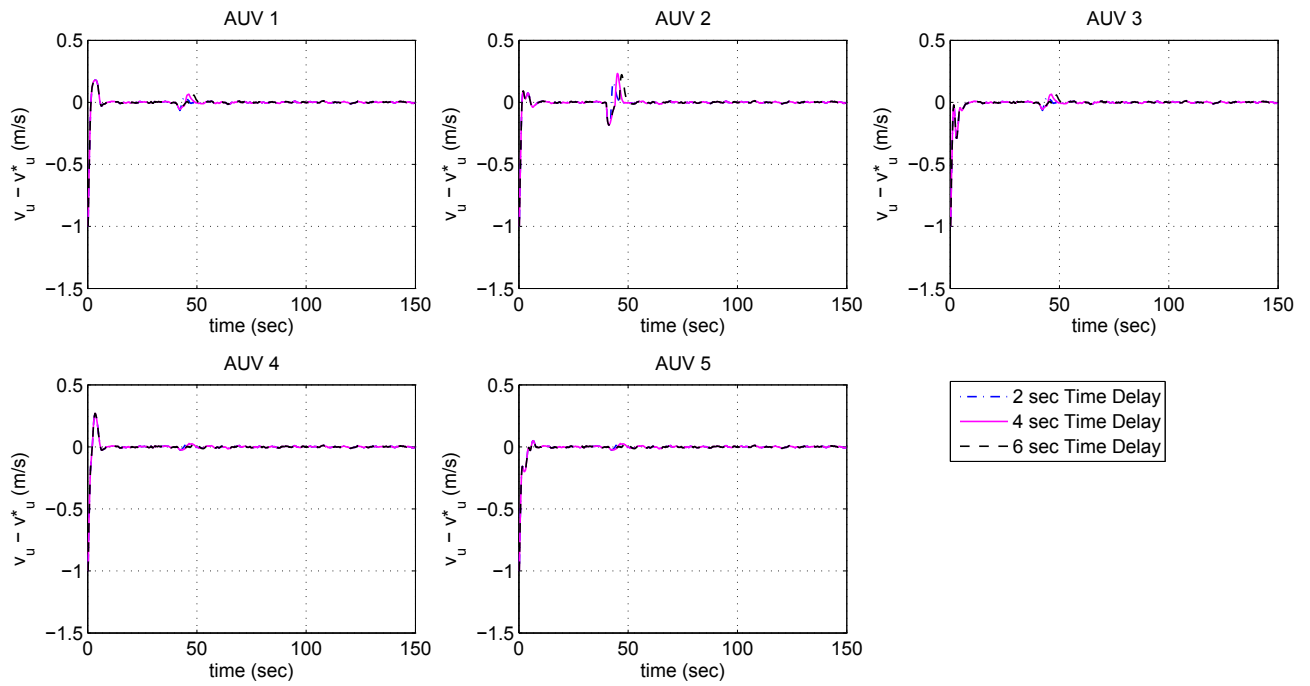


**Figure 4.11:** Surge Velocity Error Signals for Semi-Decentralized MPC-Based Accommodation Scheme, Fault Scenario 4

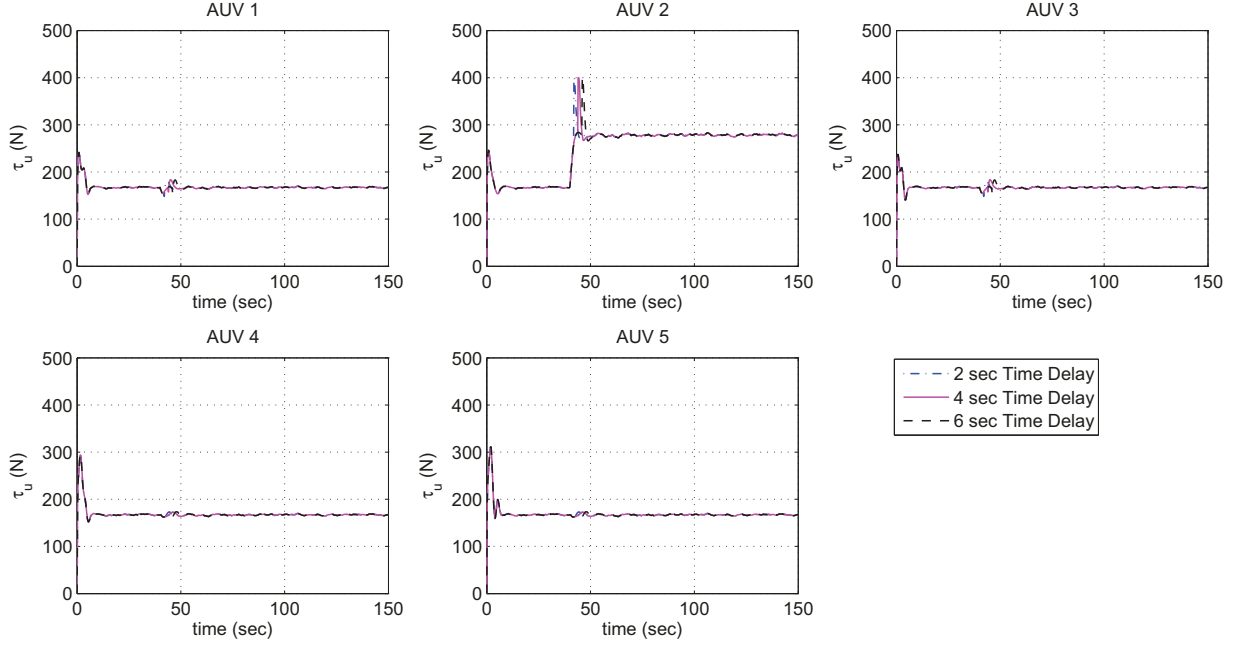


**Figure 4.12:** Thruster Forces along  $X$ -axis for Semi-Decentralized MPC-Based Accommodation Scheme, Fault Scenario 4

#### 4.5.1.5 Scenario 5: Multiple Faulty Agents in the Team

In this part, the performance of MPC-based centralized and semi-decentralized accommodation schemes are compared when there are multiple faulty agents in the team. The first set of simulations are conducted when 40% LOE fault is injected to the actuators along  $X$ -axis of AUV #2 and #4 at time  $t_f = 40 \text{ sec}$ . The second set of simulations are conducted when AUVs #2, #4, and #5 are considered faulty with different fault severities. It is assumed that AUV #2 and #5 have 40% LOE fault and AUV #4 has 20% LOE fault. The LOE faults are injected at time  $t_f = 40 \text{ sec}$ . In both cases, the time delay associated with FDI module of each agent is assumed to be  $t_d = 4 \text{ sec}$ . Additionally, the maximum allowable FDI inaccuracy of each agent is supposed to be 7% for 40% LOE fault and 20% for 20% LOE fault.

In Figures 4.13, 4.14, and 4.15, position errors, surge velocity errors, and thruster forces along  $X$ -axis for MPC-based centralized and semi-decentralized schemes are

presented under the first faulty case of scenario 5. Similarly, Figures 4.16, 4.17, and 4.18 represent position errors, surge velocity errors, and thruster forces along  $X$ -axis for all aforementioned schemes under the second faulty case of scenario 5. In addition, the performance measures and time response characteristics are quantitatively summarized in Tables 4.5 and 4.6.

**Table 4.5:** Performance and Time Response Evaluation of Centralized and Semi-Decentralized MPC-Based Fault Accommodation Mechanisms, 40% LOE Fault with 7% FDI Inaccuracy in AUVs #2 and #4

	Centralized MPC	Semi-Decentralized MPC
$J_x$	0.02	0.01
$J_{\tilde{x}}$	0.08	0.07
$J_x^s$	0.15	0.13
$J_{\tilde{x}}^s$	0.11	0.09
$J_u$	$1.75e + 04$	$1.76e + 04$
$J_{total}$	81	69
$t_s$	32	28
$\tilde{t}_s$	8	8.8
$t_{solve}$	0.9	0.07

**Table 4.6:** Performance and Time Response Evaluation of Centralized and Semi-Decentralized MPC-Based Fault Accommodation Mechanisms, Different LOE Faults in AUVs #2, #4, and #5

	Centralized MPC	Semi-Decentralized MPC
$J_x$	0.027	0.023
$J_{\tilde{x}}$	0.07	0.05
$J_x^s$	0.16	0.13
$J_{\tilde{x}}^s$	0.12	0.10
$J_u$	$1.87e + 04$	$1.874e + 04$
$J_{total}$	76	61
$t_s$	35	29
$\tilde{t}_s$	7	8
$t_{solve}$	0.53	0.08

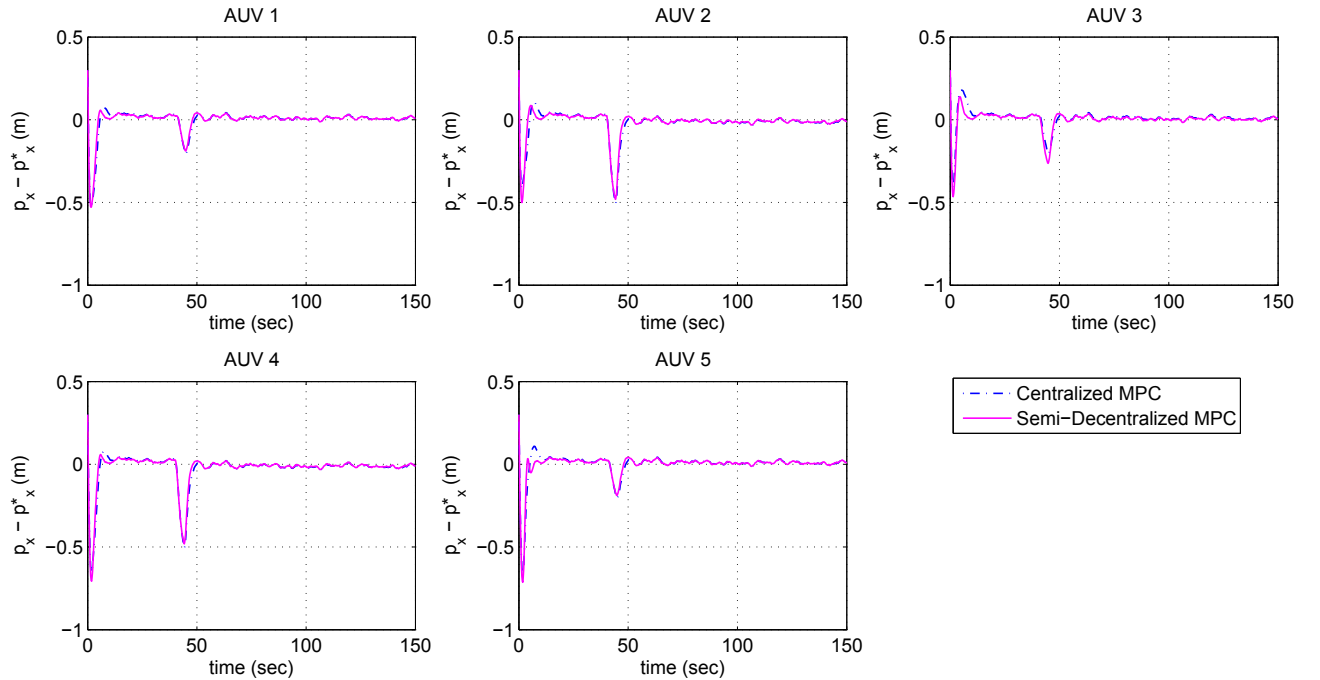


**Figure 4.13:** Error Signals Along  $X$ -axis for Centralized and Semi-Decentralized MPC-Based Accommodation Schemes, First Case in Fault Scenario 5

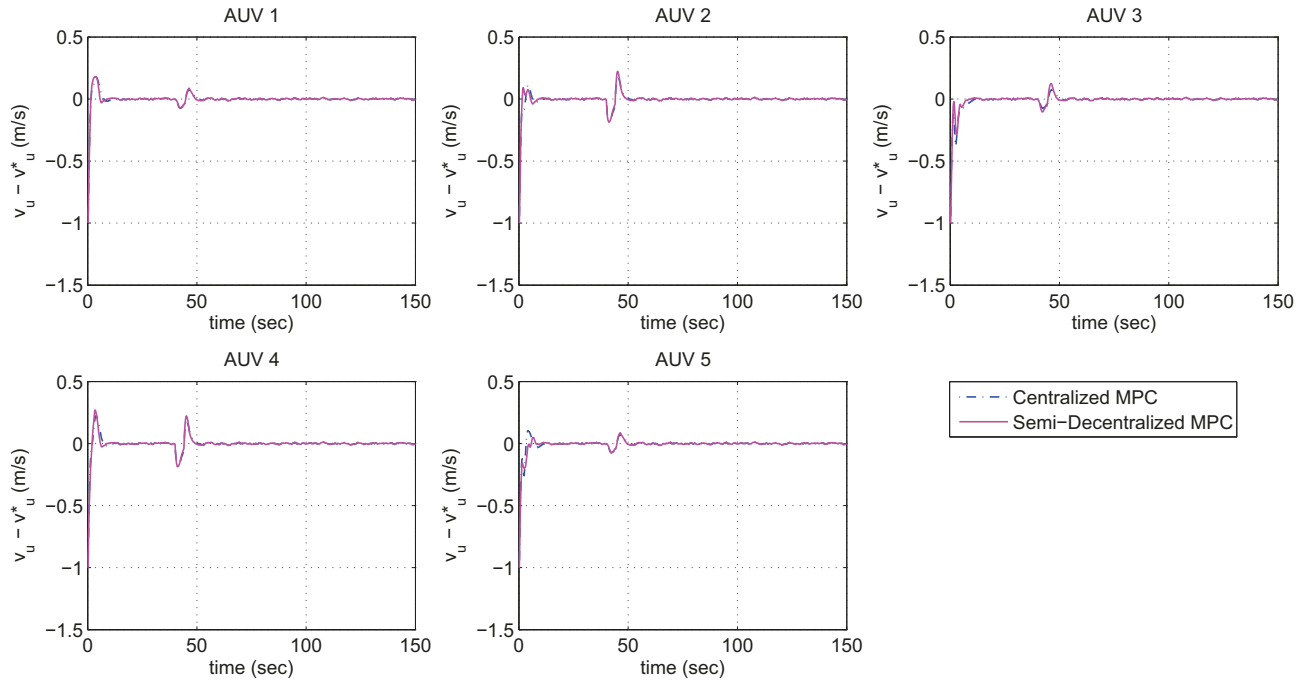


**Figure 4.14:** Surge Velocity Error Signals for Centralized and Semi-Decentralized MPC-Based Accommodation Schemes, First Case in Fault Scenario 5

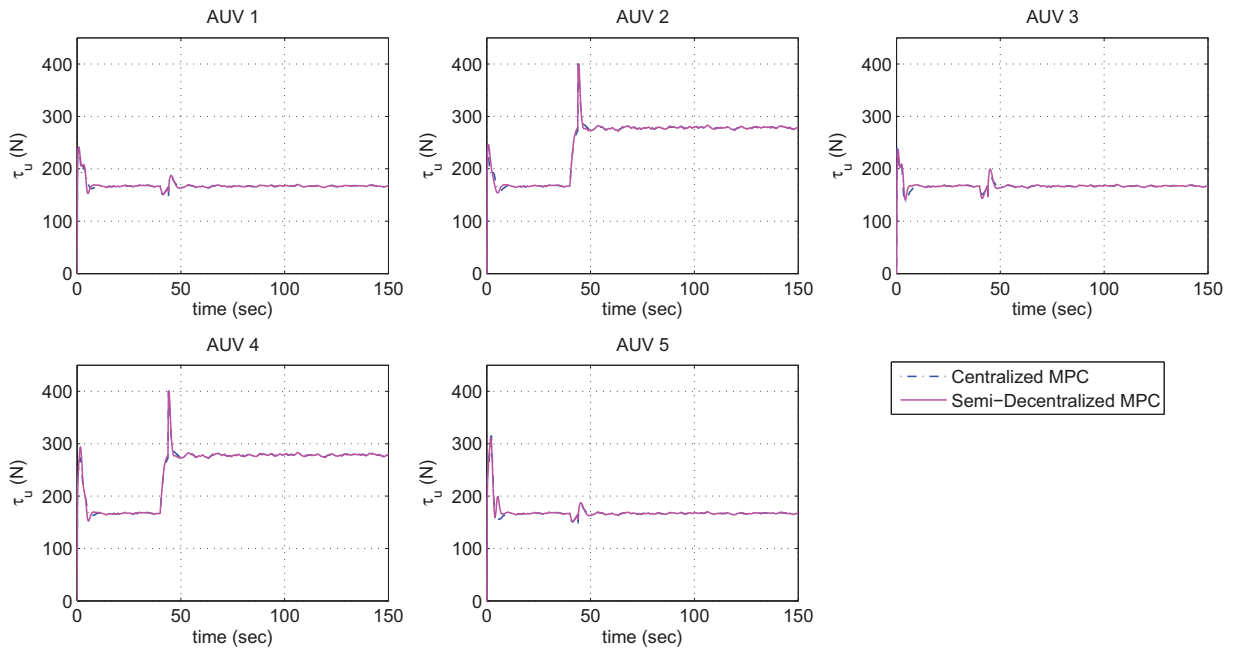


**Figure 4.15:** Thruster Forces along X-axis for Centralized and Semi-Decentralized MPC-Based Accommodation Schemes, First Case in Fault Scenario 5

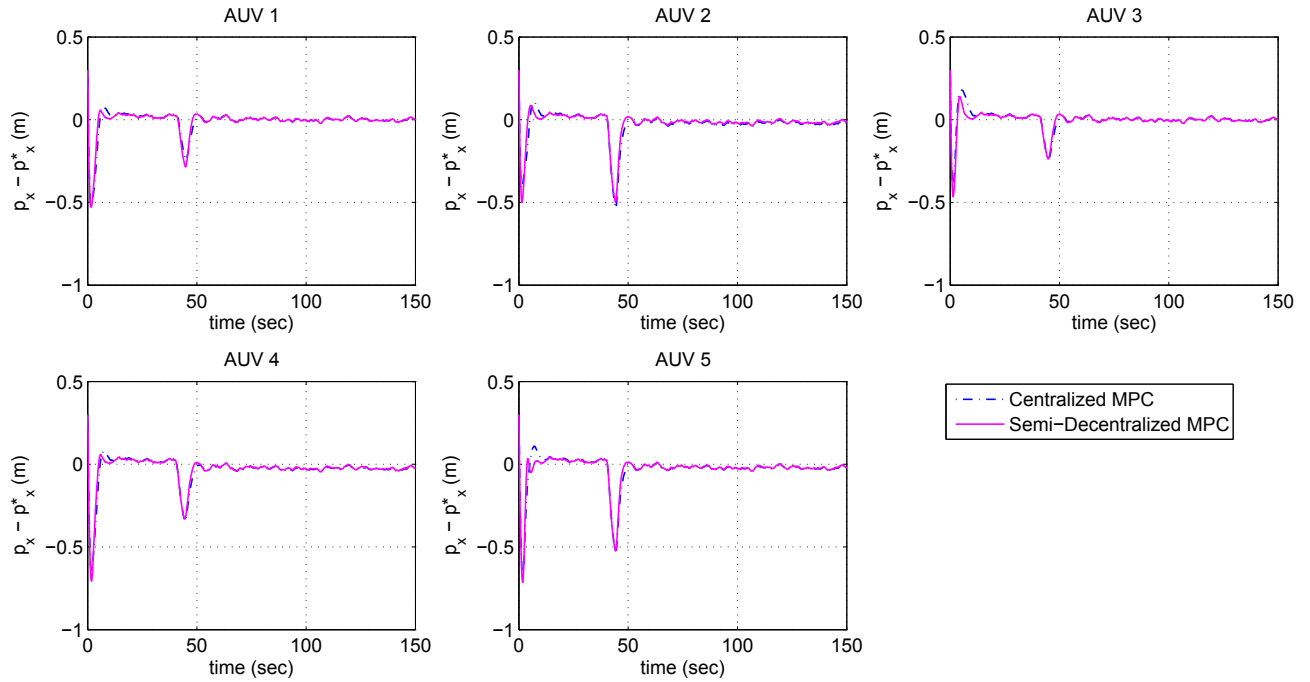


**Figure 4.16:** Error Signals Along  $X$ -axis for Centralized and Semi-Decentralized MPC-Based Accommodation Schemes, Second Case in Fault Scenario 5

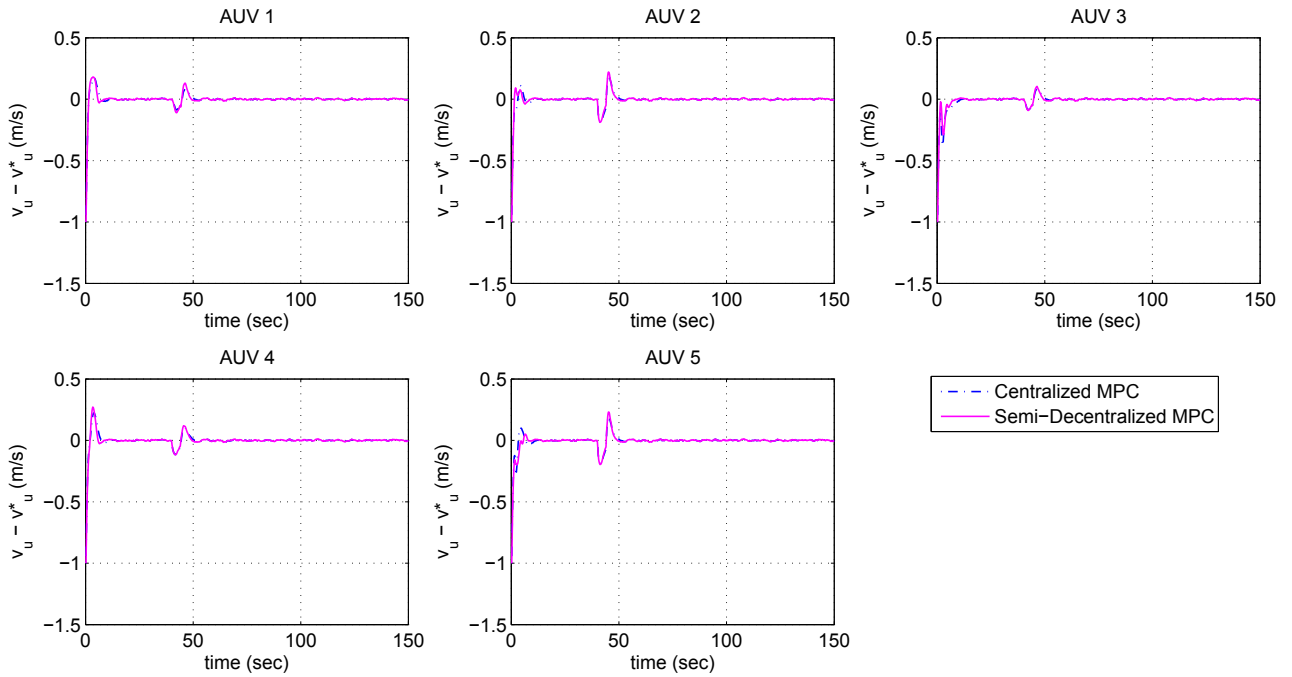


**Figure 4.17:** Surge Velocity Error Signals for Centralized and Semi-Decentralized MPC-Based Accommodation Schemes, Second Case in Fault Scenario 5

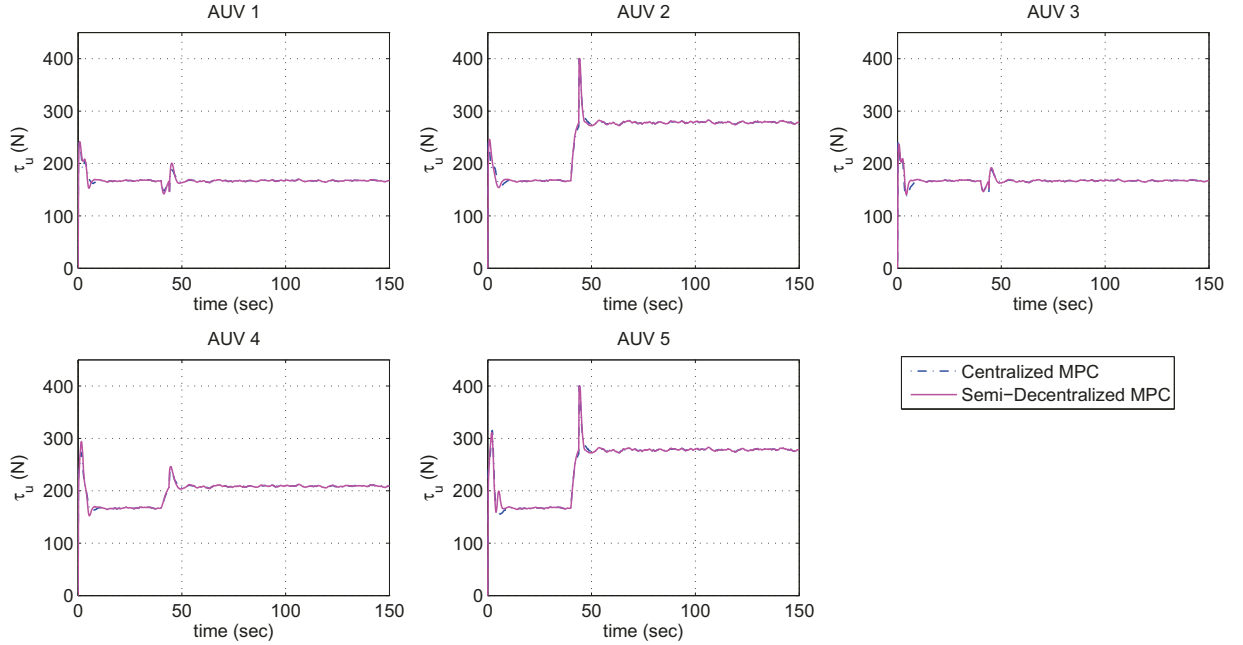


**Figure 4.18:** Thruster Forces along  $X$ -axis for Centralized and Semi-Decentralized MPC-Based Accommodation Schemes, Second Case in Fault Scenario 5

## 4.5.2 Simulation Scenarios for Semi-Decentralized Fault Accommodation Based on Non-Cooperative Dynamic Game

In this subsection, the performance of centralized, semi-decentralized, and decentralized active fault accommodation mechanisms are compared under various fault scenarios and also different conditions on the availability and accuracy of fault estimates provided by FDI module.

### 4.5.2.1 Scenario 1: 5% LOE Fault

In this part, simulations are related to a scenario where 5 % LOE fault has occurred in the actuator along  $X$ -axis of AUV #2 at time  $t_f = 40 \text{ sec}$ . In Figures 4.19, 4.20, and 4.21, position errors, surge velocity errors, and thruster forces along  $X$ -axis for Non-cooperative dynamic game-based centralized, semi-decentralized, and decentralized

schemes are presented under the faulty scenario 1. In addition, the performance measures and time response characteristics of aforementioned accommodation schemes are quantitatively summarized in Table 4.7.

The simulation results show that the nominal centralized and semi-decentralized controllers can mitigate the effect of low severity LOE fault without the need for any fault recovery mechanism. However, the nominal decentralized controller can not maintain acceptable steady-state tracking performance even for low severity LOE fault. Moreover, the control effort cost and total cost of centralized scheme are lower than two other schemes, and these cost values are lower in the semi-decentralized scheme in comparison to the decentralized scheme. However, based on the obtained tracking cost value  $J_x$ , the transient tracking performance deterioration of semi-decentralized controller due to occurrence of low severity fault is lower than two other schemes.

**Table 4.7:** Performance and Time Response Evaluation of Centralized, Semi-Decentralized, and Decentralized Controllers Based on Non-Cooperative Dynamic Game, 5% LOE Fault with No FDI and Recovery

	Centralized Non-Cooperative	Semi-Decentralized Non-Cooperative	Decentralized Non-Cooperative
$J_x$	0.003	0.002	0.005
$J_{\tilde{x}}$	0.005	0.008	0.01
$J_x^s$	0.09	0.08	0.13
$J_{\tilde{x}}^s$	0.08	0.10	0.12
$J_u$	120	124	126
$J_{total}$	6	8	12
$t_s$	22.6464	23.0967	28.1578
$\tilde{t}_s$	—	—	—
$t_{Iter}$	43	34	37

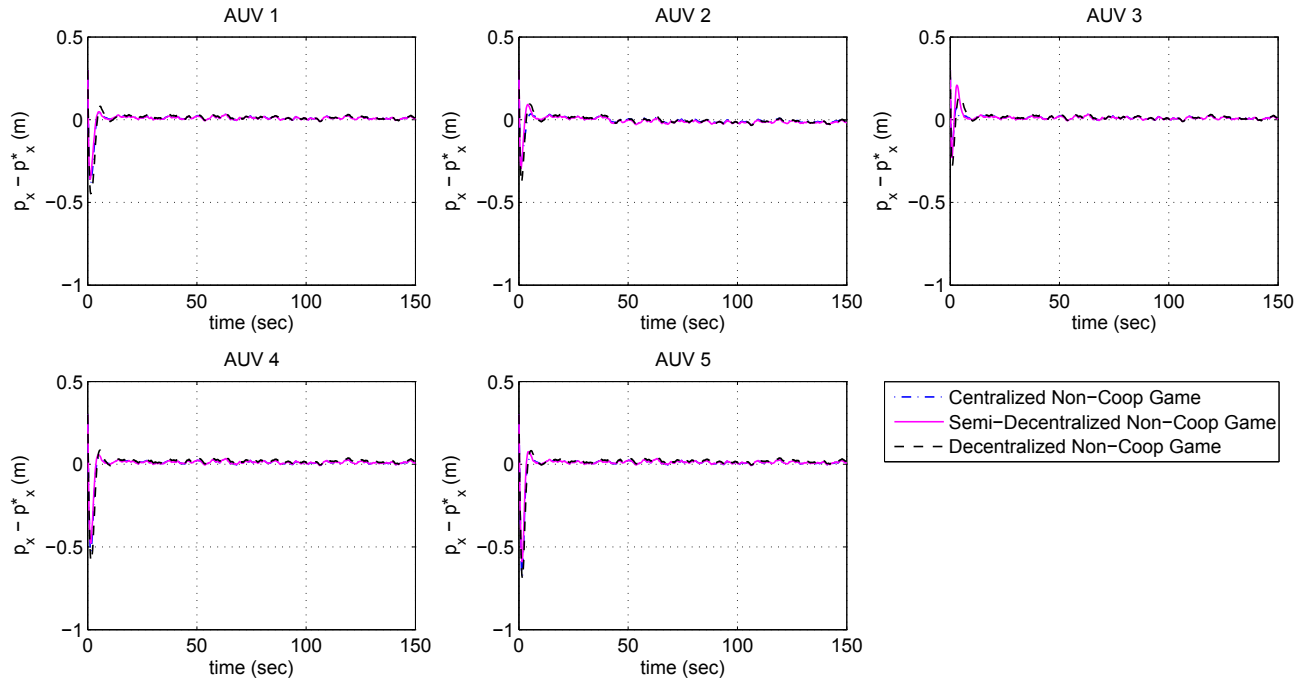


**Figure 4.19:** Error Signals Along  $X$ -axis for Centralized, Semi-Decentralized, and Decentralized Accommodation Schemes Based on Non-Cooperative Game, Fault Scenario 1

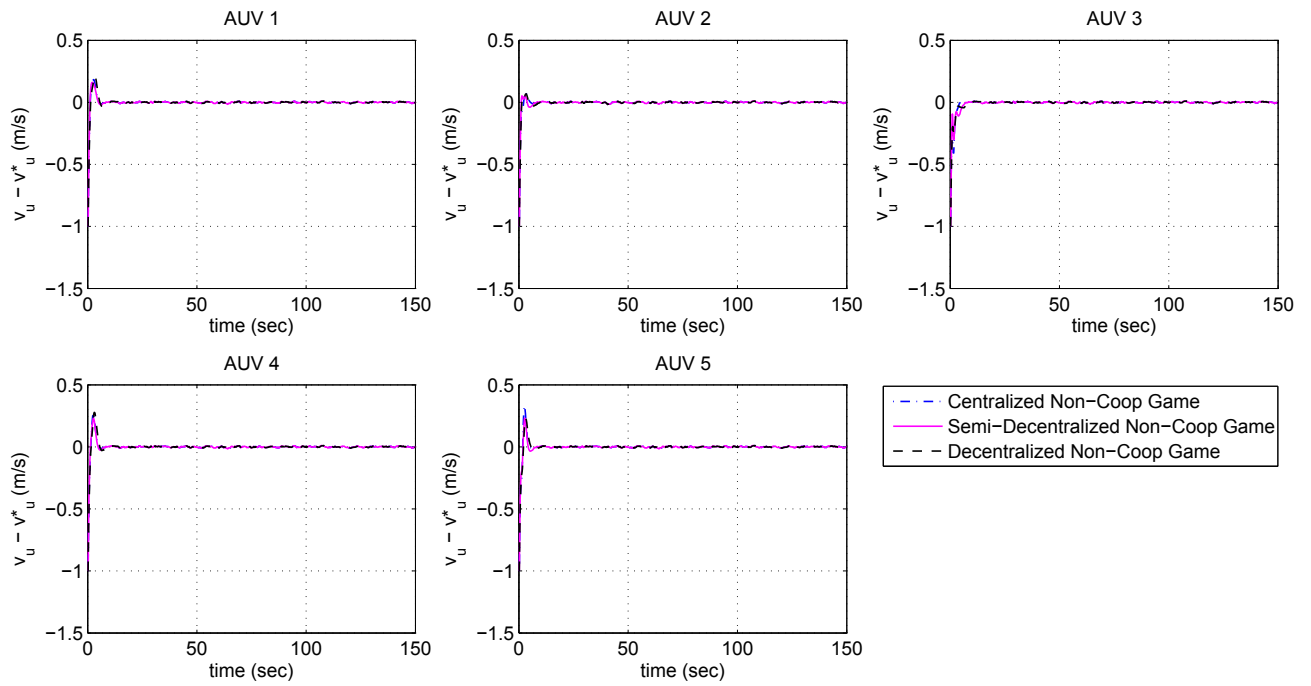


**Figure 4.20:** Surge Velocity Error Signals for Centralized, Semi-Decentralized, and Decentralized Accommodation Schemes Based on Non-Cooperative Game, Fault Scenario 1

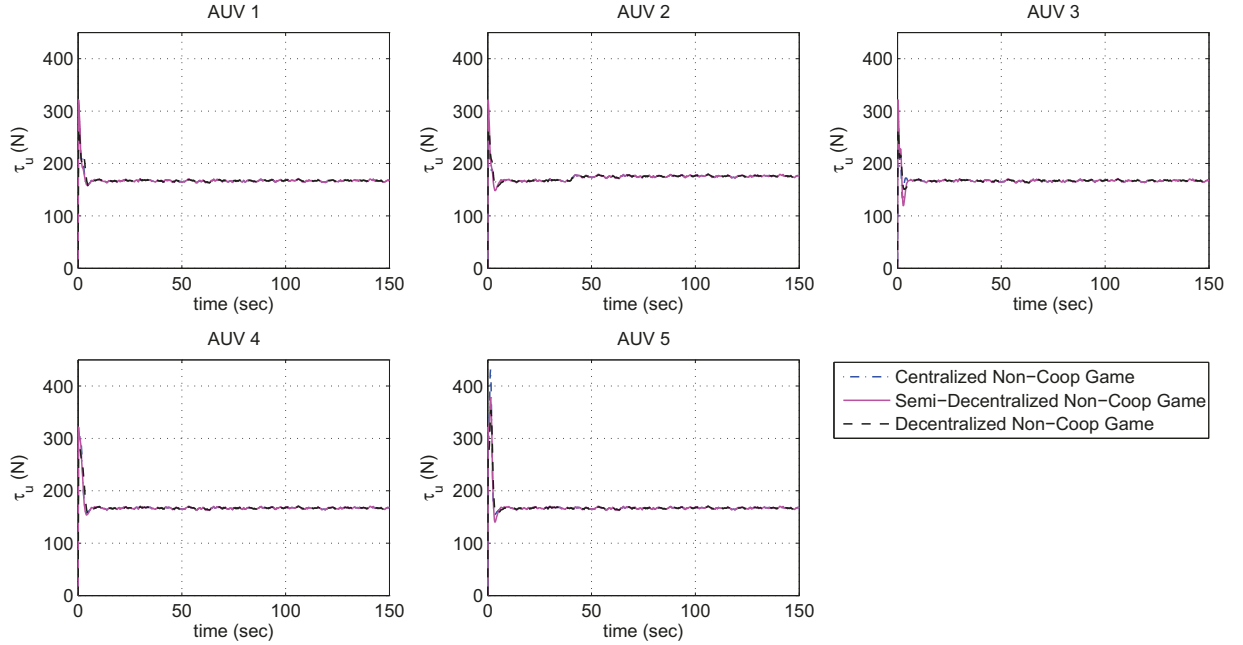


**Figure 4.21:** Thruster Forces along  $X$ -axis for Centralized, Semi-Decentralized, and Decentralized Accommodation Schemes Based on Non-Cooperative Game, Fault Scenario 1

#### 4.5.2.2 Scenario 2: 20% LOE Fault

In this part, simulations are related to a scenario where 20 % LOE fault has occurred in the actuator along  $X$ -axis of AUV #2 at time  $t_f = 40 \text{ sec}$ . Moreover, the time delay associated with the FDI module is assumed to be  $t_d = 4 \text{ sec}$ . The maximum allowable FDI inaccuracies of semi-decentralized and centralized schemes in which the acceptable degraded steady-state performance can be maintained are evaluated to be 20% and 40%, respectively. In this respect, we compare the performance of decentralized, semi-decentralized, and centralized active fault accommodation mechanisms in the presence of 20% inaccuracy in FDI information. In Figures 4.22, 4.23, and 4.24, position errors, surge velocity errors, and thruster forces along  $X$ -axis for all accommodation schemes are presented under the faulty scenario 2. In addition, the performance measures and time response characteristics of aforementioned accommodation schemes are quantitatively summarized in Table 4.8.

These figures and also steady-state performance measures  $J_x^s$  and  $J_{\tilde{x}}^s$  show that the acceptable tracking and formation keeping specifications in faulty situation are met, and the centralized and semi-decentralized accommodation schemes can mitigate the effect of moderate severity LOE fault. However, the steady-state tracking error of decentralized accommodation scheme violates the acceptable specification. Based on the obtained tracking cost value  $J_x$ , the semi-decentralized scheme has the lowest deterioration in its transient tracking performance among all schemes, and after that the centralized scheme has lower performance deterioration than the decentralized scheme. Moreover, the centralized scheme impose lower control effort and total costs to mitigate the effect of fault in the team. The semi-decentralized scheme has also obtained  $J_u$  and  $J_{total}$  cost values very close to centralized scheme.

**Table 4.8:** Performance and Time Response Evaluation of Centralized, Semi-Decentralized, and Decentralized Fault Accommodation Based on Non-Cooperative Dynamic Game, 20% LOE Fault with 20% FDI Inaccuracy

	Centralized Non-Cooperative	Semi-Decentralized Non-Cooperative	Decentralized Non-Cooperative
$J_x$	0.003	0.002	0.006
$J_{\tilde{x}}$	0.011	0.016	0.02
$J_x^s$	0.09	0.08	0.13
$J_{\tilde{x}}^s$	0.09	0.11	0.12
$J_u$	$1.201e + 03$	$1.205e + 03$	$1.298e + 03$
$J_{total}$	10	14	19
$t_s$	22	23	28
$\tilde{t}_s$	5.7	6.1	6.2
$t_{Iter}$	16	13	15

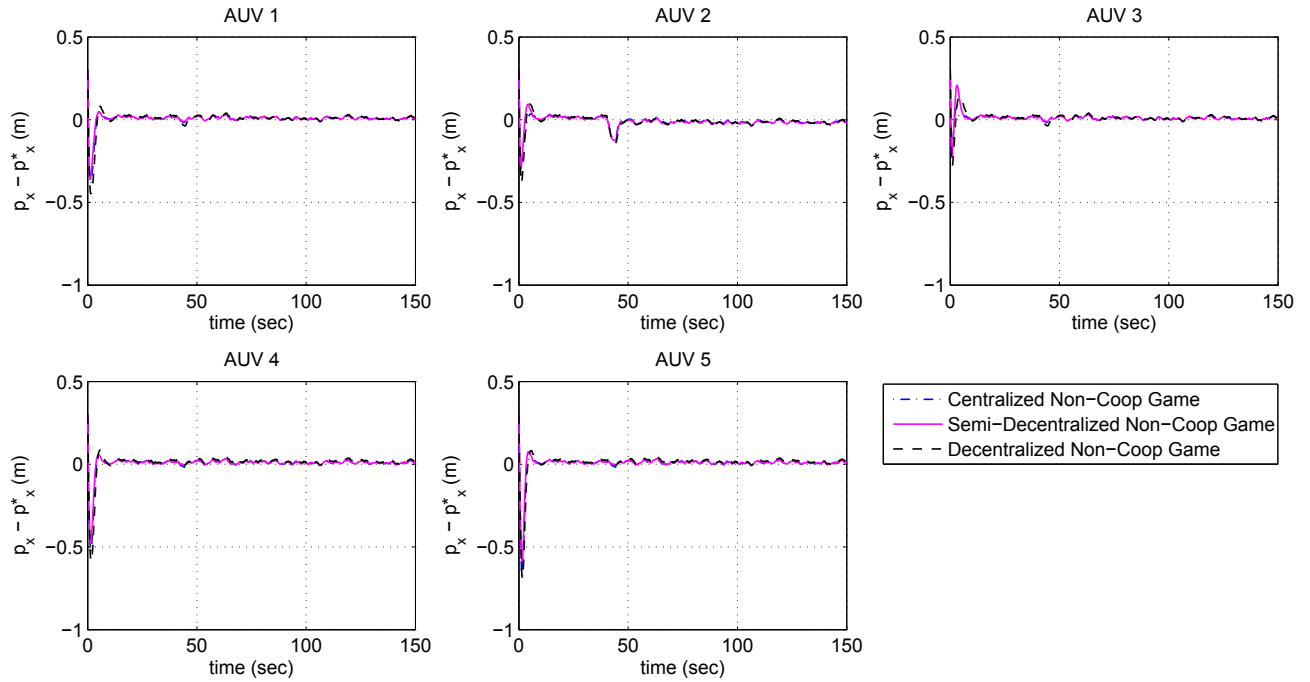


**Figure 4.22:** Error Signals Along  $X$ -axis for Centralized, Semi-Decentralized, and Decentralized Accommodation Schemes Based on Non-Cooperative Game, Fault Scenario 2

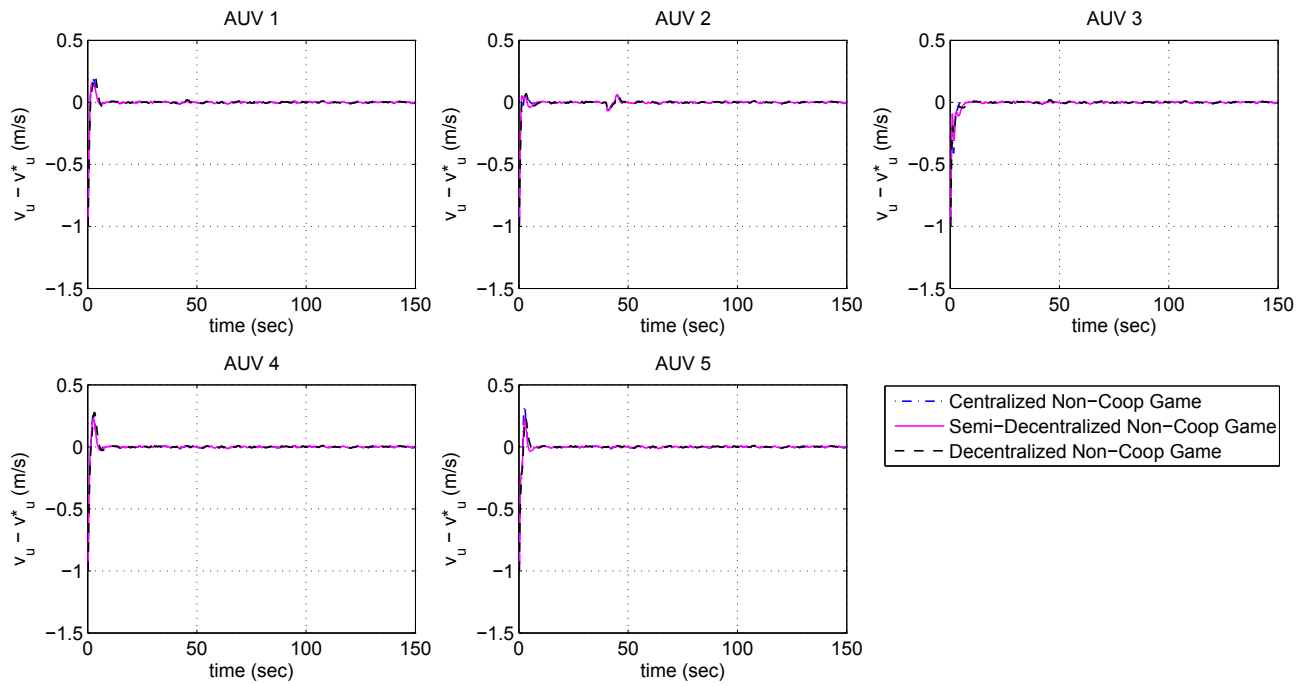


**Figure 4.23:** Surge Velocity Error Signals for Centralized, Semi-Decentralized, and Decentralized Accommodation Schemes Based on Non-Cooperative Game, Fault Scenario 2

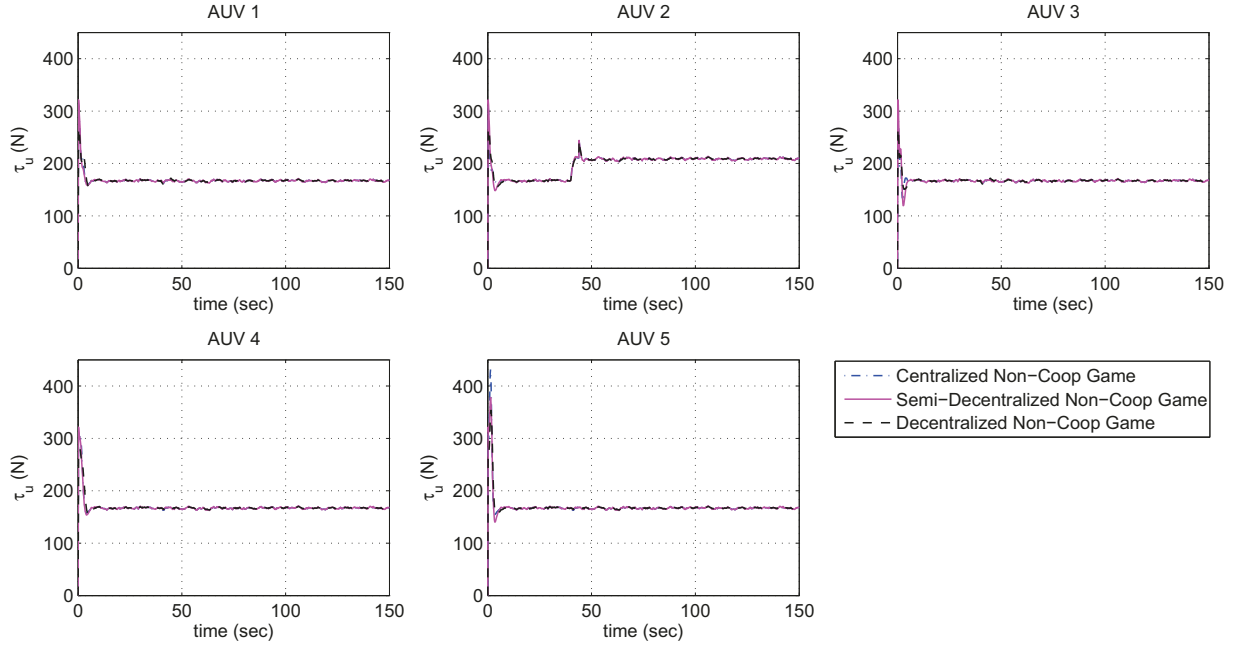


**Figure 4.24:** Thruster Forces along  $X$ -axis for Centralized, Semi-Decentralized, and Decentralized Accommodation Schemes Based on Non-Cooperative Game, Fault Scenario 2

#### 4.5.2.3 Scenario 3: 40% LOE Fault

In this part, simulations are related to 40% LOE fault that is injected to the actuator along  $X$ -axis of AUV #2 at time  $t_f = 40\text{sec}$ . Moreover, the time delay associated with FDI module is assumed to be  $t_d = 4\text{sec}$ . The maximum allowable FDI inaccuracies of semi-decentralized and centralized schemes in which the acceptable degraded steady-state performance can be maintained are evaluated to be 7% and 13%, respectively. In this respect, we compare the performance of decentralized, semi-decentralized, and centralized active fault accommodation mechanisms in the presence of 7% inaccuracy in FDI information. In Figures 4.25, 4.26, and 4.27, position errors, surge velocity errors, and thruster forces along  $X$ -axis for all accommodation schemes are presented under the faulty scenario 3. In addition, the performance measures and time response characteristics of aforementioned accommodation schemes are quantitatively summarized in Table 4.9.

The steady-state errors, verify that the acceptable tracking and formation keeping specifications in faulty situation are met, and the centralized and semi-decentralized accommodation schemes can mitigate the effect of high severity LOE fault. However, the steady-state tracking error of decentralized accommodation scheme violates the acceptable specification. Based on the obtained tracking cost value  $J_x$ , the semi-decentralized scheme has the lowest deterioration in its transient tracking performance among all schemes, and after that the centralized scheme has lower performance deterioration than the decentralized scheme. Moreover, the centralized scheme impose lower control effort and accommodation costs to mitigate the effect of fault in the team, and after that the semi-decentralized scheme has lower  $J_u$  and  $J_{total}$  cost values than the decentralized scheme. It is worth noting that, the semi-decentralized scheme can achieve a performance close to centralized scheme without that much increase in  $J_u$  and  $J_{total}$  cost values.

**Table 4.9:** Performance and Time Response Evaluation of Centralized, Semi-Decentralized, and Decentralized Fault Accommodation Based on Non-Cooperative Dynamic Game, 40% LOE Fault with 7% FDI Inaccuracy

	Centralized Non-Cooperative	Semi-Decentralized Non-Cooperative	Decentralized Non-Cooperative
$J_x$	0.005	0.005	0.009
$J_{\tilde{x}}$	0.04	0.05	0.06
$J_x^s$	0.09	0.08	0.13
$J_{\tilde{x}}^s$	0.08	0.10	0.11
$J_u$	$8.771e + 03$	$8.783e + 03$	$8.782e + 03$
$J_{total}$	34	48	58
$t_s$	39	23	43
$\tilde{t}_s$	6.5	7.0	7.2
$t_{Iter}$	21	17	19

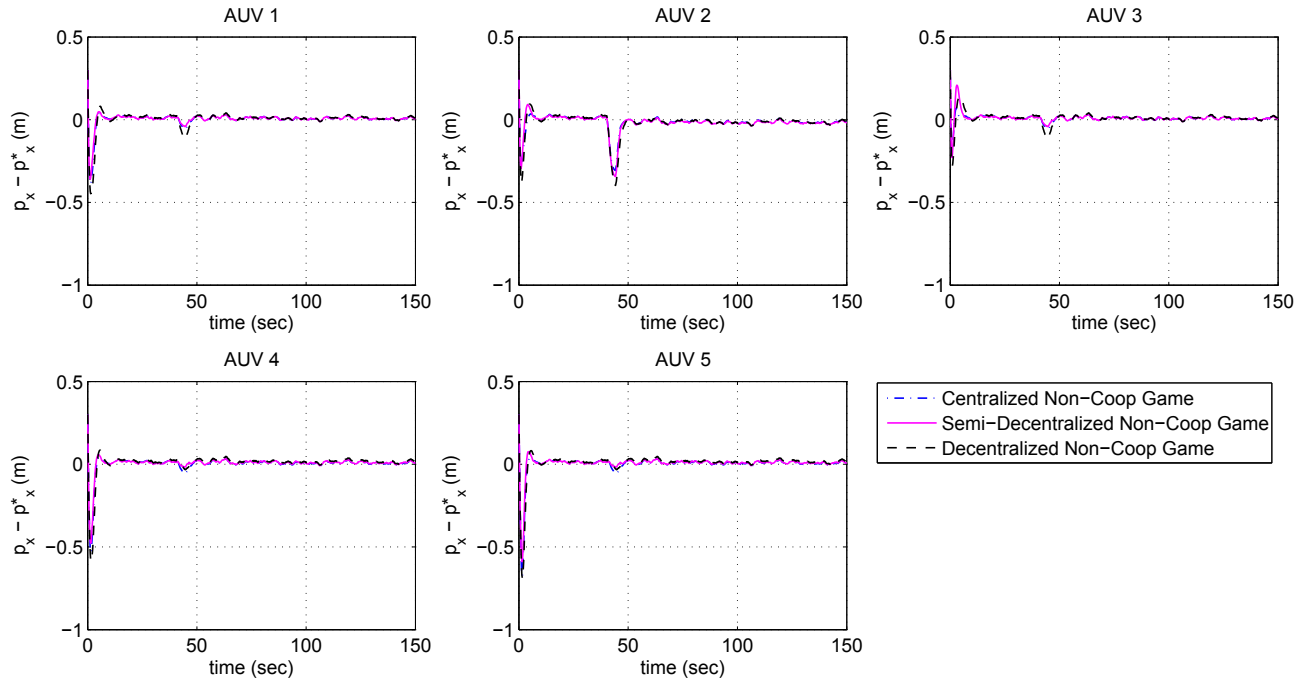


**Figure 4.25:** Error Signals Along  $X$ -axis for Centralized, Semi-Decentralized, and Decentralized Accommodation Schemes Based on Non-Cooperative Game, Fault Scenario 3

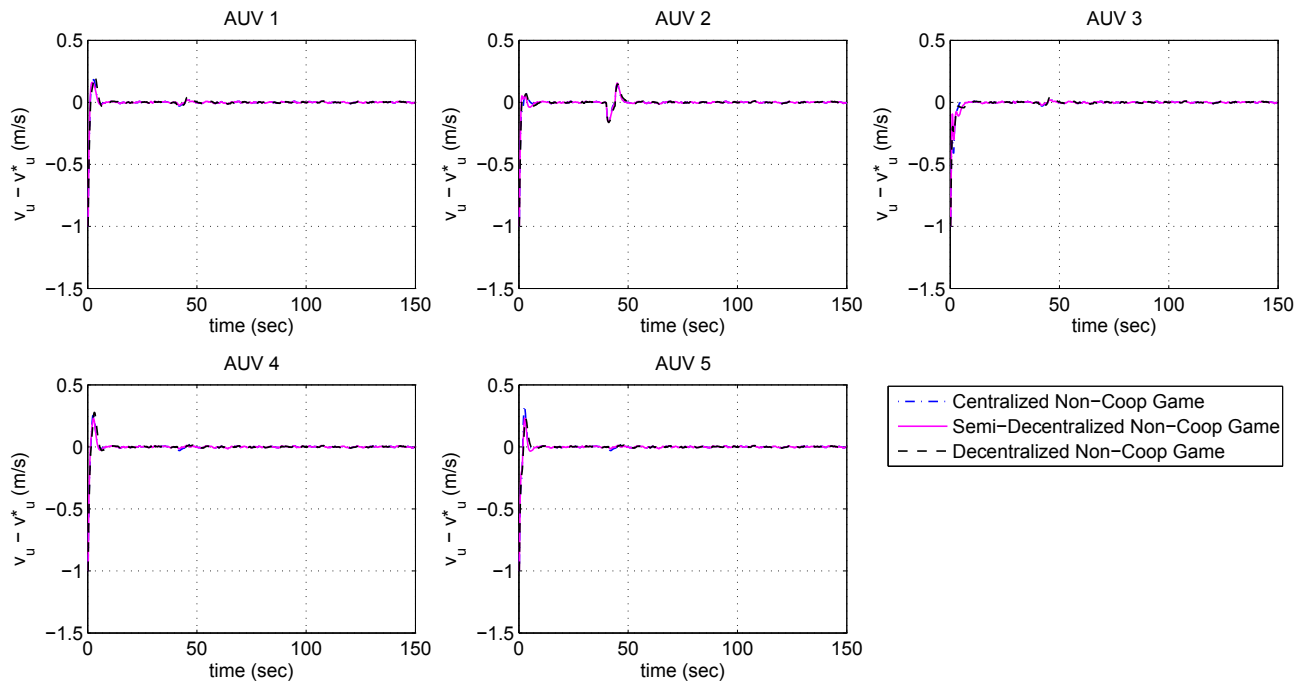


**Figure 4.26:** Surge Velocity Error Signals for Centralized, Semi-Decentralized, and Decentralized Accommodation Schemes Based on Non-Cooperative Game, Fault Scenario 3

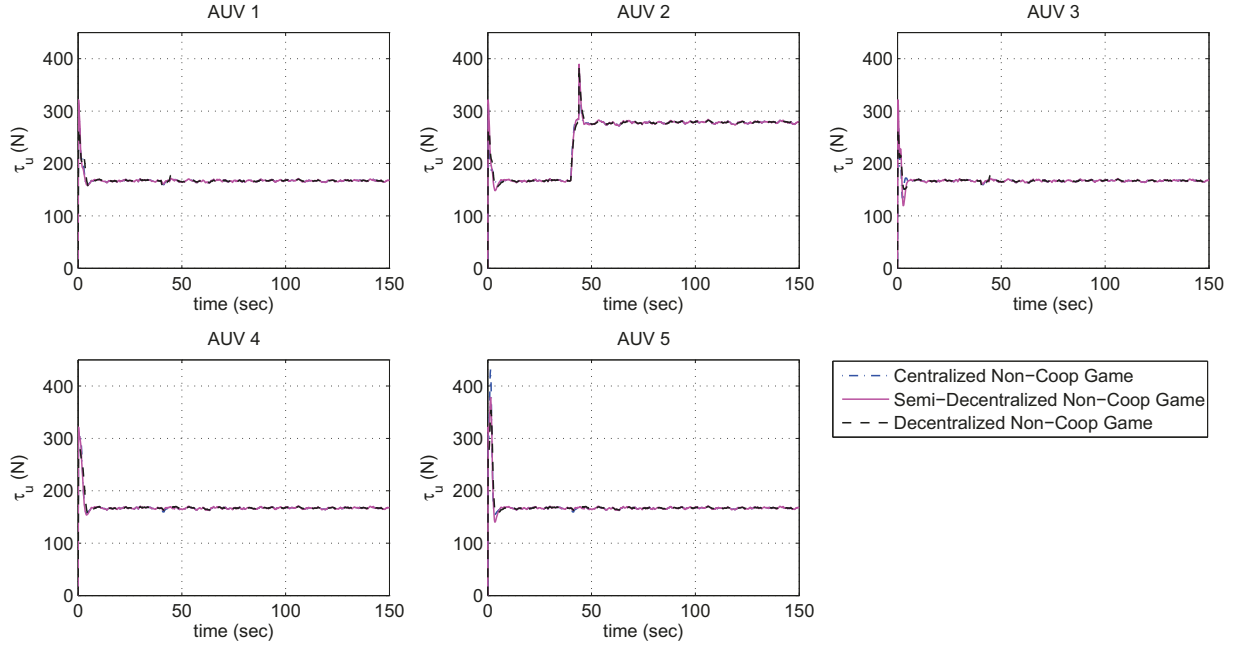


**Figure 4.27:** Thruster Forces along  $X$ -axis for for Centralized, Semi-Decentralized, and Decentralized Accommodation Schemes Based on Non-Cooperative Game, Fault Scenario 3

#### 4.5.2.4 Scenario 4: Influence of FDI Time Delay

In this part, the effect of fault detection time delay on the performance of semi-decentralized accommodation mechanism is investigated. In this regard, high severity LOE fault of 40% is injected to the system. Additionally, the maximum allowable FDI estimation error of 7% is considered. The simulations are conducted under three different FDI time delays, namely  $t_d = 2 \text{ sec}$ ,  $4 \text{ sec}$ , and  $6 \text{ sec}$ . In Figures 4.28, 4.29, and 4.30, position errors, surge velocity errors, and thruster forces along  $X$ -axis for semi-decentralized scheme are presented under fault scenario 4. In addition, the performance measures and time response characteristics for this scheme are quantitatively summarized in Table 4.10. It can be observed that the semi-decentralized accommodation mechanism can recover multi-agent system from LOE fault for larger values of FDI time delay, however larger time delay will result in poor transient behavior, higher tracking, formation keeping, and total accommodation cost values.

**Table 4.10:** Performance and Time Response Evaluation of Semi-Decentralized Fault Accommodation Based on Non-Cooperative Dynamic Game under Various FDI Time Delays, 40% LOE Fault with 7% FDI Inaccuracy

	Semi-Decentralized Non-Cooperative		
	$t_d = 2 \text{ sec}$	$t_d = 4 \text{ sec}$	$t_d = 6 \text{ sec}$
$J_x$	0.003	0.005	0.006
$J_{\tilde{x}}$	0.03	0.05	0.08
$J_x^s$	0.08	0.08	0.08
$J_{\tilde{x}}^s$	0.1	0.1	0.1
$J_u$	$8.7835e + 03$	$8.7838e + 03$	$8.7776e + 03$
$J_{total}$	26	48	68
$t_s$	23	23	23
$\tilde{t}_s$	5	7	8

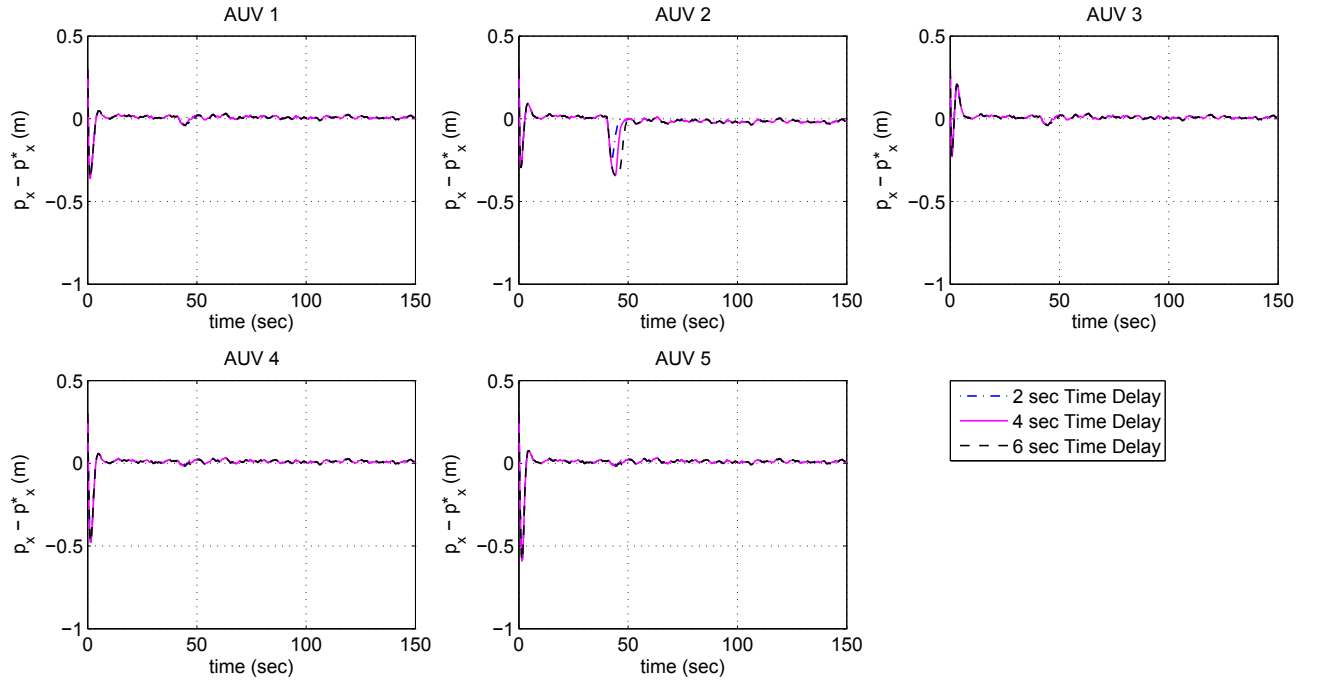


**Figure 4.28:** Error Signals Along X-axis for Semi-Decentralized Accommodation Scheme Based on Non-Cooperative Game, Fault Scenario 4

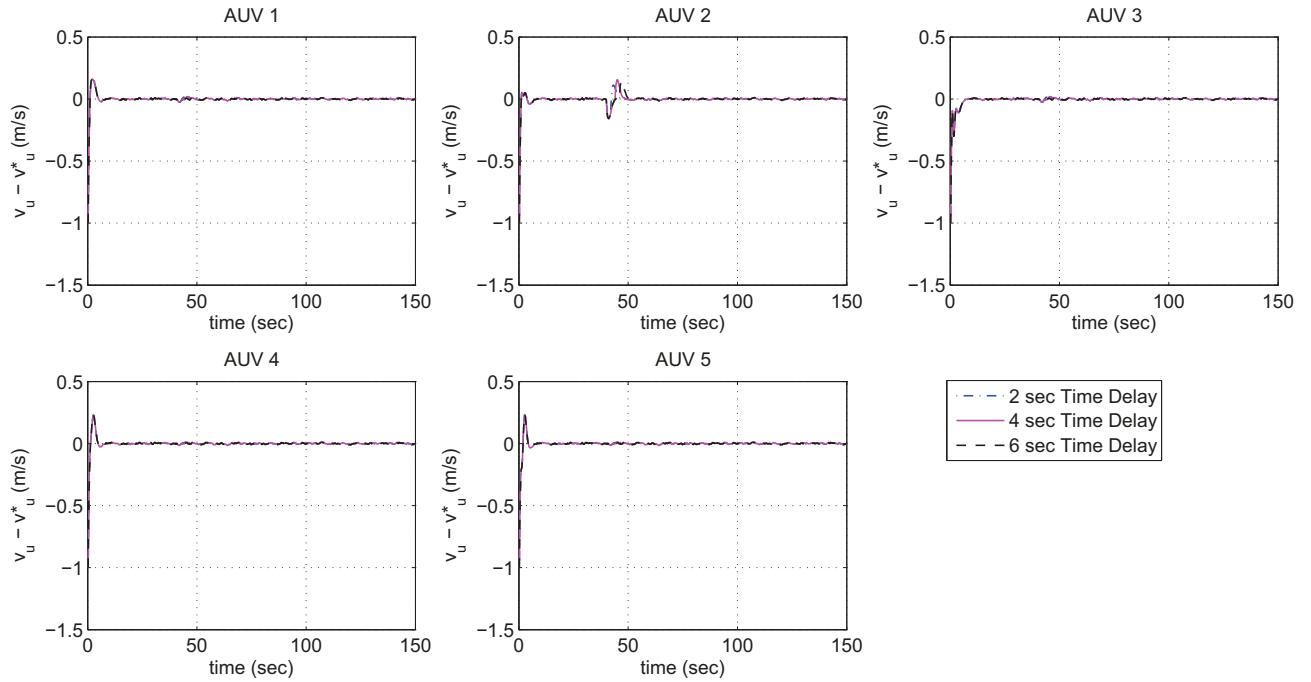


**Figure 4.29:** Surge Velocity Error Signals for Semi-Decentralized Accommodation Scheme Based on Non-Cooperative Game, Fault Scenario 4

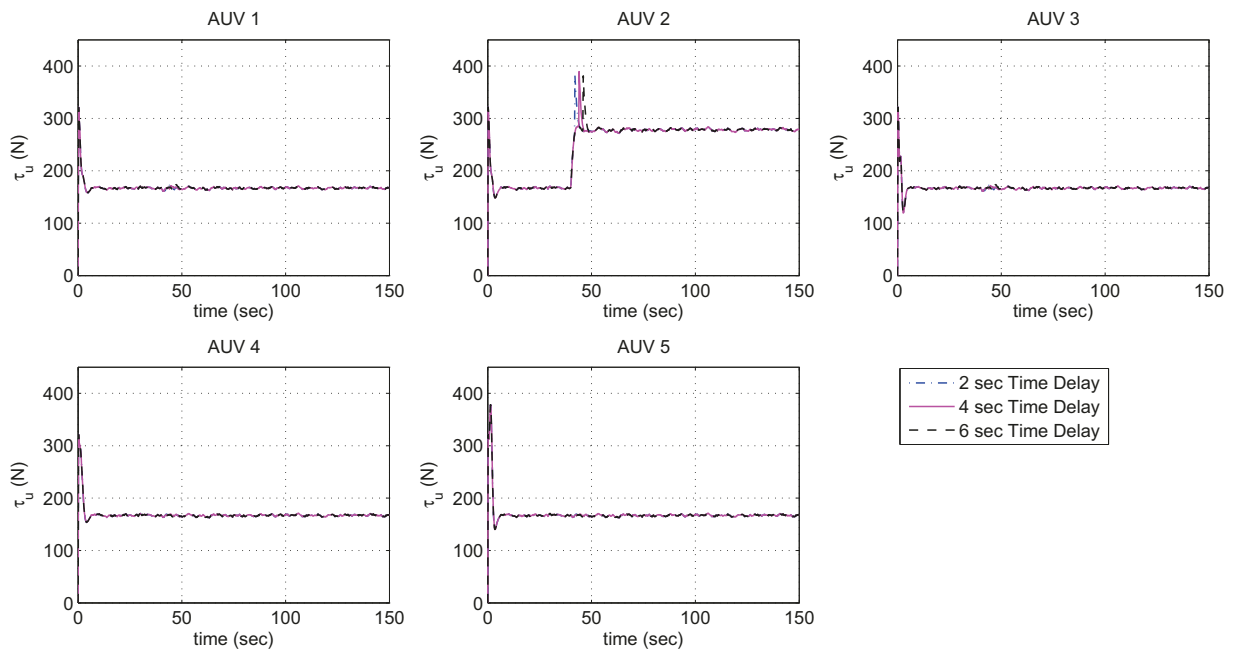


**Figure 4.30:** Thruster Forces along X-axis for Semi-Decentralized Accommodation Scheme Based on Non-Cooperative Game, Fault Scenario 4

#### 4.5.2.5 Scenario 5: Multiple Faulty Agents in the Team

In this part, the performance of centralized, semi-decentralized, and decentralized accommodation schemes are compared when there are multiple faulty agents in the team. The first set of simulations are conducted when 40% LOE fault is injected to the actuators along  $X$ -axis of AUV #2 and #4 at time  $t_f = 40 \text{ sec}$ . The second set of simulations are conducted when AUVs #2, #4, and #5 are considered faulty with different fault severities. It is assumed that AUV #2 and #5 have 40% LOE fault and AUV #4 has 20% LOE fault. Moreover, the time delay associated with the FDI module of each agent in both case is assumed to be  $t_d = 4 \text{ sec}$ . As previously mentioned, the maximum allowable FDI inaccuracy of each agent is assumed to be 7% for 40% LOE fault and 20% for 20% LOE fault.

Figures 4.31, 4.32, and 4.33 show position errors, surge velocity errors, and thruster forces along  $X$ -axis for centralized, semi-decentralized, and decentralized accommodation schemes are presented under the first faulty case of scenario 5. Similarly, Figures 4.34, 4.35, and 4.36 represent position errors, surge velocity errors, and thruster forces along  $X$ -axis for all aforementioned schemes under the second faulty case of scenario 5. In addition, the performance measures and time response characteristics are quantitatively summarized in Tables 4.11 and 4.12.

These figures and also steady-state performance measures  $J_x^s$  and  $J_{\dot{x}}^s$  show that the acceptable tracking and formation keeping specifications in faulty situation are met, and the centralized and semi-decentralized accommodation schemes can mitigate the effect of multiple faulty agents in the team. However, the steady-state tracking error of decentralized accommodation scheme violates the acceptable specification. Based on the obtained tracking cost value  $J_x$ , the semi-decentralized scheme has the lowest deterioration in its transient tracking performance among all schemes, and

after that the centralized scheme has lower performance deterioration than the decentralized scheme. Moreover, the centralized scheme impose lower control effort and total accommodation costs to mitigate the effect of fault in the team, and after that the semi-decentralized scheme has lower  $J_u$  and  $J_{total}$  cost values than the decentralized scheme. However, the semi-decentralized scheme has higher transient formation keeping cost than two other schemes. The reason for higher value of  $J_{\tilde{x}}$  is that the transient tracking performance of healthy agents are less deteriorated which result in higher formation keeping cost of semi-decentralized scheme accordingly.

**Table 4.11:** Performance and Time Response Evaluation of Centralized, Semi-Decentralized, and Decentralized Fault Accommodation Based on Non-Cooperative Dynamic Game, 40% LOE Fault with 7% FDI Inaccuracy in AUVs #2 and #4

	Centralized Non-Cooperative	Semi-Decentralized Non-Cooperative	Decentralized Non-Cooperative
$J_x$	0.01	0.009	0.016
$J_{\tilde{x}}$	0.05	0.07	0.06
$J_x^s$	0.10	0.08	0.13
$J_{\tilde{x}}^s$	0.10	0.12	0.11
$J_u$	$1.745e + 04$	$1.746e + 04$	$1.747e + 04$
$J_{total}$	50	65	59
$t_s$	39	42	45
$\tilde{t}_s$	6	7	8
$t_{Iter}$	23	18	19

**Table 4.12:** Performance and Time Response Evaluation of Centralized, Semi-Decentralized, and Decentralized Fault Accommodation Based on Non-Cooperative Dynamic Game, Different LOE Faults in AUVs #2, #4, and #5

	Centralized Non-Cooperative	Semi-Decentralized Non-Cooperative	Decentralized Non-Cooperative
$J_x$	0.013	0.010	0.021
$J_{\tilde{x}}$	0.04	0.06	0.04
$J_x^s$	0.10	0.09	0.13
$J_{\tilde{x}}^s$	0.10	0.12	0.11
$J_u$	$1.856e + 04$	$1.857e + 04$	$1.858e + 04$
$J_{total}$	46	57	52
$t_s$	39	42	45
$\tilde{t}_s$	6	7	8
$t_{Iter}$	23	19	17

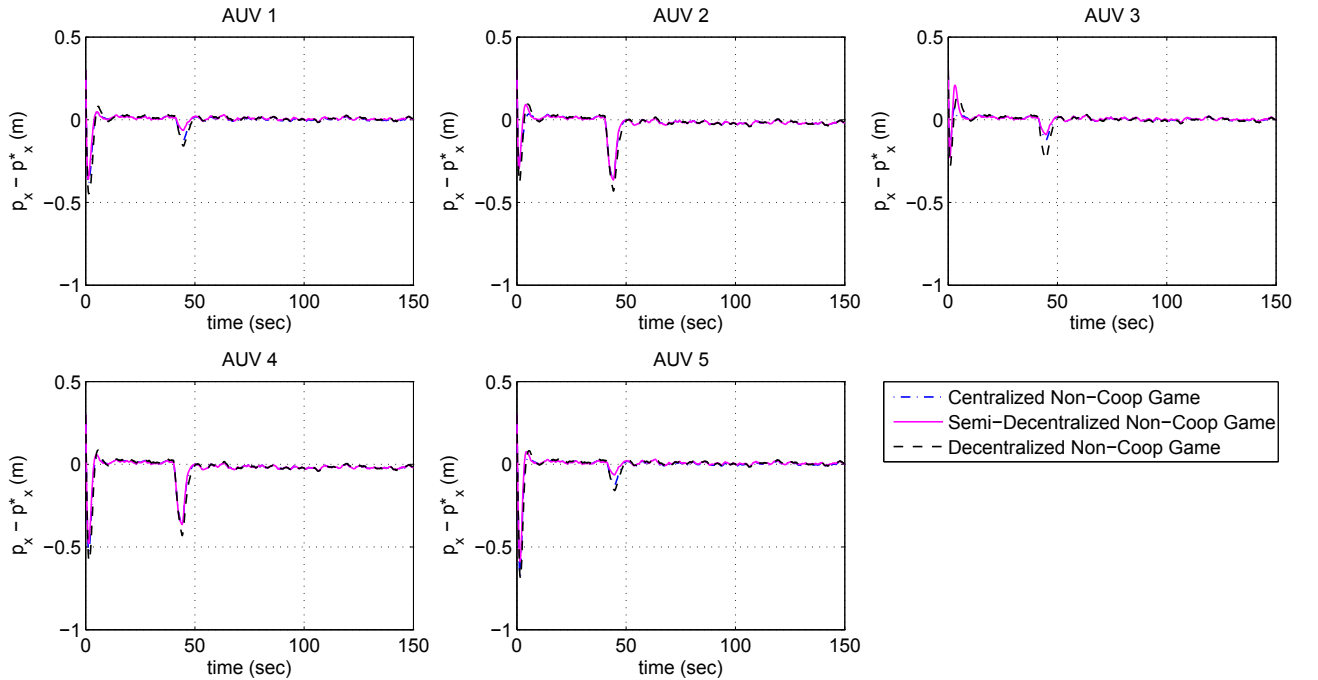


**Figure 4.31:** Error Signals Along  $X$ -axis for Centralized, Semi-Decentralized, and Decentralized Accommodation Schemes Based on Non-Cooperative Game, Fault Scenario 5.1

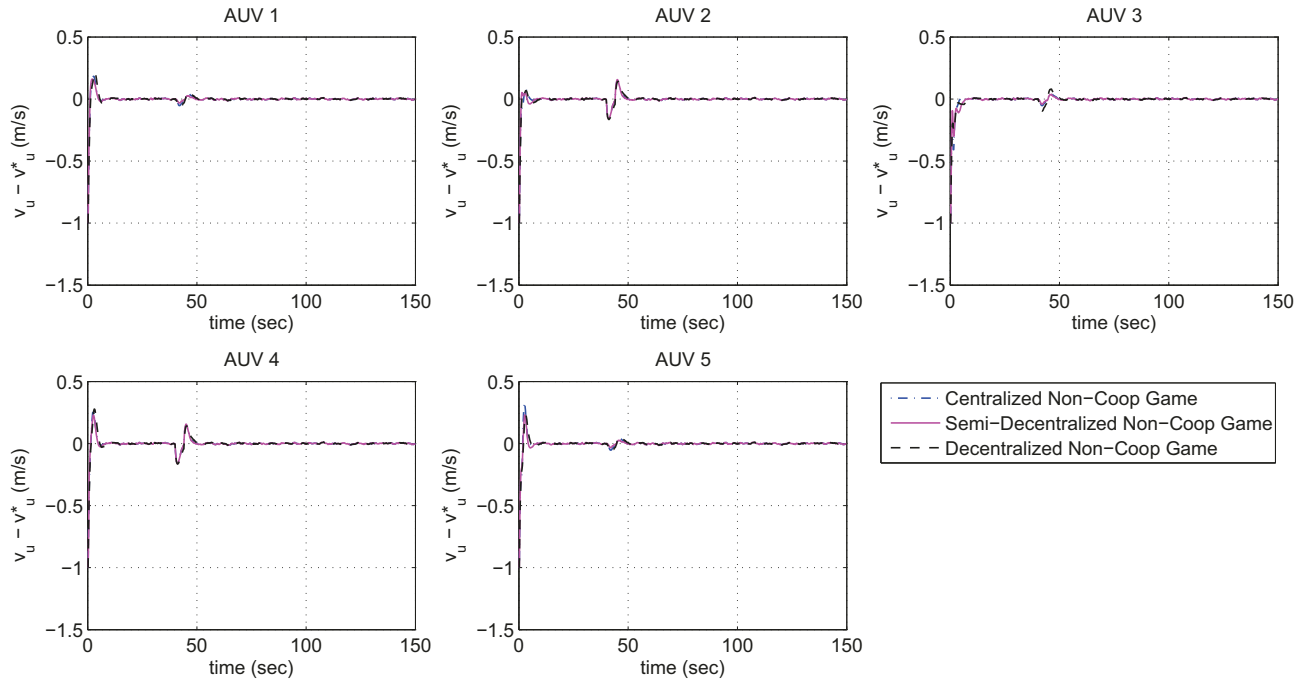


**Figure 4.32:** Surge Velocity Error Signals for Centralized, Semi-Decentralized, and Decentralized Accommodation Schemes Based on Non-Cooperative Game, Fault Scenario 5.1

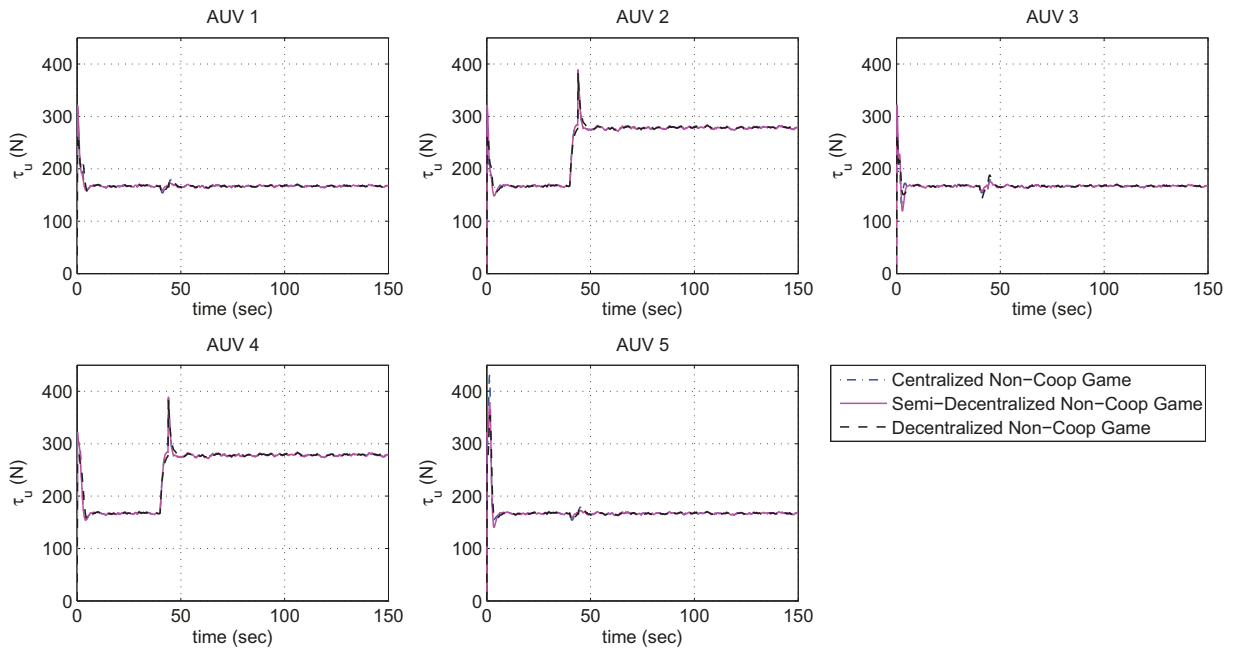


**Figure 4.33:** Thruster Forces along  $X$ -axis for Centralized, Semi-Decentralized, and Decentralized Accommodation Schemes Based on Non-Cooperative Game, Fault Scenario 5.1

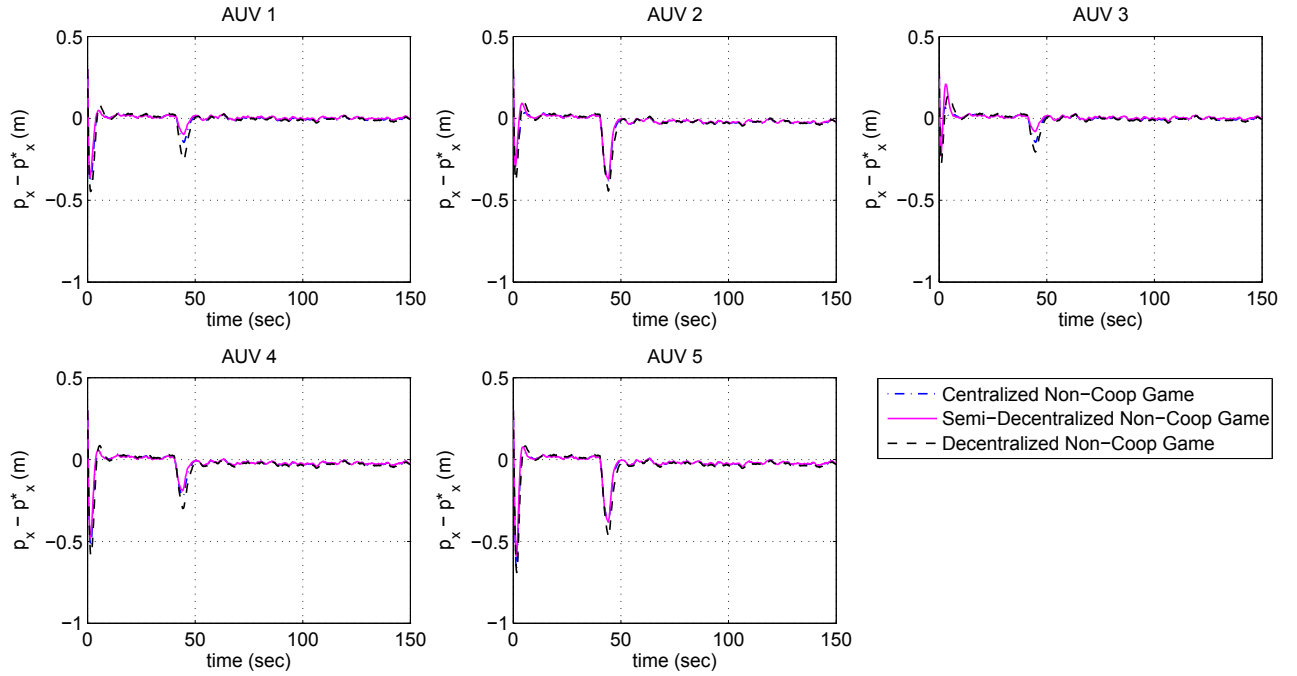


**Figure 4.34:** Error Signals Along  $X$ -axis for Centralized, Semi-Decentralized, and Decentralized Accommodation Schemes Based on Non-Cooperative Game, Fault Scenario 5.2

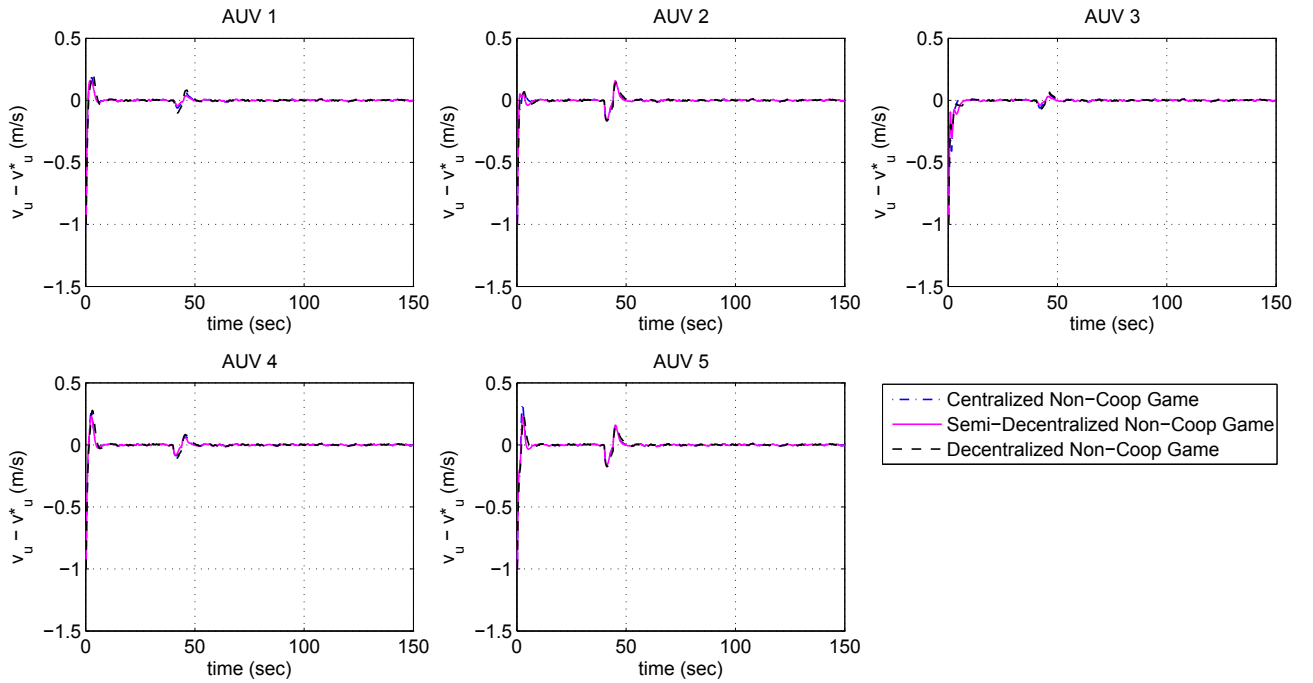


**Figure 4.35:** Surge Velocity Error Signals for Centralized, Semi-Decentralized, and Decentralized Accommodation Schemes Based on Non-Cooperative Game, Fault Scenario 5.2

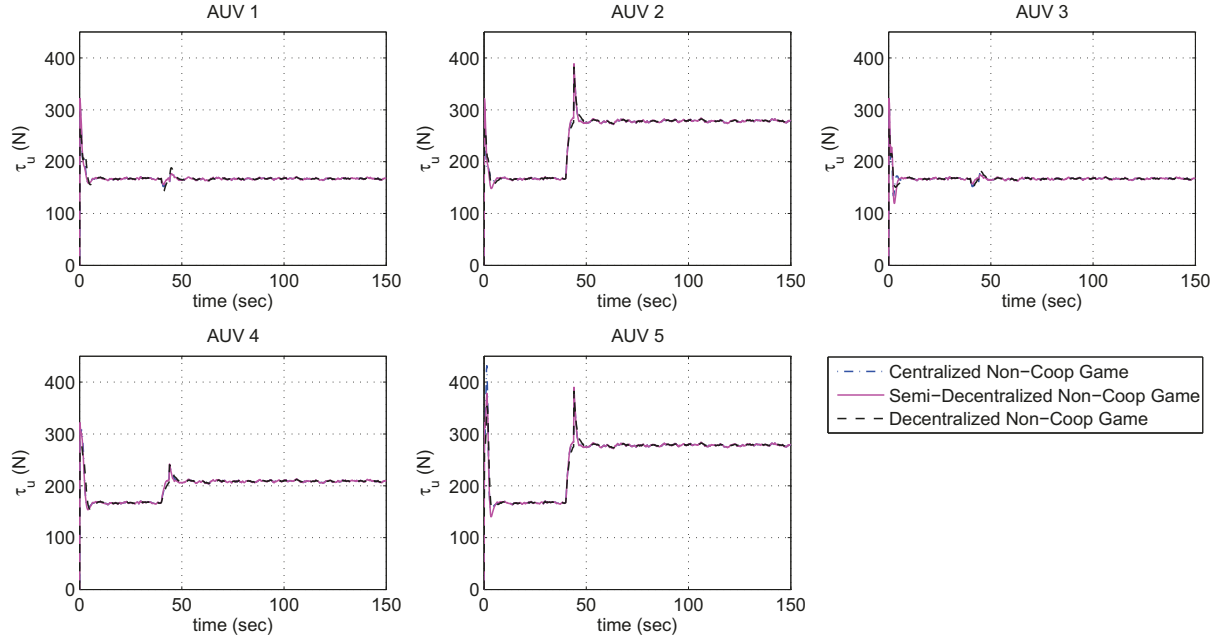


**Figure 4.36:** Thruster Forces along  $X$ -axis for Centralized, Semi-Decentralized, and Decentralized Accommodation Schemes Based on Non-Cooperative Game, Fault Scenario 5.2

### 4.5.3 Simulation Scenario for Centralized Cooperative vs. Centralized Non-Cooperative Dynamic Game

In this subsection, the performance of both cooperative and non-cooperative dynamic game approaches to centralized accommodation scheme are compared under a general fault scenario in which AUVs #2, #4, and #5 are considered faulty with different fault severities. It is assumed that AUV #2 and #5 have 40% LOE fault and AUV #4 has 20% LOE fault. The LOE faults are injected at time  $t_f = 40 \text{ sec}$ . Moreover, the time delay associated with FDI module of each agent is assumed to be  $t_d = 4 \text{ sec}$ . As previously mentioned, the maximum allowable FDI inaccuracy of each agent is assumed to be 7% for 40% LOE fault and 20% for 20% LOE fault. Figures 4.37, 4.38, and 4.39 represent position errors, surge velocity errors, and thruster forces along  $X$ -axis for these

two centralized schemes under this fault scenario. In addition, the performance measures and time response characteristics are quantitatively summarized in Table 4.13. This faulty scenario is investigated to show that how bargaining protocol of cooperative scheme can handle inconsistencies among agents. In this case, the bargaining weighting parameter is computed to be  $\alpha = [0.2222, 0.1748, 0.2222, 0.2059, 0.1748]$ . As can be seen, lower weights are allocated to faulty agents, and therefore the cost of cooperation is decreased during the fault recovery process. Moreover, it can be observed that the tracking performance of healthy agents are more deteriorated in transient time, since the cooperative centralized scheme puts more emphasis on cooperative aspect of the team, i.e. formation keeping.

**Table 4.13:** Performance and Time Response Evaluation of Centralized Fault Accommodation Based on Non-Cooperative and Cooperative Dynamic Game, Different LOE Faults in AUVs #2, #4, and #5

	Centralized Non-Cooperative	Centralized Cooperative
$J_x$	0.01	0.03
$J_{\tilde{x}}$	0.04	0.03
$J_x^s$	0.10	0.19
$J_{\tilde{x}}^s$	0.10	0.09
$J_u$	$1.856e + 04$	$1.858e + 04$
$J_{total}$	46	54
$t_s$	39	28
$\tilde{t}_s$	6.8	6.9
$t_{Iter}$	23	24

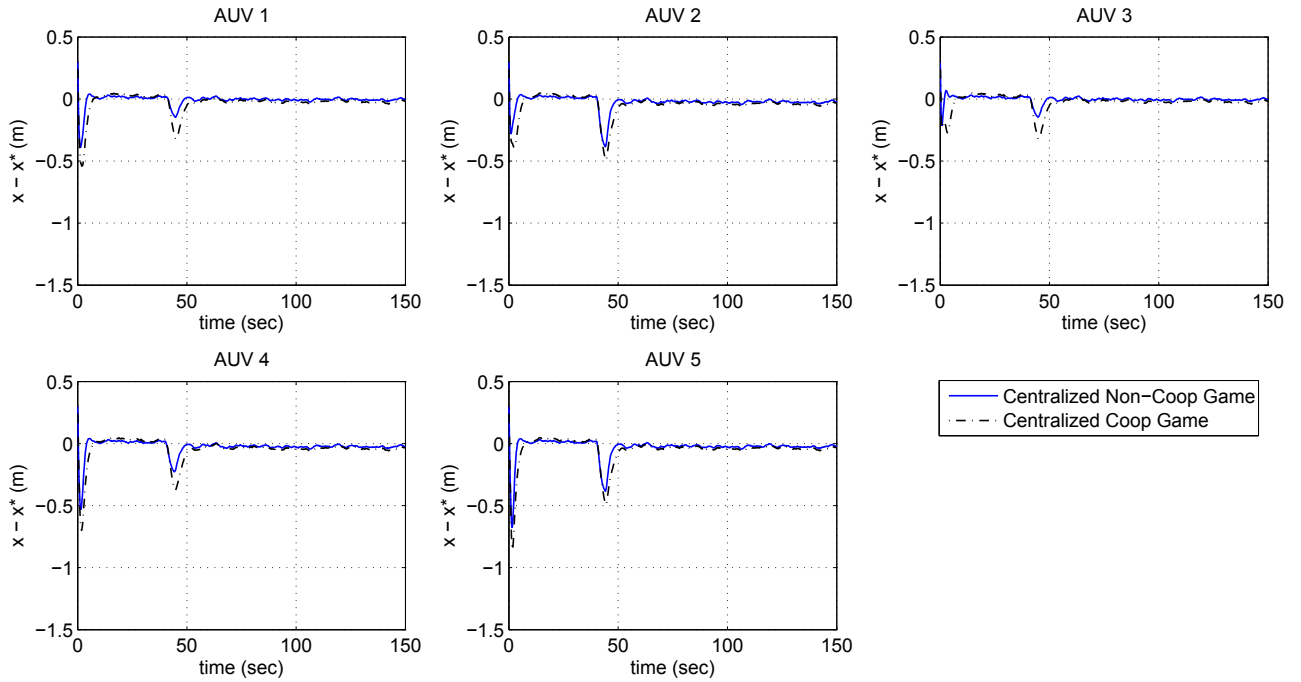


**Figure 4.37:** Error Signals Along  $X$ -axis for Centralized Accommodation Scheme Based on Cooperative and Non-Cooperative Game

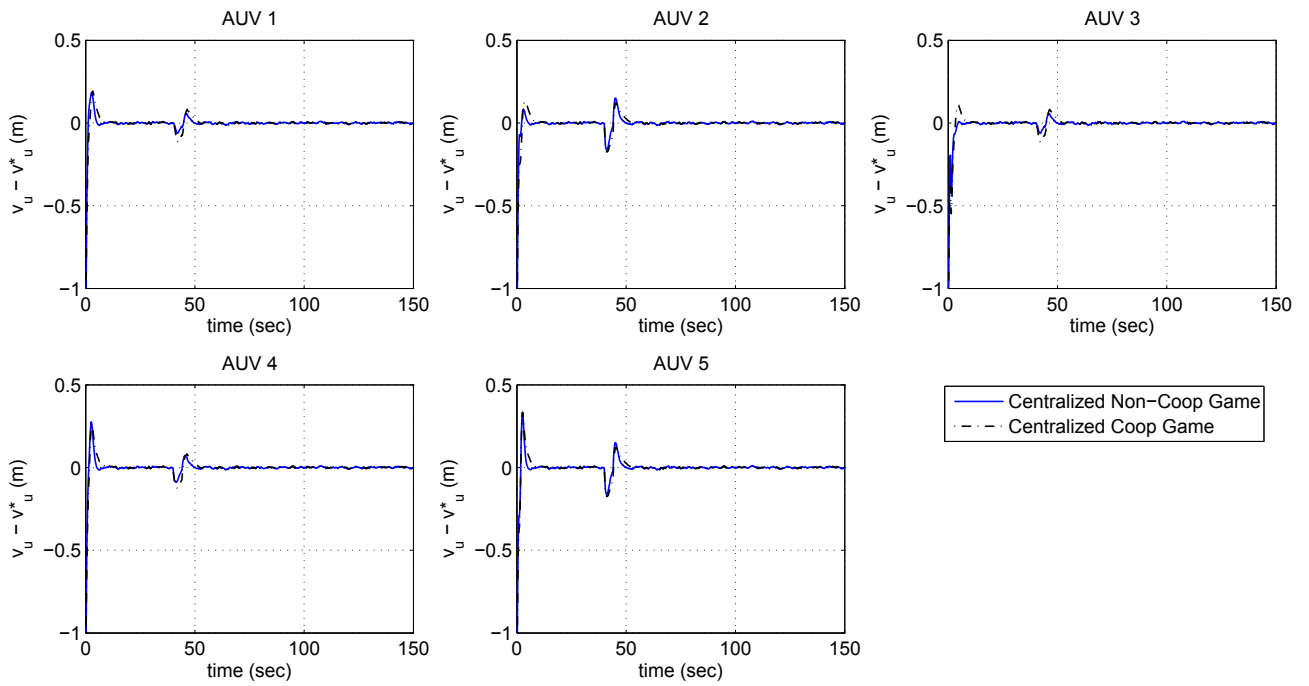


**Figure 4.38:** Surge Velocity Error Signals for Centralized Accommodation Scheme Based on Cooperative and Non-Cooperative Game

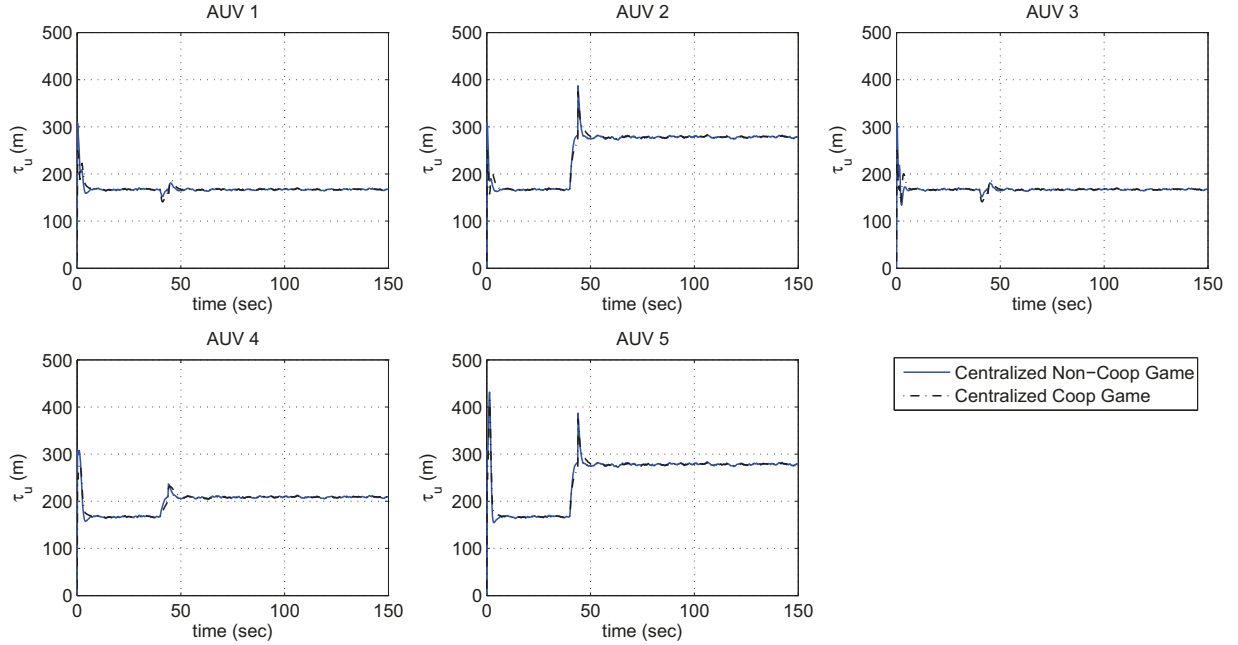


**Figure 4.39:** Thruster Forces along  $X$ -axis for Centralized Accommodation Scheme Based on Cooperative and Non-Cooperative Game

## 4.6 Summary

In this chapter, centralized, semi-decentralized, and decentralized active fault accommodation schemes are introduced to recover a team of AUVs from LOE actuator faults. The proposed active recovery schemes incorporate available online FDI fault information to redesign the nominal controllers introduced in the previous chapter. For each active recovery scheme, we proposed two recovery strategies, namely MPC-based recovery strategy and dynamic game-based recovery strategy to ensure that the tracking and formation keeping performance of the team are maintained in the presence of faulty individuals. Moreover, FDI imperfections such as the fault estimation error and time delay are considered in the redesign process. Then, a performance index is provided to have a measure of the impact of FDI imperfections on the performance of the team members.

At the end of the chapter, comparative simulations are performed to investigate the effectiveness and performance of proposed centralized, semi-decentralized, and decentralized fault accommodation schemes. To this end, various fault scenarios are considered such as different LOE fault severities, different FDI time delays, and multiple faulty agents in the team. All these fault scenarios are investigated in the presence of FDI imperfections such as estimation error and time delay. Tables 4.14, 4.15, and 4.16 summarize the quantitative results we have obtained in this chapter. Furthermore, the following conclusions briefly state our obtained result.

The simulation results under various fault scenarios show that the centralized and semi-decentralized accommodation schemes satisfy steady-state design specifications, i.e.  $J_x^s$  and  $J_{\tilde{x}}^s$ . However, the decentralized accommodation scheme violates acceptable specifications. Additionally, both MPC-based and dynamic game based semi-decentralized schemes have a performance very close to their centralized counterparts without imposing high communication requirement.

In all investigated faulty scenarios, inaccuracy of FDI estimates for LOE actuator fault does not violate the closed-loop system stability, and it only impose higher steady-state error. In the simulation scenarios related to different LOE fault severities, it is shown that high severity LOE actuator fault is more sensitive to FDI estimation error. Moreover, the centralized accommodation scheme can handle higher FDI estimation error than the semi-decentralized controller.

The fault scenario related to the low severity LOE fault reveals that both centralized and semi-decentralized nominal controllers can mitigate the effect of low severity LOE fault. In this fault scenario, it is shown that both MPC-based and dynamic game-based semi-decentralized control schemes have better transient tracking performance, i.e. lower  $J_x$  value, than centralized scheme. Moreover, the fault scenarios related to moderate and high severity LOE faults verify that the MPC-based

and dynamic game-based semi-decentralized accommodation schemes have also better tracking performance than the centralized scheme.

In fault scenarios (4.5.1.4) and (4.5.2.4), the effect of different FDI time delays is investigated. The simulation results show that both MPC-based and dynamic game-based semi-decentralized fault accommodation schemes can handle larger values of FDI time delay. However, it is shown that larger time delay results in poor transient performance and higher accommodation cost.

In fault scenarios (4.5.1.5) and (4.5.2.5), the effect of multiple faulty agents is investigated. In MPC-based fault accommodation framework, the total cost of semi-decentralized accommodation scheme is lower than the centralized scheme, but their control effort costs are very close to each other. Moreover, the tracking behavior of healthy agents in both schemes are almost identical. In dynamic game-based accommodation framework, the control and accommodation costs of semi-decentralized scheme are higher than centralized scheme. The reason is that the tracking behavior of healthy agents are less deteriorated, which in turn result in higher formation keeping cost and total accommodation cost values of semi-decentralized scheme accordingly.

**Table 4.14:** Summary of Performance and Time Response Characteristics of Centralized, Semi-Decentralized, and Decentralized fault Accommodation Schemes, Fault Scenarios 1, 2, 3

	MPC			Non-Cooperative Dynamic Game		
	Centralized		Decentralized	Centralized		Decentralized
	Centralized	Semi-Decentralized	Decentralized	Semi-Decentralized	Centralized	Decentralized
<b>Scenario 1 (5% LOE)</b>						
$J_x$	0.008	0.0059	1.957	0.002	0.003	0.005
$J_{\bar{x}}$	0.010	0.011	0.013	0.008	0.005	0.010
$J_x^s$	0.12	0.13	1.74	0.08	0.09	0.13
$J_{\bar{x}}^s$	0.16	0.12	0.13	0.10	0.08	0.12
$J_u$	116	115	4.49e + 03	124	120	126
$J_{total}$	14	12	1.4e + 03	8	6	12
$t_s$	24	23	67	23	22	28
$\tilde{t}_s$	—	—	—	—	—	—
$t_{solve}, t_{Iter}$	0.5152	0.00823	0.2671	34	43	37
<b>Scenario 2 (20% LOE)</b>						
$J_x$	0.009	0.006	1.95	0.002	0.003	0.006
$J_{\bar{x}}$	0.018	0.020	0.024	0.016	0.011	0.02
$J_x^s$	0.16	0.13	1.74	0.08	0.09	0.13
$J_{\bar{x}}^s$	0.114	0.116	0.13	0.11	0.9	0.12
$J_u$	1.200e + 03	1.201e + 03	5.17e + 03	1.205e + 03	1.201e + 03	1.298e + 03
$J_{total}$	20	19	1.48e + 03	14	10	19
$t_s$	33	23	75	23	22	28
$\tilde{t}_s$	6	7.2	7.3	6.1	5.7	6.2
$t_{solve}, t_{Iter}$	0.51	0.08	0.26	13	16	15
<b>Scenario 3 (40% LOE)</b>						
$J_x$	0.013	0.01	1.96	0.005	0.005	0.009
$J_{\bar{x}}$	0.06	0.07	0.08	0.05	0.40	0.06
$J_x^s$	0.16	0.13	1.74	0.08	0.09	0.13
$J_{\bar{x}}^s$	0.095	0.097	0.108	0.10	0.08	0.11
$J_u$	8.82e + 03	8.85e + 03	1.15e + 04	8.783e + 03	8.77e + 03	8.782e + 03
$J_{total}$	56	64	1.5e + 03	48	34	58
$t_s$	39	28	87	23	39	43
$\tilde{t}_s$	7.0	9.1	9.7	7.0	6.5	7.2
$t_{solve}, t_{Iter}$	0.49	0.07	0.27	17	21	19

**Table 4.15:** Summary of Performance and Time Response Characteristics of MPC-Based and Non-Cooperative Dynamic Game-Based Semi-Decentralized fault Accommodation Schemes, Fault Scenario 4

	MPC						Non-Cooperative Dynamic Game																									
	$t_d = 2 \text{ sec}$		$t_d = 4 \text{ sec}$		$t_d = 6 \text{ sec}$		$t_d = 2 \text{ sec}$	$t_d = 4 \text{ sec}$	$t_d = 6 \text{ sec}$																							
	$J_x$	$J_{\tilde{x}}$	$J_x^s$	$J_{\tilde{x}}^s$	$J_u$	$J_{total}$	$t_s$	$\tilde{t}_s$																								
Scenario 4 (FDI Time Delay)	0.007	0.03	0.13	0.09	8.83e + 03	31	27	6	0.013	0.10	0.13	0.09	8.84e + 03	90	29	11	0.003	0.005	0.006	0.08	0.08	0.10	8.783e + 03	26	23	5	48	23	7	68	23	8

**Table 4.16:** Summary of Performance and Time Response Characteristics of Centralized and Semi-Decentralized fault Accommodation Schemes, Fault Scenario 5, Multiple Faulty Agents

	MPC		Non-Cooperative Dynamic Game	
	Centralized	Semi-Decentralized	Centralized	Semi-Decentralized
<b>Scenario 5 (1<sup>st</sup> Case)</b>				
$J_x$	0.022	0.018	0.01	0.009
$J_{\tilde{x}}$	0.08	0.07	0.05	0.07
$J_x^s$	0.15	0.13	0.10	0.08
$J_{\tilde{x}}^s$	0.11	0.09	0.10	0.12
$J_u$	1.75e + 04	1.76e + 04	1.745e + 04	1.746e + 04
$J_{total}$	81	69	50	65
$t_s$	32	28	39	42
$\tilde{t}_s$	8	8.8	6.8	7.2
$t_{solve}, t_{Iter}$	0.9	0.07	23	18
<b>Scenario 5 (2<sup>nd</sup> Case)</b>				
$J_x$	0.0272	0.0231	0.0130	0.0109
$J_{\tilde{x}}$	0.07	0.05	0.04	0.06
$J_x^s$	0.16	0.13	0.10	0.09
$J_{\tilde{x}}^s$	0.12	0.109	0.103	0.12
$J_u$	1.870e + 04	1.874e + 04	1.856e + 04	1.857e + 04
$J_{total}$	76	61	46	57
$t_s$	35	29	39	42
$\tilde{t}_s$	7.7	8.7	6.8	7.3
$t_{solve}, t_{Iter}$	0.53	0.08	23	19

## Chapter 5

# Conclusions and Future Work

In this thesis, the formation control and accommodation of a team of autonomous underwater vehicles were addressed. The purpose of this work is to solve the tracking and formation keeping control problems with the lower communication requirement while acquiring performance that is close to the centralized case. Our second goal is to develop efficient active recovery strategies that can recover the team from LOE actuator faults such that the performance of healthy agents is less deteriorated and the whole team can maintain a graceful degraded performance. To this end, the MPC control technique and non-cooperative dynamic game theory are utilized. The reason to choose the MPC control technique is that it can compute control inputs in real-time based on the available current information from the team. Hence, this control technique can be redefined to reflect any changes or abnormalities in the system and environment such as faults and disturbances. Moreover, the non-cooperative dynamic game theory is an effective tool to model formation control and accommodation problem in which each agent has its own objective function and is coupled to other agents through its dynamical model. Moreover, with the occurrence of faults, the non-cooperative aspect of this framework led to less tracking performance deterioration in healthy individuals.

Toward aforementioned goals, MPC-based and dynamic game-based centralized, semi-decentralized, and decentralized control schemes are developed. In the centralized control scheme, the formation control problem is solved using the global information from the entire team. Although the centralized scheme can achieve the best possible performance due to solving the global minimization problem, it has the problem of high computational and communication requirements, and reliability issues in case of failure in the central unit. To overcome the aforementioned issues, a semi-decentralized scheme is proposed that divides the centralized formation problem into sub-problems of lower dimensions with local objective functions and locally coupled dynamics which leads to lower computational, and communication requirements and lifts the problem of having a single point of failure. The simulation results show that both MPC-based and dynamic game-based semi-decentralized schemes can acquire tracking and formation keeping performance very close to the corresponding centralized schemes with less control effort costs.

Moreover, MPC-based and dynamic game-based centralized, semi-decentralized, and decentralized active recovery schemes are developed to handle the most common actuator faults in underwater vehicles, namely LOE actuator faults. Then, a performance index is provided to have a measure of the impact of FDI imperfections such as the estimation error and time delay on the team members. In order to investigate the performance of the semi-decentralized accommodation scheme, comparative simulations are performed with various fault scenarios such as different LOE fault severities, different FDI time delays, and multiple faulty agents in the team. All these fault scenarios are investigated in the presence of FDI imperfections. It is shown that both MPC-based and dynamic game-based semi-decentralized accommodation schemes have a performance very close to their centralized counterparts without imposing high communication requirements. Moreover, it is shown that the tracking

performance of healthy agents in dynamic game-based semi-decentralized accommodation scheme are less deteriorated, which in turn leads to an increase in transient formation keeping cost.

Based on the results obtained in this thesis, the suggested future work can be listed as

- In this thesis, a 3-DOF model of the AUV is considered. Considering the 6-DOF AUV model can extend the functionality of the team for wider range of underwater missions. Moreover, considering the nonlinear model of the AUV can enhance the formation precision to a great deal.
- The proposed control and accommodation strategies are developed for dynamically identical AUVs. The development of both MPC-based and dynamic game-based control and accommodation strategies to control and accommodate a team of heterogeneous autonomous agents can be considered as another extension to this work.
- Besides the centralized control and accommodation scheme based on cooperative dynamic game theory that is developed in this work, the cooperative dynamic game theory provides a suitable framework for the development of distributed control and accommodation scheme in which a weighted sum of neighboring agents costs are considered as a common goal.
- The performance of proposed non-cooperative dynamic game-based semi-decentralized control and accommodation scheme can be enhanced by utilizing approximate dynamic programming approaches to compute and implement control actions in real-time.
- In this thesis, a performance index is provided to have the measure of the minimum cost value in presence of FDI uncertainties. As a future work, one

can design guaranteed cost accommodated controller such that the cost of the closed-loop system is guaranteed to be within a certain bound for all admissible FDI uncertainties.

- The fault recovery strategies developed in this thesis can be adopted to accommodate any other types of actuator faults and sensor faults.

# Bibliography

- [1] Available at: [http:// www.grex-project.eu](http://www.grex-project.eu).
- [2] K. D. Do and J. Pan, *Control of ships and underwater vehicles: design for underactuated and nonlinear marine systems*. Springer, 2009.
- [3] R. Cui, S. S. Ge, B. Voon Ee How, and Y. S. Choo, “Leader-follower formation control of underactuated auvs with leader position measurement,” in *Robotics and Automation, 2009. ICRA '09. IEEE International Conference on*, pp. 979–984, IEEE, 2009.
- [4] B. Fletcher, “Uuv master plan: a vision for navy uuv development,” in *OCEANS 2000 MTS/IEEE Conference and Exhibition*, vol. 1, pp. 65–71, IEEE, 2000.
- [5] R. Ghabcheloo, A. P. Aguiar, A. Pascoal, C. Silvestre, I. Kaminer, and J. Hespanha, “Coordinated path-following control of multiple underactuated autonomous vehicles in the presence of communication failures,” in *Decision and Control, 2006 45th IEEE Conference on*, pp. 4345–4350, IEEE, 2006.
- [6] R. Ghabcheloo, A. P. Aguiar, A. Pascoal, C. Silvestre, I. Kaminer, and J. Hespanha, “Coordinated path-following in the presence of communication losses and time delays,” *SIAM Journal on Control and Optimization*, vol. 48, no. 1, pp. 234–265, 2009.

- [7] R. M. Murray, “Recent research in cooperative control of multivehicle systems,” *Journal of Dynamic Systems, Measurement, and Control*, vol. 129, no. 5, pp. 571–583, 2007.
- [8] Y. Cao, W. Yu, W. Ren, and G. Chen, “An overview of recent progress in the study of distributed multi-agent coordination,” *Industrial Informatics, IEEE Transactions on*, vol. 9, no. 1, pp. 427–438, 2013.
- [9] R. Carelli, C. De la Cruz, and F. Roberti, “Centralized formation control of non-holonomic mobile robots,” *Latin American applied research*, vol. 36, no. 2, pp. 63–69, 2006.
- [10] R. W. Beard, J. Lawton, F. Y. Hadaegh, *et al.*, “A coordination architecture for spacecraft formation control,” *IEEE Transactions on control systems technology*, vol. 9, no. 6, pp. 777–790, 2001.
- [11] J. Lawton, R. W. Beard, and F. Y. Hadaegh, “An adaptive control approach to satellite formation flying with relative distance constraints,” 1999.
- [12] N. Burlutskiy, Y. Touahmi, and B. H. Lee, “Power efficient formation configuration for centralized leader–follower auvs control,” *Journal of marine science and technology*, vol. 17, no. 3, pp. 315–329, 2012.
- [13] E. Yang and D. Gu, “Nonlinear formation-keeping and mooring control of multiple autonomous underwater vehicles,” *Mechatronics, IEEE/ASME Transactions on*, vol. 12, no. 2, pp. 164–178, 2007.
- [14] A. S. Brandao, M. Sarcinelli-Filho, R. Carelli, and T. F. Bastos-Filho, “Decentralized control of leader-follower formations of mobile robots with obstacle avoidance,” in *Mechatronics, 2009. ICM 2009. IEEE International Conference on*, pp. 1–6, IEEE, 2009.

- [15] W. Ren and R. Beard, “Decentralized scheme for spacecraft formation flying via the virtual structure approach,” *Journal of Guidance, Control, and Dynamics*, vol. 27, no. 1, pp. 73–82, 2004.
- [16] E. Børhaug, A. Pavlov, E. Panteley, and K. Y. Pettersen, “Straight line path following for formations of underactuated marine surface vessels,” *Control Systems Technology, IEEE Transactions on*, vol. 19, no. 3, pp. 493–506, 2011.
- [17] D. J. Stilwell and B. E. Bishop, “Platoons of underwater vehicles,” *Control Systems, IEEE*, vol. 20, no. 6, pp. 45–52, 2000.
- [18] R. Skjetne, S. Moi, and T. I. Fossen, “Nonlinear formation control of marine craft,” in *Decision and Control, 2002, Proceedings of the 41st IEEE Conference on*, vol. 2, pp. 1699–1704, IEEE, 2002.
- [19] P. L. Kempker, A. C. Ran, and J. H. van Schuppen, “A formation flying algorithm for autonomous underwater vehicles,” in *CDC-ECE*, pp. 1293–1298, 2011.
- [20] E. Børhaug, A. Pavlov, and K. Pettersen, “Cross-track formation control of underactuated autonomous underwater vehicles,” in *Group Coordination and Cooperative Control*, pp. 35–54, Springer, 2006.
- [21] E. S. Kazerooni and K. Khorasani, “Semi-decentralized optimal control technique for a leader-follower team of unmanned systems with partial availability of the leader command,” in *Control and Automation, 2007. ICCA 2007. IEEE International Conference on*, pp. 475–480, IEEE, 2007.
- [22] W. B. Dunbar and R. M. Murray, “Distributed receding horizon control for multi-vehicle formation stabilization,” *Automatica*, vol. 42, no. 4, pp. 549–558, 2006.

- [23] W. Li and C. G. Cassandras, “Centralized and distributed cooperative receding horizon control of autonomous vehicle missions,” *Mathematical and computer modelling*, vol. 43, no. 9, pp. 1208–1228, 2006.
- [24] R. L. Raffard, C. J. Tomlin, and S. P. Boyd, “Distributed optimization for cooperative agents: Application to formation flight,” in *Decision and Control, 2004. CDC. 43rd IEEE Conference on*, vol. 3, pp. 2453–2459, IEEE, 2004.
- [25] Y. Q. Chen and Z. Wang, “Formation control: a review and a new consideration,” in *Intelligent Robots and Systems, 2005.(IROS 2005). 2005 IEEE/RSJ International Conference on*, pp. 3181–3186, IEEE, 2005.
- [26] J. P. Desai, “A graph theoretic approach for modeling mobile robot team formations,” *Journal of Robotic Systems*, vol. 19, no. 11, pp. 511–525, 2002.
- [27] Y. Wang, W. Yan, and W. Yan, “A leader-follower formation control strategy for auvs based on line-of-sight guidance,” in *Mechatronics and Automation, 2009. ICMA 2009. International Conference on*, pp. 4863–4867, IEEE, 2009.
- [28] F. Fahimi, “Sliding-mode formation control for underactuated surface vessels,” *Robotics, IEEE Transactions on*, vol. 23, no. 3, pp. 617–622, 2007.
- [29] M. Saffarian and F. Fahimi, “Control of helicopters’ formation using non-iterative nonlinear model predictive approach,” in *American Control Conference, 2008*, pp. 3707–3712, IEEE, 2008.
- [30] I.-A. Ihle, R. Skjetne, and T. I. Fossen, “Nonlinear formation control of marine craft with experimental results,” in *Decision and Control, 2004. CDC. 43rd IEEE Conference on*, vol. 1, pp. 680–685, IEEE, 2004.
- [31] H. Rezaee and F. Abdollahi, “A synchronization strategy for three dimensional decentralized formation control of unmanned aircrafts,” in *IECON 2011-37th*

- Annual Conference on IEEE Industrial Electronics Society*, pp. 462–467, IEEE, 2011.
- [32] A. Sadowska, D. Kostic, N. van de Wouw, H. Huijberts, and H. Nijmeijer, “Distributed formation control of unicycle robots,” in *Robotics and Automation (ICRA), 2012 IEEE International Conference on*, pp. 1564–1569, IEEE, 2012.
- [33] E. Kyrkjebo and K. Y. Pettersen, “A virtual vehicle approach to output synchronization control,” in *Decision and Control, 2006 45th IEEE Conference on*, pp. 6016–6021, IEEE, 2006.
- [34] T. Balch and R. C. Arkin, “Behavior-based formation control for multirobot teams,” *Robotics and Automation, IEEE Transactions on*, vol. 14, no. 6, pp. 926–939, 1998.
- [35] S. S. Ge, C.-H. Fua, and K. W. Lim, “Multi-robot formations: queues and artificial potential trenches,” in *Robotics and Automation, 2004. Proceedings. ICRA ’04. 2004 IEEE International Conference on*, vol. 4, pp. 3345–3350, IEEE, 2004.
- [36] F. Arrichiello, S. Chiaverini, and T. I. Fossen, “Formation control of underactuated surface vessels using the null-space-based behavioral control,” in *Intelligent Robots and Systems, 2006 IEEE/RSJ International Conference on*, pp. 5942–5947, IEEE, 2006.
- [37] N. E. Leonard and E. Fiorelli, “Virtual leaders, artificial potentials and coordinated control of groups,” in *Decision and Control, 2001. Proceedings of the 40th IEEE Conference on*, vol. 3, pp. 2968–2973, IEEE, 2001.

- [38] V. Gupta\*, B. Hassibi, and R. M. Murray, “A sub-optimal algorithm to synthesize control laws for a network of dynamic agents,” *International Journal of Control*, vol. 78, no. 16, pp. 1302–1313, 2005.
- [39] F. Borrelli and T. Keviczky, “Distributed lqr design for identical dynamically decoupled systems,” *Automatic Control, IEEE Transactions on*, vol. 53, no. 8, pp. 1901–1912, 2008.
- [40] M. A. Müller, M. Reble, and F. Allgöwer, “Cooperative control of dynamically decoupled systems via distributed model predictive control,” *International Journal of Robust and Nonlinear Control*, vol. 22, no. 12, pp. 1376–1397, 2012.
- [41] E. Semsar-Kazerooni and K. Khorasani, “Optimal consensus seeking in a network of multiagent systems: an lmi approach,” *Systems, Man, and Cybernetics, Part B: Cybernetics, IEEE Transactions on*, vol. 40, no. 2, pp. 540–547, 2010.
- [42] K. H. Movric and F. L. Lewis, “Cooperative optimal control for multi-agent systems on directed graph topologies,” *Automatic Control, IEEE Transactions on*, vol. 59, no. 3, pp. 769–774, 2014.
- [43] D. Q. Mayne, J. B. Rawlings, C. V. Rao, and P. O. Scokaert, “Constrained model predictive control: Stability and optimality,” *Automatica*, vol. 36, no. 6, pp. 789–814, 2000.
- [44] C. E. Garcia, D. M. Prett, and M. Morari, “Model predictive control: theory and practice—a survey,” *Automatica*, vol. 25, no. 3, pp. 335–348, 1989.
- [45] D. Jia and B. Krogh, “Min-max feedback model predictive control for distributed control with communication,” in *American Control Conference, 2002. Proceedings of the 2002*, vol. 6, pp. 4507–4512, IEEE, 2002.

- [46] W. B. Dunbar, *Distributed receding horizon control of multiagent systems*. PhD thesis, California Institute of Technology, 2004.
- [47] T. Keviczky, F. Borrelli, and G. J. Balas, “Decentralized receding horizon control for large scale dynamically decoupled systems,” *Automatica*, vol. 42, no. 12, pp. 2105–2115, 2006.
- [48] E. Franco, T. Parisini, and M. M. Polycarpou, “Design and stability analysis of cooperative receding-horizon control of linear discrete-time agents,” *International Journal of Robust and Nonlinear Control*, vol. 17, no. 10-11, pp. 982–1001, 2007.
- [49] Y. Kuwata, A. Richards, T. Schouwenaars, and J. P. How, “Distributed robust receding horizon control for multivehicle guidance,” *Control Systems Technology, IEEE Transactions on*, vol. 15, no. 4, pp. 627–641, 2007.
- [50] M. Vaccarini and S. Longhi, “Formation control of marine vehicles via real-time networked decentralized mpc,” in *Control and Automation, 2009. MED’09. 17th Mediterranean Conference on*, pp. 428–433, IEEE, 2009.
- [51] F. Fahimi, “Non-linear model predictive formation control for groups of autonomous surface vessels,” *International Journal of Control*, vol. 80, no. 8, pp. 1248–1259, 2007.
- [52] W. B. Dunbar and R. M. Murray, “Receding horizon control of multi-vehicle formations: A distributed implementation,” in *Decision and Control, 2004. CDC. 43rd IEEE Conference on*, vol. 2, pp. 1995–2002, IEEE, 2004.
- [53] W. B. Dunbar and R. M. Murray, “Model predictive control of coordinated multi-vehicle formations,” in *Decision and Control, 2002, Proceedings of the 41st IEEE Conference on*, vol. 4, pp. 4631–4636, IEEE, 2002.

- [54] T. Keviczky, F. Borrelli, K. Fregene, D. Godbole, and G. J. Balas, “Decentralized receding horizon control and coordination of autonomous vehicle formations,” *Control Systems Technology, IEEE Transactions on*, vol. 16, no. 1, pp. 19–33, 2008.
- [55] T. Keviczky, K. Fregene, F. Borrelli, G. J. Balas, and D. Godbole, “Coordinated autonomous vehicle formations: decentralization, control synthesis and optimization,” in *American Control Conference, 2006*, pp. 6–pp, IEEE, 2006.
- [56] A. Richards and J. How, “Decentralized model predictive control of cooperating uavs,” in *Decision and Control, 2004. CDC. 43rd IEEE Conference on*, vol. 4, pp. 4286–4291, IEEE, 2004.
- [57] M. Vaccarini and S. Longhi, “Networked decentralized mpc for formation control of underwater glider fleets,” in *Control Applications in Marine Systems*, vol. 7, pp. 63–68, 2007.
- [58] O. Morgenstern and J. Von Neumann, “Theory of games and economic behavior,” 1953.
- [59] J. F. Nash *et al.*, “Equilibrium points in n-person games,” *Proceedings of the national academy of sciences*, vol. 36, no. 1, pp. 48–49, 1950.
- [60] J. Engwerda, *LQ dynamic optimization and differential games*. John Wiley & Sons, 2005.
- [61] E. Semsar-Kazerooni and K. Khorasani, “Multi-agent team cooperation: A game theory approach,” *Automatica*, vol. 45, no. 10, pp. 2205–2213, 2009.
- [62] D. Gu, “A differential game approach to formation control,” *Control Systems Technology, IEEE Transactions on*, vol. 16, no. 1, pp. 85–93, 2008.

- [63] W. Lin, “Distributed uav formation control using differential game approach,” *Aerospace Science and Technology*, vol. 35, pp. 54–62, 2014.
- [64] F. Shamsi, F. Abdollahi, and K. Nikravesh, “Time varying formation control using differential game approach,” in *World Congress*, vol. 18, pp. 1114–1119, 2011.
- [65] K. G. Vamvoudakis, F. L. Lewis, and G. R. Hudas, “Multi-agent differential graphical games: Online adaptive learning solution for synchronization with optimality,” *Automatica*, vol. 48, no. 8, pp. 1598–1611, 2012.
- [66] S. L. Waslander, G. Inalhan, and C. J. Tomlin, “Decentralized optimization via nash bargaining,” *Theory and algorithms for cooperative systems*, vol. 4, pp. 565–585, 2004.
- [67] D. Bauso, L. Giarré, and R. Pesenti, “Non-linear protocols for optimal distributed consensus in networks of dynamic agents,” *Systems & Control Letters*, vol. 55, no. 11, pp. 918–928, 2006.
- [68] Y. Zhang and J. Jiang, “Bibliographical review on reconfigurable fault-tolerant control systems,” *Annual reviews in control*, vol. 32, no. 2, pp. 229–252, 2008.
- [69] M. Verhaegen, S. Kanev, R. Hallouzi, C. Jones, J. Maciejowski, and H. Smail, “Fault tolerant flight control-a survey,” in *Fault Tolerant Flight Control*, pp. 47–89, Springer, 2010.
- [70] D. Zhang, Z. Wang, and S. Hu, “Robust satisfactory fault-tolerant control of uncertain linear discrete-time systems: an lmi approach,” *International Journal of Systems Science*, vol. 38, no. 2, pp. 151–165, 2007.

- [71] D. Ye and G.-H. Yang, "Adaptive fault-tolerant tracking control against actuator faults with application to flight control," *Control Systems Technology, IEEE Transactions on*, vol. 14, no. 6, pp. 1088–1096, 2006.
- [72] T. Miksch, A. Gambier, and E. Badreddin, "Real-time implementation of fault-tolerant control using model predictive control," in *World Congress*, vol. 17, pp. 11136–11141, 2008.
- [73] S. Sun, L. Dong, L. Li, and S. Gu, "Fault-tolerant control for constrained linear systems based on mpc and fdi," *International Journal of information and systems sciences*, vol. 4, no. 4, pp. 512–23, 2008.
- [74] Y. Zhang and J. Jiang, "Integrated active fault-tolerant control using imm approach," *Aerospace and Electronic Systems, IEEE Transactions on*, vol. 37, no. 4, pp. 1221–1235, 2001.
- [75] M. Bodson and J. E. Groszkiewicz, "Multivariable adaptive algorithms for reconfigurable flight control," *Control Systems Technology, IEEE Transactions on*, vol. 5, no. 2, pp. 217–229, 1997.
- [76] R. F. Stengel and C. Y. Huang, "Restructurable control using proportional-integral implicit model following," *Journal of Guidance, Control, and Dynamics*, vol. 13, no. 2, pp. 303–309, 1990.
- [77] R. J. Patton, R. N. Clark, and P. M. Frank, *Issues of fault diagnosis for dynamic systems*. Springer, 2000.
- [78] E. Semsar-Kazerooni and K. Khorasani, "Team consensus for a network of unmanned vehicles in presence of actuator faults," *Control Systems Technology, IEEE Transactions on*, vol. 18, no. 5, pp. 1155–1161, 2010.

- [79] G. Godard and K. D. Kumar, “Fault tolerant reconfigurable satellite formations using adaptive variable structure techniques,” *Journal of guidance, control, and dynamics*, vol. 33, no. 3, pp. 969–984, 2010.
- [80] A. R. Mehrabian, S. Tafazoli, and K. Khorasani, “Reconfigurable control of networked nonlinear euler-lagrange systems subject to fault diagnostic imperfections,” in *Decision and Control and European Control Conference (CDC-ECC), 2011 50th IEEE Conference on*, pp. 6380–6387, IEEE, 2011.
- [81] H. Yang, M. Staroswiecki, B. Jiang, and J. Liu, “Fault tolerant cooperative control for a class of nonlinear multi-agent systems,” *Systems & Control Letters*, vol. 60, no. 4, pp. 271–277, 2011.
- [82] S. Azizi and K. Khorasani, “A hierarchical architecture for cooperative fault accommodation of formation flying satellites in deep space,” in *American Control Conference, 2009. ACC’09.*, pp. 4178–4183, IEEE, 2009.
- [83] B. Zhou, W. Wang, and H. Ye, “Cooperative control for consensus of multi-agent systems with actuator faults,” *Computers & Electrical Engineering*, vol. 40, no. 7, pp. 2154–2166, 2014.
- [84] Q. Xu, H. Yang, B. Jiang, D. Zhou, and Y. Zhang, “Fault tolerant formations control of uavs subject to permanent and intermittent faults,” *Journal of Intelligent & Robotic Systems*, vol. 73, no. 1-4, pp. 589–602, 2014.
- [85] M. Qian, B. Jiang, and D. Xu, “Fault tolerant control scheme design for the formation control system of unmanned aerial vehicle,” *Proceedings of the Institution of Mechanical Engineers, Part I: Journal of Systems and Control Engineering*, p. 0959651813495134, 2013.

- [86] Y.-H. Chang, W.-S. Chan, C.-Y. Yang, C.-W. Tao, and S.-F. Su, “Adaptive dynamic surface control for fault-tolerant multi-robot systems,” in *System Science and Engineering (ICSSE), 2013 International Conference on*, pp. 25–30, IEEE, 2013.
- [87] Z. Gallehdari, N. Meskin, and K. Khorasani, “Cost performance based control reconfiguration in multi-agent systems,” in *American Control Conference (ACC), 2014*, pp. 509–516, IEEE, 2014.
- [88] Z. Gallehdari, N. Meskin, and K. Khorasani, “Robust cooperative control reconfiguration/recovery in multi-agent systems,” in *Control Conference (ECC), 2014 European*, pp. 1554–1561, IEEE, 2014.
- [89] J. Li and K. D. Kumar, “Decentralized fault-tolerant control for satellite attitude synchronization,” *Fuzzy Systems, IEEE Transactions on*, vol. 20, no. 3, pp. 572–586, 2012.
- [90] T. I. Fossen, *Marine control systems: guidance, navigation and control of ships, rigs and underwater vehicles*. Marine Cybernetics Trondheim, 2002.
- [91] T. Fossen and A. Ross, “Nonlinear modelling, identification and control of auvs,” *IEE CONTROL ENGINEERING SERIES*, vol. 69, p. 13, 2006.
- [92] G. Antonelli, S. Chiaverini, N. Sarkar, and M. West, “Adaptive control of an autonomous underwater vehicle: experimental results on odin,” *Control Systems Technology, IEEE Transactions on*, vol. 9, no. 5, pp. 756–765, 2001.
- [93] J. E. G. Refsnes, “Nonlinear model-based control of slender body auvs,” *Norwegian University of Science and Technology*, vol. 30, no. 226, pp. 229–231, 2007.

- [94] A. P. Aguiar and A. M. Pascoal, “Dynamic positioning and way-point tracking of underactuated auvs in the presence of ocean currents,” *International Journal of Control*, vol. 80, no. 7, pp. 1092–1108, 2007.
- [95] F. Alonge, F. D’Ippolito, and F. Raimondi, “Trajectory tracking of underactuated underwater vehicles,” in *Decision and Control, 2001. Proceedings of the 40th IEEE Conference on*, vol. 5, pp. 4421–4426, IEEE, 2001.
- [96] D. J. Panagou, G. C. Karras, and K. J. Kyriakopoulos, “Towards the stabilization of an underactuated underwater vehicle in the presence of unknown disturbances,” in *OCEANS 2008*, pp. 1–8, IEEE, 2008.
- [97] E. Børhaug and K. Y. Pettersen, “Adaptive way-point tracking control for underactuated autonomous vehicles,” in *Decision and Control, 2005 and 2005 European Control Conference. CDC-ECC’05. 44th IEEE Conference on*, pp. 4028–4034, IEEE, 2005.
- [98] R. J. Patton, “Fault-tolerant control systems: The 1997 situation,” in *IFAC symposium on fault detection supervision and safety for technical processes*, vol. 3, pp. 1033–1054, 1997.
- [99] V. Venkatasubramanian, R. Rengaswamy, K. Yin, and S. N. Kavuri, “A review of process fault detection and diagnosis: Part i: Quantitative model-based methods,” *Computers & chemical engineering*, vol. 27, no. 3, pp. 293–311, 2003.
- [100] J. M. Maciejowski, *Predictive control: with constraints*. Pearson education, 2002.
- [101] A. Bemporad, M. Morari, V. Dua, and E. N. Pistikopoulos, “The explicit linear quadratic regulator for constrained systems,” *Automatica*, vol. 38, no. 1, pp. 3–20, 2002.

- [102] S. a. Keerthi and E. G. Gilbert, “Optimal infinite-horizon feedback laws for a general class of constrained discrete-time systems: Stability and moving-horizon approximations,” *Journal of optimization theory and applications*, vol. 57, no. 2, pp. 265–293, 1988.
- [103] J. B. Rawlings and K. R. Muske, “The stability of constrained receding horizon control,” *Automatic Control, IEEE Transactions on*, vol. 38, no. 10, pp. 1512–1516, 1993.
- [104] K. R. Muske and J. B. Rawlings, “Linear model predictive control of unstable processes,” *Journal of Process Control*, vol. 3, no. 2, pp. 85–96, 1993.
- [105] P. O. Scokaert and J. B. Rawlings, “Constrained linear quadratic regulation,” *Automatic Control, IEEE Transactions on*, vol. 43, no. 8, pp. 1163–1169, 1998.
- [106] W. Thomson, “Cooperative models of bargaining,” vol. 2 of *Handbook of Game Theory with Economic Applications*, pp. 1237 – 1284, Elsevier, 1994.
- [107] T. Basar, G. J. Olsder, G. Clsder, T. Basar, T. Baser, and G. J. Olsder, *Dynamic noncooperative game theory*, vol. 200. SIAM, 1995.
- [108] C. D. Godsil, G. Royle, and C. Godsil, *Algebraic graph theory*, vol. 207. Springer New York, 2001.
- [109] J. A. Fax and R. M. Murray, “Information flow and cooperative control of vehicle formations,” *Automatic Control, IEEE Transactions on*, vol. 49, no. 9, pp. 1465–1476, 2004.
- [110] D. Blueschke, R. Neck, and D. A. Behrens, “Optgame3: a dynamic game solver and an economic example,” in *Advances in Dynamic Games*, pp. 29–51, Springer, 2013.

- [111] L. Cherfi, Y. Chitour, and H. Abou-Kandil, “A new algorithm for solving coupled algebraic riccati equations,” in *Computational Intelligence for Modelling, Control and Automation, 2005 and International Conference on Intelligent Agents, Web Technologies and Internet Commerce, International Conference on*, vol. 1, pp. 83–88, IEEE, 2005.